SEDIMENTOLOGY, CORAL REEF ZONATION, AND LATE PLEISTOCENE COASTLINE MODELS OF THE SODWANA BAY CONTINENTAL SHELF, NORTHERN ZULULAND

by

Peter John Ramsay BSc (Hons)

Submitted in partial fulfilment of the requirements

for the degree of Doctor of Philosophy

in the

Department of Geology and Applied Geology

University of Natal

Durban

December 1991

PREFACE

This thesis represents original work by the author and has not been submitted in any form to another university. Where use has been made of the work of others, it has been duly acknowledged in the text.

The research was carried out in the Department of Geology and Applied Geology at the University of Natal, during the period January 1988 to January 1989 and completed during 1990 and 1991 at the Joint Geological Survey - University of Natal Marine Geoscience Unit. The project was supervised by Professor T.R. Mason.

DEDICATION

This thesis is dedicated to the memory of my late father Dave Ramsay, who instilled in me a love of the sea at an early age.

ABSTRACT

This geostrophic current-controlled Zululand/Natal shelf displays a unique assemblage of interesting physical, sedimentological and biological phenomena. The shelf in this area is extremely narrow compared to the global average of 75km, and is characterised by submarine canyons, coral reefs, and steep gradients on the continental slope. A shelf break occurs 2.1km to 4.1km offshore and the shelf can be divided into a northern region and a southern region based on the presence or absence of a defined shelf break. The southern shelf has a poorly-defined shelf break whilst the northern shelf has a well-defined break at -65m. The poor definition of the shelf break on the southern shelf can possibly be attributed to the presence of giant, climbing sand dunes offshore of Jesser Point at depths of -37m to -60m. The northern shelf has a series of coast-parallel oriented patch coral reefs which have colonised carbonate-cemented, coastal-facies sequences.

The northern shelf can be divided into three distinct zones: inner-, mid-, and outer-shelf zones. The inner-shelf is defined as the area landward of the general coral reef trend, with depths varying from 0m to -15m and having an average gradient of 1.1°. The mid-shelf is defined by the general coral reef trend, varying from -9m over the shallow central axis of the reefs to -35m along the deep reef-front environments. The outer-shelf is seaward of the coral reefs and occurs at a depth range of -35m to -65m. Gradients vary from 1° in the south to 2.5° in the northern part of the study area, and are steep compared to world average shelf gradient of 0.116°.

Four submarine canyons occur in the study area and are classified as mature- or youthful-phase canyons depending on the degree to which they breach the shelf. The origin of these canyons is not related to the position of modern river mouths but can probably be linked to palaeo-outlets of the Pongola and Mkuze River systems. It is suggested that the canyons are mass-wasting features which were exploited by palaeo-drainage during regressions. The youthful-phase canyons appear to be mass-

wasting features associated with an unstable, rapidly-deposited, progradational late Pliocene sequence and a steep upper continental slope. The mature-phase canyons were probably initiated by mass-wasting but have advanced shoreward, breaching the shelf, due to their link with the palaeo-outlets of the Pongola and Mkuze Rivers during late Pleistocene regressions.

Evidence of modern canyon growth has been noted on numerous SCUBA diving surveys carried out on the canyon heads. These take the form of minor wall slumps and small-scale debris flows. The canyons are also supplied with large quantities of sand in the form of large-scale shelf subaqueous dunes generated and transported by the Agulhas Current. As these bedforms meet the canyons the sediment cascades down the canyon thalweg and causes erosion and downcutting of the canyon walls and floor thereby increasing the canyon dimensions.

Late Pleistocene beachrock and aeolianite outcrops with or without an Indo-Pacific coral reef veneer are the dominant consolidated lithology on the shelf. These submerged, coast-parallel, carbonate-cemented, coastal facies extend semi-continuously from -5m to -95m, and delineate late Pleistocene palaeocoastline events. The rock fabric of these high primary porosity lithologies shows grains floating in a carbonate cement with occasional point-contacts. Grains are mostly quartz (80-90%), minor K-feldspar and plagioclase (5-10%), and various lithic fragments. The rocks contain conspicuous organic grains including foraminifera, bivalve, echinoid, bryozoan, red algal, and occasional sponge spicule fragments; these commonly display replacement fabrics or iron-stained rims. The dominant sedimentary structures found in these sandstone outcrops include high-angle planar cross-bedding and primary depositional dip bedding. Palaeocurrent directions suggest a palaeoenvironment dominated by a combination of longitudinal and transverse dunes with wind directions similar to those observed forming the modern dune systems. Erosional features evident on the submerged beachrocks and aeolianites include gullies trending in two different directions and sea-level planation surfaces with or without the presence of potholes.

The unconsolidated sediment on the shelf is either shelf sand, composed mainly of terrigenous quartz grains; or bioclastic sediment which is partially derived from biogenic sources.

The quartzose sand from the inner-shelf is generally fine-grained, moderately- to well-sorted, and coarsely- to near symmetrically-skewed. Carbonate content is low, and varies between 4-13%. Quartzose sand from the outer-shelf is fine-grained, moderately- to well-sorted, and coarsely- to very coarsely-skewed. The inner-shelf quartzose sand is better sorted than the outer-shelf sand due to increased reworking of this sediment by the high-energy swell regime. Sediment from the shallower areas of the outer-shelf (< -50m) is better sorted than sediment from depths of greater than -50m. Generally wave-reworking of quartzose shelf sand from the Sodwana Bay shelf results in greater sediment maturity than that observed from geostrophic current effects or a combination of geostrophic and wave-reworking. This sediment was derived by reworking of aeolian and beach sediments, deposited on the shelf during the period leading up to the Last Glacial Maximum (15 000 - 18 000 years B.P.) when sea-level was -130m, during the Holocene (Flandrian) transgression.

Bioclastic sediment on the Sodwana Bay shelf is defined as having a $CaCO_3$ content of greater than 20% and is a mixture of biogenically-derived debris and quartzose sand. The distribution of bioclastic sediment in the study area is widespread, with reef-derived and outer-shelf-derived populations being evident. This sediment consists of skeletal detritus originating from the mechanical and biological destruction of carbonate-secreting organisms such as molluscs, foraminifera, alcyonaria, scleractinia, cirripedia, echinodermata, bryozoa, porifera. The reef-derived bioclastic population is confined to depths less than -40m in close proximity to reef areas, whereas the shelf-derived bioclastic population occurs at depths greater than -40m and is derived from carbonate-producing organisms on deep water reefs and soft-substrate environments on the shelf.

Large-scale subaqueous dunes form in the unconsolidated sediment on the outer-shelf due to the

Agulhas flow acting as a sediment conveyor. These dunes are a common feature on the Sodwana Bay shelf occurring as two distinct fields at depths of -35m to -70m, the major sediment transport direction being towards the south. The two dune fields, the inner- and outer subaqueous dune fields, are physically divided by Late Pleistocene beachrock and aeolianites ledges. A bedform hierarchy has been recognised. The larger, outer dune field appears to have originated as a system of climbing bedforms with three generations of bedforms being superimposed to form a giant bedform, while the inner dune field has a less complex construction. The largest bedforms are those of the outer dune field off Jesser Point, being up to 12 m high, 4 km long and 1.2 km wide. A major slip face, with a slope of 8° is present.

Bedload parting zones exist where the bedform migration direction changes from south to north. Three bedload parting zones occur in the study area at depths of -60m, -47m and -45m; two in the inner dune field and one in the outer dune field. These zones are invariably located at the southern limits of large clockwise eddy systems. Such eddies appear to be the result of topographically induced vorticity changes in the geostrophic flow and/or the response to atmospheric forcing caused by coastal low-pressure system moving up the coastline.

It has been demonstrated that the inner subaqueous dune sediment conveyor is not active all the time but only during periods of increased current strength when the Agulhas Current meanders inshore. The smaller bedforms in the outer dune field undergo continuous transport due to the current velocity on the shelf edge outer dune field being higher than the velocity experienced on the inner dune field. The very large 2-D dune which forms the outer dune field is probably not active at present: this is inferred due to the shallow angle of the mega-crest lee slope (8°).

The very large Sodwana Bay subaqueous dune fields may be compared with the very large, reconstructed, subaqueous dunes which occur in Lower Permian sediments of the Vryheid Formation,

northern Natal. These Permian dunes are represented, in section, as a fine- to medium-grained distal facies sandstone with giant crossbeds. These large-scale bedforms are unidirectional, but rare directionally-reversed, climbing bedforms do occur, this directional reversal may be related to bedload parting zones. On the evidence presented in this thesis, it is proposed that these Permian subaqueous dunes may be ancient analogues of the modern subaqueous dune field on the Sodwana Bay shelf.

Positive-relief hummocks and negative-relief swale structures are fairly common in the fine-grained, quartzose shelf sand at depths of -30m to -60m. These appear to be transitional bedforms related to the reworking by storms of medium 2-D subaqueous dunes. These hummocky structures may be the modern equivalent of hummocky cross-stratification noted in the geological record, and if so, they are probably the first to have ever been observed underwater.

The occurrences of ladderback ripples on the Sodwana Bay shelf at depths of -4m to -17m, suggest that subtidal ladderback ripples may be more common than previously thought. Ladderback ripples are common features of tidal flats and beaches where they form by late-stage emergence run-off during the ebb tide. They are generally considered diagnostic of clastic intertidal environments. The mode of formation on the Sodwana Bay shelf is different from the classic late-stage emergence run-off model of intertidal occurrences, being a subtidal setting. Subaqueous observations indicate that ladderback ripples are not environment-specific, and that additional evidence of emergence is therefore necessary to support an intertidal setting in the rock record: ladderback ripples alone are insufficient to prove an intertidal environment.

The coral patch reefs of the northern Natal coast are unique, being the most southerly reefs in Africa, and totally unspoilt. The Zululand reefs are formed by a thin veneer of Indo-Pacific type corals which have colonised submerged, late Pleistocene beachrocks and aeolianites. Two-Mile Reef at Sodwana Bay has been used to develop a physiographic and biological zoning model for Zululand coral reefs, which

has been applied to other reefs in the region. Eight distinct zones can be recognised and differentiated on the basis of physiographic and biological characteristics. The reef fauna is dominated by an abundance of alcyonarian (soft) corals, which constitute 60-70% of the total coral fauna. The Two-Mile Reef zoning model has been successfully applied to larger reefs such as Red Sands Reef, and smaller patch reefs (Four-Mile and Seven-Mile Reefs) in the same general area.

In this thesis extensive use has been made of Hutton's uniformitarian principles. Hutton's doctrine is particularly relevant to the study of depositional processes and relict shorelines. Coastal processes and weather patterns during the late Pleistocene were broadly similar to modern conditions enabling direct comparisons to be made. A computer-aided facies analysis model has been developed based on textural statistics and compositional features of carbonate-cemented coastal sandstones. Many attempts have been made to distinguish different ancient sedimentary depositional environments, most workers in this field having little success. The new method of facies reconstruction is based on:

(1) underwater observations of sedimentary structures and general reef morphology;

(2) a petrographic study of the reef-base enabling five facies: aeolianite, backbeach, forebeach, swash, and welded bar facies to be recognised, which control the geomorphology of Two-Mile Reef;

(3) cluster and discriminant analysis comparing graphic settling statistics of acid-leached reef-base samples with those of modern unconsolidated dune/beach environments.

The results of this analysis demonstrated that the beachrocks and aeolianites on the shelf formed during a regression and that late Pleistocene coastal facies are similar to modern northern Zululand coastal environments, which have been differentiated into aeolian, backbeach, forebeach, swash, & welded bar.

A late Pleistocene and Holocene history of the shelf shows that during the late Pleistocene, post-

Eemian regressions resulted in deposition and cementation of coast-parallel beachrocks and aeolianites, which define a series of four distinct palaeocoastline episodes with possible ages between 117 000 and 22 000 years B.P. The beachrock/aeolianites formed on the shelf during stillstands and slow regressions, and the gaps between these strandline episodes represent periods of accelerated sea-level regression or a minor transgressive phase which hindered deposition and cementation. The formation of these lithologies generated a considerable sediment sink in the nearshore zone. This reduced sediment supply and grain transport in the littoral zone during the Holocene, and probably enhanced landward movement of the shoreline during the Flandrian transgression.

Prior to the Last Glacial Maximum, the beachrock/aeolianite sedimentary sequence was emergent and blanketed by shifting aeolian sands. The Pongola River, which flowed into Lake Sibaya, reworked the unconsolidated sediments on the shelf, and exploited the route of least resistance: along White Sands and Wright Canyon axes. The erosion resulting from fluvial denudation in Wright Canyon has caused this canyon to erode some of the beachrock/aeolianite outcrops which form palaeocoastline episode 2 and entrench the canyon to a deeper level; this eroded the shelf to a distance of 2km offshore.

During the Flandrian transgression the unconsolidated sediment cover was eroded, exposing and submerging the beachrock/aeolianite sequence. Flandrian stillstands caused erosional features such as wave-planed terraces, potholes, and gullies to be incised into beachrock and aeolianite outcrops; these are seen at present depths of -47m, -32m, -26m, -22m, -17m to -18m, and -12m. High energy sediment transfers, in an onshore direction, resulted in the deposition of sand bars across the outlet of Lake Sibaya's estuary and the development of a 130m+ coastal dune barrier on a pre-existing, remnant Pleistocene dune stub. Sea-level stabilised at its present level 7 000-6 000 years B.P. and coral reef growth on the beachrock/aeolianite outcrops probably started at 5 000 years B.P. A minimum age for the formation of the northern Zululand coral reefs has been established at 3780 ± 60 years B.P.

A mid Holocene transgression relating to the Climatic Optimum deposited a +2m raised beachrock sequence. This transgression eroded the coastal dune barrier and caused a landward shoreline translation of approximately 40m. A minor transgression such as this can be used as a model for coastal erosion which will result from the predicted 1.5m rise in sea-level over the next century. This rise in sea-level could result in a 30m landward coastline translation of the present coastline, ignoring the influence that storms and cyclones will have on the coastline configuration.

ACKNOWLEDGEMENTS

This thesis was funded by the South African Geological Survey and completed while the author was employed by Geological Survey's Marine Geoscience Unit.

There are numerous persons and organisations to whom I would like to express my sincere thanks. Special thanks are due to the Natal Parks Board (NPB) for granting permission to undertake research in the St Lucia and Maputaland Marine Reserves and for providing accommodation at Sodwana Bay. R. Broker, W. Howells, F. Junor, L. Fearnhead, and D. Densham of the NPB provided invaluable logistic support to the project. Dr Allan Ramm of the CSIR (Durban) provided assistance in the initial phase of the study. The officers and crew of the RV Benguela deserve thanks for their hard work and enthusiasm.

This project would not have been possible without Peter Bova's astounding technical expertise. Peter spent a considerable amount of time preparing all the geophysical instrumentation for the various cruises and kept the instruments running in perfect working order during those long sea cruises. I am greatly indebted Ian Wright, Dr. Alan Smith, and Wade Kidwell for their considerable scientific and technical assistance on the RV Benguela and Geocat cruises. My fearless diving companions and surface support team, consisting of Ian Wright, Wade Kidwell, Andrew Cooper, and Arjoon Singh, braved all sorts of weather and mishaps to accomplish the scientific diving objectives. D.H. Hattingh spent many long hours drafting the maps and diagrams and I am greatly indebted to him.

Thanks to Dr. Alan Smith and Andrew Cooper for all the fruitful discussions, those during office hours and those over a few beers, on the origin, formation, and evolution of the northern Zululand continental shelf.

My fiancèe, Silvia, and my mother provided constant support on the domestic front, bearing my occasional moods in the final write-up phase of this thesis.

I am especially grateful to my supervisor Professor Tom Mason for his wise guidance and useful comments, and for always being available for consultations on a variety of subjects.

AUTHOR'S PUBLICATION LIST

(Topics related to the thesis)

INTERNATIONAL REFEREED JOURNAL PAPERS

Ramsay, P.J. (1990). The use of computer graphics to produce a three-dimensional morphological and bathymetric model of a Zululand coral reef. S.A. Jour. Sci., 86(3), 130-131.

Ramsay, P.J., Cooper, J.A.G., Wright, C.I. & Mason, T.R. (1989). The occurrence and formation of ladderback ripples in subtidal, shallow marine sands, Zululand, South Africa. Marine Geology, 86(2/3), 229-235.

Ramsay, P.J. & Mason, T.R. (1990). Development of a type zoning model for Zululand coral reefs, Sodwana Bay, South Africa. Journal of Coastal Research, 6(4), 829-852.

CONFERENCE ABSTRACTS

Mason, T.R., Cooper, J.A.G., Grobbler, N.G., Ramsay, P.J., Wright, C.I. (1987). Natal Coastal Research Programme: S.E.A.L. Project (Abstract). 6th National Oceanographic Symposium, Stellenbosch, Paper B-96.

Ramsay, P.J. (1988). Physiographic and biological zoning of Two-Mile Reef, Sodwana Bay. Extended Abstract: 22nd Earth Science Congress of the Geological Society of South Africa, University of Natal, Durban, 483-486.

Ramsay, P.J. & Mason, T.R. (1990). Zululand coral reefs as palaeocoastline indicators. Abstract: Oceans '90, 7th National Oceanographic Conference, San Lameer, South Africa.

Ramsay, P. J. (1990). The coral reefs of Maputaland. Abstract: Barologia, UCT, South Africa, September 1990.

Ramsay, P. J. (1990). A new method for reconstructing late Pleistocene coastal environments. Abstract: Natal Branch GSSA 10th Anniversary Colloquium, University of Natal, Pietermaritzburg, October 1990.

Smith, A.M., Mason, T.R., Ramsay, P.J., Watkeys, M., & Wright, C.I. (1991). Modern, ancient and deformed sedimentary structures compared and sources of error highlighted. Terra Nova, 3, Abstracts Supplements 3, 26.

THESES

Ramsay, P.J. (1987). The Sedimentation, Distribution and Zonation of Two-Mile Reef, Sodwana Bay. (unpubl.) Bsc (Hons) thesis, 63 pp.

REPORTS

Ramsay, P.J. (1987). A pilot study of the sedimentation, distribution and zonation of Two-Mile Reef, Sodwana Bay. Natal Parks Board Report, CM 16/6/2, 63 pp.

Mason, T.R., Ramsay, P.J., Wright, C.I. (1987). Report on pilot sedimentological studies of Two-Mile Reef, Sodwana Bay and Lake Sibaya, Zululand. Report presented to Kwazulu Bureau of Natural Resources and Young Yamaha organisation.

Ramsay, P.J., Cacchione, S.A. & Mason, T.R. (1989). A photographic record of the Boshoff coral collection, Oceanographic Research Institute, Durban. Joint Geological Survey - University of Natal Durban Marine Geoscience Unit, Special Report, 1, 195 pp.

Ramsay, P.J. (1989). A computer-generated model and bathymetry of Two-Mile Reef, Sodwana Bay. Natal Parks Board Report SM 3/9/2 No.1, 9 pp.

Mason T.R. & Ramsay P.J. (1989). Report on access roads to the beach: Sodwana Bay. Joint Geological Survey - University of Natal Durban Marine Geoscience Unit, Special Report, Natal Parks Board, 18 pp.

Ramsay, P.J. & Mason, T.R. (1989). The development of a type zoning model for Zululand coral reefs, Sodwana Bay, South Africa. Joint Geological Survey - University of Natal Durban Marine Geoscience Unit, Special Report, 2, 49 pp.

Mason, T.R. & Ramsay, P.J. (1990). Environmental assessments on the Maputaland coastline. Natal Parks Board Consultancy Report, 32 pp.

Ramsay, P.J. (1990). Geological history and coral reef formation of the Bazaruto Archipelago. In : Dutton, T. P., Conservation Master Plan for the sustained development of the Bazaruto Archipelago, People's Republic of Mozambique, Oceanographic Research Institute, Durban, 13-16 & 31-32.

Ramsay P.J. (1990). A new method for reconstructing late Pleistocene coastal environments, Sodwana Bay, Zululand. SA Geological Survey Report, 1990-0227, 44 pp.

POPULAR PAPERS

Ramsay, P.J. (1988). A detailed look at Two-Mile Reef,Sodwana Bay. Underwater, 7, 7-8 & 26-27.

Cooper, J.A.G. & Ramsay, P.J. (1989). Diving in the Kosi Lakes. Underwater, 12, 46-47.

CONTENTS

PREFACE I

DEDICATION II

ABSTRACT III

ACKNOWLEDGEMENTS XI

AUTHOR'S PUBLICATION LIST XIII

CONTENTS XVI

CHAPTER 1

INTRODUCTION 1

CHAPTER 2

REGIONAL SETTING OF THE STUDY AREA 5

2.1 CLIMATE 5

2.2 OCEANOGRAPHY 7

2.3 GEOLOGICAL SETTING 11

CHAPTER 3

METHODS 23

3.1 FIELDWORK 23

3.1.1 Navigation 23

3.1.2 Echo-sounding survey 26

3.1.3 Side-scan sonar survey 26

3.1.4 Sampling and SCUBA diving observations 27

3.2 DATA REDUCTION 30

3.2.1 Track chart 30

3.2.2 Bathymetry 30

3.2.3 Side-scan sonar data 32

3.2.4 Sediment sample analysis 34

CHAPTER 4

SHELF BATHYMETRY & THREE-DIMENSIONAL REEF MODELLING 35

4.1 METHODOLOGY 35

4.2 SEAFLOOR MORPHOLOGY OF THE STUDY AREA 40

4.2.1 The northern shelf 40

4.2.2 The southern shelf 42

4.2.3 Submarine canyons 42

4.3 DISCUSSION 47

CHAPTER 5

SHELF SEDIMENTOLOGY BASED ON SIDE-SCAN SONAR INTERPRETATION 50

5.1 CONSOLIDATED LITHOLOGIES 52

5.1.1 Beachrocks and aeolianites 52

5.1.1.1 Sedimentary structures and features 58

5.1.2 Coral reefs 63

5.2 UNCONSOLIDATED LITHOLOGIES 68

5.2.1 Quartzose shelf sand 68

5.2.2 Bioclastic sediment 70

5.3 UNCONSOLIDATED SEDIMENTARY STRUCTURES 74

5.3.1 Subaqueous dunes 74

5.3.1.1 Outer subaqueous dune field 81

5.3.1.2 Inner subaqueous dune field 84

5.3.1.3 Ancient analogue for the subaqueous dunes 88

5.3.2 Hummocky and swaley structures 93

5.3.3 Ripples 94

5.3.3.1 Oscillatory ripples 94

5.3.3.2 Ladderback ripples 96

5.4 DISCUSSION 101

CHAPTER 6

PHYSIOGRAPHIC AND BIOLOGICAL ZONING OF CORAL REEFS 110

6.1 METHODS 112

6.2 REEF SETTING 112

6.3 REEF ZONING 113

6.4 APPLICATION OF THE TWO-MILE ZONING MODEL TO OTHER ZULULAND REEFS 127

6.4.1 Four-Mile Reef 127

6.4.2 Seven-Mile Reef 132

6.4.3 Other Sodwana Bay reefs 133

6.4.4 Red Sands Reef 134

6.5 DISCUSSION 136

CHAPTER 7

COMPUTER-AIDED REEF-BASE FACIES AND LITHOLOGICAL ANALYSIS 138

7.1 METHODS 138

7.2 PETROGRAPHIC ANALYSIS OF AEOLIANITE/BEACHROCK 139

7.2.1 Review of carbonate cementation and beachrock/aeolianite formation 146

7.2.2 Cementing history of the Sodwana Bay beachrock/aeolianite 149

7.3 PALAEOENVIRONMENTAL RECONSTRUCTION 150

7.3.1 Comparative reef-base settling analysis 151

7.3.2 Cluster and discriminant results 154

7.4 DISCUSSION 160

CHAPTER 8

SEA-LEVEL CHANGES, AEOLIANITE/BEACHROCK FORMATION, AND PALAEOCOASTLINE HISTORY 164

8.1 LATE PLEISTOCENE SEA-LEVEL CONTROVERSY 164

8.2 AEOLIANITE/BEACHROCK PALAEOCOASTLINE EPISODES 166

8.3 LATE PLEISTOCENE AND HOLOCENE HISTORY OF THE SHELF 170

REFERENCES 178

APPENDIX 202

MAP 1 - BATHYMETRY OF THE SODWANA BAY CONTINENTAL SHELF, NORTHERN ZULULAND

MAP 2 - SEDIMENTOLOGY OF THE SODWANA BAY CONTINENTAL SHELF INTERPRETTED FROM SIDE-SCAN SONAR IMAGERY

CHAPTER 1: INTRODUCTION

This thesis is the first detailed sedimentological study to be undertaken on the northern Zululand shelf and deals with diverse research topics such as shelf morphology, shelf sedimentology, biology of coral reefs, computer facies analysis of submerged coastlines, and late Pleistocene to Holocene sea-level changes and coastline evolution. In the past, studies along this coastline have been more superficial or on a regional basis and have not attempted to describe or understand the physical processes which operate on the northern Zululand shelf. This thesis represents a synopsis of data collected by the author over a period of 5 years beginning in January 1987. The maps enclosed also represent the only accurate maps to have been produced of the Natal or Zululand shelf.

The research area is located 300km north-northeast of Durban and comprises a 59km^2 section of the northern Zululand continental shelf, from 3km south of Jesser Point (Sodwana Bay) to Gobey's Point (Fig. 1.1). Sodwana Bay falls into the St Lucia Marine Reserve and is a protected natural area administered by the Natal Parks Board. This reserve is bounded by Cape Vidal in the south and White Sands in the north, and extends three nautical miles seaward. Eighty thousand recreational SCUBA dives are undertaken each year on the coral reefs around Sodwana Bay and in recent years Sodwana Bay has become a very popular tourist resort. The popularity of the area has necessitated the development of an integrated management plan for the area based on predicted tourism growth rates. The bathymetry and side-scan sonar maps of the shelf in this area are an extremely valuable asset to the Natal Parks Board environmental management strategy for the St Lucia Marine Reserve. These maps are used to define areas of low- and high intensity use and areas of restricted access, and show an accurate distribution of coral reefs along this coastline. These maps are also used by the Natal Parks Board, in conjunction with a Global Positioning System (GPS), to locate skiboats found contravening the marine reserve regulations. The maps play an important part in the successful prosecution of law-breakers in the area, by allowing NPB personnel to define the offenders position within the Marine Reserve.

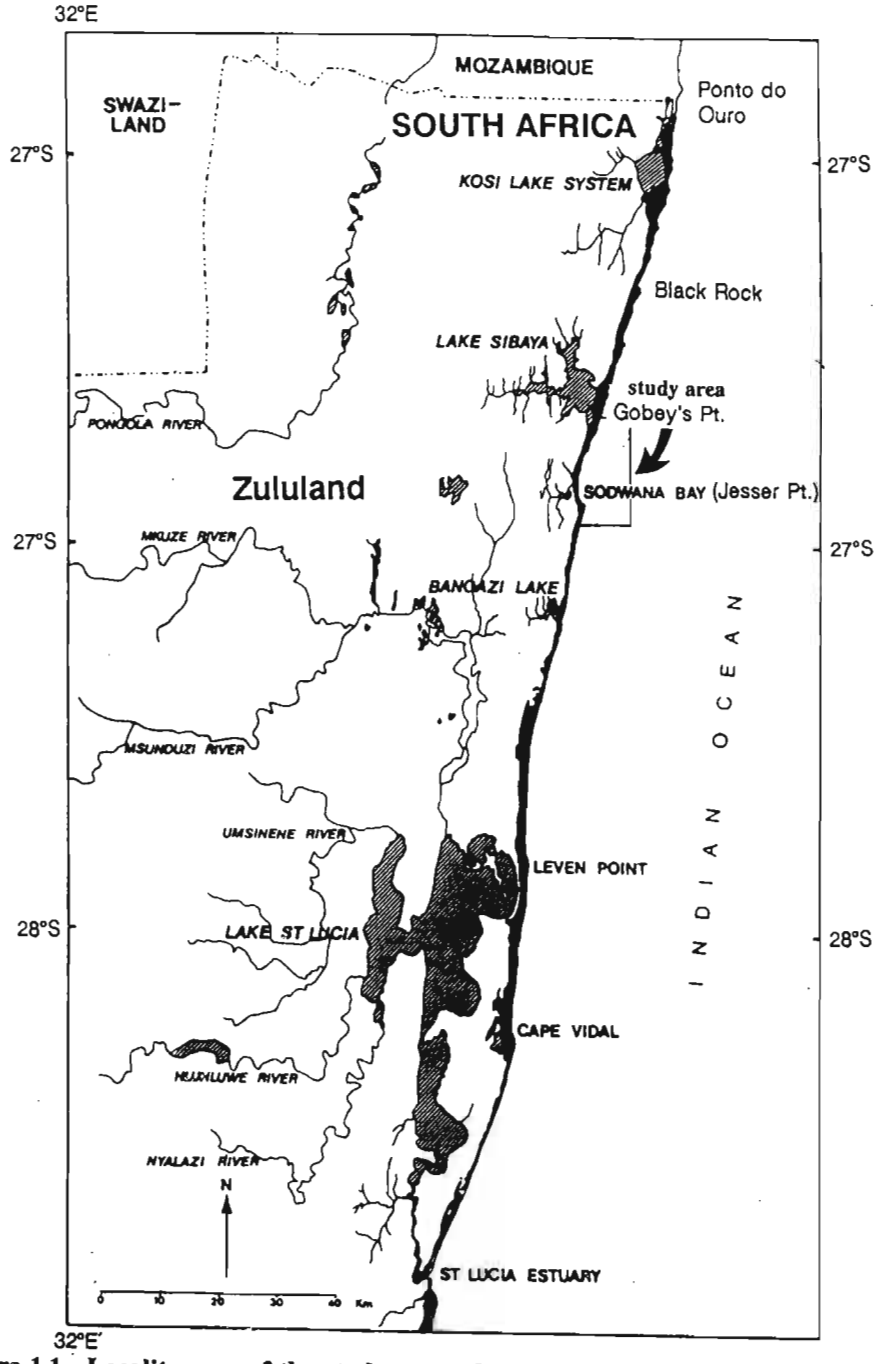

Figure 1.1. Locality map of the study area. Coastal dune forest is indicated in black.

The aims of this study were:

1) to produce accurate bathymetric and sedimentological maps of the Sodwana Bay shelf and to understand the processes operating on the shelf;

2) to describe the coral reefs in the area and formulate a physiographic and biological zoning scheme for these reefs;

3) to develop a method to define the facies associations of the submerged, carbonate-cemented, coastal sandstone sequences on the shelf;

4) to define the palaeocoastline episodes which formed the submerged, coastal sandstones and describe the late Pleistocene and Holocene evolution of the shelf.

The study commences with discussion of the regional setting of the area followed by a description of data-collection methods and data analysis. Certain detailed data-analysis procedures are dealt with at the beginning of the relevant chapters. Seafloor morphology and shelf zones are described using the bathymetric data base together with a discussion on submarine canyon morphology, classification, and mode of formation. A three-dimensional computer-generated reef model and a shelf model were produced from various data sources. The Sodwana Bay shelf has yielded a unique assemblage of sedimentological features produced by the dominant hydrological processes which control shelf sedimentation. The sedimentology was based on an interpretation of side-scan sonar imagery and extensive ground-truth SCUBA diving observations and sampling. Shelf sediments are described as unconsolidated- and consolidated subdivisions; followed by an explanation of the sedimentary structures on the shelf. A zonation scheme was devised for the northern Zululand coral reefs based on physiographic and biological criteria. Computer-aided facies analysis techniques were used to define coastal facies units of carbonate-cemented, sandstone outcrops on the shelf. A late Pleistocene

and Holocene history of the area is proposed, dealing with sea-level changes related to the palaeocoastline episodes observed on the shelf.

CHAPTER 2: REGIONAL SETTING OF THE STUDY AREA

2.1 CLIMATE

According to the Köppen Classification (Boucher, 1975), the climate of the Natal coastal belt is given the symbol Ca as it has a humid sub-tropical climate with a warm summer; this climatic zone being dominated by the southern sub-tropical high-pressure belt (STHP) (Hunter, 1988). The now abandoned Lake Sibaya Research Station (operational from 1973 to 1977) was the closest weather station to Sodwana Bay, therefore these climatic data, where available, were used in preference to other weather stations further south along the coastline (data summarised from Van Bruggen & Appleton, 1977; Allanson, 1979; & Maud, 1980).

Figure 2.1 depicts average, seasonal wind roses for Cape St Lucia, 98km south of the study area. The coastline trends roughly north-northeast/south-southwest, and the dominance of coast-parallel winds is apparent (Hunter, 1988). North to northeasterly winds dominate the December wind rose while the June wind rose demonstrates a rough balance in frequency between southerly and northerly winds (Fig. 2.1; Hunter, 1988). Data from Voluntary Observing Ships (VOS) show that southwesterly through to southerly winds generally have the highest speeds (Hunter, 1988). The Agulhas Current gives the region an enhanced land breeze circulation offshore, and there may be a link between this circulation and the initiation of convection both over the Agulhas Current and, at times, over the coast (Hunter, 1988).

Rainfall along the Maputaland coast averages 1 000-1 100mm annually, but this declines progressively westward (inland) to only 600mm at the base of the Lebombo Mountains (Maud, 1980). The Lake Sibaya weather station recorded annual rainfalls of 1 130mm and a mean annual temperature of 21.6°C (in 1976) varying from 11.5°C in July to 28.7°C in January. The air temperature in the region

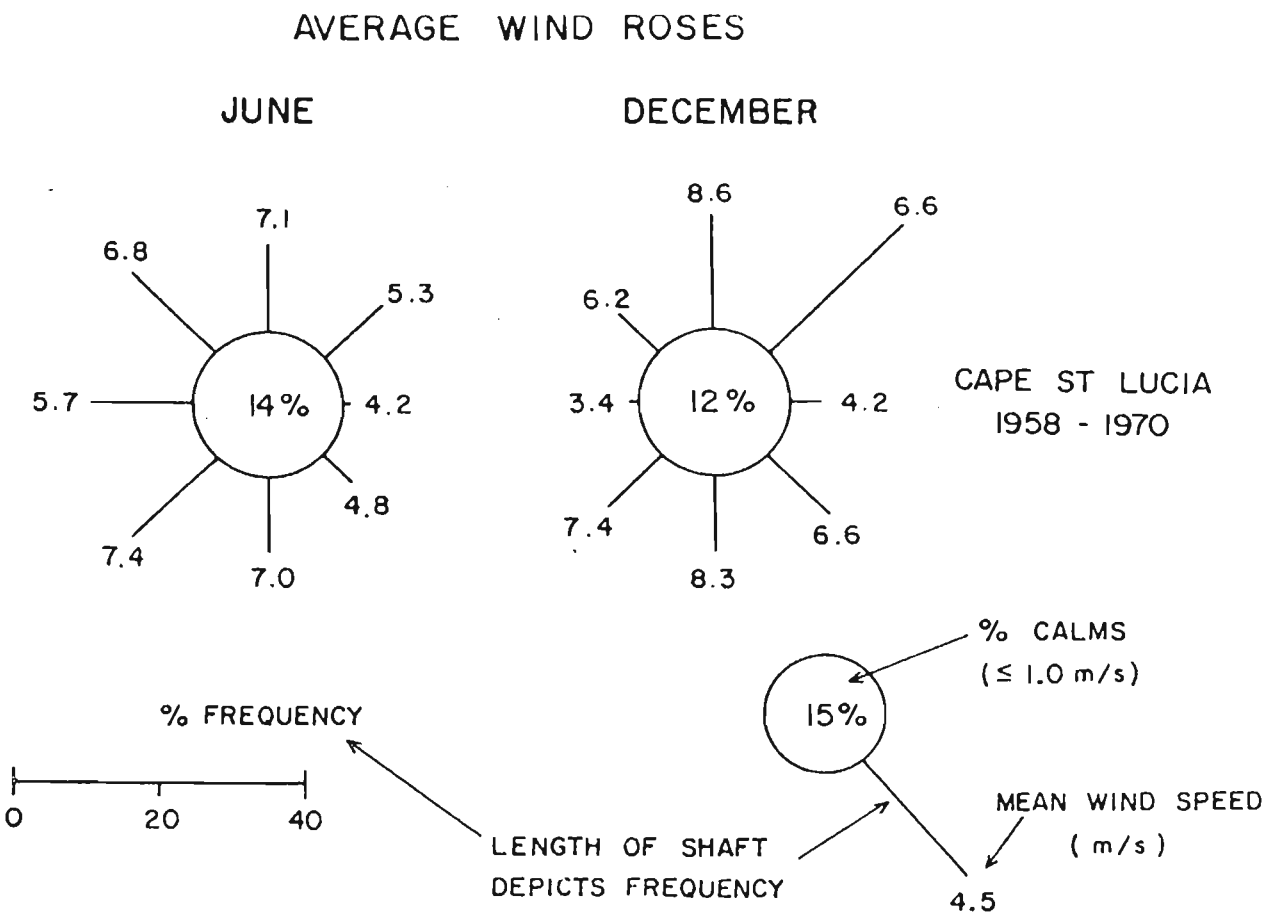

Figure 2.1. Average wind conditions at Cape St Lucia for June and December over the period 1958-1970. (From Hunter, 1988).

is characterised by a relatively low seasonal range which is due to the damping effect of the adjacent ocean (Hunter, 1988). Relative humidity shows maximum and minimum values of 88% and 56% respectively for the winter months of 1973, the comparable summer month values for the same period being 83% and 60%. The evaporation rate measured in a Symons Tank averaged 4.1mm per day.

Monthly mean atmospheric pressures are significantly higher in winter than in summer. This is due to an increase in the average intensity of migratory highs which also track closer to the Natal coast during the winter months (Hunter, 1988). VOS reports give an absolute minimum pressure of 992 mb offshore, with an absolute maximum near 1 040 mb (Hunter, 1988).

The occurrence of tropical cyclones threatening northern Natal is not a common one, although cyclones in 1984, 1987 & 1988, during the months of September to February, caused extensive wave and flood damage (Hunter, 1988). The author witnessed the effects that the 1987 and 1988 cyclones had on the coastline and offshore reefs. These cyclones were responsible for short duration, heavy rainfalls exceeding 400mm south of the study area and 10m swells at sea (Hunter, 1988). Maud (1980) noted that cyclonic rainfall on the Maputaland coastline accounted for 700mm of rainfall in 3 days in early 1976. These tropical cyclones develop northeast of Madagascar between November and April, with an average of one each year affecting the southern Mozambique coast and Maputaland (Hunter, 1988).

2.2 OCEANOGRAPHY

The most important large-scale oceanographic feature in the area is undoubtedly the Agulhas Current (Schumann, 1988). It is generally accepted that this western boundary current forms off the northern Natal/Mozambique coast, from the confluence of waters which follow complex paths in the Mozambique Channel and areas south of Madagascar (Lutjeharms, Bang & Duncan, 1981; Gründlingh & Pearce, 1984; Saetre & Da Silva, 1984; Fig 2.2). The Agulhas Current is recognised as one of the

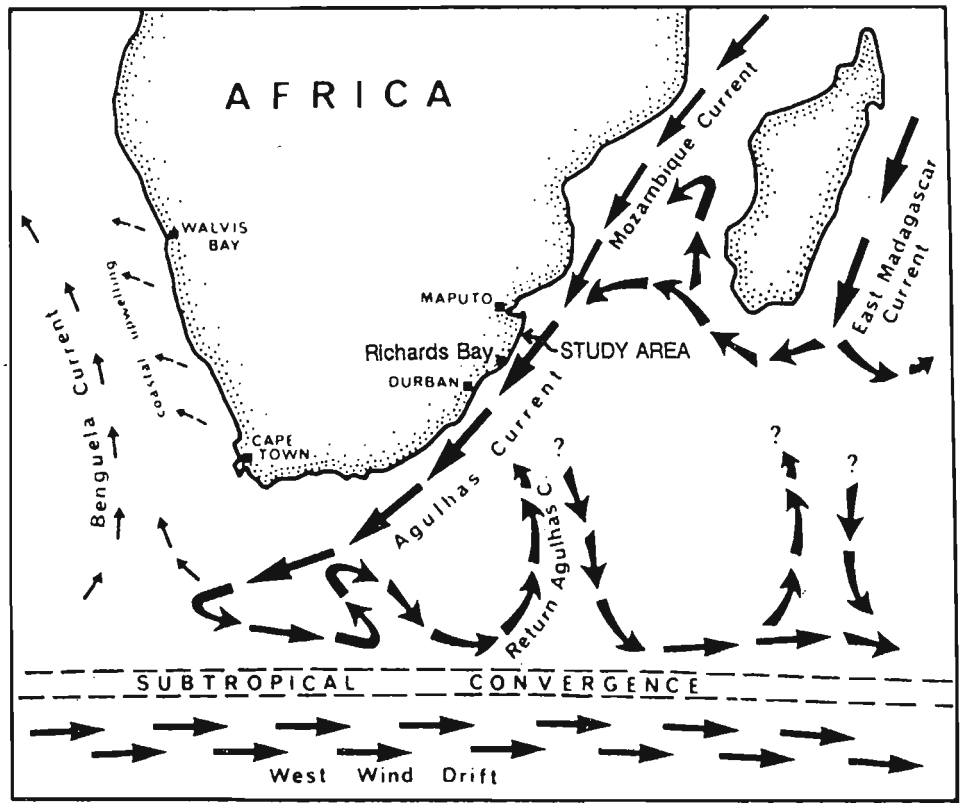

Figure 2.2. The regional setting the Agulhas Current system. (From Flemming, 1981).

world's major currents, and sweeps polewards with a core generally just offshore of the shelf break; this markedly affects the waters on the shelf (Schumann, 1988). Bang & Pearce (1978) found the mean width of the Current to be about 100km and there appears to be no distinct seasonal variation in the volume flow (Schumann, 1988). The daily variability of the Current masks any seasonal variability that may be present (Schumann, 1988).

Figure 2.3 shows the seasonal variabilities in temperature and salinity in the water column on the inner- and outer-shelf off Richards Bay, 150km south-southwest of the study area. In the shallower, inshore regions there is a about a 4°C temperature decline from summer to winter, with a maximum of about 25°C in February (Schumann, 1988). There is also a fairly uniform vertical temperature structure, indicating a well-mixed regime (Schumann, 1988). Further offshore there is also a 4°C temperature decline from summer to winter in the upper 50m of the water column, with maximum temperatures greater than 26°C (Schumann, 1988). There does not appear to be a distinct thermal gradient on the inner boundary of the Current (Schumann, 1988). The author has recorded water temperature extremes in the study area of 18°C in September (spring) and 28°C in February (summer). Figure 2.3 indicates that salinity variations are not as conspicuous, although there is evidence of lower salinity water over the shelf in late summer (Schumann, 1988). Pearce (1978) analysed the same data from Figure 2.3 and found an annual temperature range of 4.8°C, with the inshore water being 1.4°C cooler than that at the shelf break. He postulated that water in the -40m to -60m layer at the shelf break moves shorewards along an appropriate sigma-t surface in a mild but continuous upwelling process. The author has noticed a thermocline at -45m in submarine canyon heads with temperature extremes being 20°C at the bottom and 28°C 5m above the sea floor: this is probably related to minor upwelling along canyon axes.

As a consequence of a narrow shelf in the study area, the Agulhas Current flows close inshore and can attain velocities of up to 3m/sec (Martin, 1984); however, Schumann (1988) quotes a maximum speed

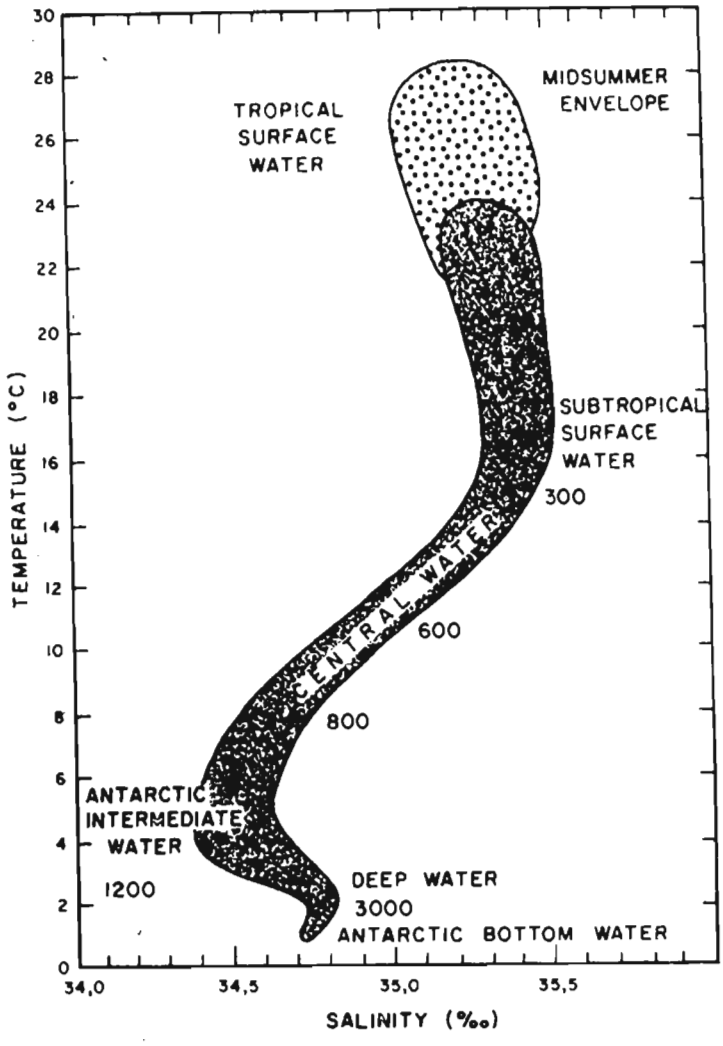

Figure 2.3. Temperature/salinity distribution of values measured off the southeast coast of Southern Africa. Water types are given, along with approximate depths (in metres) where such water is commonly found. (From Schumann, 1988).

of approximately 1.5m/sec. Satellite imagery has revealed the existence of an eddy situated offshore of Maputo. It is probable that the northern Natal shelf is not as strongly influenced by the Agulhas Current as the southern portion of the Natal coast. Harris (1978) found the percentage of northeastward currents increased to the north. However, current velocities tended to be less than 0.25m/sec, while those of southwestward currents generally exceeded 0.5m/sec.

The tidal range in the area averages 2m (Schumann & Orren, 1980) and the coast is therefore high microtidal (Davies, 1964) or low mesotidal (Hayes, 1979). Microtidal coasts typically show a narrow and steep beach profile with offshore bars and an offshore-fining trend (Reineck & Singh, 1973; Leeder, 1982): this is typical of the Zululand coastline. The coast is dominated by persistent high-energy waves and prevailing large-amplitude swells from the southeast (40% of the year) (Begg, 1978; Swart & Serdyn, 1981; Rossouw, 1984; Van Heerden & Swart, 1986; Fig. 2.4 & 2.5) with northeasterly to easterly onshore swells prevailing for a further 40% of the time (Van Heerden & Swart, 1986). There is negligible influence of the seasons on wave directional distributions (Rossouw, 1984). Subordinate low-amplitude, short-period, northeasterly swells are formed when a northeasterly wind blows. Under these conditions the smaller northeasterly swell is superimposed on the southeasterly swell. Only when a northeasterly wind blows for a considerable period does it become the dominant swell direction (Ramsay et al., 1989).

2.3 GEOLOGICAL SETTING

The Zululand coast extends for 320km south-southwest from Ponta do Ouro on the Mozambican/South Africa border to the Tugela River mouth and the area between Cape Vidal and Ponta do Ouro is oriented 010° to 020°. The northern Zululand coast is characterised by a linear, clastic, sandy shoreline which receives little sediment input from non-marine sources (Cooper, 1991). The long barrier beaches, of Holocene age, are backed by well-vegetated Pleistocene and Holocene sand dunes

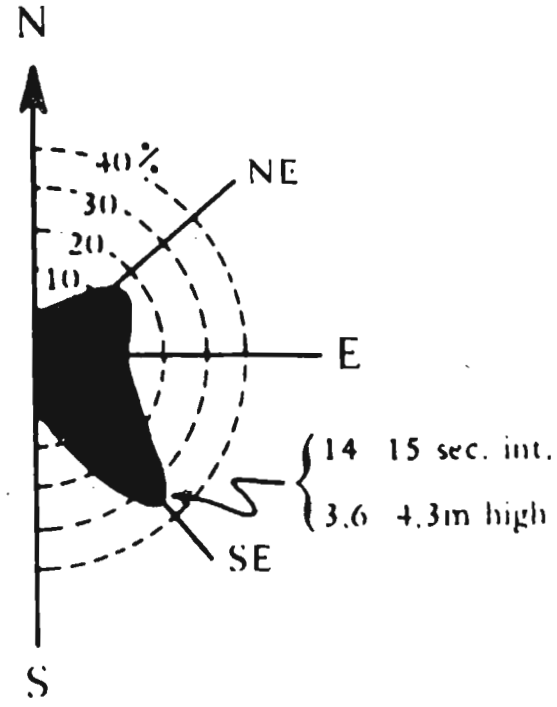

Figure 2.4. Swell observations (direction and height) at Cape St Lucia. (After Begg, 1978).

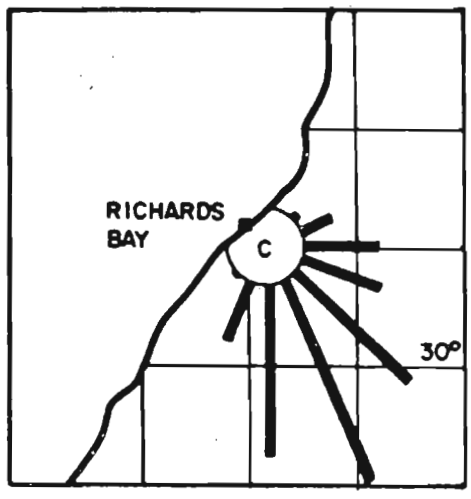

Figure 2.5. Wave direction distribution recorded from deepsea clinometer data for the Richards Bay area. (After Rossouw, 1984).

up to 180m high, behind which lie extensive swamps, lagoons and old dune ridges (Orme, 1973). The Holocene dune barrier has grown in response to high energy and material transfer during and since the Flandrian transgression (Orme, 1973). Older nearshore sediments, dune sands, and swamp deposits indicate Pleistocene sea-level oscillations across this coast, and show that the present barrier is superimposed upon the remnants of a major Pleistocene barrier system represented by the Port Durnford Beds (Orme, 1973; Hobday, 1979). Maud's (1980) geological cross-section of the northern Zululand coastal plain is presented in Figure 2.6.

During late Pleistocene times, the glacial maximum low produced a sea-level at least -100m below the present level (Zeuner, 1959; Fairbridge, 1961; Maud, 1968; Shepard, 1963; Curray, 1965; Mörner, 1971; Siesser, 1972a; Orme, 1973; Bloom et al., 1974; Chappell, 1983), and probably as low as -130m (Milliman & Emery, 1968; Shackleton & Opdyke, 1973; Chappell, 1974; Tankard, 1976; Williams et al., 1981; Hails, 1983). This caused rivers to rejuvenate, cutting through earlier deposits and spreading a blanket of reworked marine, fluvial and aeolian sands across the continental shelf. The shallow Zululand shelf (< -65m) has thus been subaerially exposed for most of the Quaternary. Onshore, weathering and eluviation transformed the Pleistocene sands in the vadose zone into red and grey clayey sands, but in the phreatic zone calcareous cementation transformed similar sands into aeolianite and beachrock (Orme, 1973). During the Holocene transgression the sea submerged these cemented aeolianites and beachrocks to form the base of modern coral reef structures (Ramsay, 1990a).

The continental shelf is narrow in the area, approximately 3km wide with a shelf break between -45m to -70m (Flemming 1981, Martin & Flemming, 1986; Fig. 2.7) and owes its origin to transform fault systems (Martin, 1984; Fig 2.8). Rugged, linear aeolianite shoals are some of the most prominent features on the Natal shelf (Martin & Flemming, 1988; Fig 2.9). The presence of several semi-continuous beachrock and aeolianite zones both on the shelf (Martin & Flemming, 1988; Ramsay

1990a; Ramsay & Mason 1990a) and onshore (Hobday, 1976; Cooper & Flores, 1991) indicates that several phases of beachrock formation have occurred during the Pleistocene sea-level fluctuations (Cooper, 1991). The approximate volume of beachrock along the shoreline is 120 000 m^3/km (Cooper,

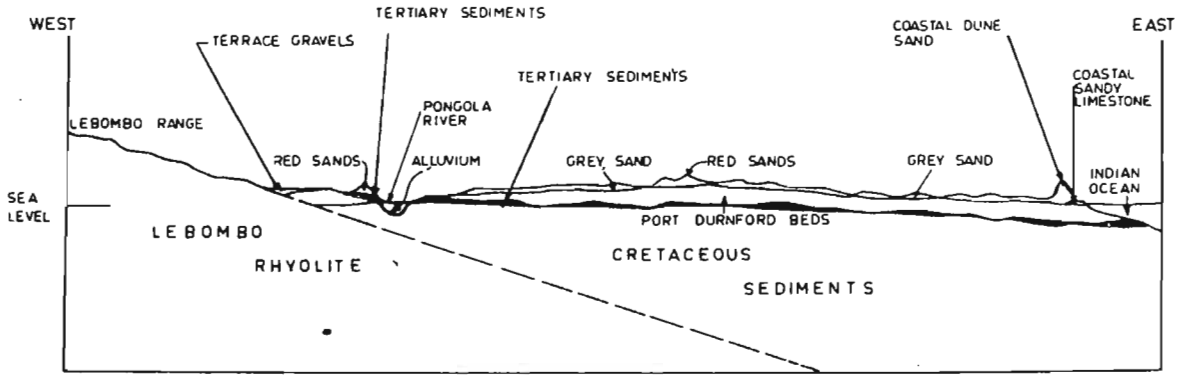

Figure 2.6. Schematic geological cross-section of northern Zululand (not to scale). (From Maud, 1980).

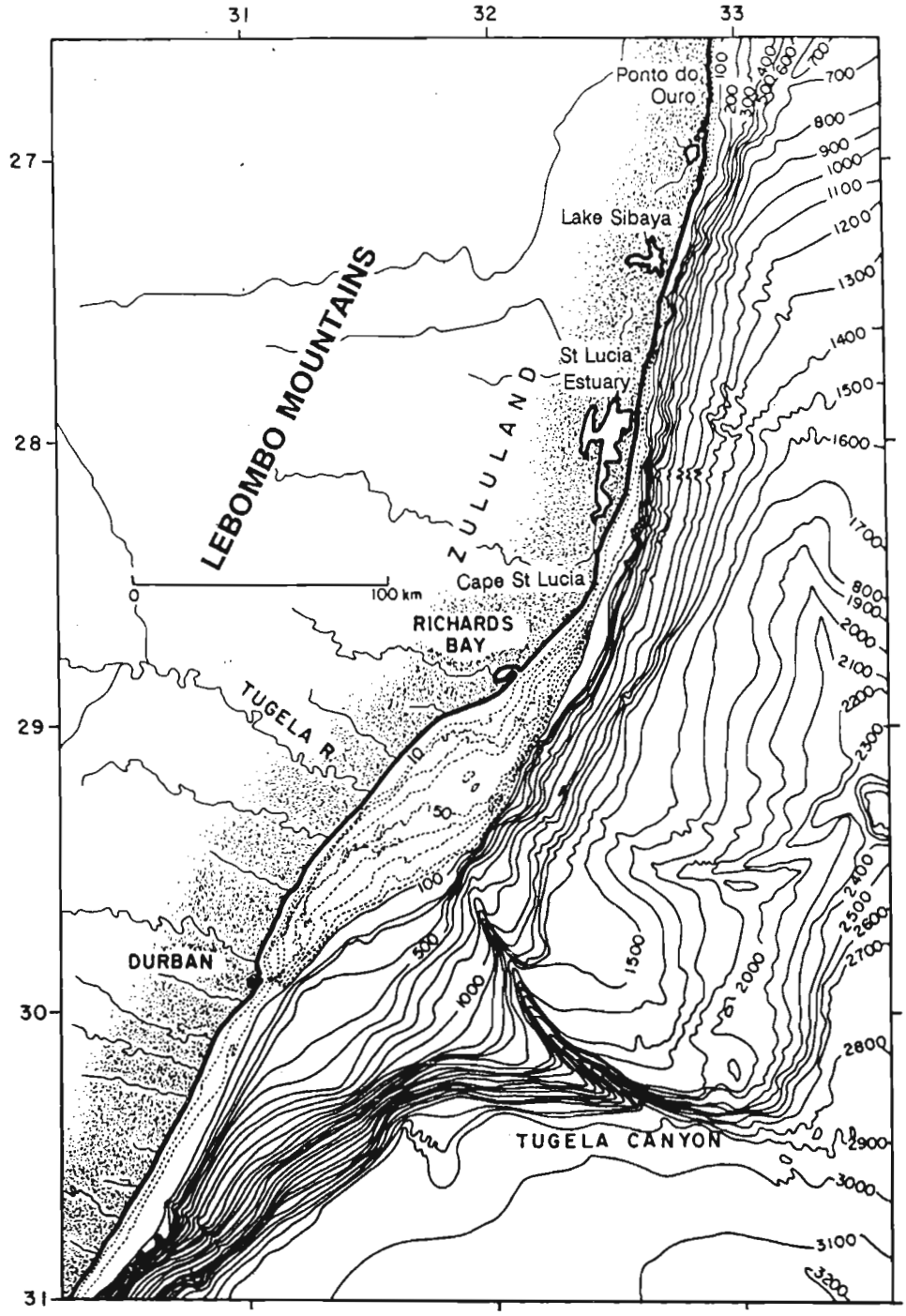

Figure 2.7. Bathymetry of the continental margin, with isobaths in metres. (From Martin & Flemming, 1988).

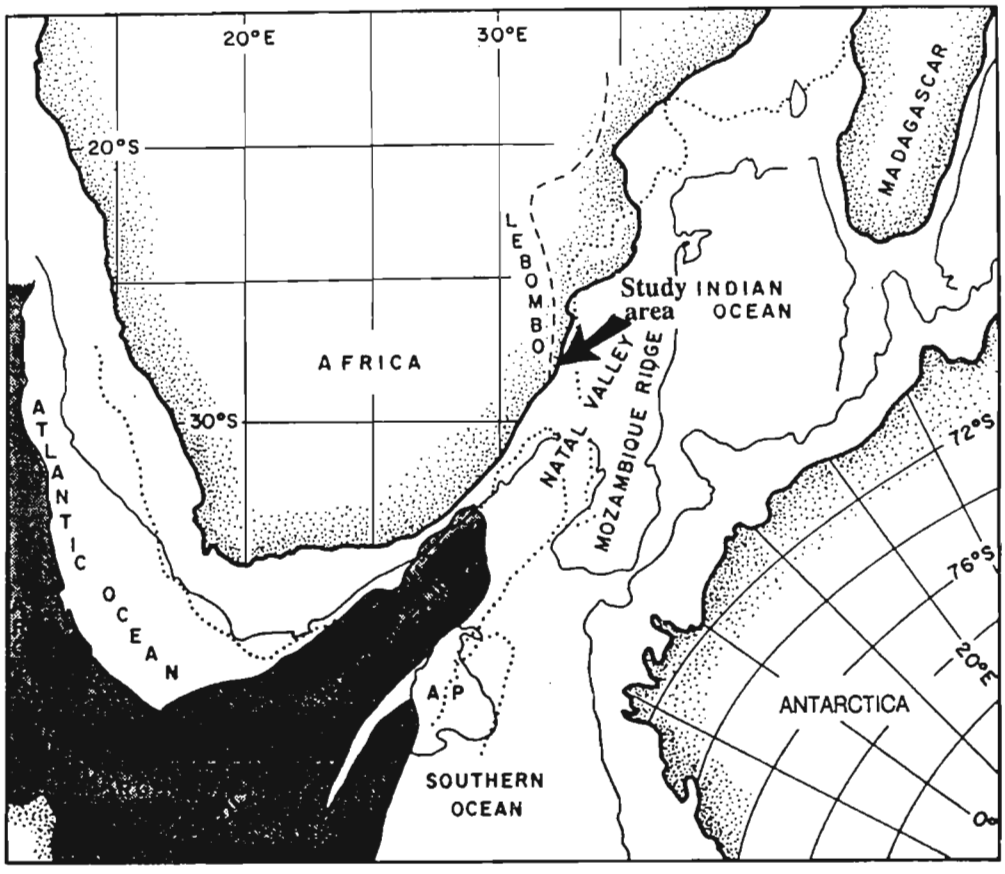

Figure 2.8. A reconstruction of Africa, Madagascar, Antarctica, and South America as they were at the time of sea-floor spreading magnetic anomaly M2 (123 Ma); each continent is outlined by the 3 000m isobath. Dotted lines mark the 3 000m isobaths of South America, the Falkland Plateau, and East Antarctica in their pre-break-up positions, prior to 153 Ma. A.P. = Agulhas Plateau. (From Martin & Flemming, 1988).

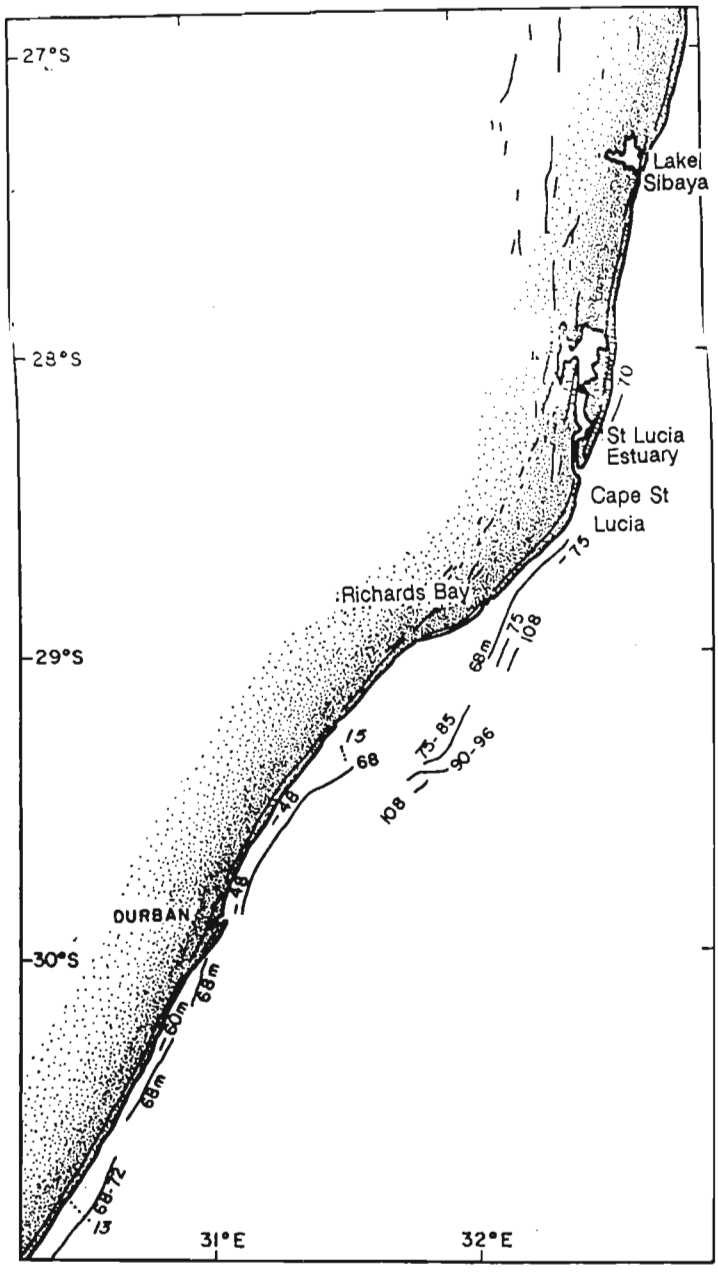

Figure 2.9. Pleistocene aeolianite cordons of the Natal continental shelf mapped from over 5 000km of seismic profiles. The numbers refer to the dune cordon base depth which marks the inferred sea-level. (From Martin & Flemming, 1988).

1991). Onshore and offshore aeolianites extend from Mozambique to the western Cape (McCarthy, 1967; Maud, 1968; Siesser, 1974; Coetzee, 1975a&b; Davies, 1976; Birch, 1981; Flemming, 1981; Barwis & Tankard, 1983; Martin & Flemming, 1986). Maud (1968) relates the northeast-trending reefs off the Zululand coast to the 'first aeolianite' although, in the author's opinion, they are probably better compared to his description of the 'third aeolianite' which formed during the major regression, during the late Pleistocene, leading to the Last Glacial Maximum. On the south coast of South Africa, observations by SCUBA divers and on-land fieldwork shows that the aeolianites are associated with beach, wash-over fan, lagoonal and estuarine facies, pointing to their formation as coastal dunes associated with barrier beaches (Martin & Flemming, 1986). Re-evaluation of micropalaeontological data (McLachlan & McMillan, 1979) and available ^{14}C-dates (Deacon, 1966; Barwis & Tankard, 1983) suggest formation of these shoals during the last interglacial between 120 000 and 30 000 years ago (Martin & Flemming, 1988).

The present sea-level stillstand is responsible for the formation of the series of broad, marine, intertidal beachrock platforms which are intermittently present along the Zululand coastline (Coetzee, 1975a&b). During spring low-tides the planed platforms are completely exposed and the horizontal surfaces are covered with marine organisms. The platforms are characterised by slightly "raised rims" on their outer edges followed by broad intermediate benches (Fig. 2.10, Black Rock). At low-tide the water surges over the rim to form shallow pools on the platforms. The seawater in these shallow intertidal pools dissolves $CaCO_3$ during the night due to a drop in temperature causing a reduction in pH and increase in the $CaCO_3$-solubility product (Coetzee, 1975b). The raised rims escape solution (as well as mechanical wave erosion) as they are protected by a hard, dense encrustation of Lithothamnion algae. The existence of the raised rims is therefore a product of differential solution on the platform rather than of upward growth of the organisms (Coetzee, 1975a). Guilcher (1988) relates the algal encrustation around incipient rimmed pools on intertidal calcareous outcrops in Morocco, Madagascar, and the Society Islands to Porolithon and not to Lithothamnion.

Coral patch reefs are common on this coastline and owe their existence to clear, warm water carried southward by the warm water Agulhas Current and the absence of silt-carrying rivers in the coastal hinterland. These reefs are the most southerly in Africa and are thoroughly documented by Ramsay (1987), Ramsay (1988), Ramsay et al. (1989), Ramsay (1990a&b), Ramsay & Mason (1990a&b), and Williams (1989a&b).

Along this coast a number of steep-sided submarine canyons begin at depths of -30m to -40m within 1 or 2km of the shore and plunge to -650m within 8km of the shore. Bang (1968) lists six prominent canyons between St. Lucia and Lake Sibaya, although the author has discovered 13 such canyons on geophysical sea-cruises during 1990. The origin of these canyons is not related to the position of modern river mouths but can probably be linked to palaeo-outlets of the Pongola and Mkuze River systems (Orme, 1973 ; Hill, 1975; Wright, 1990). Sydow (1988) suggests that the canyons are mass-wasting features which have later been exploited by palaeo-drainage during regressions.

Continuity of the modern, open sandy beaches along the Zululand coast attest to the abundance of beach-forming materials and to the powerful onshore and alongshore movement of these materials throughout the coastal zone (Orme, 1973). The beaches are composed predominantly of medium- to coarse-grained quartz sand with significant heavy mineral concentrations of ilmenite, rutile and zircon (Orme, 1973). Beach sediment supports foreshore slopes of 7-12° and backshore slopes of up to 4°; the steeper foreshore slopes correlate with increased moisture content. The mean beach width is approximately 60m (Cooper, 1991), with berm elevations reaching ±2m above mean sea-level (Orme, 1973). At intervals along the coast, blowouts occur in the vegetated Holocene dune; one of the largest lies 10km north of Sodwana Bay and is colloquially known as "White Sands" (Fig. 2.11).

The southeasterly swell regime leads to a net northward longshore drift capable of transporting 1 x 10^6 m^3 of sediments per year (Van Heerden & Swart, 1986). Littoral drift is predominantly toward

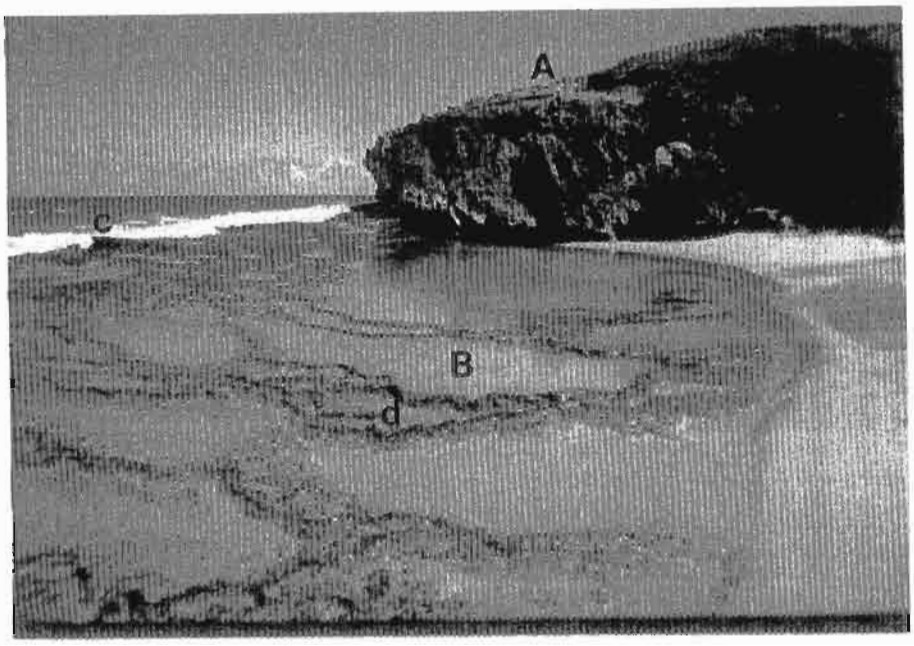

Figure 2.10. Carbonate-cemented aeolianite (A) overlying an intertidal beachrock outcrop (B) with a "raised ridge" (c) and "raised rims" (d).

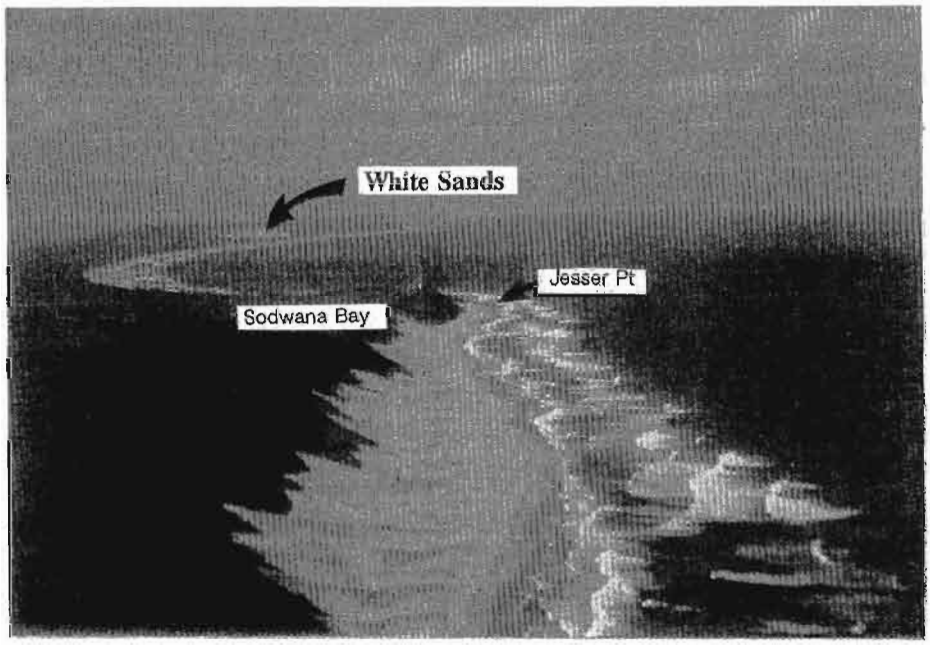

Figure 2.11. Oblique aerial photograph, looking north, of the log-spiral curve bay at Sodwana. Note the transverse dune field in the foreground.

Figure 2.12. View of Sodwana Bay looking south across the intertidal beachrock outcrop at Jesser Point and Mgobezeleni estuary.

the north and intertidal beachrock ledges serve to trap beach sediments on their southern or updrift side while allowing erosion on the downdrift side (Orme, 1973). This leads to the development of small log-spiral curve bays along the coastline (Fig. 2.11). Cooper (1991) refers to these embayments as zeta bays. These embayments produce a series of coastal cells in quasi-equilibrium and this reduces longshore drift to a minimum (Cooper, 1991).

CHAPTER 3: METHODS

Geophysical data were collected on the continental shelf between Leven Point and Gobey's Point on two separate cruises over the period 1990-1991 on the RV *Benguela* (Fig. 3.1) and the research skiboat *Geocat* (Fig. 3.2 & 3.3). The data collection involved bathymetric profiling, side-scan sonar seafloor mapping and shallow-penetration seismic profiling (pinger seismics). Most of the survey lines were oriented coast parallel to obtain the maximum coverage of coast parallel geological features previously identified by the author on numerous diving surveys. Two lines were run coast perpendicular to obtain bathymetric profiles of one submarine canyon and across the major subaqueous sand dune field. The seismic profiling data has not been included in this thesis.

The research vessels' statistics are outlined below:

VESSEL	RV *BENGUELA*	*GEOCAT*
OWNERSHIP	Sea Fisheries Research Institute	SA Geological Survey
LENGTH	44m	6.4m
DRAUGHT	3m	0.5m
TONNAGE	560 T	2 T
TRANSDUCER DEPTH	3m	0.5m (1991)

3.1 FIELDWORK

3.1.1 Navigation

Position fixes were made using a Global Positioning System (GPS) receiver (JRL 4200 GPS system) and corrected to the Cape Datum. A GPS system receives positioning data on the geodetic datum WGS 84, which requires a correction to be made to standardise the data to the South African geodetic

Figure 3.1. The Research Vessel *Benguela* used for the geophysical surveys on the Sodwana Bay shelf.

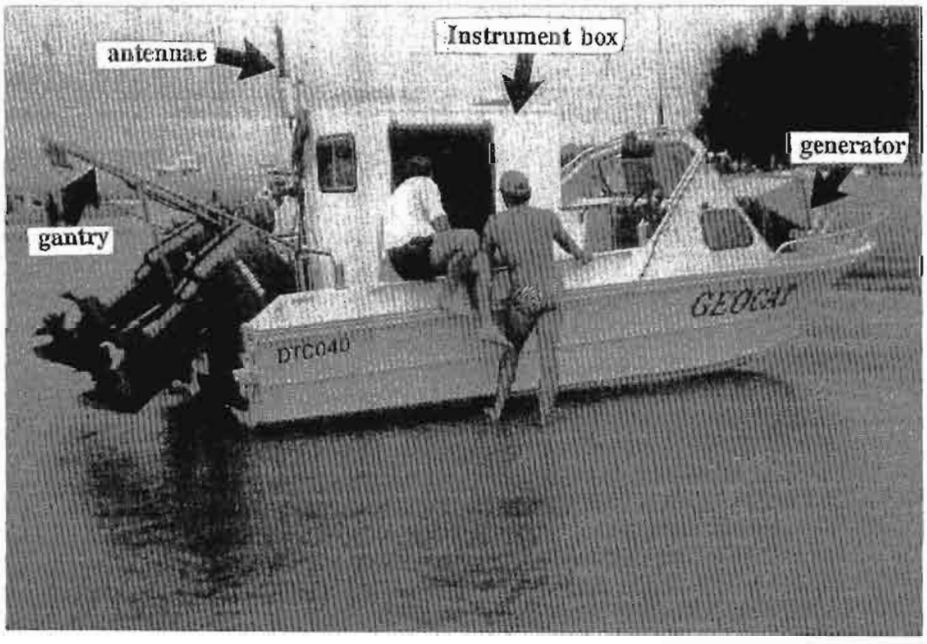

Figure 3.2. The skiboat *Geocat* used to undertake inshore side-scan sonar and bathymetric surveys.

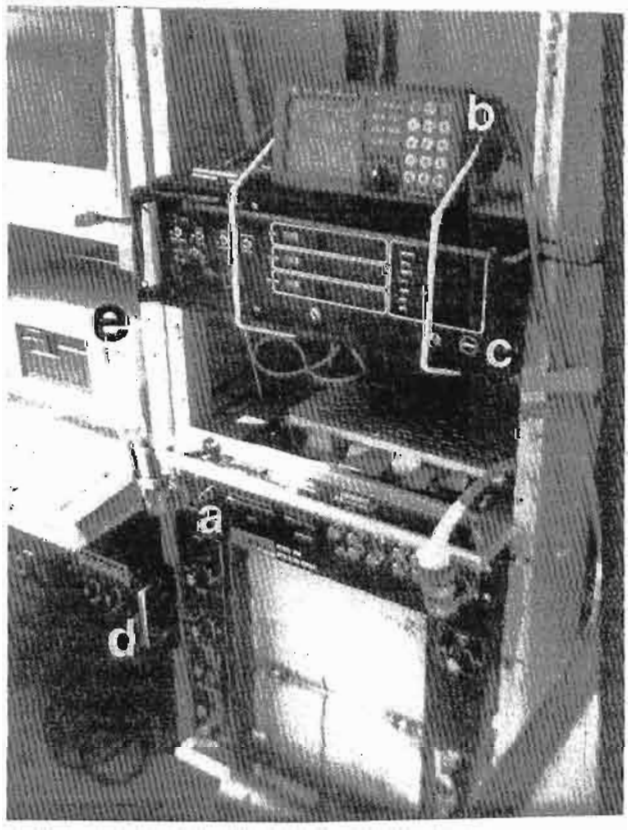

Figure 3.3. A view of the instrument box on *Geocat*. Instruments include: side-scan sonar recorder (a), GPS (b), MRD-1 Tellurometer (c), digital echo-sounder (d), and computer (e).

datum (Cape Datum). WGS 84 positioning data were corrected to the Cape Datum by applying a latitude and longitude correction factor. The correction factor applied to the Sodwana Bay navigation data was:

WGS 84 latitude - 1.7"

WGS 84 longitude + 0.8"

The accuracy of the GPS in the dynamic mode was tested by placing marker buoys at specified co-ordinates using the GPS, these points were triangulated using two theodolites stationed on the shore on top of benchmarks co-ordinated by the Kwa-Zulu Department of Works. The mean accuracy for 25 points between the GPS position and the triangulated position was 48m with the most accurate being 8m.

The positioning data were downloaded, at 30 second intervals via an RS 232 serial port interface, to an IBM-compatible AT computer. The computer runs a specially designed, integrated survey system package developed by the Institute of Maritime Technology (IMT), Simon's Town. This program allows the user to define the survey track line parameters on the computer, these are then displayed on the computer screen. The position of the research vessel is also displayed on the screen via the GPS, thereby making it a comparatively easy job for the helmsman to keep the vessel on the predetermined survey track lines. The program also converts the geometrical co-ordinates (latitude & longitude) to Lo 33° System (Longitude Origin) on the Cape Datum. Lo co-ordinates are practical for local surveys, because the X- and Y-axis scales are equal (orthogonal) making it easy to measure distance and calculate scales (De Decker, 1987).

For the above-mentioned surveys the track lines were defined as coast-parallel lines with a line spacing of 250m. This covered the continental shelf between the -5m and the -100m isobaths.

3.1.2 Echosounding survey

The data for the bathymetry map were taken from records obtained with a hull-mounted SIMRAD Model EK 120 scientific echosounder on the RV *Benguela* and a 12 Khz ELAC digital echosounder on the skiboat *Geocat*. The paper chart output from the SIMRAD sounder was annotated every 10 minutes. The output from the digital echosounder was downloaded into the integrated survey system package on an AT computer together with the time and position fix. A total of 226km of bathymetric lines were accumulated in this way on the Sodwana Bay shelf.

3.1.3 Side-scan sonar survey

The side-scan sonar survey lines were undertaken at a scan range of 150m with a line spacing of 250m; this resulted in a 33% overlap of adjacent swathes. This overlap give a degree of leeway for vessel divergence from the predetermined survey line. The instrument used was an EG & G Model 260 image-correcting side-scan sonar with a Model 272-T Saf-T-Link 105 kHz tow-fish attached to a 600m Kevlar cable. The selection of a scan range of 150m resulted in a scale factor on the isometric record of 1 to 1500. The records were annotated every 10 minutes and the ship's speed manually corrected on the recorder from the speed-over-ground reading displayed by the GPS. The survey speed varied from 3.5 to 5.5 knots with an average of 5 knots; this is well within the speed specifications to obtain high-quality records. Tow-fish height off the bottom was kept at the optimum of approximately 20% of the range setting or 30m above the seafloor as recommended by the EG & G manual (1986). In shallow water, such as over the reef-crests, the tow-fish height was raised to avoid collision with the seabed. A total of 18 coast-parallel side-scan sonar lines, amounting to a total distance of 188km, were collected on the shelf off Sodwana Bay: an area of 59km^2 was insonified by side-scan sonar.

3.1.4 Sampling and SCUBA diving observations

The shelf off Sodwana Bay lends itself very well to SCUBA diving scientific observations and photography due to the warmth of the water and the extremely good underwater visibility encountered most of the year round. Underwater visibility of 30-40m is common and visibility of 50m has been encountered; the visibility is seldom less than 15m.

Thirty five unconsolidated sediment samples, from depths of -15m to 240m, were collected using a SHIPEK grab on the RV *Benguela* cruise. This was supplemented by the collection of 36 unconsolidated sediment samples during numerous SCUBA and snorkel dives (approximately 250) over the period January 1987 to February 1991. The position of 59 samples used in this thesis are located on Figure 3.4. A team of three scientific divers and backup in an inflatable craft or ski-boat sampled unconsolidated sediment and consolidated lithologies and collected data pertaining to seafloor geology and biology (Fig. 3.5). Samples were placed in pre-labelled plastic bottles or bags and stored in a "crayfish bag" around the diver's waist. Dip and strike measurements of sedimentary bedding were made using a SILVA compass/clinometer and rock samples collected using an ESTWING geological hammer. Notes were recorded on an underwater slate. Underwater photographs were taken using a NIKONOS V camera and a NIKONOS SB102 flash.

Dive sites from 1987 to 1989 were co-ordinated using horizontal sextant bearings onto landmarks on the shore, whilst the positions of dives conducted in 1990 and 1991 were determined using a GPS. The observations made on the 103 SCUBA dives in the study area are discussed in detailed in Chapters 5 & 6. These data were supplemented by extensive snorkel-diving observations and sampling (to depths of -25m) on the coral reef system.

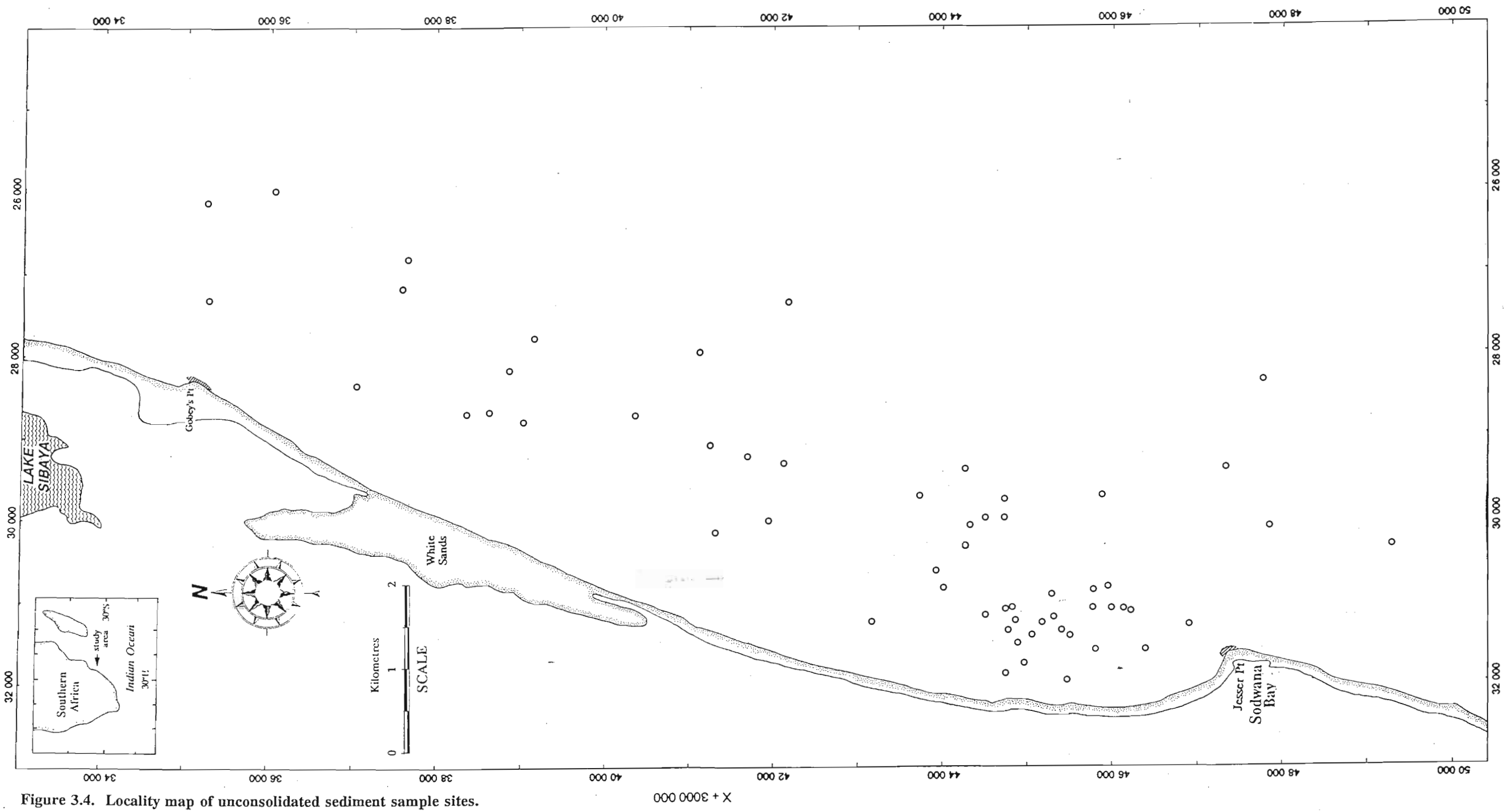

Figure 3.4. Locality map of unconsolidated sediment sample sites.

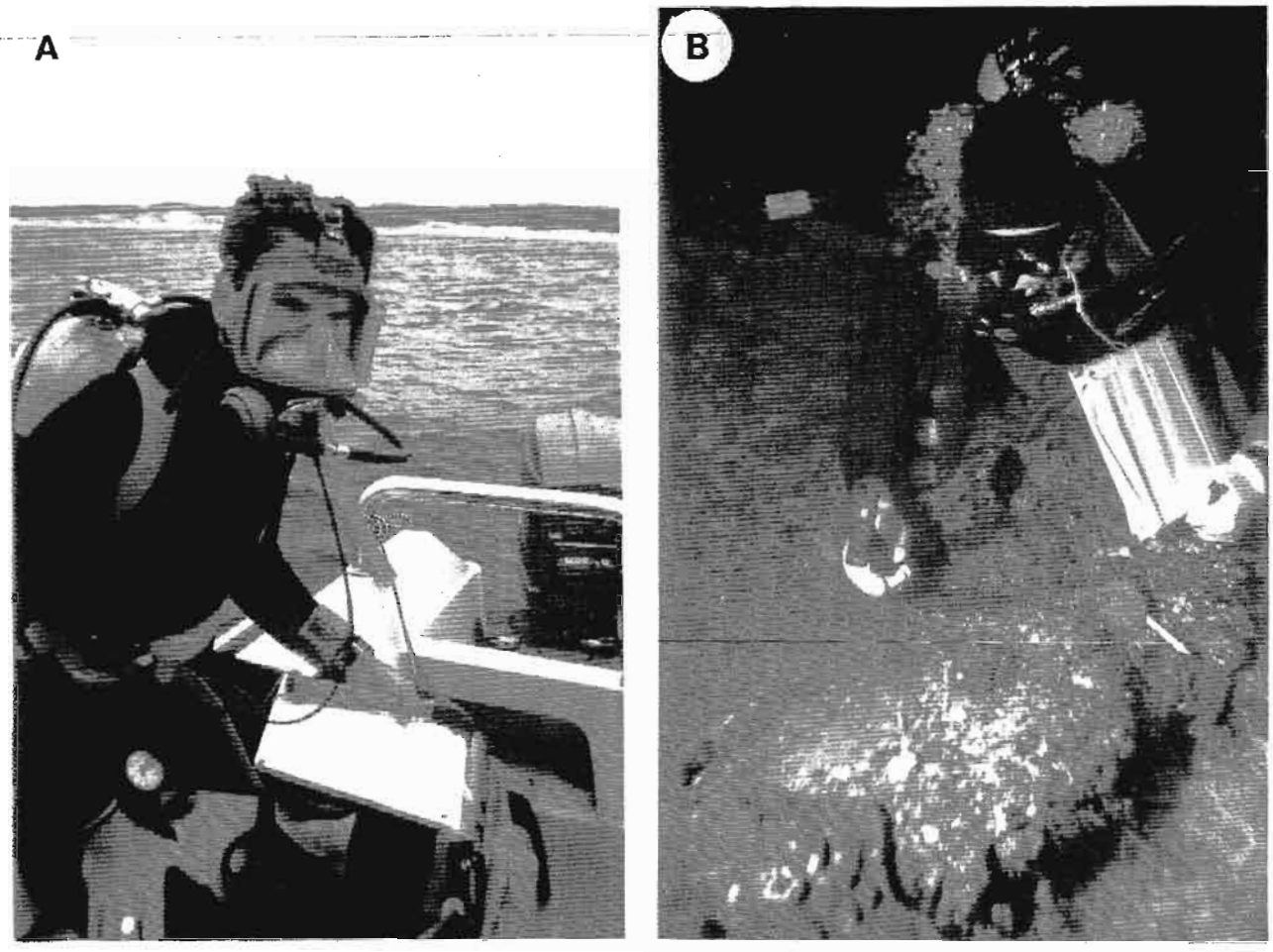

Figure 3.5. (A) The author in full SCUBA equipment with a full face-mask. (B) A marine geologist working underwater. Note the hammer, underwater writing slate, and compass clinometer. (C) Diver sampling unconsolidated sediment.

3.2 DATA REDUCTION

3.2.1 Track chart

Track lines were plotted at a scale of 1:15 000 from the computer survey data using the commercial graphics package "Grapher" and a HEWLETT PACKARD HP 7586 A0 plotter. The data were plotted at 30 second intervals to ensure a high degree of accuracy for each track line, and the fix time was annotated on each track every 2 minutes. This track chart was used as the base map for plotting the side-scan sonar surficial facies of the shelf off Sodwana Bay. Figure 3.6 is a reduced version of the track chart for the RV *Benguela* and *Geocat* cruises.

3.2.2 Bathymetry

The navigation data are in a compressed binary format and were converted to ASCII files using the program "Sidekick". These files, one for each survey line, were imported into a spreadsheet program ("Supercalc 5") which allowed the bathymetric data from the echosounder chart paper output to be entered onto the coordinate list. The echosounding profiles were annotated at 1 minute intervals in the laboratory and the depths were transposed onto a coordinate-time list. Great care was exercised in reading the depths off the profiles especially where a change in slope gradient was evident. A total of 2 154 depth data points were assimilated for the research area; these data were then corrected for transducer depth and tidal variation. The X, Y, and Z data were then exported in an ASCII format into the topographic and three-dimensional generating program "Surfer"; this was used to generate the bathymetric maps and computer-generated three-dimensional models.

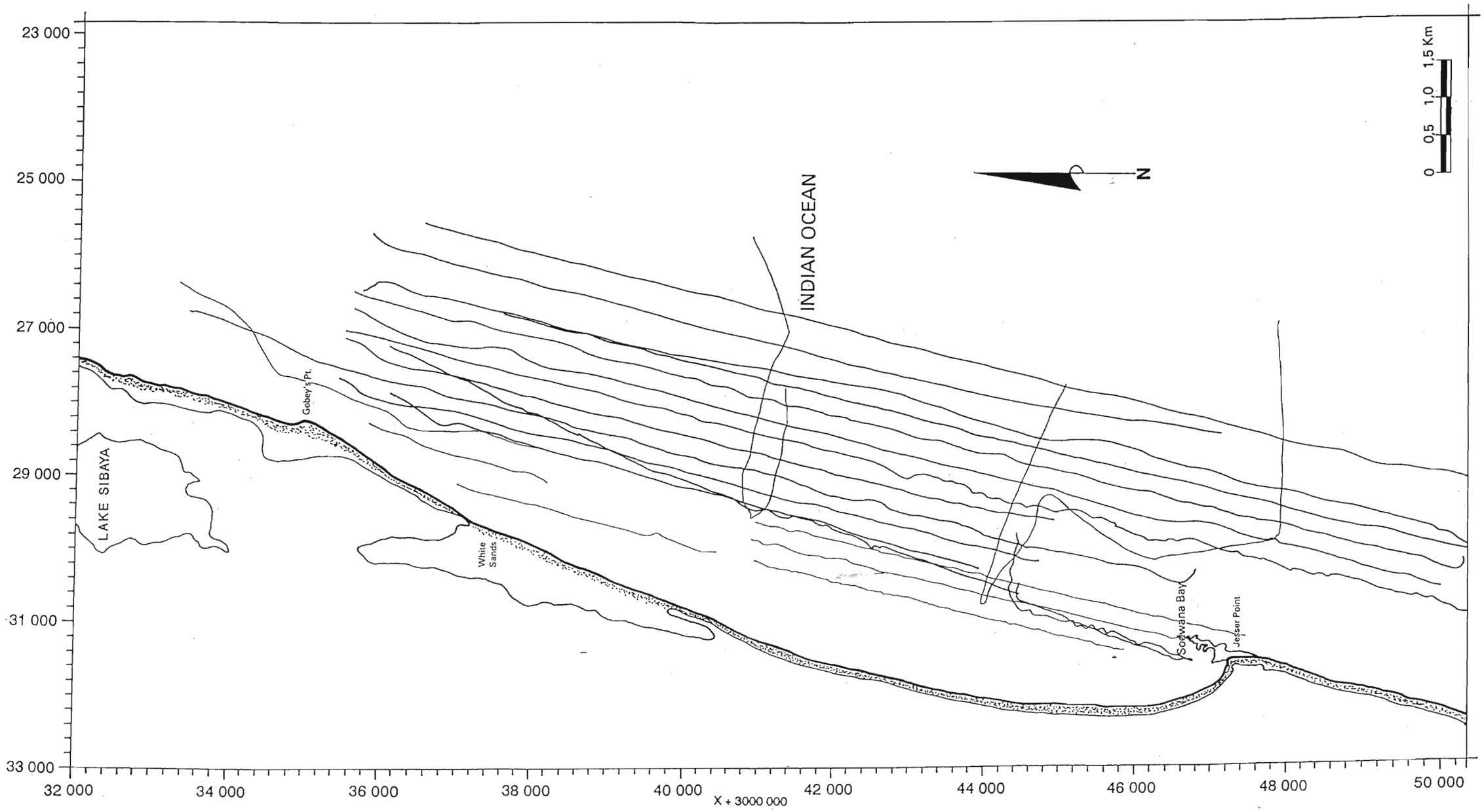

Figure 3.6. Cruise track chart of geophysical survey lines undertaken on the RV Benguela and skiboat Geocat.

3.2.3 Side-scan sonar data

Various acoustic signatures on the side-scan sonar records were photographed and compiled into a working atlas of sonograph seafloor types. These "type" acoustic facies were compared to SCUBA diving observations undertaken since 1987 and further diving sites were identified for ground-truthing. Ground-truthing of acoustic facies is essential if valid geological interpretations are to be made from side-scan sonar imagery (Williams, 1982 ; Bouma and Rappeport, 1984 ; Duck and McManus, 1985). SCUBA diving observations, sediment samples and rock samples, and bathymetric profiles were used in conjunction with the sonographic records to obtain an accurate geological interpretation of each "type" acoustic facies.

In the laboratory the side-scan sonar records were time-annotated in detail by dividing the 10 minute cruise annotations into 10 equal 1 minute annotations. A series of layback curves were plotted for various tow-fish cable lengths assuming a constant ship speed of 5 knots (2.5m/sec), an example of which is shown in Figure 3.7. These empirical curves for a light-weight Kevlar cable were derived from the tow depth versus ship speed graphs in the EG & G tow-fish manual (1984) and tow-fish depth data for a given cable length displayed by the side-scan sonar recorder during actual surveys. A layback equal to approximately 94% of the cable length is inferred assuming no current. An estimate of the effect of running side-scan sonar lines with and against a 3 knot current with respect to layback were also made. The layback of the record when running against the current is approximately 96% of the cable length whereas running lines with the current produced a layback of 80% of the cable length.

The plotting and interpretation of the side-scan imagery involved laying the record for each line next to the time-annotated track chart and accurately tracing the acoustic facies onto the 300m line swath. Each line was corrected for the calculated tow-fish layback and retraced onto drafting film.

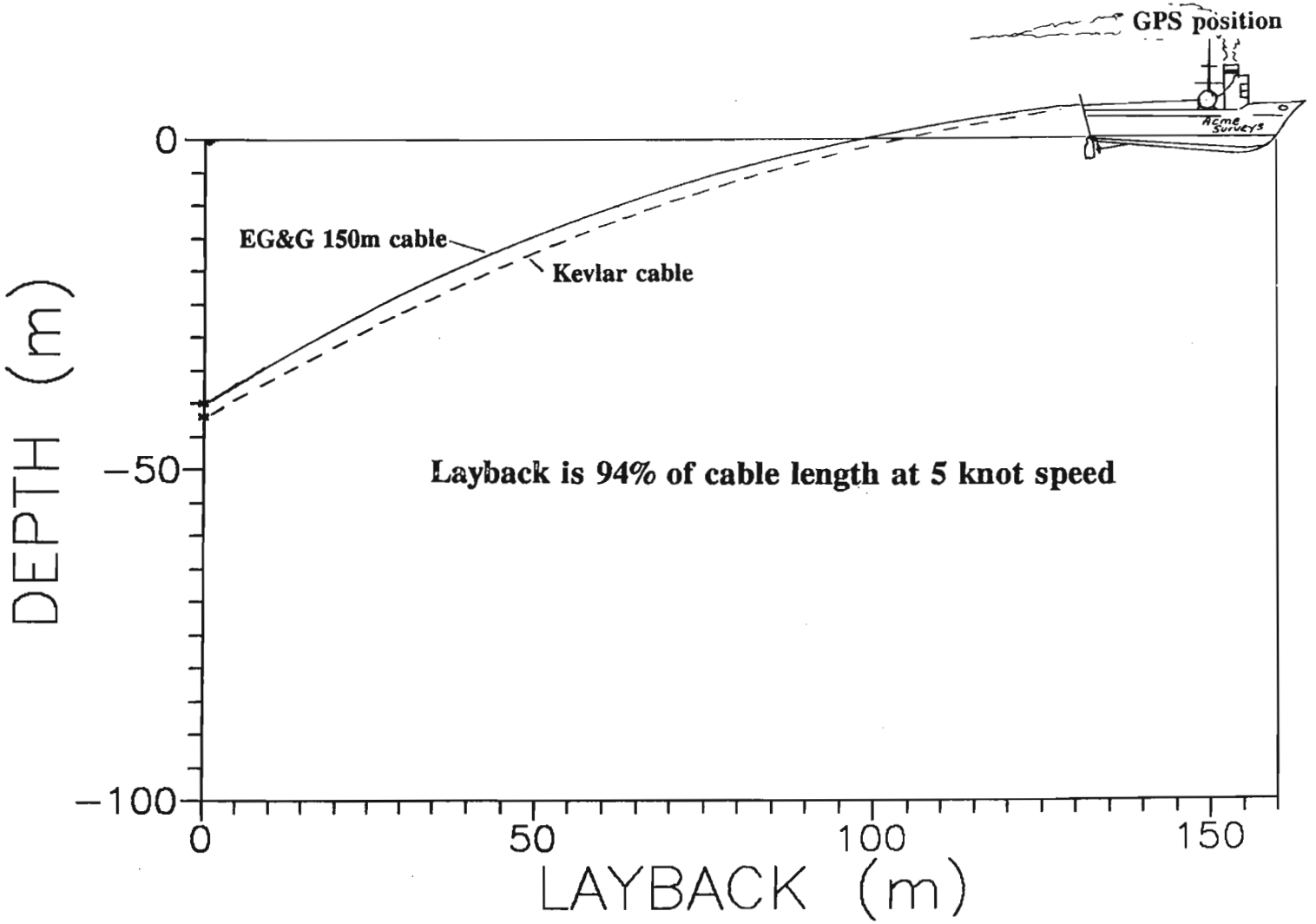

Figure 3.7. An empirical side-scan sonar layback curve for a light-weight Kevlar cable at a speed of 5 knots.

3.2.4 Sediment sample analysis

The laboratory treatment of unconsolidated sediment samples is outlined by Cooper & Mason (1987). The aim of the laboratory analysis is to determine to relative proportions of sand (63μm - 2mm) and gravel (> 2mm), carbonate content, and, in certain samples, the percentage of biogenic components. The size distribution and statistical parameters of the sediment were determined using a computer-linked settling tube. According to Esterhuysen & Reddering (1985) the accuracy of the settling tube has been tested and found to yield results comparable to standard sieving techniques. Carbonate content was determined using a slightly modified version of the "carbonate bomb" (Schink et al., 1978); organic carbon tests were not undertaken due to the lack of organic matter within these samples (Ramsay, 1987). The biogenic content of 21 shelf sediment samples was analyzed by point-counting loose grains under a binocular microscope. This was undertaken to assess the contribution of various carbonate-producing organisms to the total sediment population. The analyses of carbonate-cemented beachrock and aeolianite samples from the shelf are detailed in Chapter 7.

CHAPTER 4: SHELF BATHYMETRY AND THREE-DIMENSIONAL REEF MODELLING

Geophysical, sedimentological and biological zoning studies of the Zululand coral reefs have allowed plots of shelf bathymetry and three-dimensional underwater reef topography to be made. These maps and three-dimensional plots are useful for displaying morphological, biological, and sedimentological relationships of the various features of the shelf and the reefs. The only way to produce three-dimensional reef models, capable of being viewed from any orientation, is to use graphics software packages. The commercially available "Surfer" three-dimensional graphics package was used to produce the shelf bathymetry and three-dimensional reef images.

This section introduces:

(a) a continental shelf bathymetric map of the study area at a scale of 1:15 000 (Map 1);

(b) a detailed bathymetric and three-dimensional model of a selected reef in the study area (Two-Mile Reef) (Fig.4.1 & 4.2).

4.1 METHODOLOGY

(a) The shelf bathymetry data collection and reduction is detailed in Chapter 3 and this section discusses the methods used to produce the bathymetric images. Various grid sizes, grid methods, and search patterns available in "Surfer" were explored to find the most suitable configuration for an accurate depiction of the shelf bathymetry. The best gridding configuration for the database was found to be a 230 by 230 grid which used a kriging grid method and an octant search pattern. The kriging grid method uses geostatistical techniques

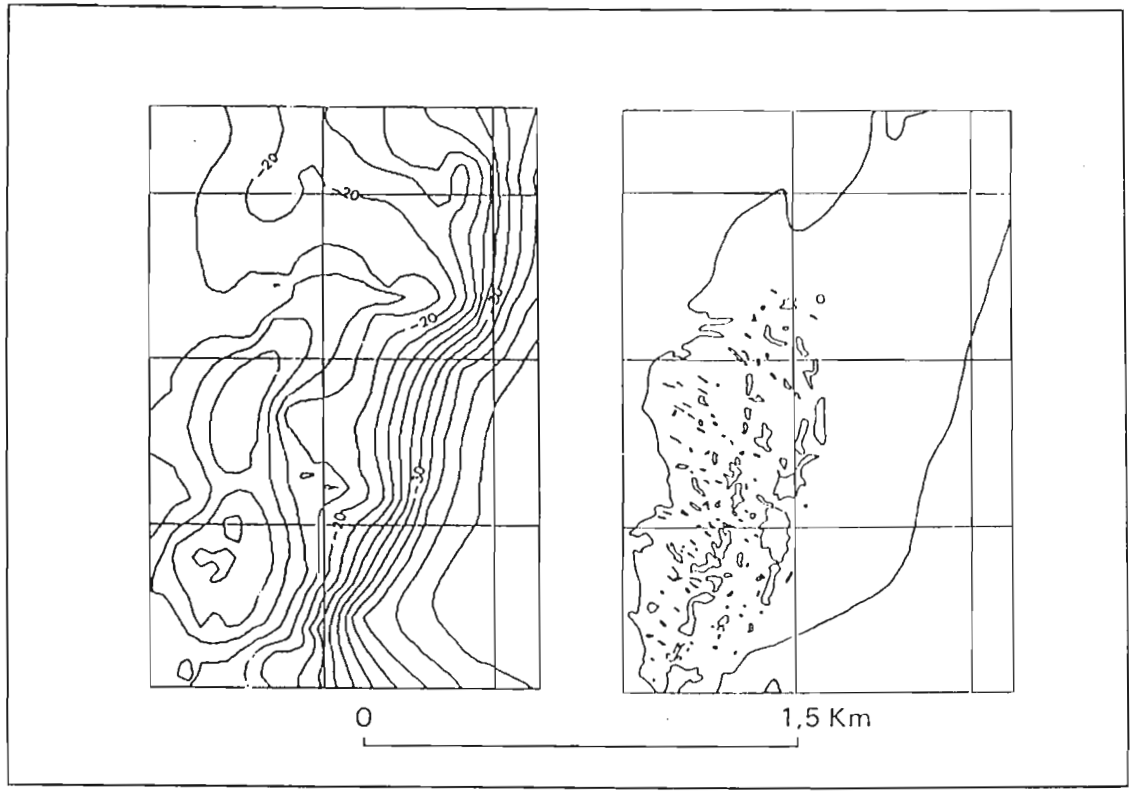

Figure 4.1. Bathymetric map and plan of Two-Mile Reef reduced to the same scale. Bathymetric contour interval is 2 metres. The map of Two-Mile Reef is derived from side-scan sonar image interpretation and aerial photographs.

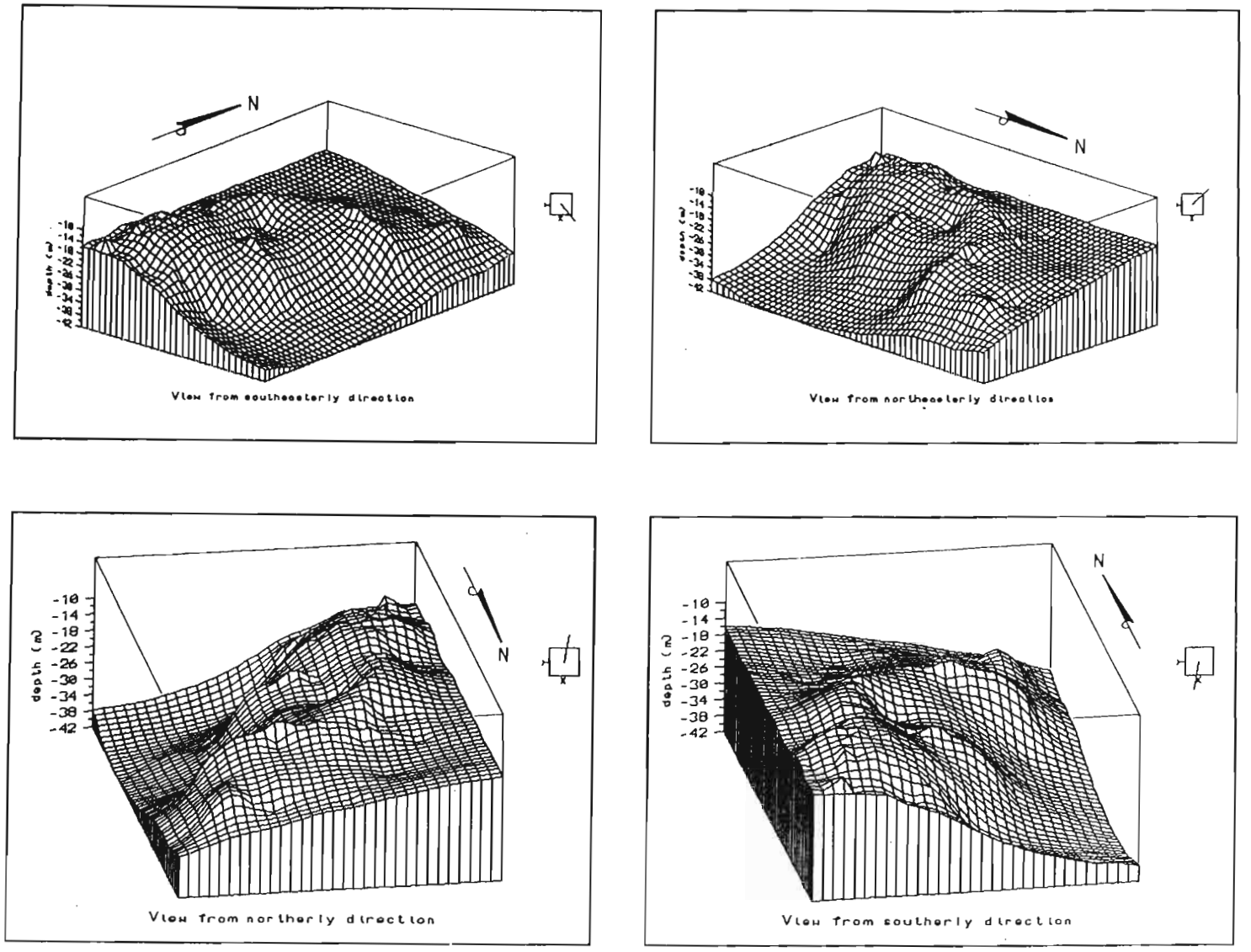

Figure 4.2. Computer-generated, three-dimensional models of Two-Mile Reef viewed from various orientations at a tilt angle of 20° above horizontal. The small legend next to the plot indicates the direction of view.

which calculate the autocorrelation between data points to produce a minimum variance unbiased estimate: in theory, no other gridding method can produce more accurate estimates (Surfer manual, 1987). It was found that a search radius of 19988.17 datapoints using the 10 nearest points was best. The calculation of this grid took approximately eighty hours on a IBM-compatible 286 computer with a maths co-processor. The gridding time was reduced to four hours on 486 machine. Once the gridding operation was complete the grid file was smoothed using a matrix smoothing technique. The smoothing technique gives the impression of hand contouring.

(b) The detailed reef survey database for the three-dimensional model and bathymetry involved mapping the extent of Two-Mile Reef using panchromatic aerial photographs. These photographs were enlarged to a scale of 1:11 500 and shading techniques were employed to enhance the visual impact of the underwater reef on the photograph. The deeper reef margins could not be observed on the photograph, but were mapped using side-scan sonar and echosounding profiles. An accurate map of the reef was produced from these data (Fig. 4.1). Seven echo-sounding traverses, two in a north-south direction, and five in an east-west direction, were used to make a three-dimensional model of Two-Mile Reef to help visualise the morphology of the reef. The echo-sounding data were supplemented by extensive, co-ordinated, spot-depth readings taken on various SCUBA dives over a period of three years. A total of 232 X, Y, and Z co-ordinates on Two-Mile Reef were obtained from the co-ordinated echo-sounding traverses (approximately every millimetre on a 1:11 500 map) and entered into "Surfer". The default setting used in "Surfer" are tabulated in Figure 4.3.

DEFAULT SETTINGS	SHELF MODELLING	REEF MODELLING
Grid size	230 x 230	50 x 32
No. data points	2125	232
Grid method	Kriging	Kriging
Search method	Octant	Octant
Search radius	19988.17	21
Nearest points	10	10
Gridding time (hours)	80 (286 computer with co-processor) 4 (486 computer)	1 (286 computer with co-processor)
Matrix smoothing	Yes	No

Figure 4.3. Default settings in "Surfer" used for shelf bathymetry and three-dimensional reef gridding.

Once the entry of grid data were completed the three-dimensional surface plot or topographic plot system could be selected. This enables viewing of the Two-Mile Reef model from any orientation and tilt angle (Fig. 4.2). The tilt angle above horizontal in Figure 4.2 has been kept constant at 20°. It is possible to plot a topographic map from the same set of X, Y, and Z data. This is especially useful in visualising the bathymetry of the reef system (Fig. 4.1). A detailed description of reef morphology is outlined in Chapters 5 & 6.

Figures 4.1 & 4.2 show that it is possible to view large scale underwater reefs in three dimensions from various orientations which would otherwise be difficult to visualise using a bathymetric chart. The three-dimensional reef image is extremely useful as a baseline into which other geological and biological data may be entered.

4.2 SEAFLOOR MORPHOLOGY OF THE STUDY AREA

Data used in this section was obtained from an interpretation of the detailed bathymetric map with an isobath interval of 5m (Map 1).

The shelf in this area is extremely narrow compared to the global average of 75km (Shepard, 1963), and is characterised by submarine canyons, coral reefs, and steep gradients on the continental slope. A shelf break occurs at -65m situated 2.1km to 4.1km offshore; the world-wide average shelf break occurs at -130m (Shepard, 1963). Sydow (1988), working at Leven Point (40km south of the study area), found the shelf break to be at -64m; this correlates well with the author's data. The shelf can be divided into a northern region and a southern region based on the presence or absence of a defined shelf break. Jesser Point defines the junction between the two shelf regions.

4.2.1 The northern shelf

The northern shelf can be divided into three distinct zones: inner-, mid-, and outer-shelf zones (Fig. 4.4). The inner-shelf is defined as the area landward of the general coral reef trend. Depths vary from 0m to -15m with an average gradient of 1.1°. Reef scour-moats are developed on the landward margins of the reefs and are thought to have formed by geostrophic current erosion of off-reef unconsolidated sediment when the Agulhas Current divides and flows around the linear reef trend. The mid-shelf in this area is defined by the general coral reef trend. These reefs lie 0.5-1km offshore, extend parallel to the coastline and attain a maximum width of 0.9km. Water depths vary from -9m over the shallow central axis of the reef to -35m along the deep reef-front environment. Reef topography is rugged on the reef-crests becoming more low relief on the reef margins. The outer-shelf is seaward of the coral reefs and occurs at a depth range of -35m to -65m. Gradients vary from 1° in the south to 2.5° in the northern part of the study area, and are steep compared to world average shelf gradient of 0.116°

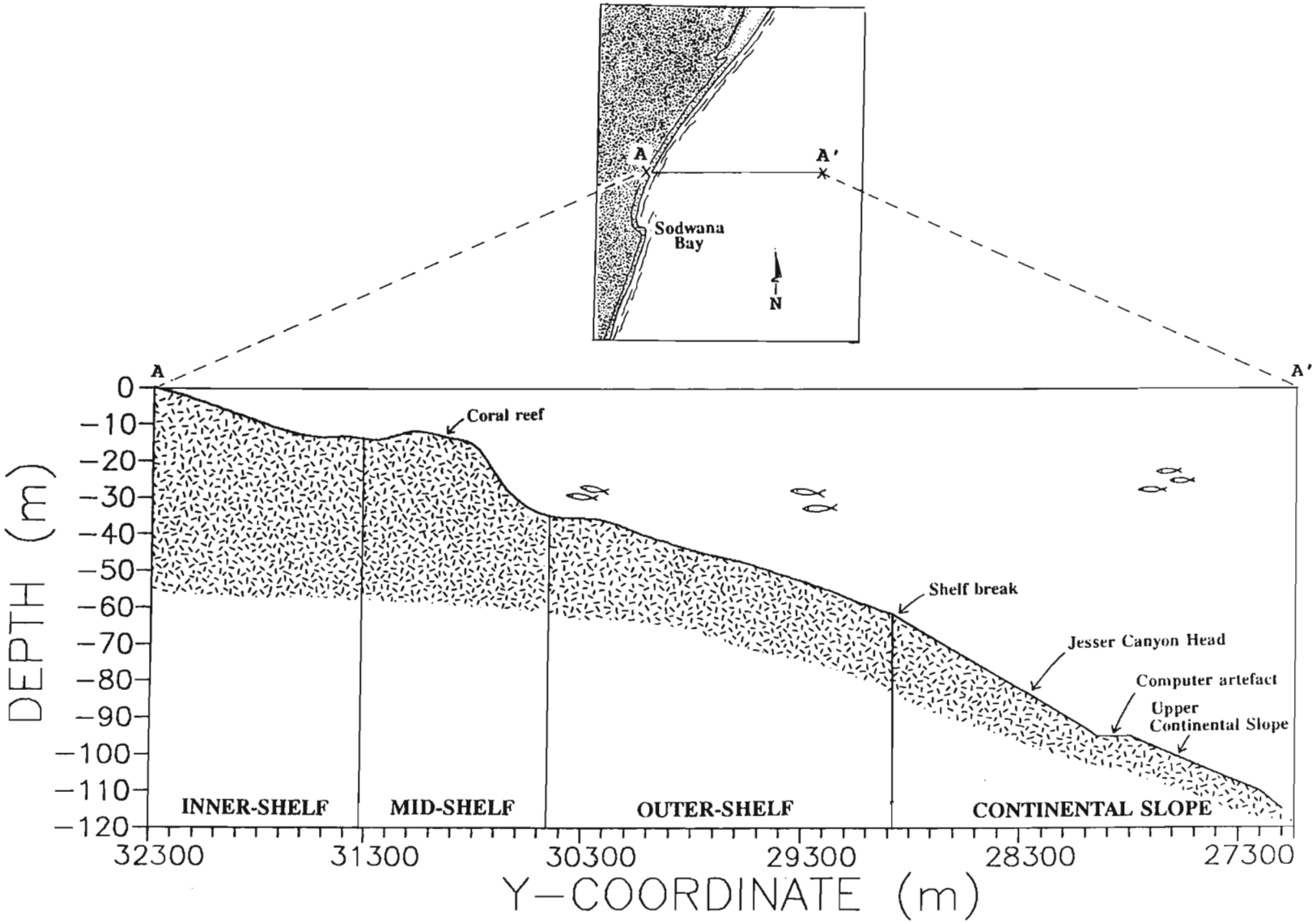

Figure 4.4. Computer-generated east-west cross-section of northern shelf showing the inner-, mid-, and outer-shelf zones. Data for this plot were edited from the bathymetric data file in "Surfer" and exported to "Grapher" to be plotted as an X-Y graph.

(Shepard, 1963) and 0.205° (Hayes, 1964). The outer-shelf is dissected by two large submarine canyons (Wright Canyon & White Sands Canyon) and two smaller canyons (Jesser Canyon & Beacon Canyon): close to the canyon head of the largest canyon, between -35m and -65m, the shelf gradient steepens to 6.23°.

4.2.2 The southern shelf

The shelf south of Jesser Point has a poorly defined shelf break and cannot be sub-divided on the basis of morphology. The gradient averages 1.3°.

In the study area off-shelf gradients of the upper continental slope, at depths of -65m to -115m, vary from 0.7° south of Jesser Point to 2.9° in the inter-canyon area 9km north-east of Jesser Point. Sydow (1988) noted that the upper continental slope, off Leven Point, is divided into a lower, moderately dipping (3.0°), hummocky surface, and an upper, steeply dipping (8.6°), relatively planar surface with occasional subtle scallops. These two surfaces are separated by a 300m wide, laterally discontinuous terrace at -250m.

4.2.3 Submarine canyons

Four submarine canyons occur on the northern shelf; from north to south they are: (1) Jesser Canyon; (2) Wright Canyon; (3) Beacon Canyon; (4) White Sands Canyon (Map 1; Fig. 4.5). These have been named either after a nearby geographical feature or after a member of the survey team. The canyons can be classified as mature- and youthful-phase canyons depending on the degree to which they have incised the shelf. Farre et al. (1983) define mature-phase canyons as deeply incised canyons which traverse the shelf and youthful-phase canyons as less deeply incised features which have not yet

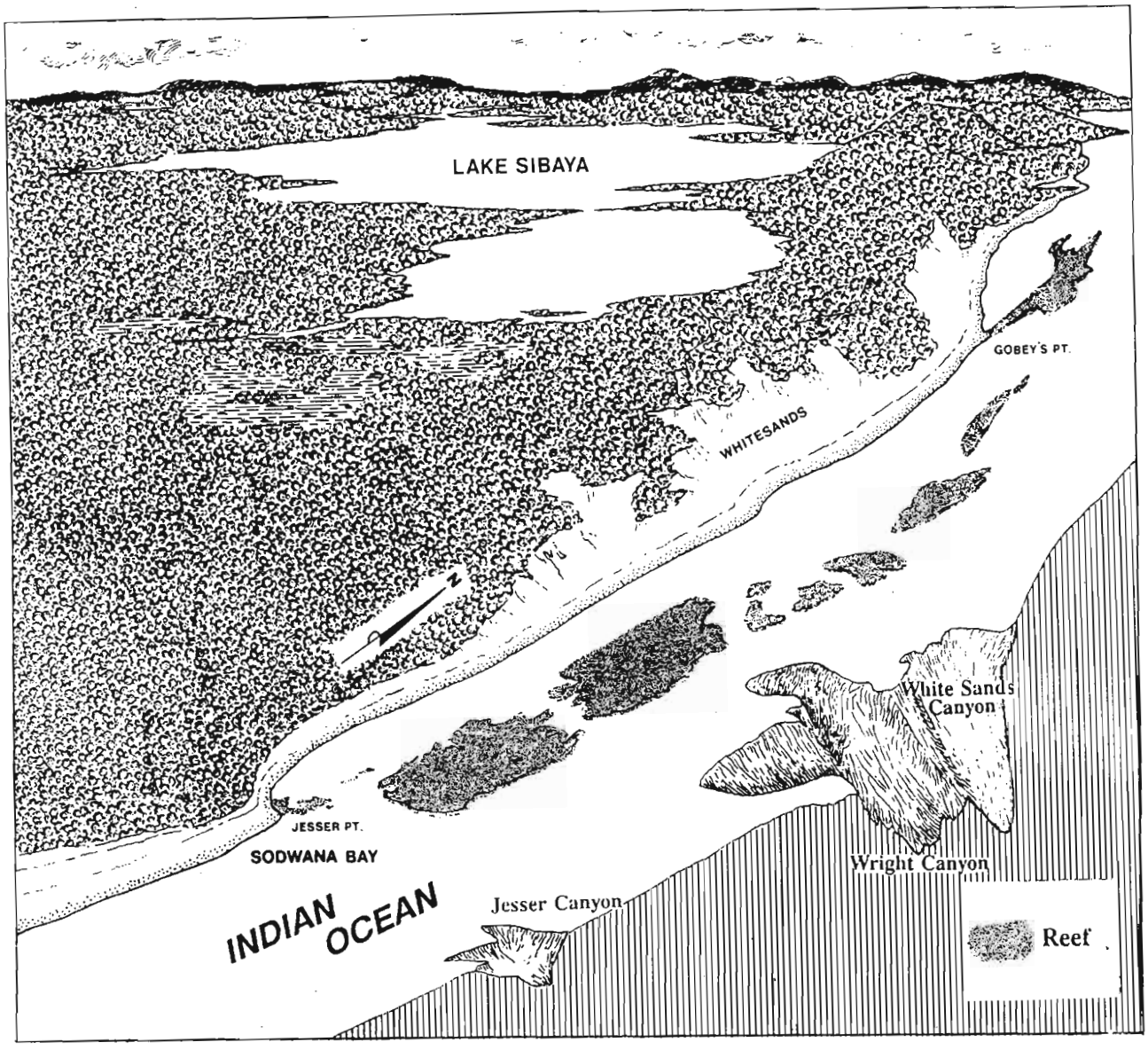

Figure 4.5. An oblique, three-dimensional sketch of Sodwana Bay shelf and adjacent coastal plain showing the nature and distribution of submarine canyons and coral reefs.

breached the shelf break.

The most southerly canyon on the northern shelf is a youthful-phase canyon (Jesser Canyon) located 4km offshore and 1.9km north of Jesser Point. The canyon head occurs at -70m with a gradient of 10.1° and an axis orientation of 100°. Jesser Canyon has a characteristic V-shaped morphology with a uniform northern wall and a large slump on the southern wall at -87m. The northern canyon wall has a steeper gradient (9.1°) than the southern wall (6.5°): this is characteristic of the canyons in the study area. The seaward extension of this canyon could not be traced below -102m on the upper continental slope due to a lack of bathymetric data in this area.

Six and a half kilometres north of Jesser Point is Wright Canyon. This is the largest canyon in the study area and as such is a mature-phase canyon (Fig. 4.5). The canyon breaches the shelf edge at a distance of 2km offshore; the canyon head occurs at -38m and the thalweg can be traced, at a gradient of 20.6°, to more than -453m deep on the continental slope. The maximum width of the canyon on the shelf is 1.2km. The canyon is V-shaped and sinuous with axis orientation changes from 093° at the canyon head, to 163° in the mid-canyon area and 102° on the upper continental slope. This sinuosity is due to the presence of a competent, shore parallel, submarine spur on the northern canyon margin at -75m to -90m. This is probably a resistant Pleistocene sandstone outcrop which delineates a palaeocoastline. In the upper reaches of Wright Canyon the gradient of the rims of the canyon walls are shallower than further down towards the thalweg. At depths of less than -100m the southern and northern canyon wall gradients are similar (5.3°); a terrace is evident on the southern canyon wall at -46m to -49m (Figs. 4.6; 4.7; & 4.8). In deeper water (-160m to -453m) the gradient of the southern canyon wall varies from 13.3-23.7° and the northern wall gradient varies from 14.3-18.6°. The northern canyon wall is usually steeper than the southern canyon wall and notable slumps are located on the southern canyon wall at -67 and -77m. The canyon thalweg is hummocky due to the accumulation of slumped sediment (Fig. 4.7). Two oval depressions are present in the upper reaches of the canyon

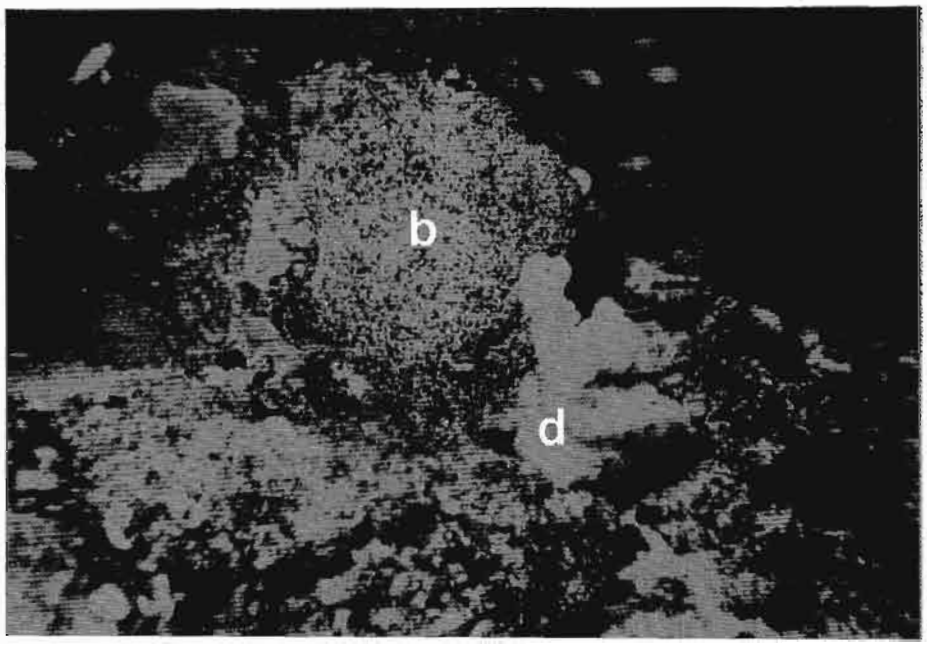

Figure 4.6. Diverse marine life encrusting a beachrock terrace outcrop on the southern wall of Wright Canyon. Basket starfish (b) and Dendronephthya soft coral (d) are very common. Depth -41m.

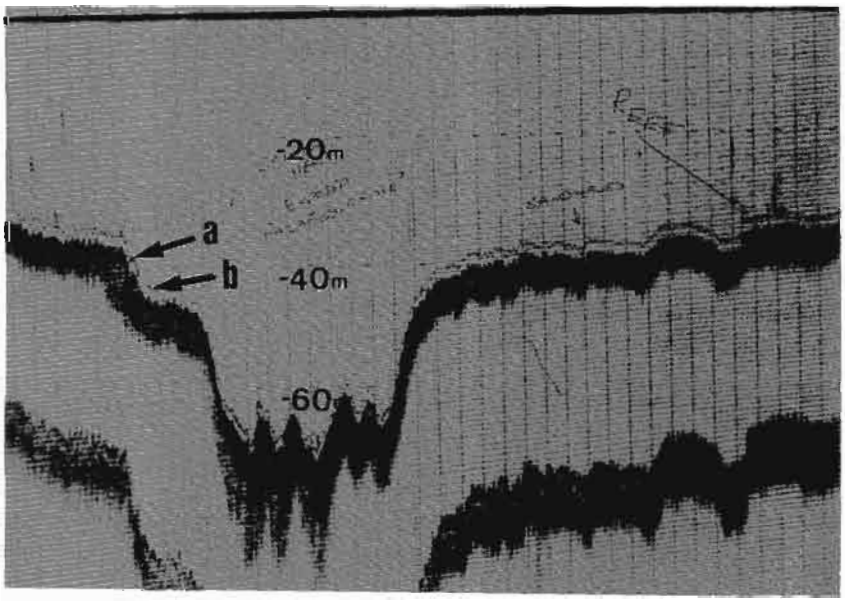

Figure 4.7. A south-north, coast-parallel, bathymetric profile across the canyon head of Wright Canyon. The canyon thalweg is hummocky due the accumulation of slumped sediment. (a) Beachrock outcrop on the southern wall noted in Fig. 4.6. (b) Position of the small-scale debris flow noted in Fig. 4.8.

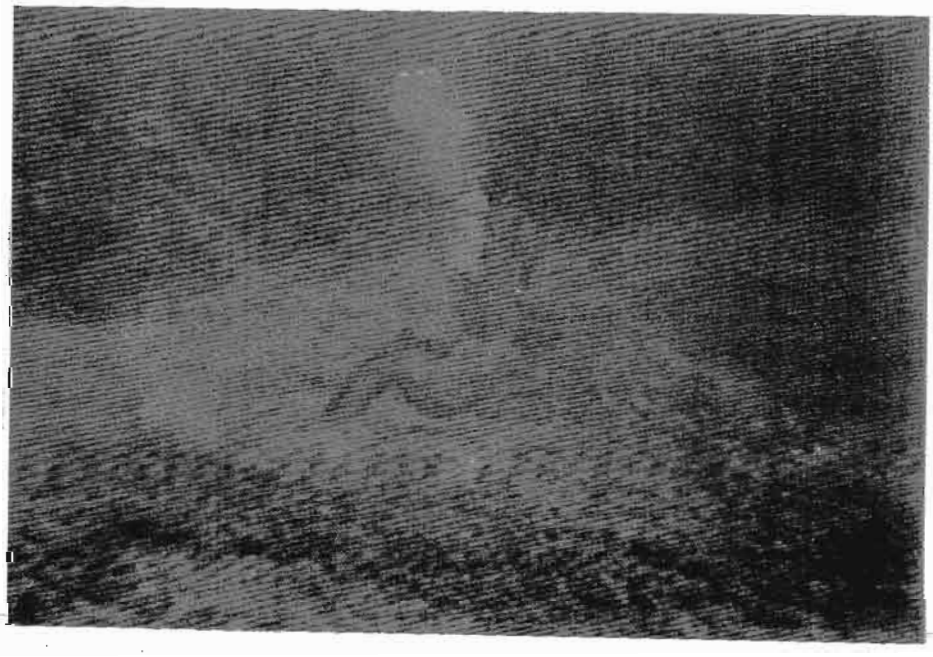

Figure 4.8. A small-scale bioclastic debris flow at the base of a beachrock terrace outcrop in Wright Canyon. Depth -48m.

thalweg; the author is unsure of the nature or origin of these features.

Between Wright Canyon and White Sands Canyon an incipient, youthful phase canyon (Beacon Canyon) occurs. The canyon head is at -70m and the canyon progresses into a characteristic V-shaped morphology which can be traced to at depth of -97m.

The second largest submarine canyon (White Sands Canyon) occurs 10.7km north of Jesser Point and has the steepest canyon head gradient (41.4°). The canyon head is 3km offshore, begins close to the shelf break at -65m and has an axis orientation of 100°. The canyon has a V-shaped morphology with the upper reaches of the canyon walls having a shallower gradient. The thalweg is hummocky with much slumped sediment being evident. Slumps generally occur on the southern canyon wall with a notable slump at -145m. The gradient of the northern canyon wall is steeper (15.6-11.2°) than the southern canyon wall (11.5-10.7°) and the canyon was traced to a maximum depth of -353m. This canyon can be classified as mature-phase due to its size, steep head gradient and extensive erosion of the shelf edge.

SUBMARINE CANYON	DISTANCE OFFSHORE	CANYON HEAD GRADIENT	AXIS ORIENTATIONS	CLASSIFICATION (Farre et al., 1983)
Jesser Canyon	4km	10.1°	100°	Youthful-phase
Wright Canyon	2km	20.6°	093°, 163° & 102°	Mature-phase
Beacon Canyon	3km	3°	100°	Youthful-phase
White Sands Canyon	3km	41.4°	100°	Mature-phase

Figure 4.9. Submarine canyon characteristics of the Zululand continental shelf around Sodwana Bay.

4.3 DISCUSSION

The narrow continental shelf (average 3km) off Sodwana Bay can be divided into two distinct zones, based on the presence or absence of a defined shelf break. The southern shelf has a poorly-defined shelf break whilst the northern shelf has a well-defined break at -65m. The poor definition of the shelf break on the southern shelf can possibly be attributed to the presence of giant climbing sand dunes offshore of Jesser Point at depths of -37m to -60m (see 5.3.1). The northern shelf has a series of coast-parallel patch coral reefs which have colonised carbonate-cemented, coastal-facies sequences (discussed further in Chapters 5 & 6), which apparently delineate late Pleistocene palaeocoastline trends.

The four submarine canyons in the study area are classified as mature- or youthful-phase canyons depending on the degree to which they breach the shelf. The canyons have a characteristic V-shaped morphology with the northern canyon walls being steeper than the southern walls. Slumps, probably debris flows, are more prevalent on the southern canyon walls and the thalwegs are hummocky due to the presence of slumped sediment in the canyon thalweg. Seaward extensions of these canyons on the upper continental slope could not be ascertained due to a lack of bathymetric data in this area.

The origin of the Zululand canyons is not related to the position of modern river mouths but can probably be linked to palaeo-outlets of the Pongola and Mkuze River systems (Orme, 1973; Hill, 1975; Wright, 1990; see Chapter 8). Sydow (1988) suggests that the canyons are mass-wasting features which have later been exploited by palaeo-drainage during regressions. The author concludes that the youthful-phase canyons are mass-wasting features associated with an unstable, rapidly-deposited, progradational late Pliocene sequence (noted by Sydow, 1988) and a steep upper continental slope (Fig. 4.10). The mature-phase canyons were probably initiated by mass-wasting but have advanced shoreward, breaching the shelf, due to their link with the palaeo-outlets of the Pongola and Mkuze Rivers during the late Pleistocene regressions.

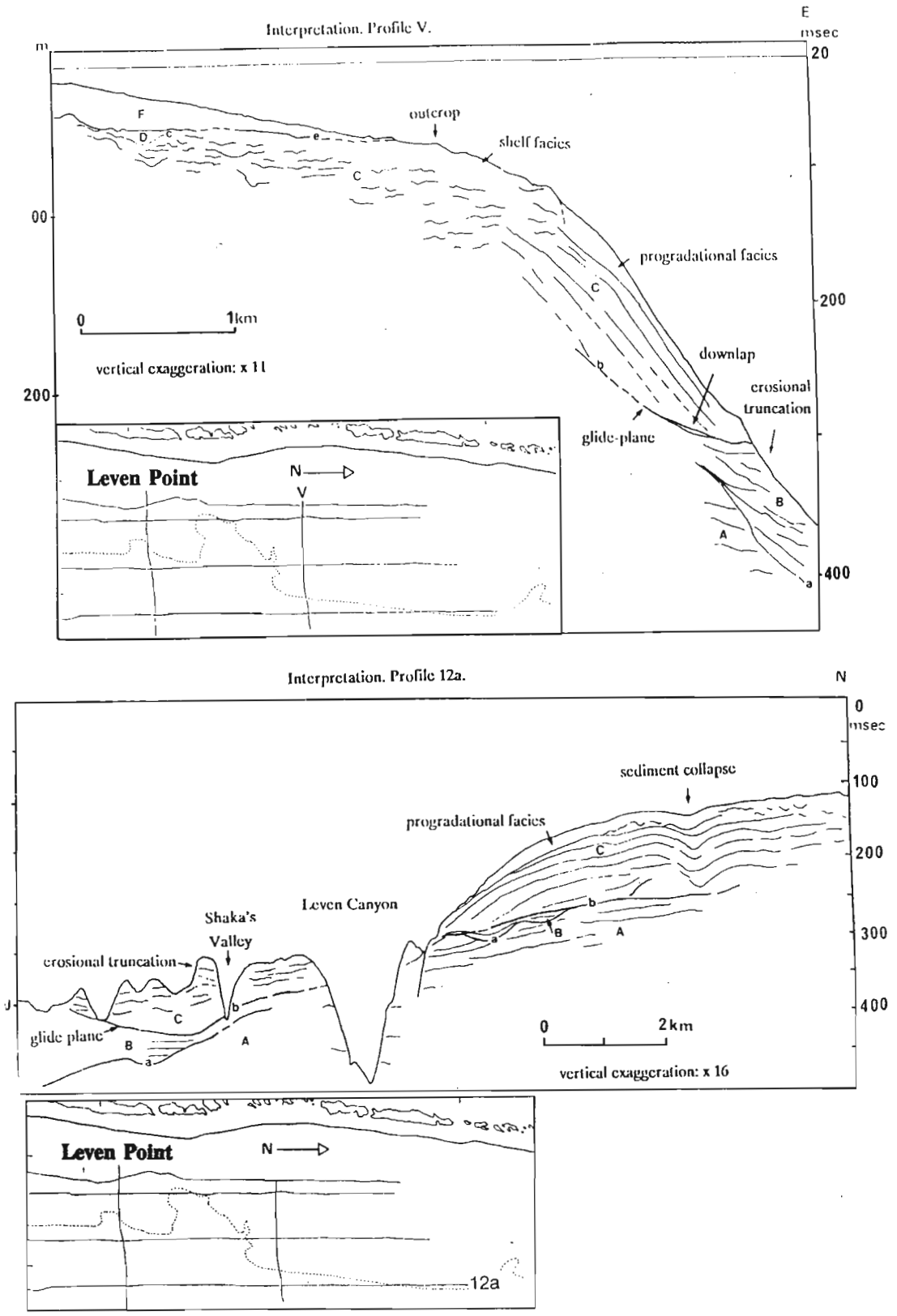

Figure 4.10. Sparker seismic profile interpretations off Leven Point. (a) Shore-perpendicular line V and (b) shore-parallel line 12a. Stratigraphic sequence interpretation: A = St Lucia Formation; a = erosive surface from Late Cretaceous/Early Palaeocene; B = marine sequence, Late Palaeocene?; b = Buried glide-plane scar, Zululand slump; C = rapidly deposited progradational sequence, Pliocene; D = shallow marine, Pleistocene; E = Pleistocene aeolianite "stump"; e = erosive surface, previous glacial maximum 16 000 years B.P.; F = inner-shelf Holocene sediment prism. (From Sydow, 1988).

Evidence of modern canyon growth has been noted on numerous diving surveys that the author has carried out on the canyon heads. This takes the form of minor wall slumps and small-scale debris flows (Fig. 4.8). The canyons are also supplied with large quantities of sand in the form of large-scale shelf sand dunes generated and moved by the Agulhas Current; discussed further in Chapter 5. These were first described by Flemming (1978, 1980, & 1981) and later by Sydow (1988). As these sand bodies intersect the canyons the sediment slumps down the canyon thalweg and causes erosion and downcutting of the canyon walls and floor thereby increasing the canyon dimensions.

CHAPTER 5: SHELF SEDIMENTOLOGY BASED ON SIDE-SCAN SONAR INTERPRETATION

The Agulhas Current controls physical and biological processes on the shelf and is undoubtedly responsible, in whole or in part, for the vast array of interesting sedimentological and biological phenomena which have recently been discovered on the Sodwana Bay shelf (Map 2). Conspicuous beachrock/aeolianite outcrops account for a substantial proportion of the surficial area of the shelf. A study of sedimentary structures visible in these outcrops has revealed palaeocurrent directions and palaeostrandline orientations during late Pleistocene times. At depths of less than -25m, corals have colonised the outcrops forming soft-coral dominated reefs. Coral reefs and deeper water gorgonian/sponge reefs, together with other carbonate-producing organisms on the shelf, contribute to the surficial bioclastic sediment on the seafloor. Most of the surficial, unconsolidated sediment on the shelf is composed of terrigenous quartz grains with a carbonate content of less than 20%. Large-scale subaqueous dunes form in the unconsolidated sediment on the outer-shelf due to the Agulhas flow forming a sediment conveyor. Within this conveyor, the main sediment transport direction is south. In isolated areas bedload parting zones exist where the sediment transport direction is reversed to a northerly flow.

This chapter deals with the geological interpretation of shelf acoustic facies obtained from sonograph images, ground-truth SCUBA diving, and remote video traverses. Side-scan sonar used in conjunction with bathymetric profiling can quantify the microtopography of the seafloor in terms of "ruggedness". The following terms are now rigorously defined to quantify the microtopographic nature of the seafloor (De Decker, 1987):

subdued - topographic differences are less than 2m;

rugged - topographic differences vary from 2-5m;

very rugged - topographic differences are more than 5m;

sediment-covered bedrock - more than 75% of the bedrock has sediment cover that can be recognised on sonograph images;

exposed, bare bedrock - less than 25% of the bedrock has a sediment veneer over it.

The seafloor is often described in terms such as "highly, moderately, and weakly reflective", "granular", "even-toned", "blotchy", etc. (Knebel et al., 1982). These descriptions group features with similar acoustic reflectivities together, even though the features themselves may be quite different (De Decker, 1987). The scale of the isometric sonograph record figures is defined by "ticks": each "tick" represents 25m of seafloor (Figs. 5.2, 5.3, 5.4).

SCUBA diving observations on sedimentary structures, sediment samples and rock samples, and bathymetric profiles were used in conjunction with the sonograph images to obtain an accurate geological interpretation of each "type" acoustic facies. Remote video camera images were also used on selected areas of the shelf. The main shelf facies have been divided into consolidated and unconsolidated lithologies and these have been further sub-divided into various facies. The sedimentary lithologies are discussed below in considerable detail with special emphasis placed on a discussion of inherent sedimentary structures in the various lithotypes. Where applicable, the sonograph image for each facies is described, followed by a detailed sedimentological interpretation based on the above-mentioned observations and analyses.

5.1 CONSOLIDATED LITHOLOGIES

5.1.1 Beachrocks and aeolianites

Beachrocks and aeolianites on the shelf at Sodwana Bay form the reef-base of coral and gorgonian/sponge reefs (Ramsay, 1987; Ramsay, 1988; Ramsay 1990a&b; Ramsay et al., 1989; Ramsay & Mason, 1990a&b). The reefs formed by these outcrops have been named in accordance with their distance north of Jesser Point or after a member of the survey team (Fig 5.1; Map 2). The author has personally discovered three previously unknown coral reefs in the study area. These rocky outcrops produce distinctive sonograph images: aeolianites display a pronounced, rugged outcrop microtopography whereas beachrocks have a more subdued microtopography (confirmed by SCUBA diving). Sonograph images from aeolianite outcrops are generally highly reflective with blotchy and rugged linear patterns (Fig 5.2) whereas beachrock outcrops are highly reflective with a less blotchy nature (Fig 5.3). Areas of highly reflective (bioclastic) sediment partially covering very subdued beachrock outcrops have also been discriminated, these produce a granular pattern (Fig 5.4).

Previously, very little was known about the rocky sandstone foundations which corals have colonised to form offshore coral reefs in northern Zululand. McCarthy (1967) related the offshore, submerged aeolianite which forms Aliwal Shoal on the Natal south coast to a regressive Pliocene deposit. Maud (1968) suggested that the northeast-trending submarine reefs in Zululand correlated with the 'first aeolianite' which post-dated the mid-Pleistocene Port Durnford Beds. The first aeolianite is similar in extent and lithology to the oldest aeolianite of the Western Australian coast described by Fairbridge & Teichert (1953). These two formations are apparently analogous and contemporaneous (Maud, 1968). Reference is made by Flemming (1981) and Martin & Flemming (1986) to offshore aeolianite ridges along the Zululand coast which trap Holocene sediment on their landward margins (Fig. 5.5). Coetzee (1975b) suggested that aeolianites at Black Rock (50km north of Sodwana Bay) formed during

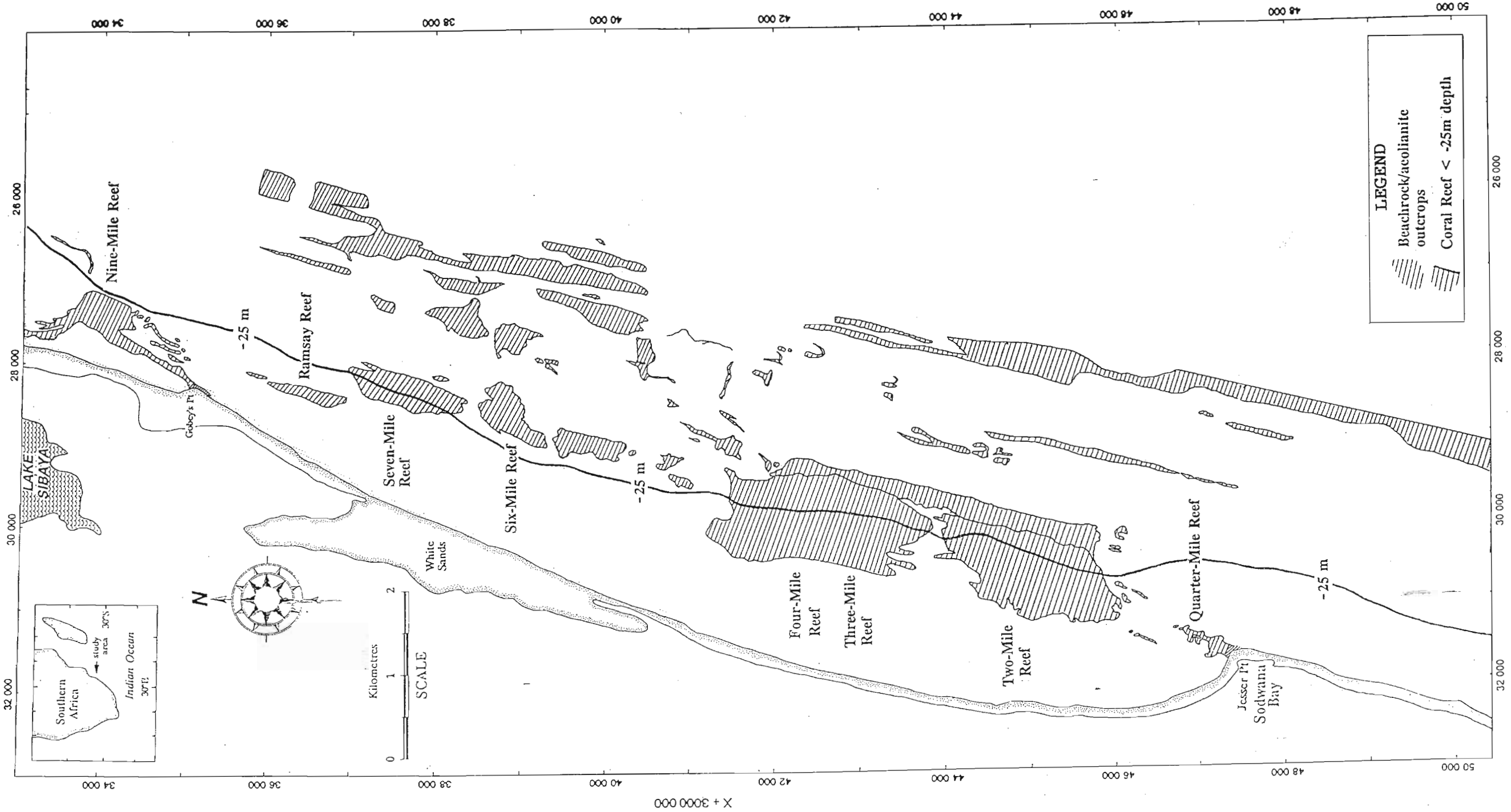

Figure 5.1. Distribution of beachrock/aeolianite outcrops on the Sodwana Bay shelf. Coral reef veneers cap the aeolianite/beachrock sequence at depths less than -25m.

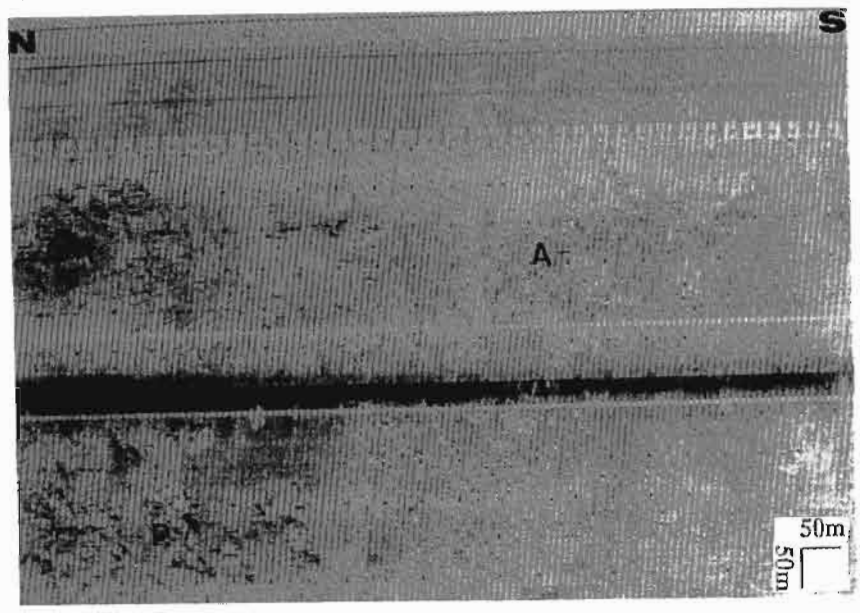

Figure 5.2. Sonargraph image of a highly reflective, rugged aeolianite outcrop (A) with a coral reef capping. Note the rugged relief pinnacles (P). (X+3042334;Y+30140).

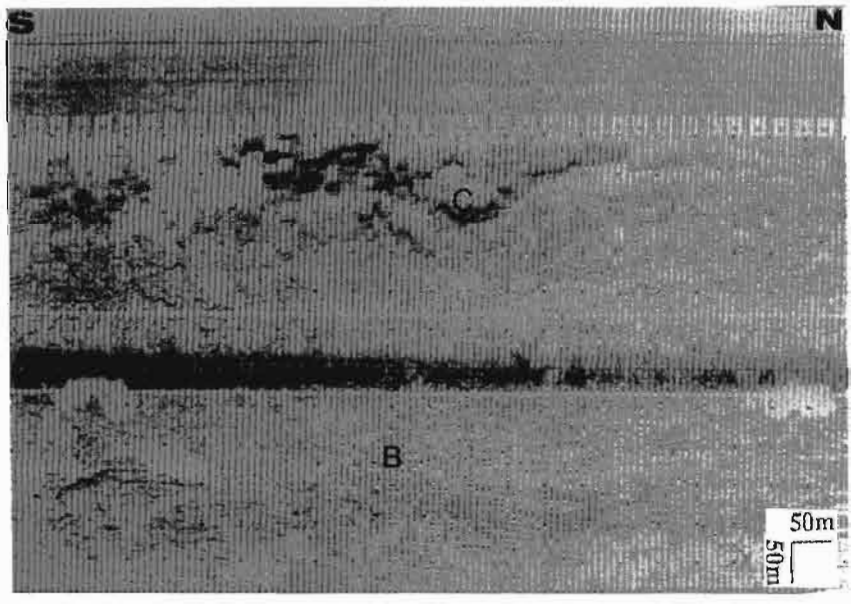

Figure 5.3. Sonargraph image of highly reflective, but less rugged beachrock outcrop (B). A regressive aeolianite outcrop that occurs stratigraphically above the beachrock is labelled (C). (X+3037682;Y+28 394).

Figure 5.4. Sonargraph image of highly reflective, granular bioclastic sediment (D) partially covering a subdued beachrock outcrop. E represents an underwater cliff (± 2m high) related to a sea-level notch incised at -32m. (X+3044427;Y+29970).

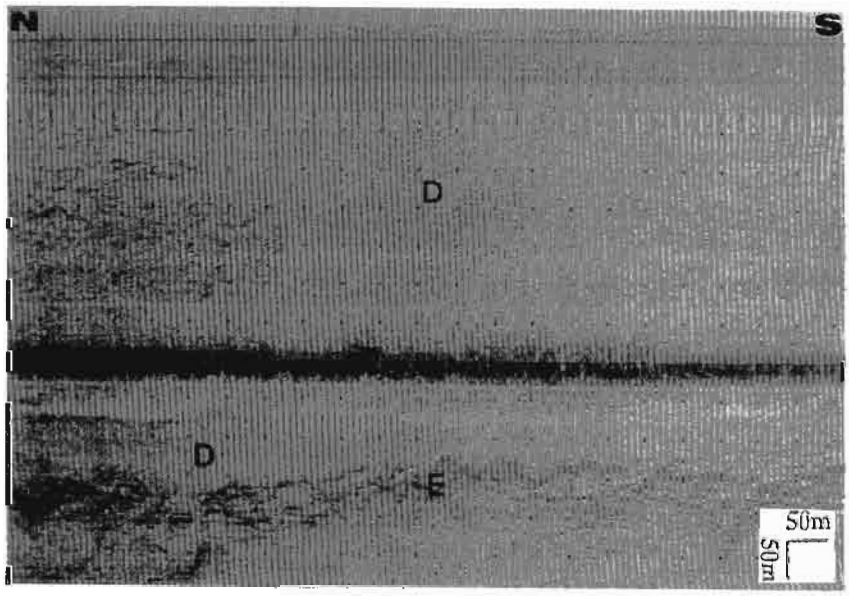

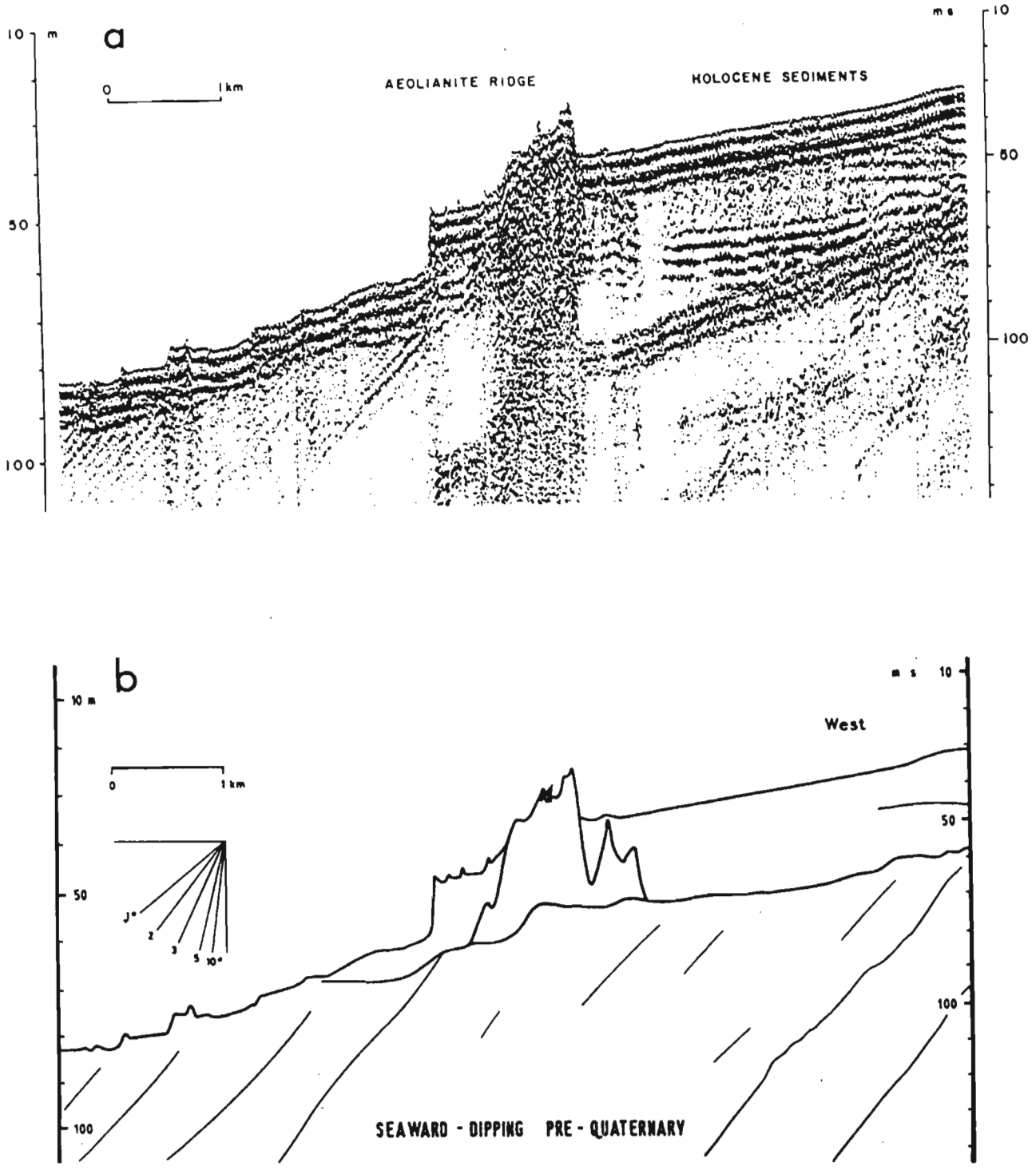

Figure 5.5. (a) A sparker seismic profile; and (b), interpretation showing stratigraphic relationships on the narrow east coast shelf, South Africa. Seaward-dipping pre-Quaternary and possibly pre-Cretaceous strata are unconformably overlain by Pleistocene aeolianites, which are in turn overlain by Holocene sediments. Note the damming effect of the aeolianite ridge. The seaward flank of the Pleistocene formation slopes seaward at 29° and may be a submerged wave-cut cliff indicating that sea-level has occupied the base of the aeolianite ridge at least twice. (From Martin & Flemming, 1986).

a Pleistocene marine regression and that the dunes were cemented by downward percolation of carbonate-rich groundwater. Cooper & Flores (1991) defined eight carbonate-cemented coastal facies at Isipingo Beach south of Durban on the basis of petrology, grainsize, internal structures and field relationships. These facies have been interpreted as deposits of surf zone, breaker zone, swash zone, backbeach, boulder beach, and dune environments.

Coral reef veneers capping beachrocks and aeolianites are found on the Natal-Recife coastline of Brazil (Guilcher, 1988) and on the western, northwestern and southern Australian shelf area (Fairbridge, 1950a). The Brazilian reefs are colloquially known as "arrecifes", a Portuguese term which means sandstone (Guilcher, 1988). The reefs are founded on submerged Holocene beachrocks and have been dated at between 7000 and 2000 B.P. (Flexor & Martin, 1979). The Australian patch reefs grow on truncated benches in Pleistocene aeolianites, which formed as coastal sand dunes in parallel ridges during various sea-level lows (Fairbridge, 1950a). Bloom (1974) described modern reef complexes as thin veneers of late Pleistocene and Holocene limestone deposited on older reefs and lithified dune fields that were exposed to subaerial weathering during the low sea-level of the Wisconsin glaciation.

Intertidal beachrocks form the prominent Jesser and Gobey's Points but also occur intermittently along the log-spiral curve (zeta bay) of Sodwana Bay. These outcrops were cemented in the intertidal zone by the action of groundwater supersaturated with $CaCO_3$ and the buffering action of seawater which triggers carbonate cementation by precipitation. This cementation mechanism is favoured by Fairbridge (1950a), Coetzee, (1975b) and Guilcher (1988) (see Chapter 7). The beachrock sedimentary structures visible include planar cross-bedded units dipping 2-5° east and trough cross-bedded units indicating "ridge and runnel structures" on a beach (Fig. 5.6). The trough cross-beds demonstrate northerly flowing palaeocurrents trending coast parallel with occasional 180° current reversals; this is typical of what is seen in the modern "ridge and runnel structures" along the Zululand coastline. These intertidal beachrocks formed during the Holocene, once sea-level had stabilised at its present

Figure 5.6. Trough cross-bedded unit in a intertidal beachrock outcrop at Gobey's Point, indicating "ridge and runnel structures". The transport direction is towards the north. The scale is 10cm long.

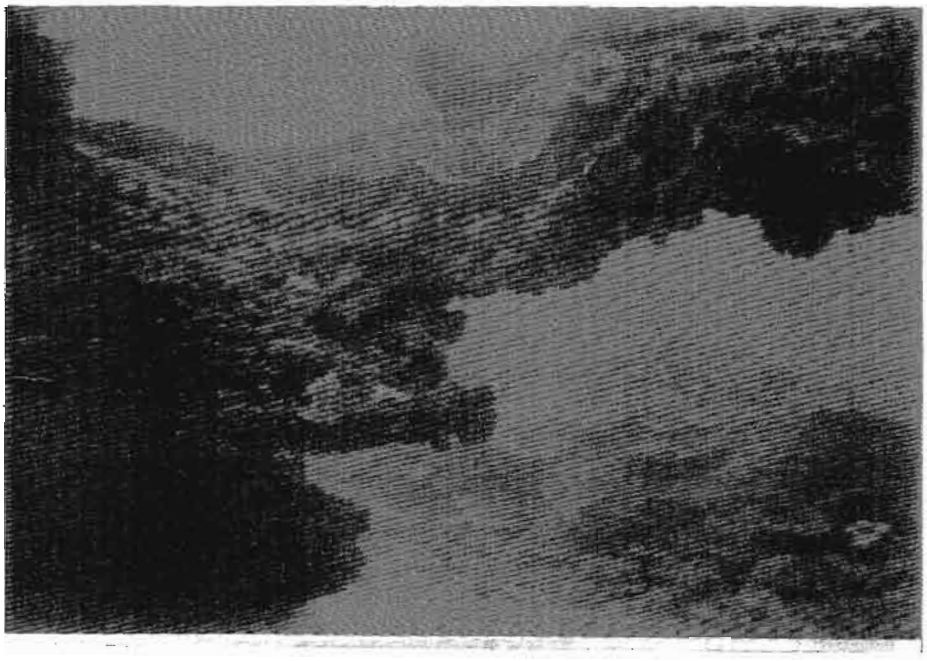

Figure 5.7. A competent aeolian foreset forming a natural underwater arch on Four-Mile Reef at -21m. Aeolian foresets on this reef give a palaeo-wind vector towards the north. The field of view is ± 4m.

level. They have a ^{14}C-age of 3780 ± 60 B.P. (laboratory analysis no. Pta-5052).

The offshore beachrocks and aeolianites on the shelf at Sodwana Bay formed during late Pleistocene regressions and may be used to delineate late Pleistocene palaeocoastlines (Ramsay, 1990a; Ramsay & Mason, 1990a&b). These submerged, coast-parallel, carbonate-cemented, coastal facies extend semi-continuously from -5m to -95m. The mineralogy, cementation history and detailed facies analysis is discussed further in Chapter 7. As mentioned earlier, aeolianites display a more rugged microtopography than beachrocks do. This topographic relief is formed by the outcropping of competently cemented, steeply dipping aeolian foresets (Fig. 5.7).

5.1.1.1 Sedimentary structures and features

The dominant primary sedimentary structures found on the carbonate-cemented sandstone outcrops include high-angle planar cross-bedding and depositional dip bedding. Orientation and dip of the foresets and dip and strike of the bedding could only be measured in isolated places. Foreset thickness could not be determined because of extensive epifaunal growth on the reef-base.

The large-scale, high-angle foresets on the reef-crest of Two-Mile Reef, dipping at 10-30°, indicate a dominant palaeocurrent transport direction towards the east (Fig. 5.8). Other minor palaeocurrent directions indicate transport directions towards the west (5° dip), the north-northeast (16-20° dip), and the southeast (15-30° dip) (Fig. 5.8). These sedimentological data define the reef-crest, carbonate-cemented sandstone as an aeolianite. These palaeocurrent directions are similar to those found in the large, vegetated, longitudinal, Holocene dunes on the present coastline.

Numerous, high-angle, planar cross-bedded units occur on the reef-crest of Four-Mile Reef. The reef-crest outcrop is a fine-grained, ferruginous, calcareous sandstone with the foreset units forming

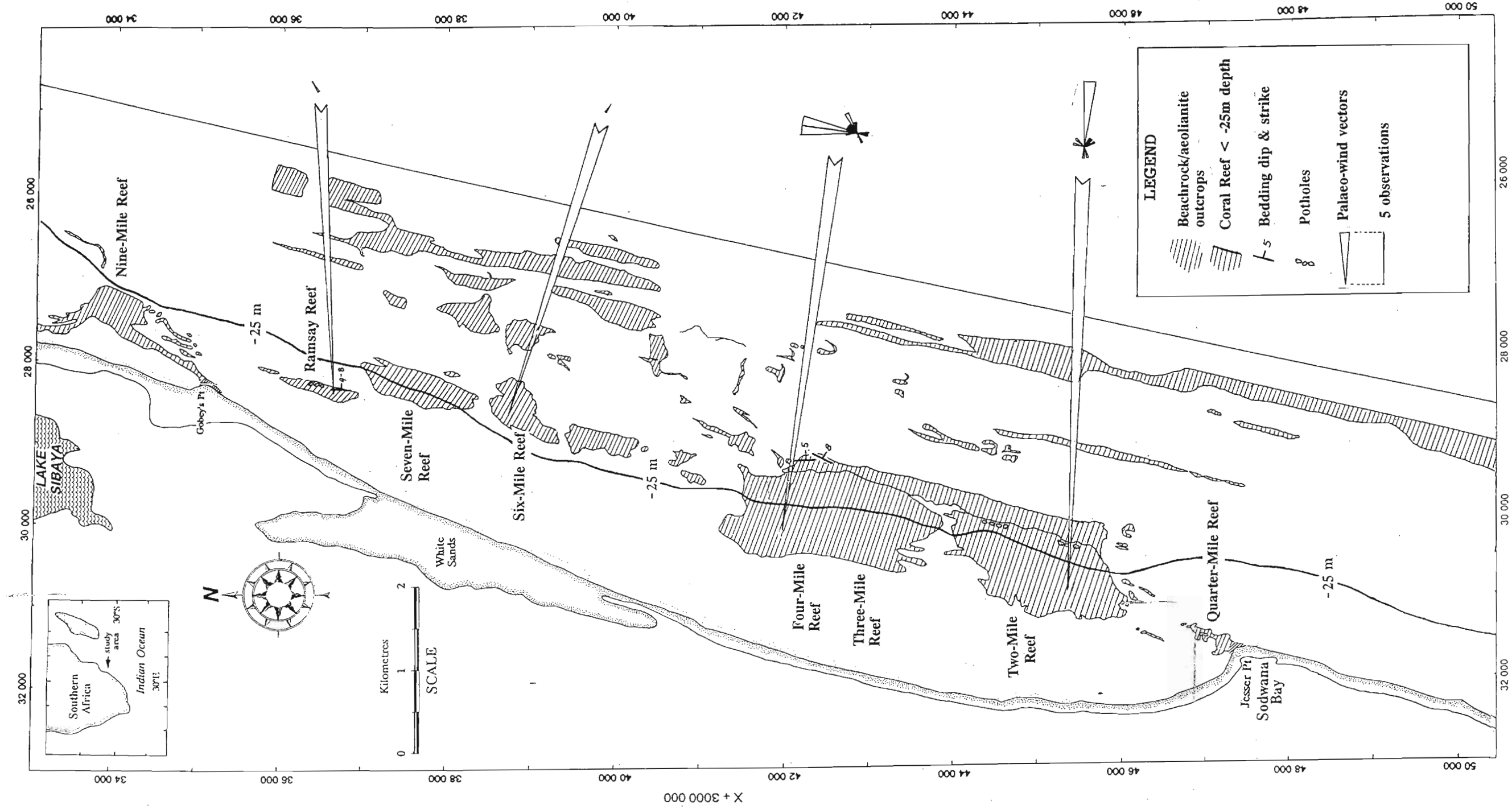

Figure 5.8. Distribution of beachrock/aeolianite outcrops on the Sodwana Bay shelf showing palaeocurrent directions, primary sedimentary dip, and outcrop erosional features.

rugged, coast-normal ridges rising 2m above the average reef level. The spacing between these ridges is approximately 50m with a lateral extent of 100m. Palaeocurrent transport directions inferred from the planar cross-bedded units indicate a transport direction towards the north (10-30° dip; Fig. 5.8). Other minor transport directions are towards the northeast (12-28° dip) and the south-southeast (10-30° dip). The reef-crest of Four-Mile Reef appears to represent a transverse dune sequence formed by a dominant southerly wind. Similar transverse dunes can be seen at the base of large, vegetated dunes along the Zululand coastline (Fig. 5.9).

Other areas where high-angle (20-30°) planar cross-bedded units have been observed include Six-Mile Reef, Seven-Mile Reef, and Ramsay Reef. These aeolian foresets indicate a palaeocurrent transport direction towards the west and southwest (Fig. 5.8). Primary sedimentary bedding was occasionally observed in the submerged beachrock outcrops. These structures typically dip 5-8° (Fig. 5.8) east and correlate with the seaward dip of beaches and Holocene beachrock along the Zululand coastline. Occasionally 5° westerly dips were noted in the beachrock sequences, these indicate the primary bedding of backbeach or washover fan facies, as found in the modern environment. As a general rule the reef-crests of the reefs are invariably aeolianites, and the fore-reef environments are beachrock or intertidal facies.

Erosional features evident on the submerged beachrocks and aeolianites include prominent gullies trending in various directions (Map 2; see also Figs. 5.11B & 6.7), and sea-level planation surfaces with or without the presence of potholes. Three sets of inter-reef gullies transect the reefs in two major directions (Map 2). Two sets strike at 010-015° and form ellipsoidal to irregularly-shaped holes up to 200m long and have a maximum relief of 3m. These two gully sets occur on what is now reef-crest and fore-reef at depths of -13m and -17m respectively. These gullies may be remnant rock pools and other erosional features incised by wave and tidal action on the consolidated beachrock/aeolianite during periods when sea-level was substantially lower than at present. The implied origin of these

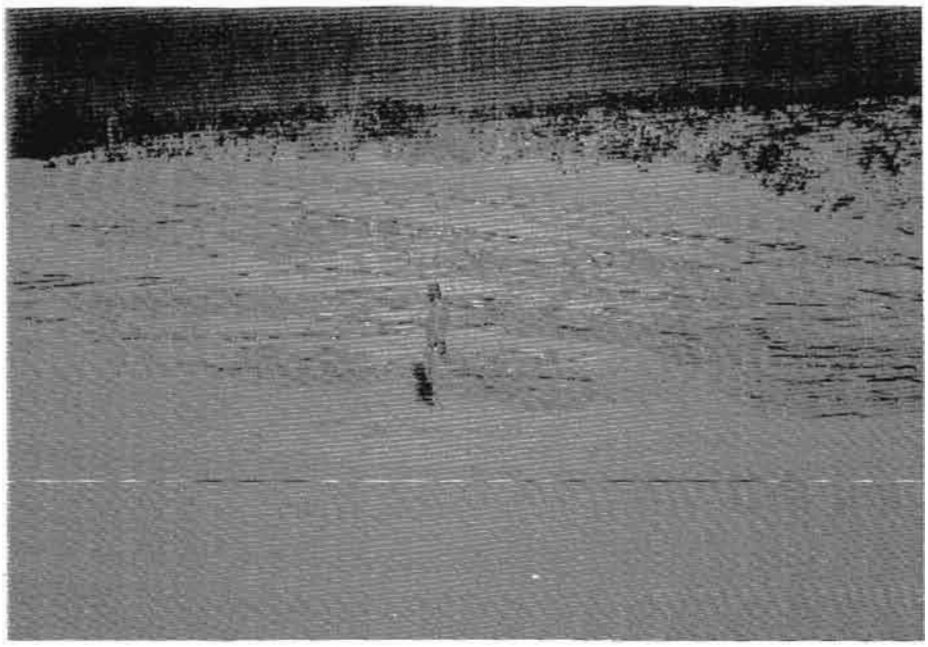

Figure 5.9. Cross-section through a transverse dune on the upper foreshore, 10km north of Jesser Point. The dominant foreset dip is towards the north and these are thought to be the modern equivalent of the aeolianite which forms the substrate of Four-Mile Reef.

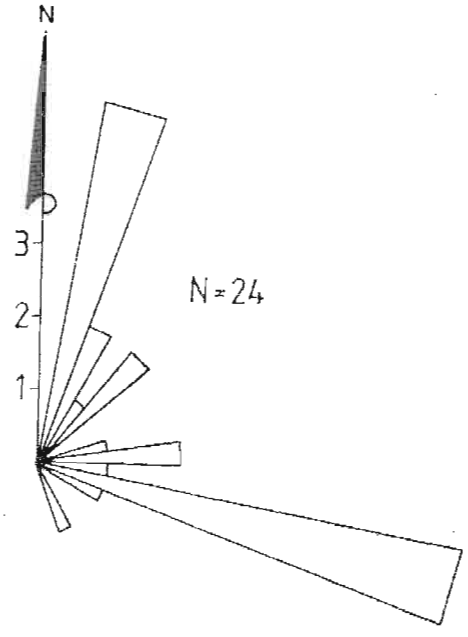

Figure 5.10. Rose diagram of intertidal beachrock joint direction trends in the study area. The two major joint trend orientations are NNE (coast parallel) and ESE (coast perpendicular).

larger, north-trending sets of gullies on the fore-reef probably relates to a sea-level still-stand at -17m during the Holocene transgression. The other north-trending set of gullies on the reef-crest at -13m relates to a later Holocene still-stand. Maud (1968) found evidence of sea-level stillstands on the Zululand continental shelf at -11m, -18m, and -36m. These first two correlate well with the sea-level stillstands that would have been necessary to produce the gully incision and pothole formation. Similar gully and pothole structures are visible on the modern wave-cut platform at Jesser Point, Sodwana Bay. A third set of inter-reef gullies strike at 120-130° and occur on the reef-crest and fore-reef. They tend to be narrow, straight to sinuous gullies, which can extend for up to a few hundred metres in length and generally have a relief of less than 1m. This gully set is probably related to erosional scouring of wave and tidal currents along joint planes in the reef-base. The strike of these inter-gullies is in agreement with readings taken on joint planes produced by wave under-cutting and block slumping on the exposed intertidal beachrocks on the shore (Fig. 5.10). Guilcher (1988) has noted similar fractures and slab slumping owing to undercutting in beachrock exposed on shorelines. Siesser (1974) describes two directions of jointing in intertidal beachrocks in the southwestern Cape; one parallel and one normal to the coast. These have become avenues of erosion, cutting the beachrock into isolated "buttes". This correlates well with the relative orientation and morphology of the gully structures observed underwater on Two-Mile Reef.

The potholed sections of the reefs occur at depths of -18m, -32m, and -47m (Fig. 5.8). These potholes were formed by diurnal solution, mechanical scouring, and biological protection of the inciplent rim during a lower sea-level. Individual mechanisms are described by Alexander (1932), Emery (1946), Coetzee (1975a&b), and Guilcher (1988). Gully development and pothole formation are related to stillstands in the Holocene (Flandrian) transgression or to post-lithification erosional features during the late Pleistocene regression.

5.1.2 Coral reefs

Coral reefs cannot be discriminated from rocky reefs on the sonograph images as coral reef morphology is controlled by the underlying lithology. Reefs at depths of less than -25m are generally true coral reefs (Map 2; Fig 5.8); this was confirmed by extensive SCUBA diving surveys. The sonograph images from coral reef areas are highly reflective and indicate a rugged microtopography consisting of pinnacles and ledges (Fig. 5.11). Numerous gullies are observed and these are filled with rippled, bioclastic sediment (Fig. 5.11). The pinnacles on the reef are defined by pronounced acoustic shadows on the record.

The coral reefs on the northern Zululand shelf are the most southerly coral reefs in Africa, and owe their existence to clear, subtropical water carried southward by the warm Agulhas Current and the absence of silt-carrying rivers in the coastal hinterland (Ramsay, 1987 & 1988; Ramsay et al., 1989; Ramsay, 1990a&b; Ramsay & Mason, 1990a&b). The depth to which significant coral cover extends is -25m and the true coral reef is assumed to be marginal beyond this depth (Ramsay & Mason, 1990b). Reduced light intensity at this depth hinders the development of the photosynthetic, symbiotic alga zooxanthellae within the coral tissue and this leads to a decrease in coral density (Ramsay & Mason, 1990b).

These reefs can be classified as patch reefs and are thin veneers of Indo-Pacific coral species which have colonised submerged, late Pleistocene aeolianites and beachrocks (= reef-base) (Ramsay, 1988, 1990b; Ramsay & Mason, 1990a&b). The maximum coral thickness capping the reef-base is 30-40cm and this thins towards the reef margins. The reefs are windward reefs with zones parallel to the north-northeast south-southwest reef/coast trend. Eight distinct zones can be recognised and differentiated on the basis of physiographic and biological characteristics (see Chapter 6). The reef fauna is dominated by an abundance of alcyonarian (soft) corals, which constitute 60-70% of the total

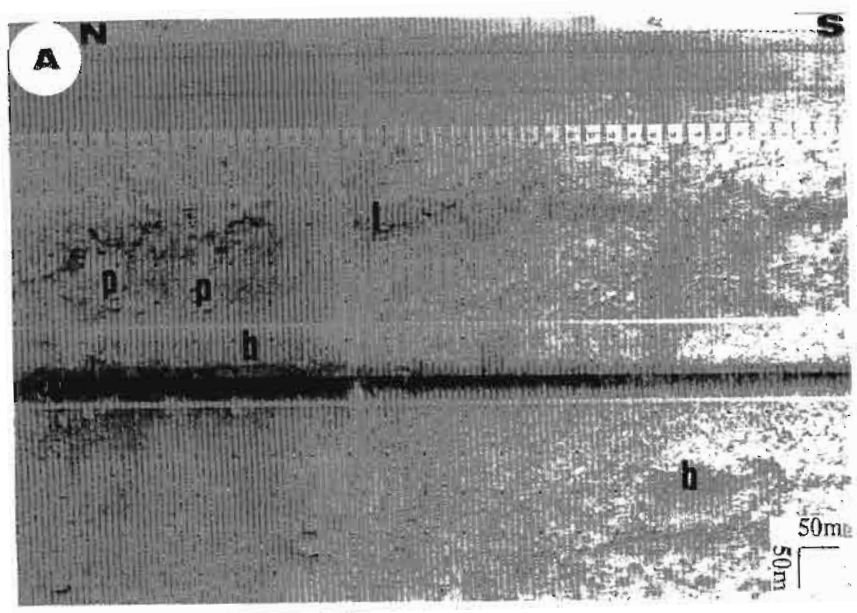

Figure 5.11. Sonargraph images from Four-Mile Reef showing the highly reflective, rugged microtopography of a coral reef (A), consisting of ledges (l) and pinnacles (p) (X+3042334;Y+30140). (B) Numerous gullies on the reef are filled with rippled, bioclastic sediment (b). (X+3043595;Y+26698).

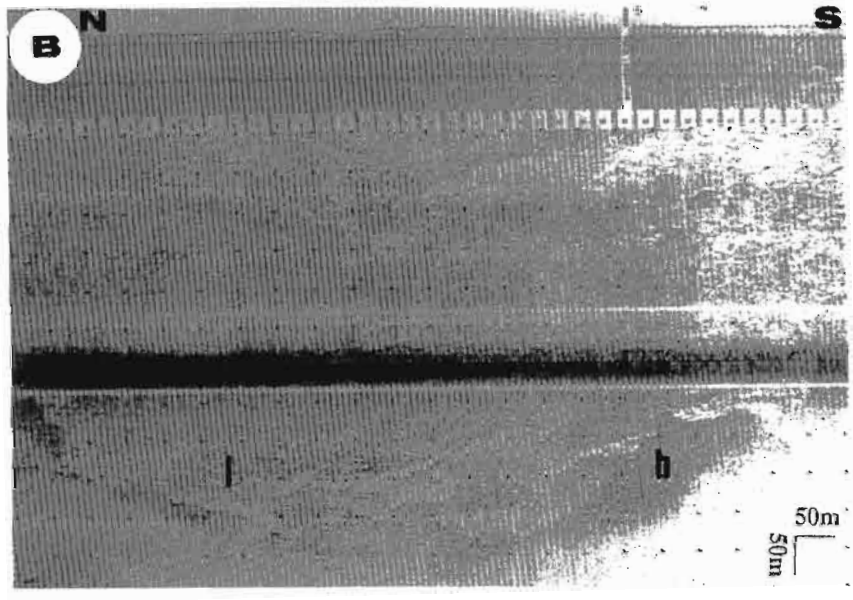

coral fauna (Fig. 5.12). Other common reef fauna elements are Scleractinia (hard corals) and two other subordinate anthozoan orders, Gorgonacea (sea fans) and Antipatharia (black corals). Molluscs, foraminifera, calcareous algae, sponges, and ascidians are also important contributors to the reef biomass.

The reefs can be divided into four morphological environments based on topography, depth, and geographical position. These are:

(1) back-reef,

(2) reef-crest,

(3) fore-reef, and

(4) deep reef-front environments (Ramsay & Mason, 1990b; Fig. 5.13).

The landward margin of a Zululand reef is the back-reef environment (-13m to -16m deep) and this zone is usually inclined at 3° to the west. The microtopography is generally subdued with occasional small pinnacles rising 1.5m above the average reef level. The reef margin is characterised by broken rocky outcrops, but "spur and groove" topography is observed at isolated places. These ridges strike perpendicular to the shore and have a maximum height of 40cm and within 20m of the reef margin, disappear under the fringe of bioclastic sediment which usually surrounds the coral reefs. This "spur and groove" topography is the marginal extension of the third set of inter-reef gullies described in 5.1.2. Inter-reef gullies are poorly developed in the back-reef environment compared to the rest of the reef.

The reef-crest is the shallow, high energy, and rugged central axis of the reef which is parallel to the coast. Numerous deep gullies, overhangs and pinnacles are developed at depths varying from -9m to -13m. This resembles the "spur and groove zone" described by Pichon (1974) on the fringing reefs of southwest Madagascar. The deep gullies on the reef-crest sometimes provide a geological window into

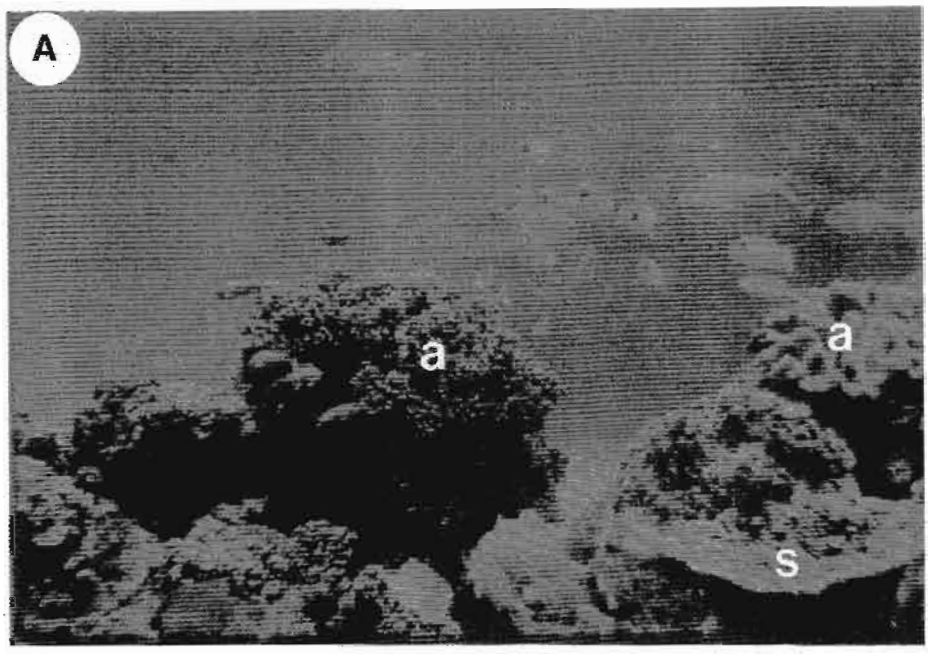

Figure 5.12. Underwater photographs taken on the reef-crest of Two-Mile Reef (-13m) showing the dominance of alcyonarian corals (a) over scleractinian corals (s). The fields of view are ± 4m (A) and 2.5m (B).

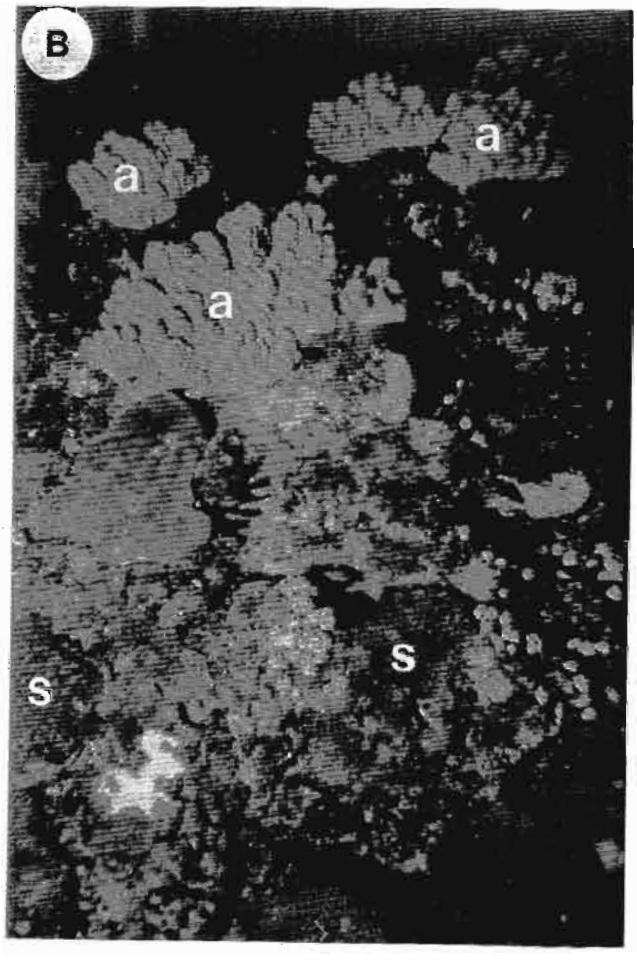

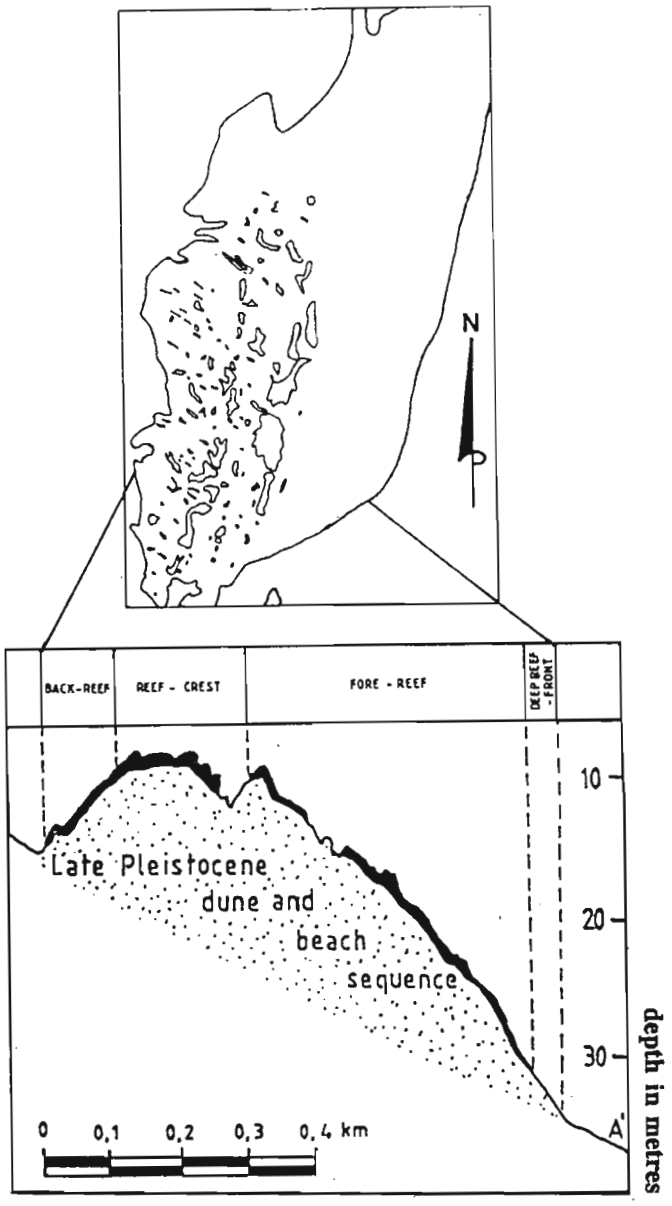

Figure 5.13. Map and cross-section of Two-Mile Reef (a typical northern Zululand coral reef) showing depths and distribution of the reef's morphological environments.

the underlying facies. The only reef-base sedimentary structures found on the coral reefs were located here.

The -13m to -30m deep seaward margin of the reefs, dipping at approximately 3.5° to the east, is the fore-reef environment. The microtopography is subdued with occasional pinnacles rising 3m above the average reef level. The fore-reef usually has two distinct sets of inter-reef gullies oriented at 010° and 120°. The deep reef-front environment is the -30m to -35m seaward extension of the coral reefs and consists of broken rocky outcrops and with occasional pothole development.

5.2 UNCONSOLIDATED LITHOLOGIES

5.2.1 Quartzose shelf sand

The most common unconsolidated sediment type on the shelf is quartzose shelf sand (Map 2). This sediment is the surficial expression of the Holocene sand prism described by Martin & Flemming (1986). Martin & Flemming (1986) noted a sediment-prism thickness of 19m south of the study area (28°S) and Sydow (1988) found a comparable thickness of 25m offshore of Leven Point, 43km south of Sodwana Bay.

Sonograph images from this sediment are weakly reflective, smooth, and even-toned due to the uniform grainsize of the sediment and lack of bedforms large enough to be resolved by side-scan sonar (Fig. 5.14). The quartzose sand from the inner-shelf is generally fine-grained, moderately- to well-sorted, and coarsely- to near symmetrically-skewed. Carbonate content is low, and varies between 4-13%. Quartzose sand from the outer-shelf is fine-grained, moderately- to well-sorted, and coarsely- to very coarsely-skewed. The inner-shelf quartzose sand is better sorted than the outer-shelf sediment due to increased reworking of this sediment by the high-energy swell regime. Sediment from the shallower

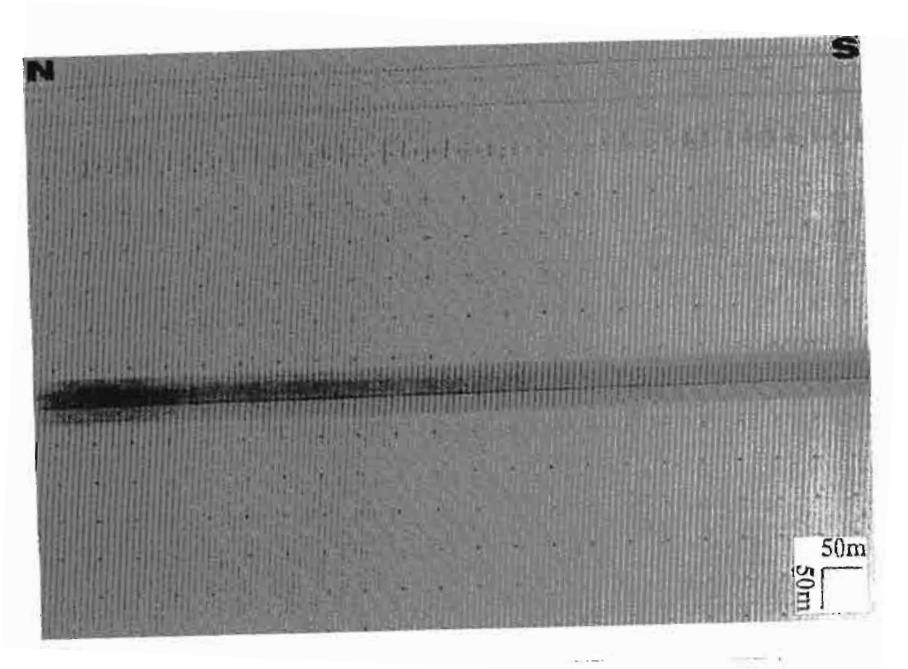

Figure 5.14. Sonargraph image of quartzose shelf sand. This sediment is weakly reflective, smooth, and even-toned due to the uniform, fine grainsize of the sediment.

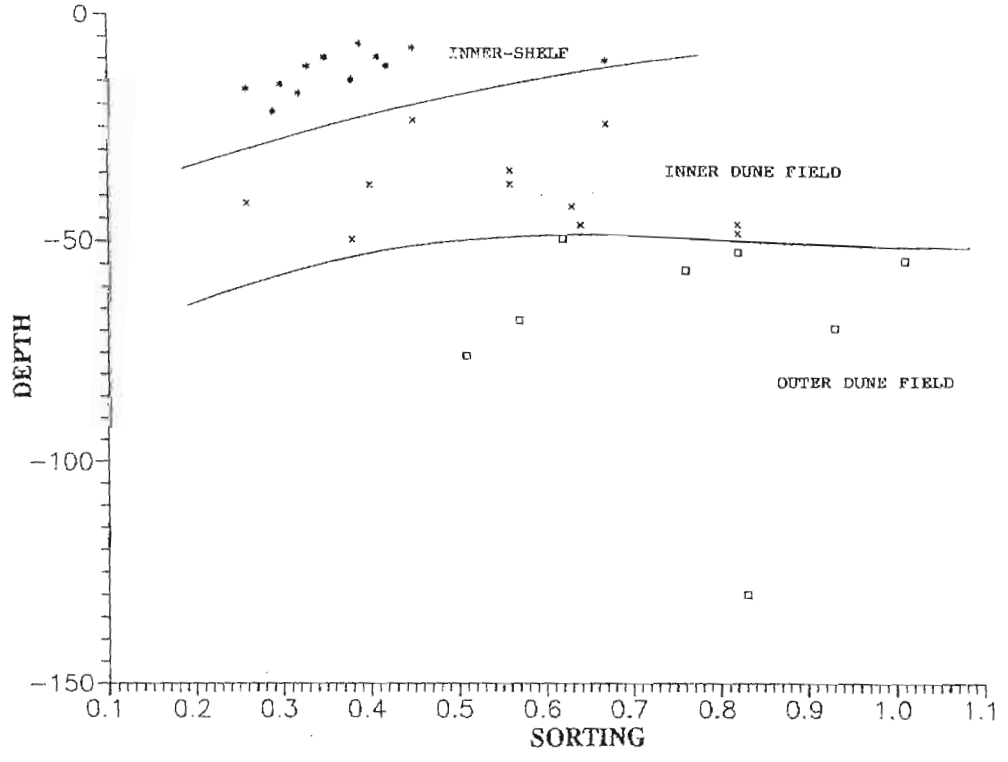

Figure 5.15. A graphical representation of the depth verse sorting relationship of inner-shelf, inner dune field, and outer dune field sediment.

areas of the outer-shelf (< -50m) is better sorted than sediment from depths of greater than -50m. A combination of wave- and geostrophic-reworking in the shallower areas of the outer-shelf result in the higher degree of sorting A graph of depth verse sorting (Fig. 5.15) has been prepared for sediment from the inner-shelf, inner dune field, and outer dune field, illustrating the decrease in sediment sorting with increasing depth.

Generally wave-reworking of sediment from the Sodwana Bay shelf results in greater sediment maturity than that observed from geostrophic current effects or a combination of geostrophic and wave-reworking.

5.2.2 Bioclastic sediment

Most of the skeletal detritus in sediments associated with coral reefs originates from the mechanical and biological destruction of the reef framework and associated organisms (Scoffin, 1987). Local and gradual variations in depth and circulation in the reef tract produce differences in fauna and flora from one area to another resulting in sediments with varying abundances of the major constituent organisms (Swinchatt, 1965). Thus the way organisms break down leads to sediment differentiation dependant on grain-size, whereas different source areas of the various organisms produce a separation according to organic composition (Maxwell, 1968).

Bioclastic sediment on the Sodwana Bay shelf is defined as having a $CaCO_3$ content of greater than 20% and is a mixture of biogenic-derived debris and quartzose sand. A regional surficial sediment study (Moir, 1975) revealed that the Zululand shelf was covered by sands containing only 5-25% carbonate. The substantial proportion of biogenic fragments imparts a highly reflective, even-toned to granular image to the sonograph record (Fig. 5.11A&B). The chief skeletal remains contributing to the bioclastic sediment on the shelf are; molluscan fragments, foraminiferal tests, sclerites of soft

corals and sea fans and cirriped fragments (Fig 5.16). Other components are echinoderm spines and test fragments, bryozoan fragments, hard coral and calcareous algae remains, as well as spicules from sponges. Figure 5.16A shows the general distribution of biogenic fragments in the carbonate fraction of shelf sand together with examples of benthic foraminiferal tests (Fig. 5.16B) and alcyonarian (soft coral) sclerites (Fig. 5.16C). Bryozoan, echinoid, and cirriped fragments (B-E-C fragments) have been summed to simplify the distribution pie-charts in Figure 5.17.

The distribution of bioclastic sediment in the study area is widespread, with reef-derived and outer-shelf-derived populations being evident (Fig. 5.17). The reef-derived bioclastic population is confined to depths of less than -40m and located in close proximity to reef areas. The shelf-derived bioclastic population occurs at depths of greater than -40m and is derived from carbonate-producing organisms from deep water reef and soft-substrate environments on the shelf.

Reef-derived bioclastic sediment, comprising coarse biogenic material (mainly of molluscan origin), forms a carbonate fringe and isolated lenses around the coral reefs, such as Two-Mile Reef (Fig. 5.17). Other important reef-derived bioclastic components include sclerite, foraminifera, bryozoan, cirriped, and coral fragments. The carbonate-rich sediment rests on and progrades in all directions from the reef environment over quartzose sand. Bioclastic sediment distributions are influenced by the interaction of the dominant swell direction and the morphology of the reef, but are controlled by the strength and response of the off-reef currents to the topographic setting around the reef (Ball, 1967). Two current shadows are developed within the bioclastic sediment which surrounds Two-Mile Reef (Fig. 5.17). A 150m long current shadow is evident on the southern margin of the reef in response to the southward-flowing Agulhas Current occasionally washing over the reef and reworking the bioclastic sediment southwards (Ramsay, 1987). The other current shadow occurs on the landward margin of the reef in response to reworking by the dominant wave-front direction (Ramsay, 1987). The general trend is a decrease in carbonate content away from the reef consistent with a decrease in effective wave

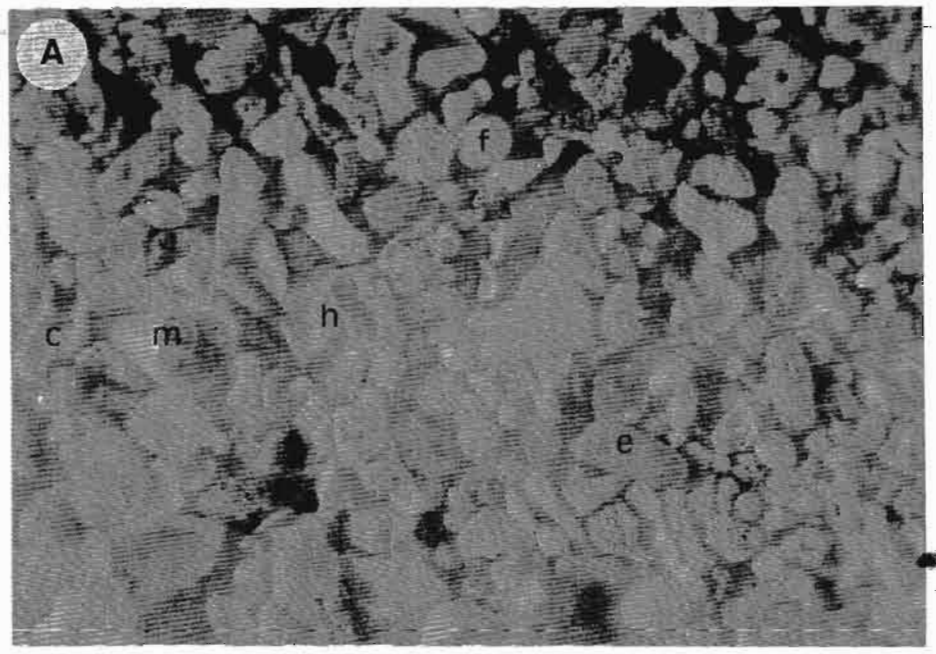

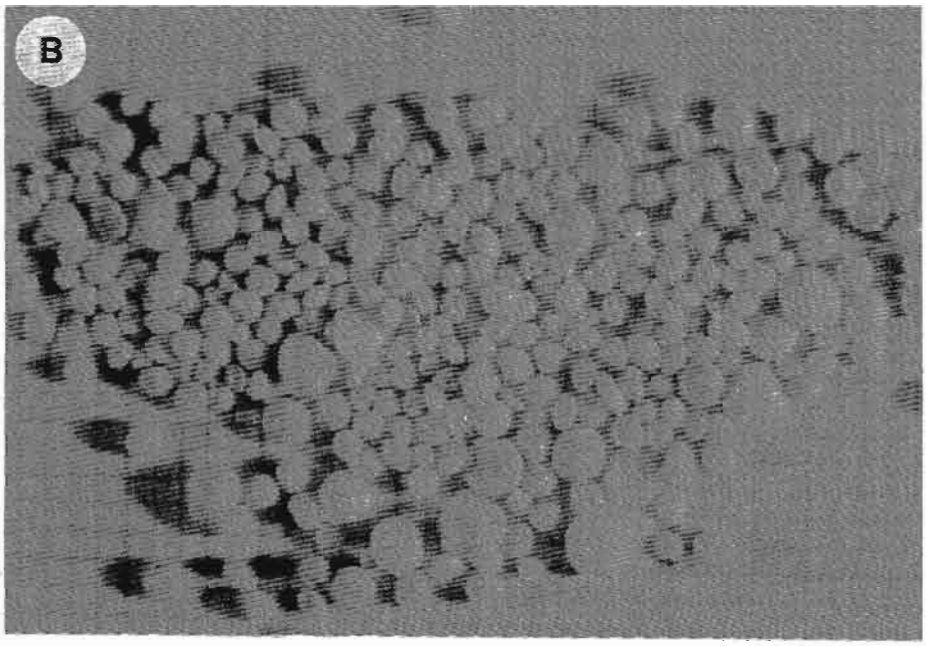

Figure 5.16. Bioclastic sediment derived from Two-Mile Reef (A). The skeletal components are: molluscan fragments (m), foraminiferal tests (f), sclerites (s), cirriped fragments (c), echinoderm spines (e), and hard coral fragments (h). (B) shows a selection of benthic foraminifera and (C) shows a selection of soft coral sclerites.

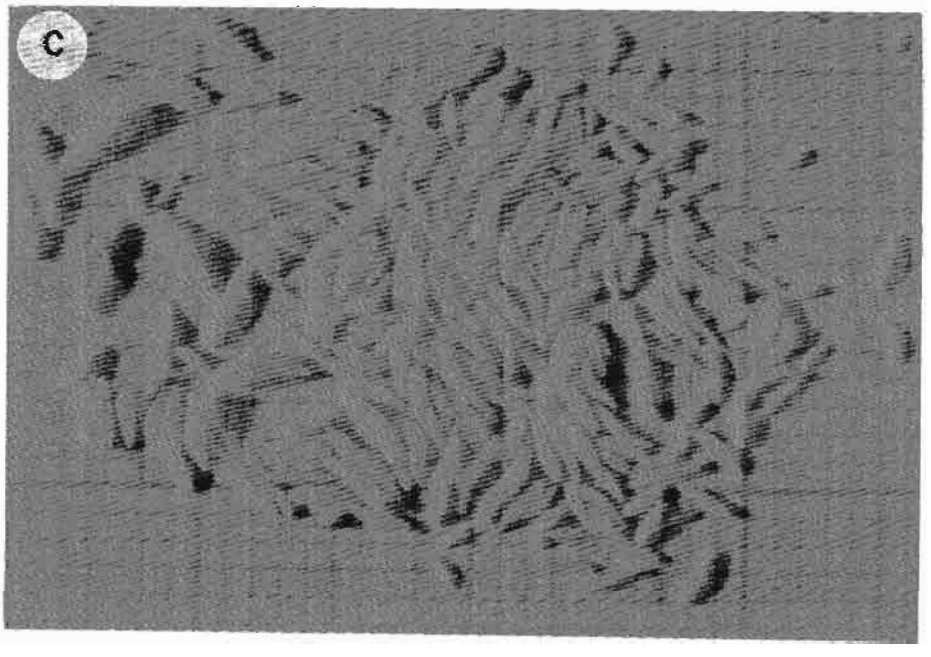

5mm

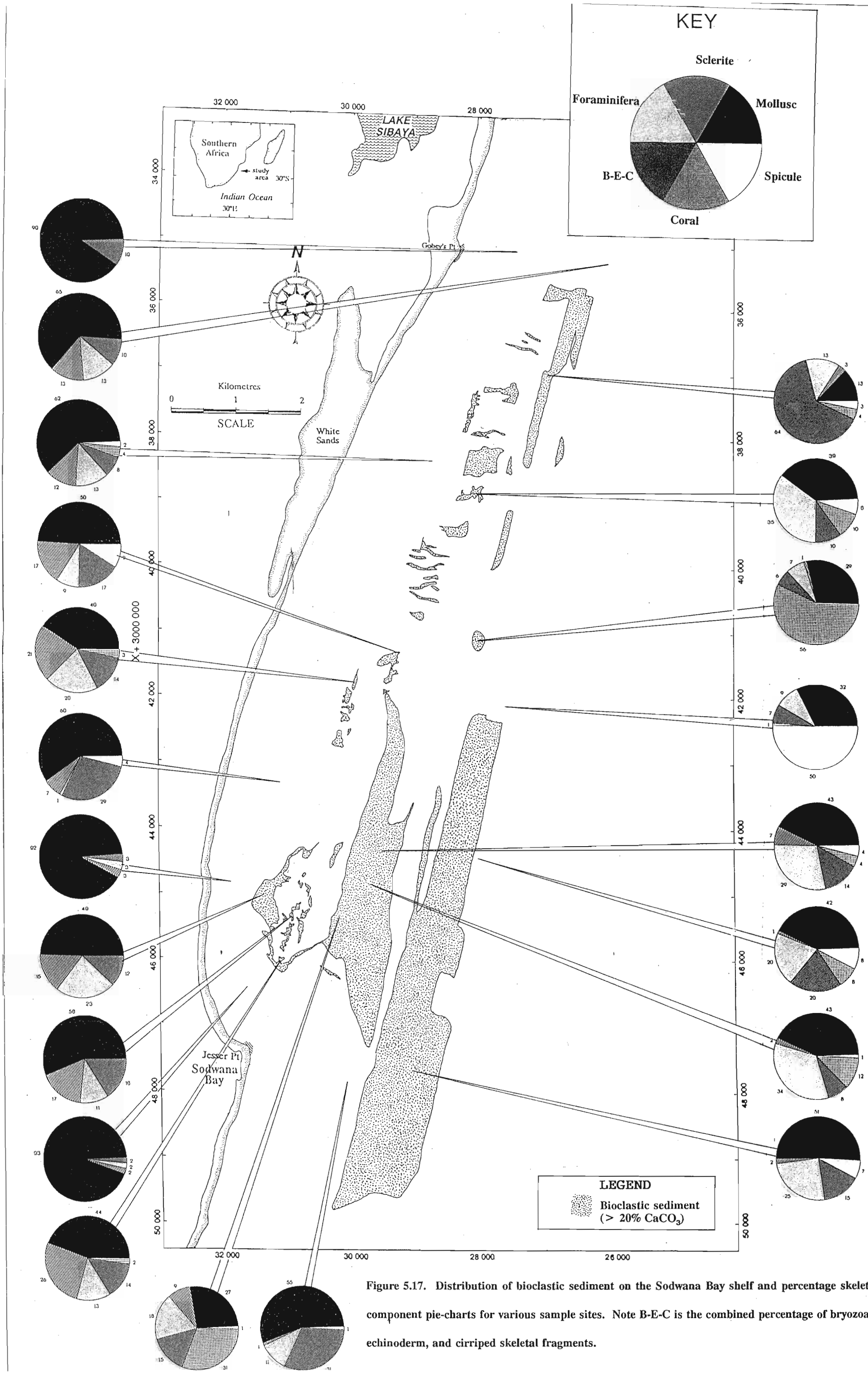

Figure 5.17. Distribution of bioclastic sediment on the Sodwana Bay shelf and percentage skeletal component pie-charts for various sample sites. Note B-E-C is the combined percentage of bryozoan, echinoderm, and cirriped skeletal fragments.

energy. The reef-derived bioclastic sediment is coarse-grained, moderately well- to poorly-sorted and finely- to very coarsely-skewed. Carbonate contents vary from 56-82%. The different hydraulic characteristics of reef-derived bioclastic sediment and quartzose shelf sand result in little or no mixing between these populations. The inner-shelf quartzose sand has reef-derived carbonate contents of less than 10%, mainly composed of molluscan fragments. Coral reef margin sediments consist of a dominant molluscan fraction with almost equal percentages of foraminifera, sclerite, and B-E-C fragments within the 40-80% carbonate content of the sediment.

The outer-shelf-derived bioclastic sediment is fine-grained, moderately- to well-sorted, and very coarsely-skewed. Carbonate contents vary from 20-35%. Flemming (1978) noted carbonate contents of 40-80% in outer-shelf sediments along the Natal coastline. Molluscan fragments dominate the bioclastic distribution with foraminiferal tests, and B-E-C fragments being common. The notable difference between the bioclastic component distributions of the reef- and shelf-derived populations is the increase in abundance of hexactinellid sponge spicule fragments on the outer-shelf as compared to the mid- and inner-shelf environments (Fig. 5.17). The canyon areas appear to have the highest spicule content with abundances reaching 50% of the total bioclastic sediment (Fig. 5.17). Sponges probably represent the dominant benthic deep-water fauna at depths of greater than -60m.

5.3 UNCONSOLIDATED SEDIMENTARY STRUCTURES

5.3.1 Subaqueous dunes

The classification of large-scale subaqueous bedforms has recently been revised by an SEPM working group (Ashley, 1990). Bedforms with a spacing of just under 1m to over 1 000m are now terms "dunes" instead megaripple and sand wave. Ashley (1990) recommends the term "dune" to be modified with a primary descriptor of shape (i.e., 2-D or 3-D; Fig 5.18) and size based on spacing: small (0.6-5m),

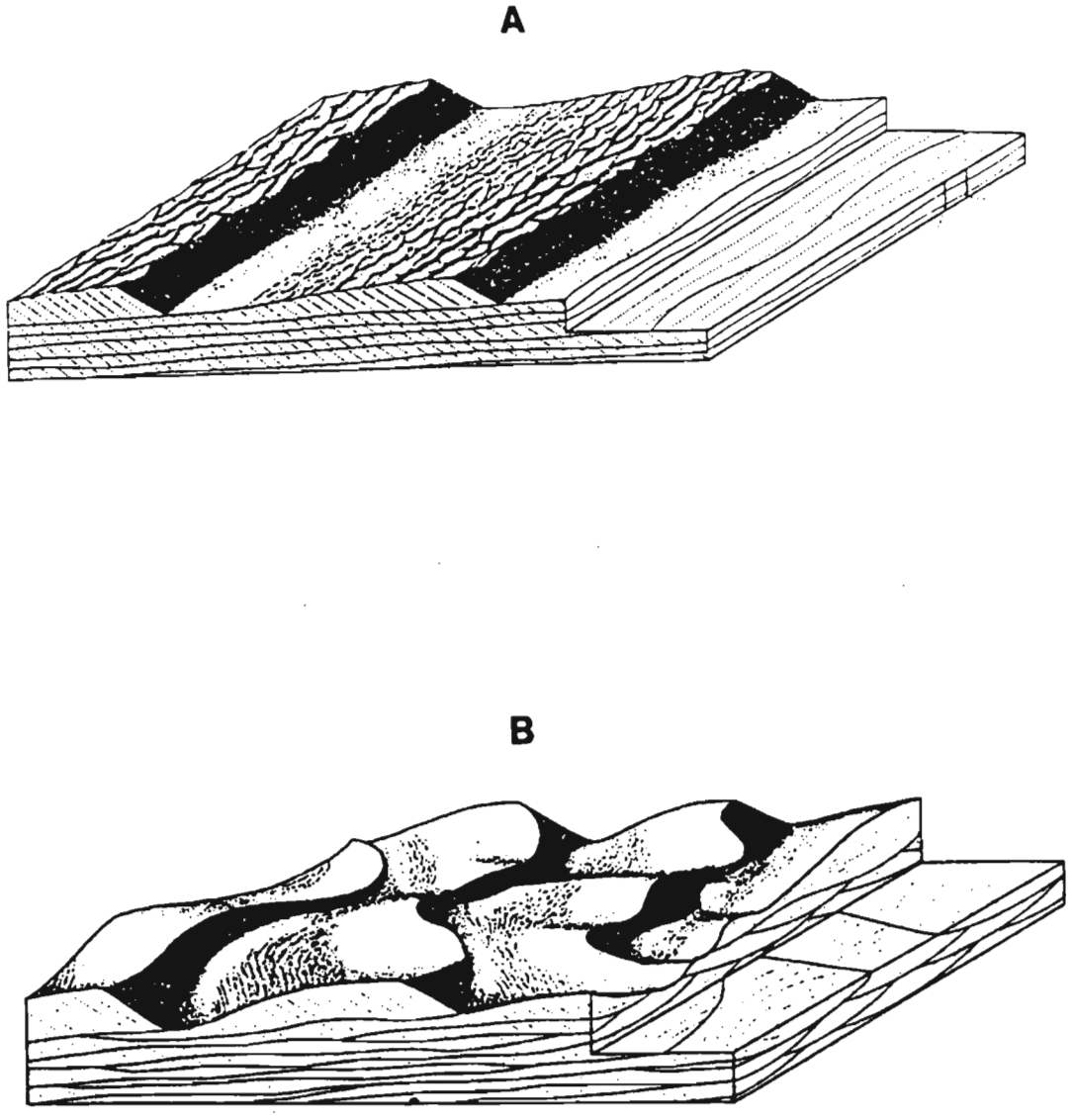

Figure 5.18. Block diagrams showing large-scale, tabular cross-stratification formed by migrating 2-D dunes (A) and large-scale trough cross-stratification formed by migrating 3-D dunes (B). Note flow in both diagrams is left to right and the length of the block could range from a few metres to as much as a few hundred metres. (From Ashley, 1990).

medium (5-10m), large (10-100m), or very large (> 100m). The adjective *subaqueous* can be used to distinguish the "dune" from *aeolian* dunes. Second order descriptors such as sediment size and bedform superposition may also be used to describe subaqueous dunes. This classification is morphologically based and descriptive and has been used to classify the large-scale subaqueous bedforms on the Sodwana Bay shelf.

The occurrence of subaqueous dunes along the southeast African continental outer-shelf is well documented (Flemming, 1978; 1980; & 1981; Flemming & Hay, 1988; Fig 5.19). From this work it is now known that sedimentary processes on the outer-shelf of this region are dominated by the Agulhas Current. These bedforms migrate south in the direction of the Agulhas Current, at depths below -50m (Flemming, 1978; Fig 5.20). The largest subaqueous dune documented by Flemming (1980) had a maximum height of 17m and a wavelength of almost 700m. Near-bottom current velocities of 1.3m/sec are necessary to produce such bedforms (Flemming, 1978). Along the northern Zululand shelf, however, 3m high dunes were noted (Flemming, 1978).

The characteristic shape of very large and large, asymmetric subaqueous dunes on the Sodwana Bay shelf can be easily recognised on the bathymetric profiles (Fig 5.21), medium-sized dunes with heights of less than 1m are however not discernible. Large- and medium-sized subaqueous dunes leave a distinct acoustic signature on the sonograph image because the dune troughs contain a substantial proportion of bioclastic debris (> 20% $CaCO_3$). These troughs show up as regularly-spaced, highly reflective, even-toned sonograph images with the finer grained dune stoss slopes giving a weakly reflective, even-toned signal (Figs 5.22; 5.23).

Subaqueous dunes occur in two depth zones on the shelf off Sodwana Bay: -45m to -70m (outer subaqueous dune field) and -35m to -55m (inner subaqueous dune field) (Figs. 5.24; 5.25; Map 2).

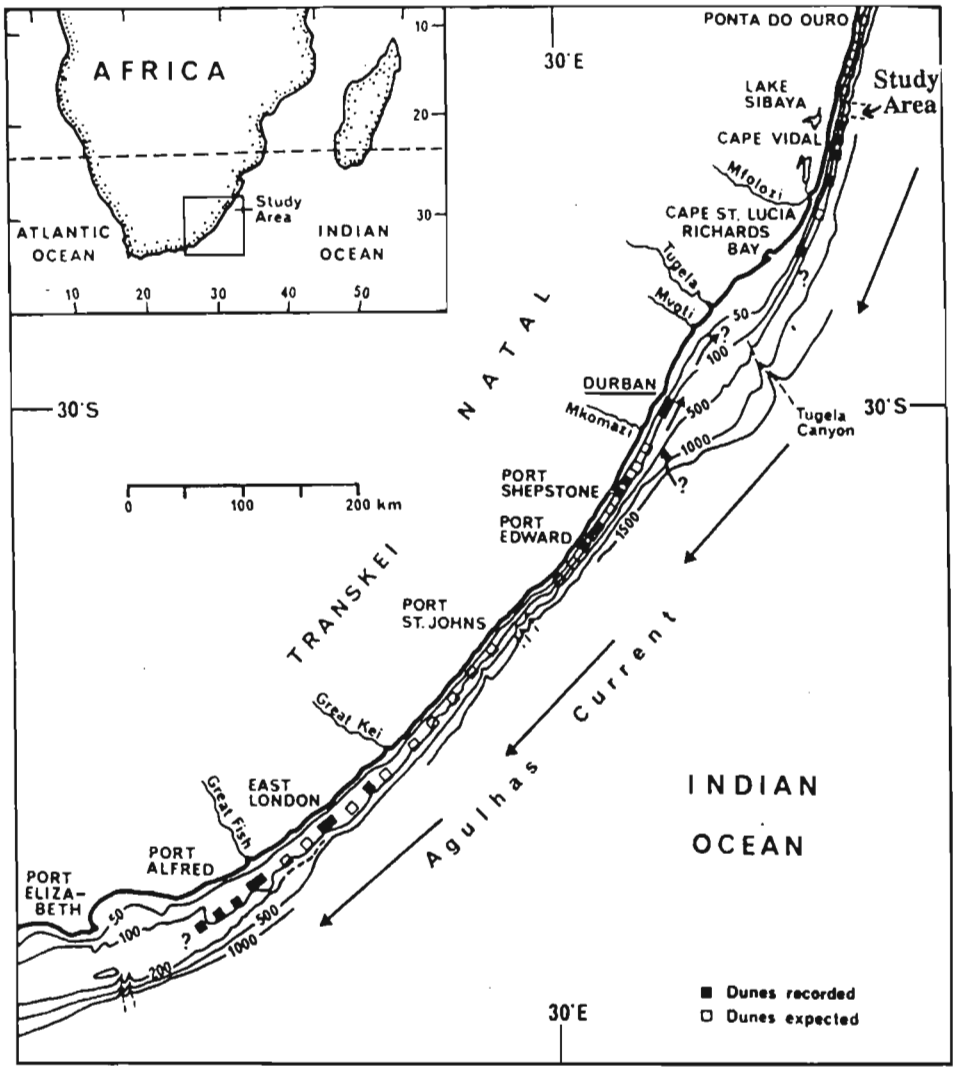

Figure 5.19. The distribution of recorded subaqueous dune fields on the southeast African continental margin. (From Flemming, 1978).

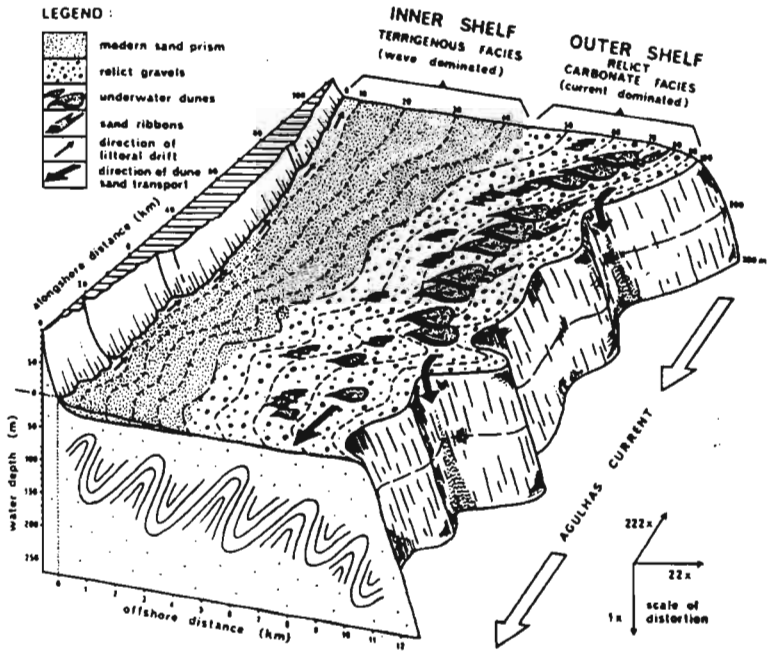

Figure 5.20. Schematic block diagram of a section of the South African shelf summarising the sedimentary features. (From Flemming, 1978).

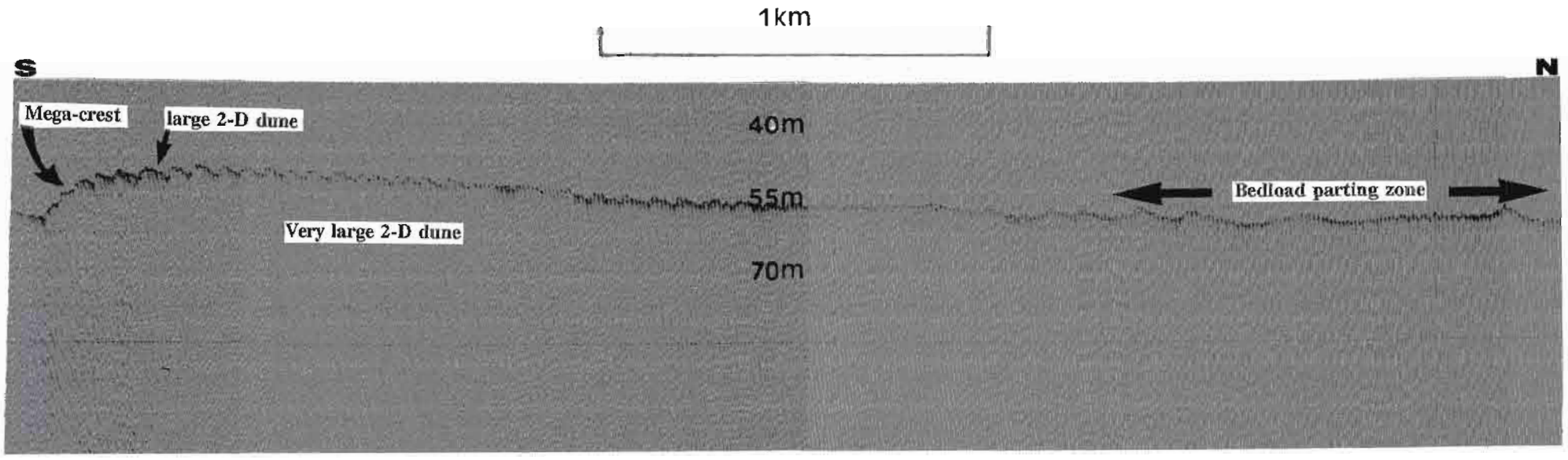

Figure 5.21. Shore-parallel bathymetric profile across the outer subaqueous dune field. Note the presence of a bedload parting zone in the large 2-D subaqueous dunes in the northern section of the dune field.

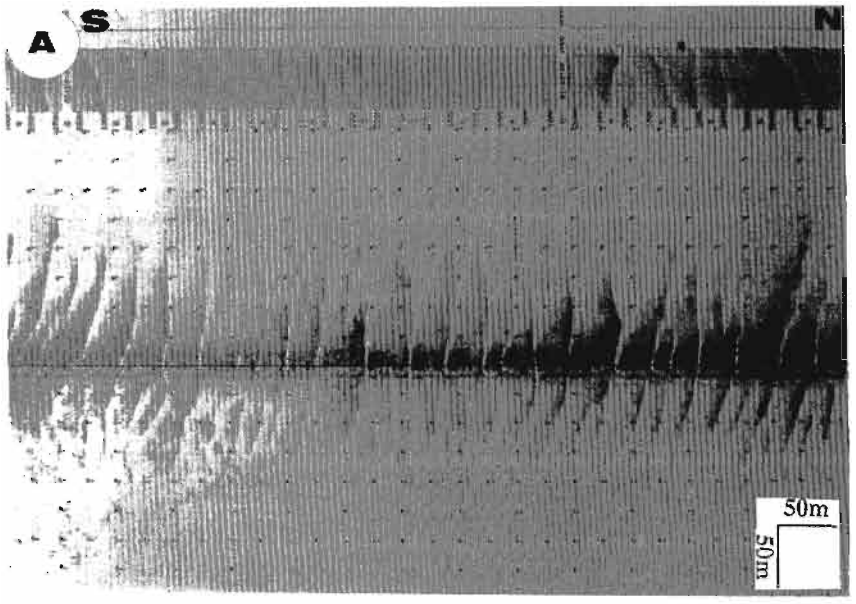

Figure 5.22. Sonargraph images of the outer subaqueous dune field. (A) Large 2-D subaqueous dune troughs are defined by regularly-spaced, highly reflective, even-toned sonargraph images with the finer grained dune stoss slopes giving a weakly reflective, even-toned signal. (B) A bedload parting zone noted in the large 2-D dunes.

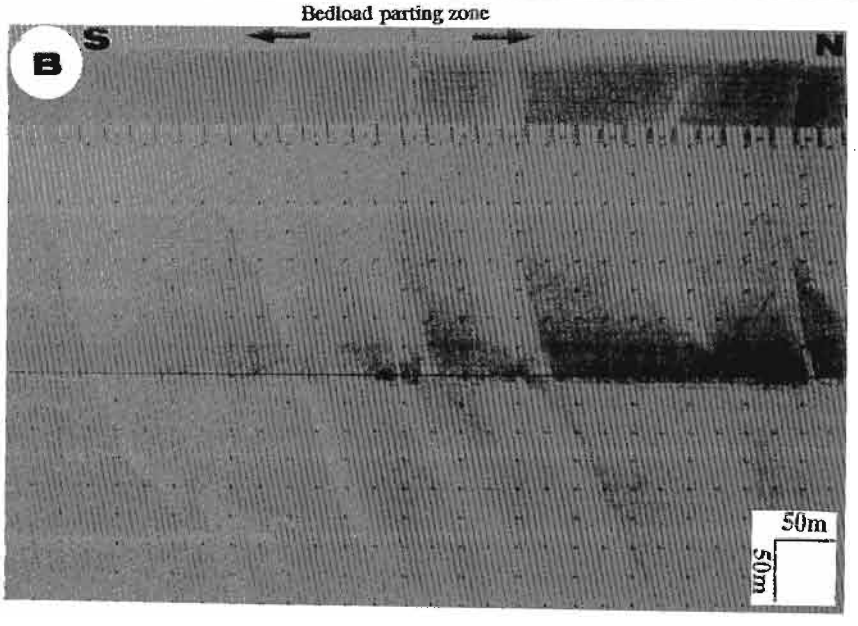

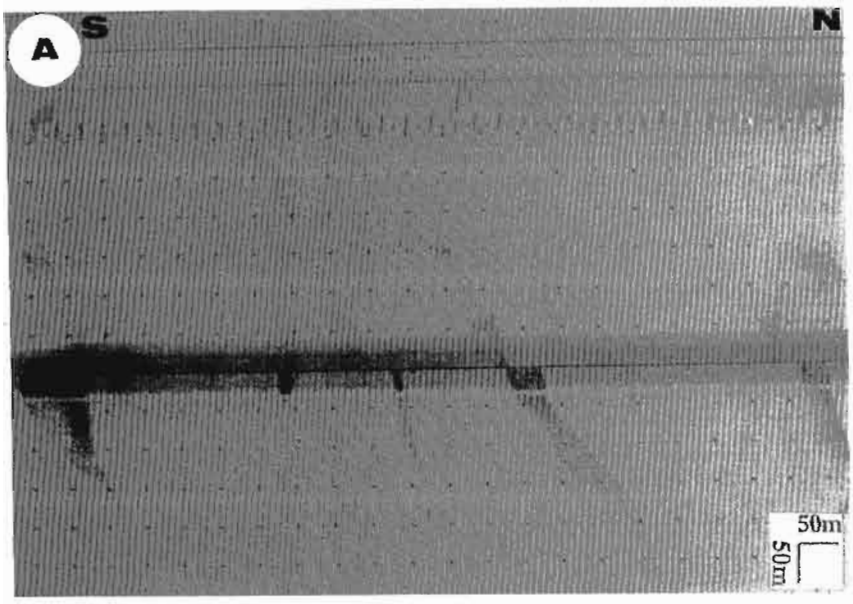

Figure 5.23. Sonargraph images (A & B) of the inner subaqueous dune field showing large 2-D dune troughs filled with bioclastic sediment (b). The sediment transport direction is towards the south. (A: X+3040084;Y+28773 B: X+3042210;Y+29783).

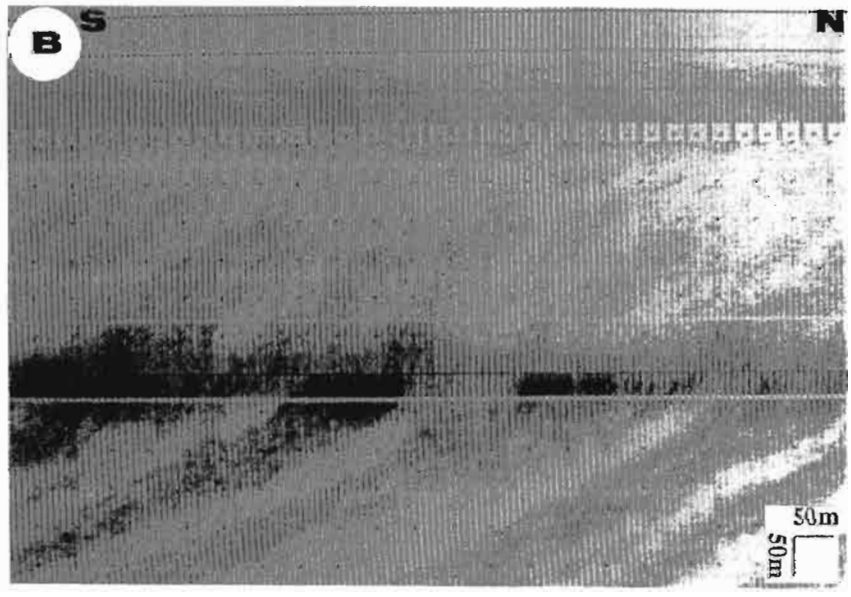

5.3.1.1 Outer subaqueous dune field

The largest, subaqueous dune field is the outer field, located 1.9km east of Jesser Point at depths of -45m to -70m (Figs. 5.24, 5.25 & Map 2). The field is confined between two linear beachrock outcrops which lie at -55m and -70m; the average depth for the subaqueous dune field being -60m. This single, very large 2-D subaqueous dune has a wavelength of 4km, a width of 1.1km and a height of 12m. This bedform is strongly asymmetrical with a long (4km) stoss slope and a very pronounced lee slope (8.1° gradient) which forms the mega-crest of the very large dune (Fig. 5.25). Two generations of bedforms are superimposed on the very large 2-D dune field: large 2-D dunes with bioclastic sediment in the troughs and small-scale sinuous to bifurcating current ripples on the stoss slopes of the large dunes. The large 2-D dunes have spacings between 45-90m and a height of 1-2m. The superimposed large 2-D dunes experience crest orientation deflections from north to south on the very large 2-D dune. The dune crest orientations vary from 110° in the north to 132-122° in the middle of the field and 090-070° in the south near the mega-crest (Fig 5.24). The mega-crest orientation is 068°. The crest orientation deflection observed in the large 2-D dunes can be related to a minor meander in the Agulhas Current due to the outer-shelf gradient becoming steeper directly east of Jesser Point. The Agulhas Current flowing along the shelf edge is forced slightly offshore in the southern part of the dune field resulting in a north to south crest orientation deflection of 60° in the large 2-D dunes. A field of large 2-D dunes with a height of 3-5m is developed due south (downstream) of the mega-crest. The sonograph image indicates that medium 2-D dunes with a spacing of 10m and a height of 0.5m are superimposed on the larger bedforms. The sediment supply required to form these southerly bedforms is derived by avalanche of the lee slope.

The dominant transport direction is south, except in the northern part of the very large 2-D dune field where a bedload parting zone exists: large 2-D dunes being transported north (Figs. 5.22B; 5.24 & 5.25). This system of migrating bedload partings in the large 2-D dunes is thought to be responsible

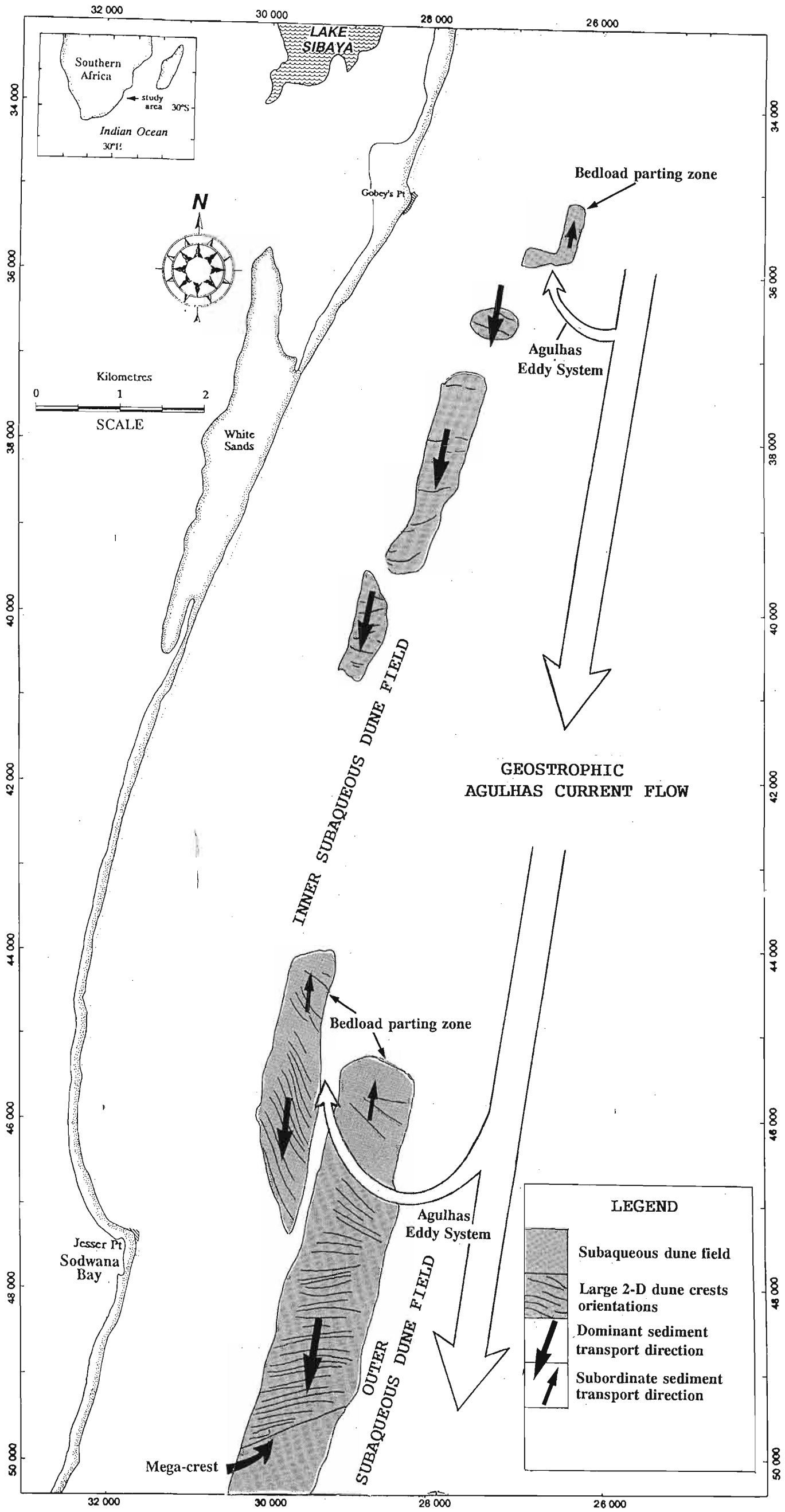

Figure 5.24. Distribution of the inner- and outer subaqueous dune fields on the Sodwana Bay shelf. The sediment transport directions and bedload parting zones are illustrated.

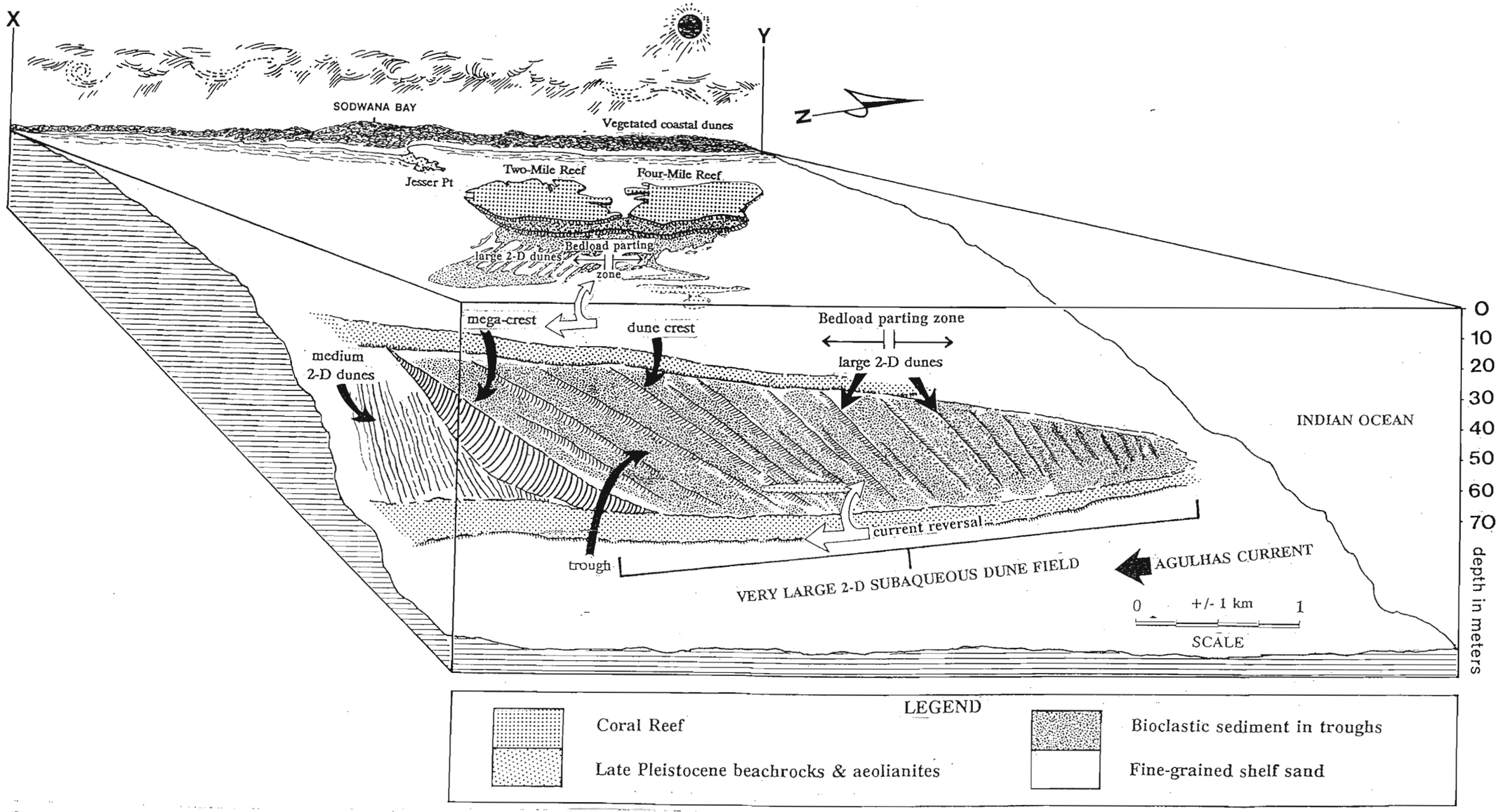

Figure 5.25. Block diagram of the features and relationships of subaqueous dunes fields on the shelf off Jesser Point. The dune fields are confined between linear beachrock outcrops.

for the formation of the very large 2-D dune field.

5.3.1.2 Inner subaqueous dune field

Part of the inner subaqueous dune field occurs 1.9km northeast of Jesser Point at depths of -40m to -50m (offshore of Two-Mile Reef; Fig. 5.24, 5.25, & Map 2). This series of large 2-D dunes, in an average water depth of -45m, is 2.9km long and 0.6km wide and is confined between two linear, coast-parallel beachrock outcrops. The dune field consists of large 2-D dunes with a spacing of 30-75m and heights of 0.5-0.75m; these features are easily recognised on sonograph images, due to the presence of bioclastic sediment in the dune troughs (Fig. 5.23). The construction of the inner subaqueous dune field is less complex than the outer field with only two generations of bedforms being evident: large 2-D dunes and superimposed small-scale current or wave ripples.

On four SCUBA dives on this bedform field, small-scale current or oscillation or interference ripples were seen superimposed on the large 2-D dunes. The large 2-D dunes do not appear to be superimposed on a larger asymmetrical bedform as occurs in deeper water off Jesser Point and no major crest azimuth changes were noted. At one locality (SCUBA dive, X + 3045750; Y + 28720), hummocks were observed in the fine-grained shelf sand (this is discussed further in 5.3.2). The dominant sediment transport direction in this dune field is towards the south. In the middle of the dune field the bioclastic dune troughs, which are usually linear, become irregularly shaped and appear to be undergoing reworking (Fig. 5.26). North of this, the large 2-D dunes begin to be transported north (Fig 5.24). This bedload parting zone is characterised by irregular bioclastic dune troughs (Fig. 5.26), and is 450m inshore and 950m north of the bedload parting zone noted in the outer subaqueous dune field.

An interesting biological phenomena occurs in the bioclastic dune troughs in the bedload parting zone:

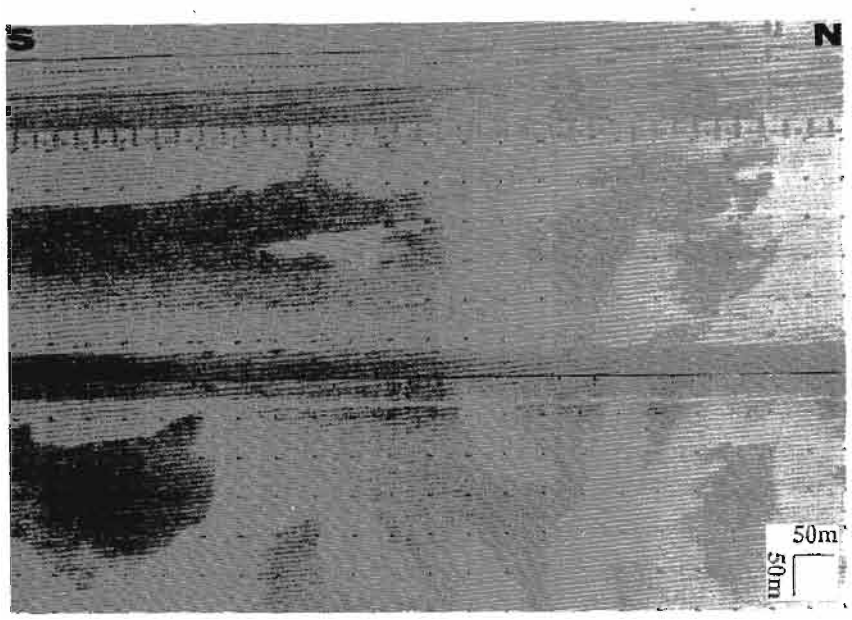

Figure 5.26. Sonargraph image of bioclastic dune troughs in the inner subaqueous dune field undergoing reworking due to the presence of a bedload parting zone. Pinna bivalve colonies occur in this area (see Fig. 5.27) (X+3045750;Y+28720).

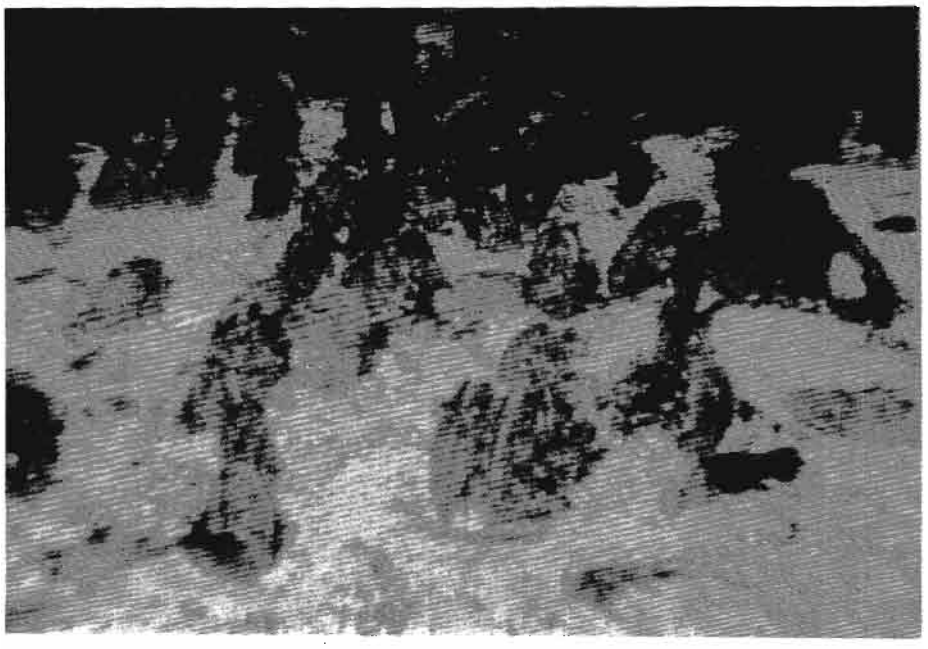

Figure 5.27. Underwater photograph of showing the great abundance of Pinna bivalves in the inner subaqueous dune field at -50m. Each bivalve is 20-25cm long. The field of view is 1m.

the great abundance of the large bivalve, Pinna muricata (Fig 5.27). The bivalves are 20-25cm in length and cover an area of approximately 83250 m^2 with a density of 20 individuals per square metre; totalling ± 1.7 million individuals.

The other inner subaqueous dune fields occur on the northern side of Wright Canyon head at depths of -35m to -55m and extend further north to 2km off Gobey's Point; a distance of 6km (Fig 5.24). This is not one continuous dune field, but a series of smaller fields comprising 2-7 individual large 2-D dunes each. These bedforms are large 2-D dunes with low heights (0.5-1m) and variable spacings (150-600m). The major crest orientation of the large dunes varies from 080-105°. The inner subaqueous dune field north of Wright Canyon is confined on the landward side by a series of beachrock/aeolianite outcrops at -25m to -35m which define the mid-shelf. The dune field is partially confined on the seaward side by beachrock/aeolianite outcrops at depths of -50m to -60m. The troughs, which are clearly defined on the sonograph image by highly reflective bioclastic sediment, are linear or irregularly shaped. Ground-truth diving on these troughs has revealed that sinuous oscillation ripples are developed in the trough bioclastic sediment. These ripples have an orientation of 028°, a wavelength of 30-40cm and an amplitude of 10cm.

The dominant transport direction in this dune field is south (Fig 5.24). Sediment moving south intersects the canyon head of Wright Canyon and cascades down the canyon walls (Fig. 5.28) as debris flows (see Chapter 4; Figs. 4.7 & 4.8). In the far north of the study area a bedload parting zone exists in the inner subaqueous dune field (Fig 5.24). North of this zone the bedform transport direction is towards the north and the fluctuation in sediment transport directions is responsible for an increase in the large dune height to 2 m just north of the bedload parting zone. Sediment starvation and a reduction in current velocity are probably the cause of the large 2-D dunes in the northern section of the inner subaqueous dune field being less well developed than those further south.

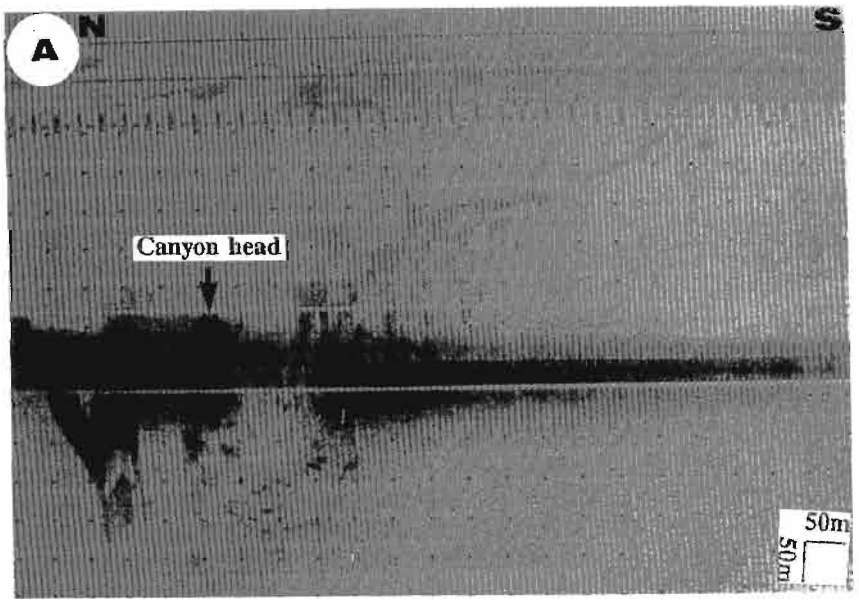

Figure 5.28. Shore-parallel sonargraph images of the southern margin of Wright Canyon head (A) and (B) showing subaqueous dunes migrating south towards the northern margin of the canyon. As these bedforms intersect the canyon head, sediment cascades down the canyon wall as debris flows and accumulates in the canyon thalweg. (X + 3042086;Y + 29317).

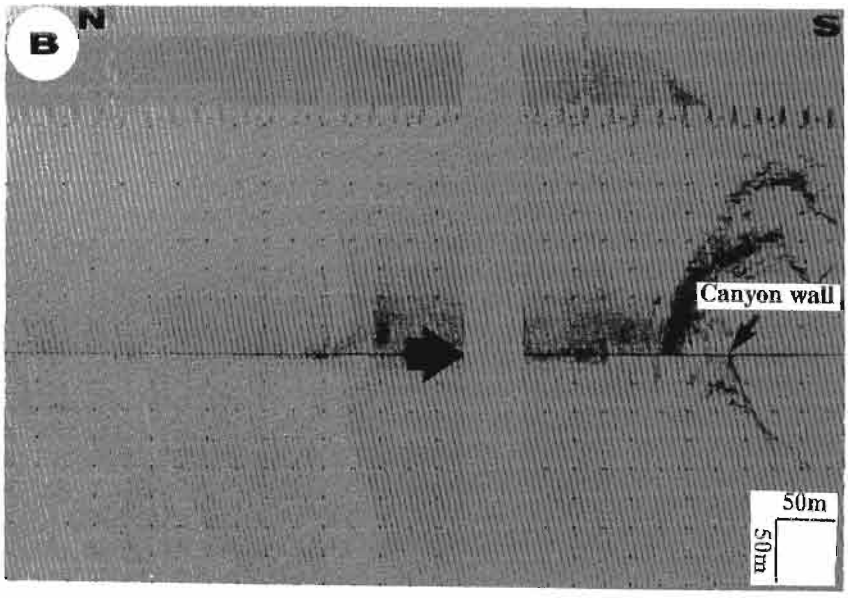

Figure 5.29 is an interpretative geological model of what the very large subaqueous dune field would look like if it was preserved in a cliff section. The preservation potential of the lee slopes of subaqueous dunes is much higher than the corresponding stoss slopes (Smith, 1989), therefore only the lee slope sections are represented in the model. The lower coset represents the medium 2-D dunes over which the very large dune is migrating. The giant foresets represent the very large subaqueous dune coset, each dune giant foreset bed is separated by a bounding surface with the dominant transport direction being parallel to the geostrophic flow. The geostrophic flow, in this case, is produced by the Agulhas Current. The upper coset represents the lithified product of the large 2-D dune lee slopes and superimposed hummocky cross-stratification structures (HCS; see 5.3.2). Localised bedload parting zones are depicted within the large 2-D dunes and it is this superimposition of bedforms and current reversals which assist in building the very large subaqueous dune field.

5.3.1.3 Ancient analogue for subaqueous dunes

The author and Dr A M Smith of the South African Geological Survey have had numerous discussions comparing the very large, Sodwana Bay subaqueous dune field to the very large, reconstructed, subaqueous dunes which occur in Lower Permian sediments of the Vryheid Formation, northern Natal (Fig 5.30). These fruitful discussions have led to the conclusion that a certain facies type, the lower Zungwini-Type facies, may be the ancient analogue of the modern subaqueous dune field on the Sodwana Bay shelf.

These reconstructed, subaqueous dunes are characterised by giant crossbeds. These giant crossbeds were previously thought to represent Gilbertian deltas (Hobday, 1973). Smith (1989; 1990) interprets these features as subaqueous dunes which formed on the palaeoshelf of the proposed Permian Southeast African Interior Seaway (Smith & Tavener-Smith, 1988), in water depths greater than -20m (Fig 5.30). These subaqueous dunes are concentrated in the lower 100m of the Ecca Group in the

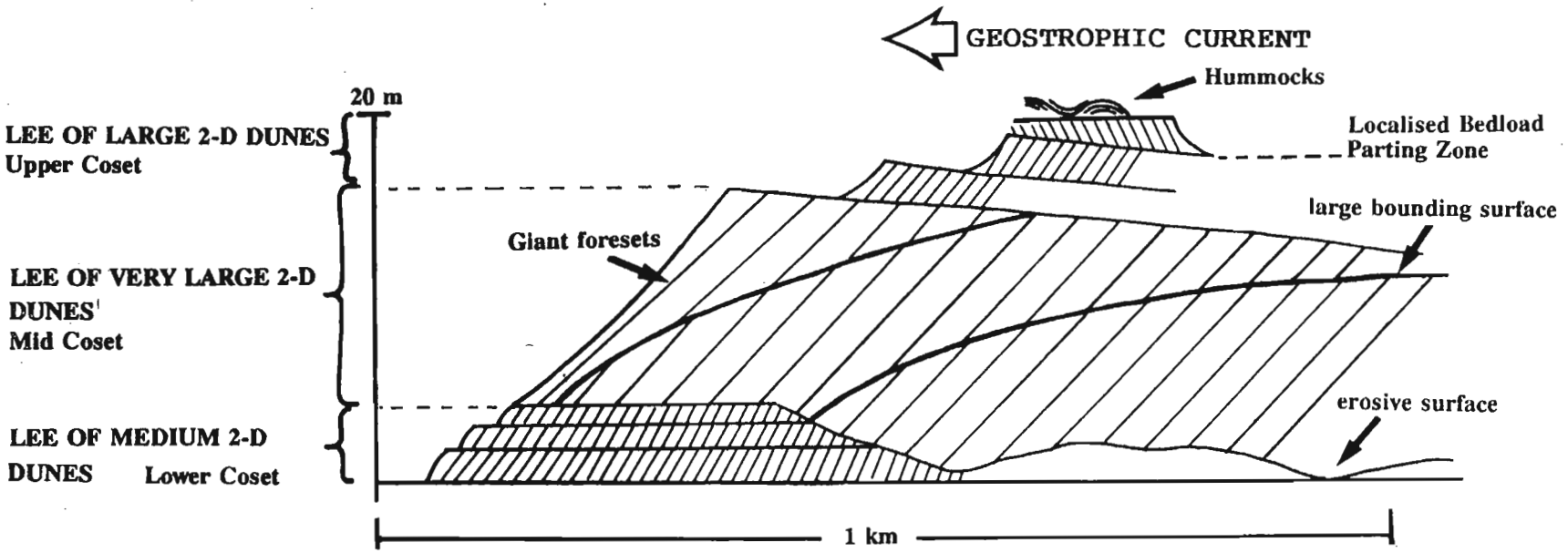

Figure 5.29. An interpretative geological model of what the very large subaqueous dune field would look like if it was preserved in a cliff section.

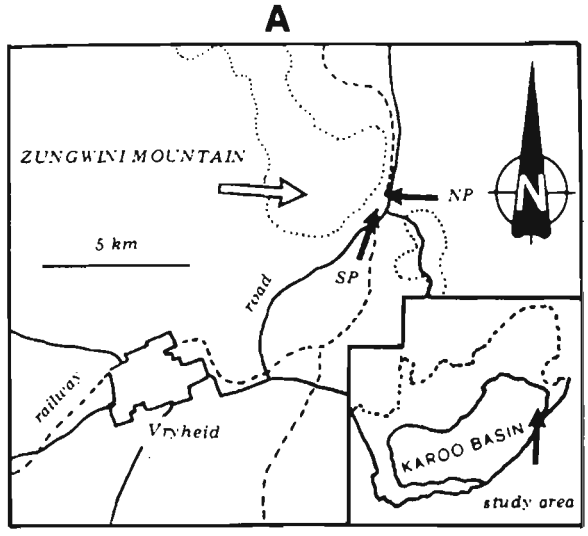

Figure 5.30. (A) Locality map of Zungwini Mountain in the Vryheid Formation and (B) a cartoon showing the depositional model for the Permian palaeo-shelf on which the large-scale sandwaves (subaqueous dunes) formed. (From Smith, 1989). Note: south and north tunnel portals are denoted as SP and NP, respectively.

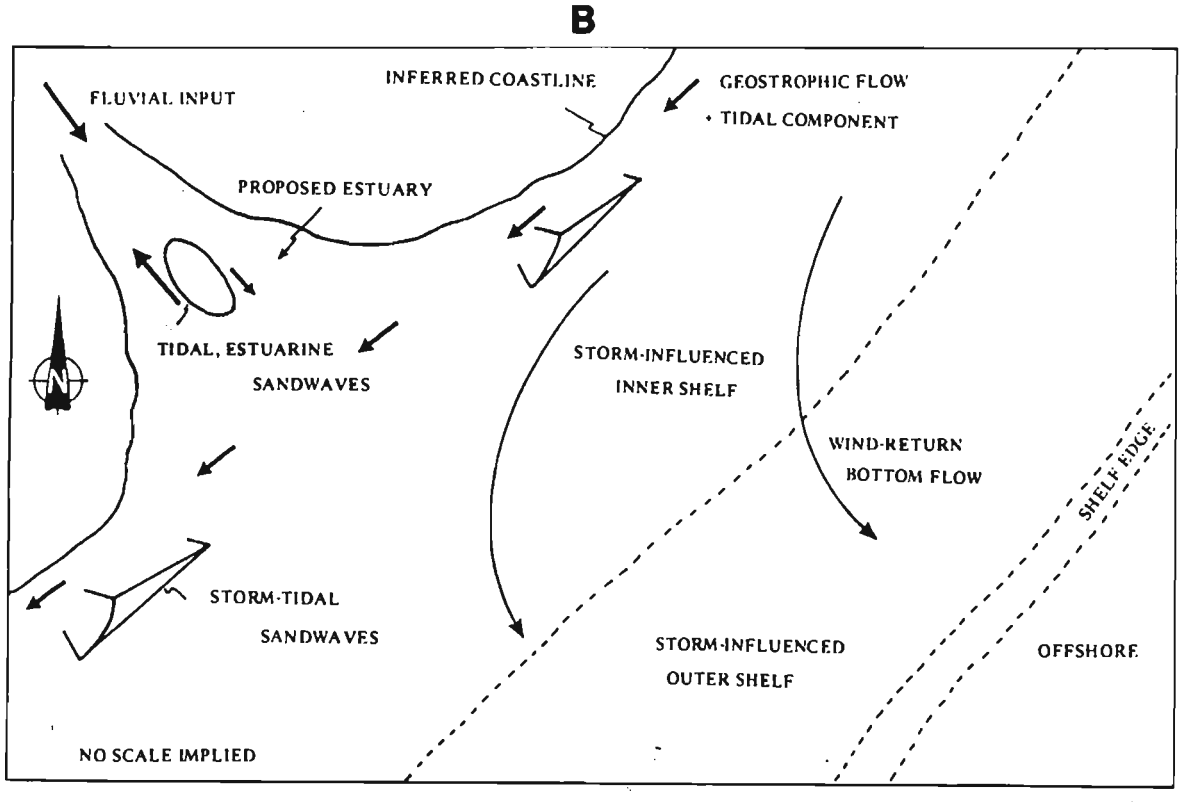

Vryheid Formation, part of the Karoo Sequence (Smith & Tavener-Smith, 1988; Smith, 1989).

The giant crossbeds represent the lee of the very large subaqueous dunes, which are spectacularly exposed in the railway tunnel excavations at the southern tip of Zungwini Mountain (Fig. 5.30). The stoss slope is represented by planar crossbedded sandstone which is less likely to be preserved (Smith & Tavener-Smith, 1988; Smith, 1989). Each bedform is divided into sets by bounding surfaces up to 20m thick (Fig. 5.31): this would infer a dune height of at least 20m or more; the spacing is not known (Smith, pers. comm. 1991). These large-scale bedforms are unidirectional, but rare directionally-reversed, climbing bedforms do occur (Smith, 1989). This directional reversal may be related to bedload parting zones. According to Smith (1989) these enormous bedforms formed above the shelf break. He recognised two facies of giant crossbedded facies association units: (a) the proximal coarse- to very coarse-grained Ngedla-Type and (b) the more distal fine- to medium-grained Zungwini-Type (Smith, 1989, 1990). Overall, the large-scale crossbed facies coarsen upward.

The lower Zungwini-Type subaqueous dunes near Vryheid are composed of three facies (Smith, 1989): (1) giant crossbedded sandstone, (2) hummocky cross-stratified sandstone (HCS), and (3) planar crossbedded sandstone facies. Very large dune migration gave rise to the giant crossbeds of the foreset beds (Fig 5.31). The HCS facies is believed to have formed between storm and fairweather wave base as a response to storms (Dott & Bourgeois, 1982). The azimuth divergence between the stoss and lee slopes of the subaqueous dunes is a consequence of current deflection caused by the dune relief (Fig 5.31; Smith, 1989).

The shelf current which moved the very large bedforms was storm-dominated and coast-parallel and Smith (1990) considers the modern southeast Bering Sea or the North Sea as a possible modern analogues for the ancient Vryheid shelf (Smith, 1990), but concedes that the Sodwana Bay shelf subaqueous dunes are an analogue for the lower Zungwini-Type subaqueous dunes near Vryheid (Smith, pers. comm. 1991). The difference between the modern subaqueous dunes and the ancient

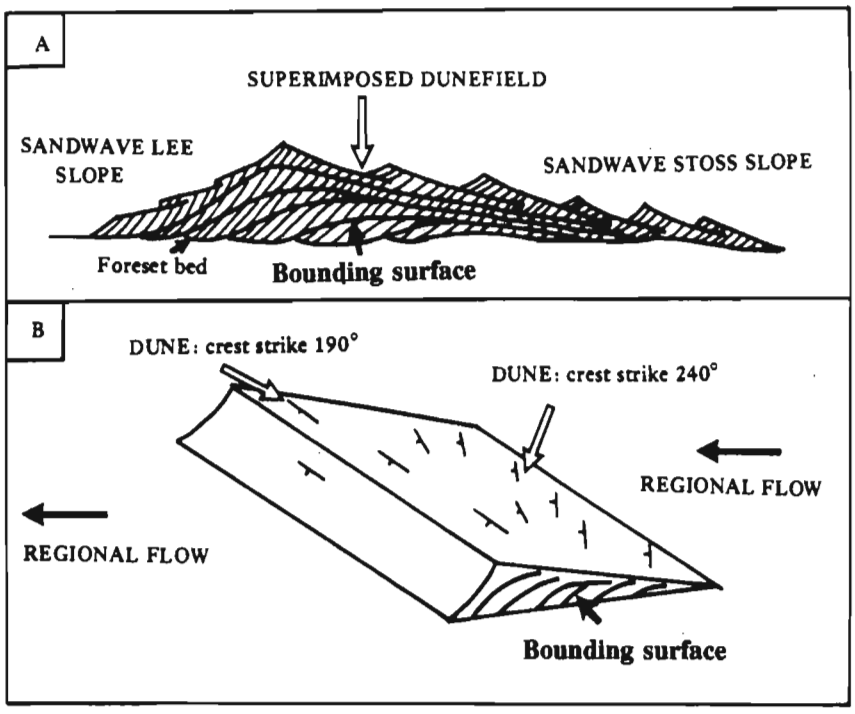

Figure 5.31. Model for the lower Zungwini Mountain reconstructed subaqueous dune. (A) Cross-section showing the climbing dunes and bounding surfaces that form this structure. (B) The relationship between bedform crests and current flow. (From Smith, 1989).

analogue is that of environment, the modern Sodwana shelf environment is open to the ocean whereas the ancient shelf analogue was probably a confined, shallow sea. Sedimentological similarities between the modern and ancient analogue are tabulated in Figure 5.32.

SODWANA BAY SHELF	LOWER ZUNGWINI-TYPE (VRYHEID)
Formed by superimposition of bedforms on the shelf	Formed as a series of climbing bedforms on a horizontal palaeoshelf
Bedload parting zones are a common feature	Directional reversals in palaeocurrent current have been observed to produce climbing bedforms
The unconsolidated lithology is fine-grained, moderately- to well-sorted quartzose sand with coarser bioclastic sediment trapped in the dune troughs	Lithology is fine-grained, relatively well-sorted quartzose sand
60° current orthogonal deflections occur across the very large dune	50° current orthogonal deflections occur across the very large dunes
Amplitude of the very large subaqueous dune is 12m	Amplitudes of the large dune features are of the order of 20m

Figure 5.32. Table of similarities between the Sodwana Bay shelf subaqueous dunes and the lower Zungwini-Type subaqueous dunes.

5.3.2 Hummocky and swale structures

Hummocky cross-stratification geometry implies low relief, oval bedforms of a few metres spacing with the orientation being poorly defined or random (Swift et al., 1983). Hummocky cross-stratification (HCS) has been ascribed to deposition between storm and fairweather wave base as a response to frequent storms (Dott & Bourgeois, 1982). Many authors believe that oscillating currents produced by storm-wave action alone are sufficient to develop this structure (Dott & Bourgeois, 1982; Duke, 1985) but others suggest that this process must work in conjunction with shore-parallel flow (Swift et al., 1983; Allen, 1985; Swift & Nummedal, 1987).

Two occurrences of hummocky (positive relief) and swaley structures (negative relief) have been observed on two dives on the inner subaqueous dune field offshore of Two-Mile Reef (Map 2; Fig. 5.8). These low-relief oval bedforms appear as small, moderately reflective blotches on an otherwise weakly reflective, smooth, and even-toned sonograph record (Fig. 5.33). These features are fairly common in the fine-grained, quartzose shelf sand at depth regimes of -30m to -60m (Map 2). The hummocky structures observed were low relief, oval bedforms with a height of 20cm and a wavelength of 1.5m. The low-relief swale structures had a wavelength of 5m and a depth of 20cm. These bedforms could be transitional from small 2-D dunes (megaripples). Evidence cited for this theory is the occurrence a single small 2-D dune, with a height of 30cm, observed in the middle of the hummocky bedform field on a SCUBA dive. Swift et al. (1983) observed the relationship between hummocky bedforms and megaripples. He noted that hummocky megaripples form as a response to a combined-flow regime consisting of a slowly varying mean flow component and a high-frequency wave orbital component. Comparison of hummocky storm-induced megaripples with megaripples induced primarily by mean flow suggests that the effect of the wave orbital current is to deform the elongate crests, so that the plan view is mound-like (Swift et al., 1983).

5.3.3 Ripples

5.3.3.1 Oscillatory ripples

Oscillation ripples are the most common sedimentary structure on the shelf of Sodwana Bay or any other wave-dominated shelf. The coast is dominated by persistent high-energy waves and prevailing large-amplitude swells from the southeast for about 40% of the year (Swart and Serdyn, 1981; Van Heerden & Swart, 1986; see 2.2), which produces oscillation ripples in quartzose shelf and bioclastic sediment (Figs. 5.34; 5.35). Large oscillation ripples, with wavelengths of up to 50cm and amplitudes of 8-15cm, occur in the reef-derived bioclastic sediment at depths of -12m to -30m (Fig. 5.35). Smaller,

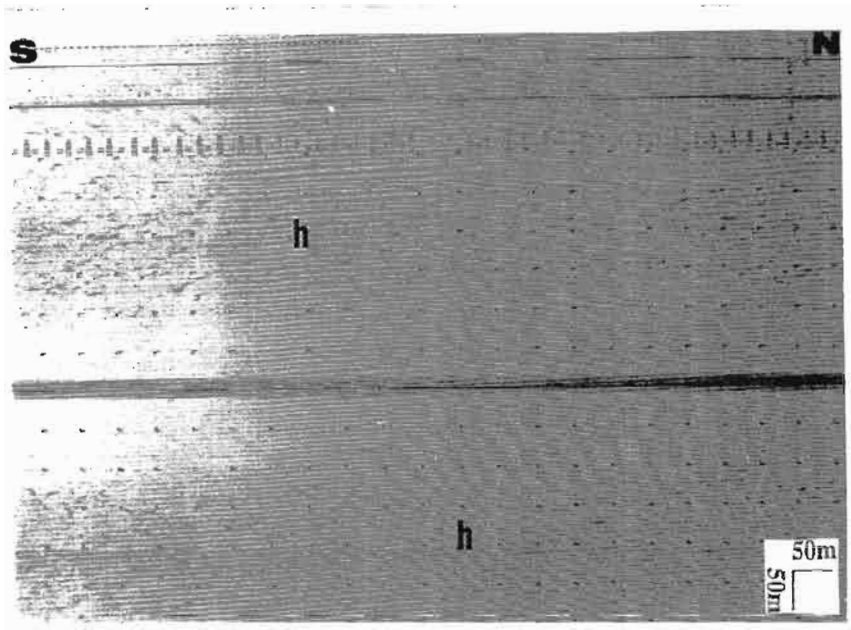

Figure 5.33. Sonargraph image of hummocky structures (h) in fine-grained quartzose shelf sand. These are low-relief oval bedforms with a maximum wavelength of 5 m. (X+3049199;Y+30370).

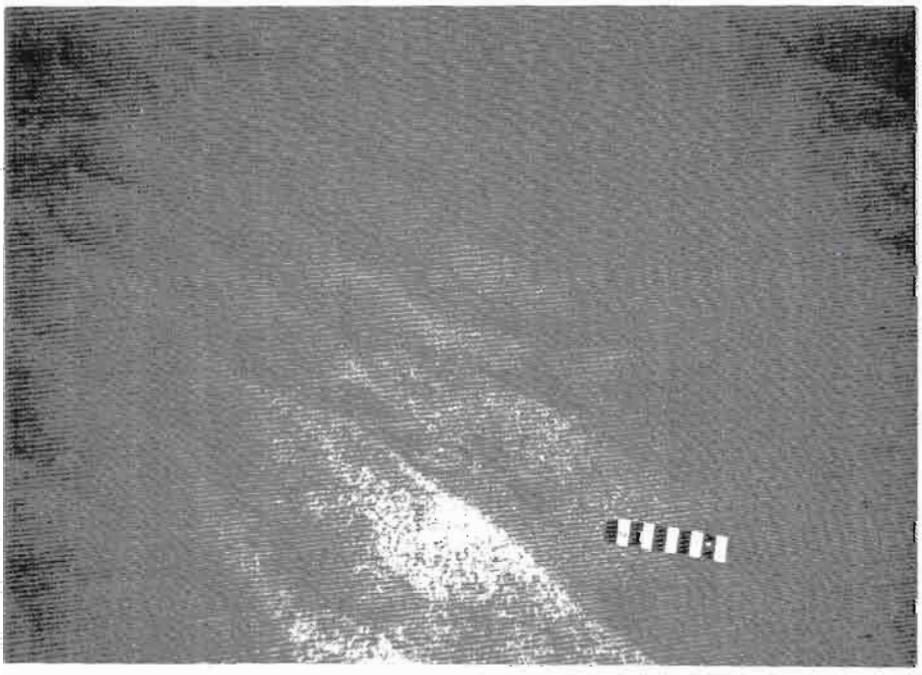

Figure 5.34. Small-scale, sinuous, oscillation ripples in quartzose shelf sand photographed at a depth of -18m. The scale is 10cm long.

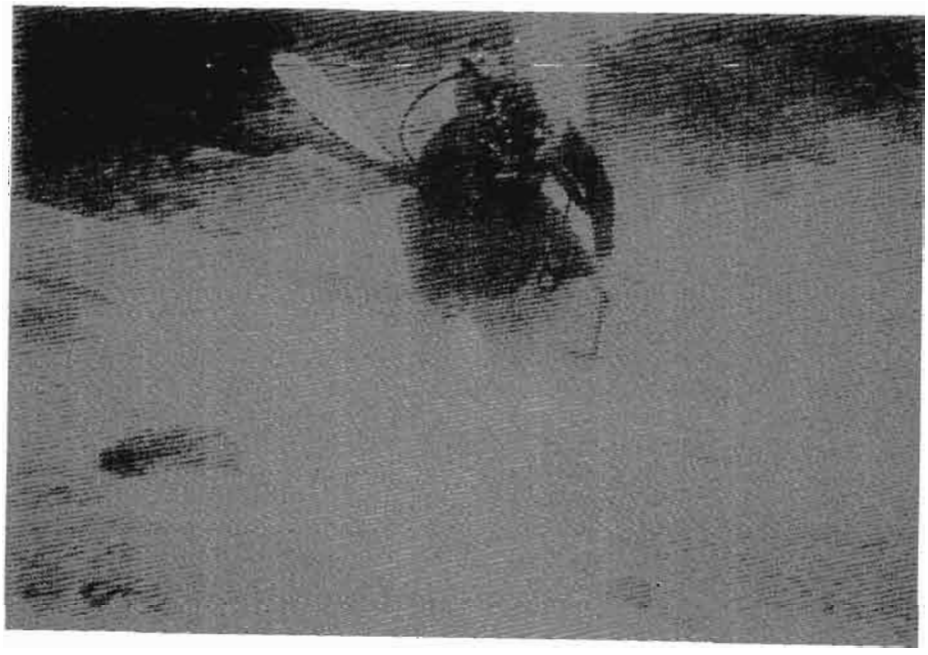

Figure 5.35. Large peaked-crest, oscillation ripples in bioclastic sediment on the landward margin of Two-Mile Reef (-17m). Amplitude is 20cm with a wavelength of 50cm.

sinuous to bifurcating oscillation ripples (wavelength 20cm; amplitude 6cm) are produced in fine-grained quartzose shelf sand (discussed further in 5.3.3.2). Ripple crests are straight to sinuous with continuous crestlines and crest orientations vary from 008-060°. Oscillation ripples have been noted on numerous SCUBA dives down to the scientific diving limit of -50m.

5.3.3.2 Ladderback ripples

Ladderback ripples are common features of tidal flats and beaches where they form by late-stage emergence run-off during the ebb tide (Klein, 1970). They are generally considered diagnostic of clastic intertidal environments (Klein, 1970, 1977; Wunderlich, 1970). Recently, this concept's exclusivity was challenged by Reddering (1987a), who documented ladderback ripples in shallow subtidal estuarine and marine environments. Flemming (1979) also described interference-type ripple patterns in water depths of -10m. These developed by a superimposition of two ripple fields produced by a change in direction of the prevailing wave regime, but were not true ladderback ripples. "Cross ripples" have been described by Clifton et al. (1971) in subtidal environments off the coasts of southern Oregon and southeastern Spain. These tend to be composed of shorter ripples that occupy the troughs of the longer set, and both are oriented obliquely to the oscillatory current. This ripple pattern resembles that of interference ripples, but the ripples only respond to the oscillatory current, which approximately bisects the angle between the two sets. These cross ripples are common in medium- to coarse-grained sand in water depths of 2-4m under conditions of intense asymmetric flow generated by long-period waves. They appear to be structurally transitional between small, asymmetric, irregular ripples and lunate megaripples (Clifton et al., 1971). During investigations of reef-derived shelf carbonates (Ramsay, 1987, 1988; Ramsay et al., 1989) the widespread occurrence of ladderback ripples in water depths between -4m and -17m was noted on the landward side of offshore reefs.

Ladderback ripples have been noted in three areas on the landward margin of Two-Mile Reef (Fig.

5.36). These localities lie in water depths between -4m and -14m in fine-grained terrigenous quartz sand and down to depths of -17m in bioclastic carbonate sand. The wave action from a southeasterly direction produces primary ripple sets comprising straight- to sinuous-crested oscillation ripples (wavelength 50cm; amplitude 15cm) in the coarse bioclastic sand and sinuous to bifurcating oscillation ripples (wavelength 20cm; amplitude 6cm) in fine-grained terrigenous quartz sand. Superimposed on these are smaller ladderback ripples of two types, each produced by different processes. These are outlined below:

Type 1 ladderback ripples consist of a superimposed oscillation ripple set developed at angles between 20° and 90° to the main oscillation ripple orientation. These ladderback ripples have wavelengths of about 16cm and amplitudes of 7-8cm in coarse bioclastic sand and tend to be smaller (wavelength 11cm; ampliltude 2-3cm) in the fine-grained quartzose shelf sand (Fig. 5.37);

Type 2 ladderback ripples consist of superimposed current ripples developed at 90° to the main oscillation ripple set. These ripples were noted only in fine-grained quartzose sand and have wavelengths of 10cm and amplitudes of 3cm. The ripple asymmetry indicates a current direction from south to north.

The formation of the two types of ladderback ripples described above may be explained in terms of grain-size and bottom hydraulic conditions. The fine-grained quartzose sand with its high degree of sorting and low porosity, is less mobile than the poorly sorted and irregularly-shaped bioclastic sand. The latter, due to poor packing, has a higher porosity. The mobility of the bioclastic sand results in its more rapid reworking by wind-driven swells from the northeast to form oscillation ladderback ripples (Type 1), without destroying the orientation of the main ripple set which is generated by the refracted, prevailing southeasterly swell. Minimum bottom-current velocities necessary to produce such reworking to form a Type 1 ladderback ripple set are approximately 0.34m/sec (Blatt, Middleton

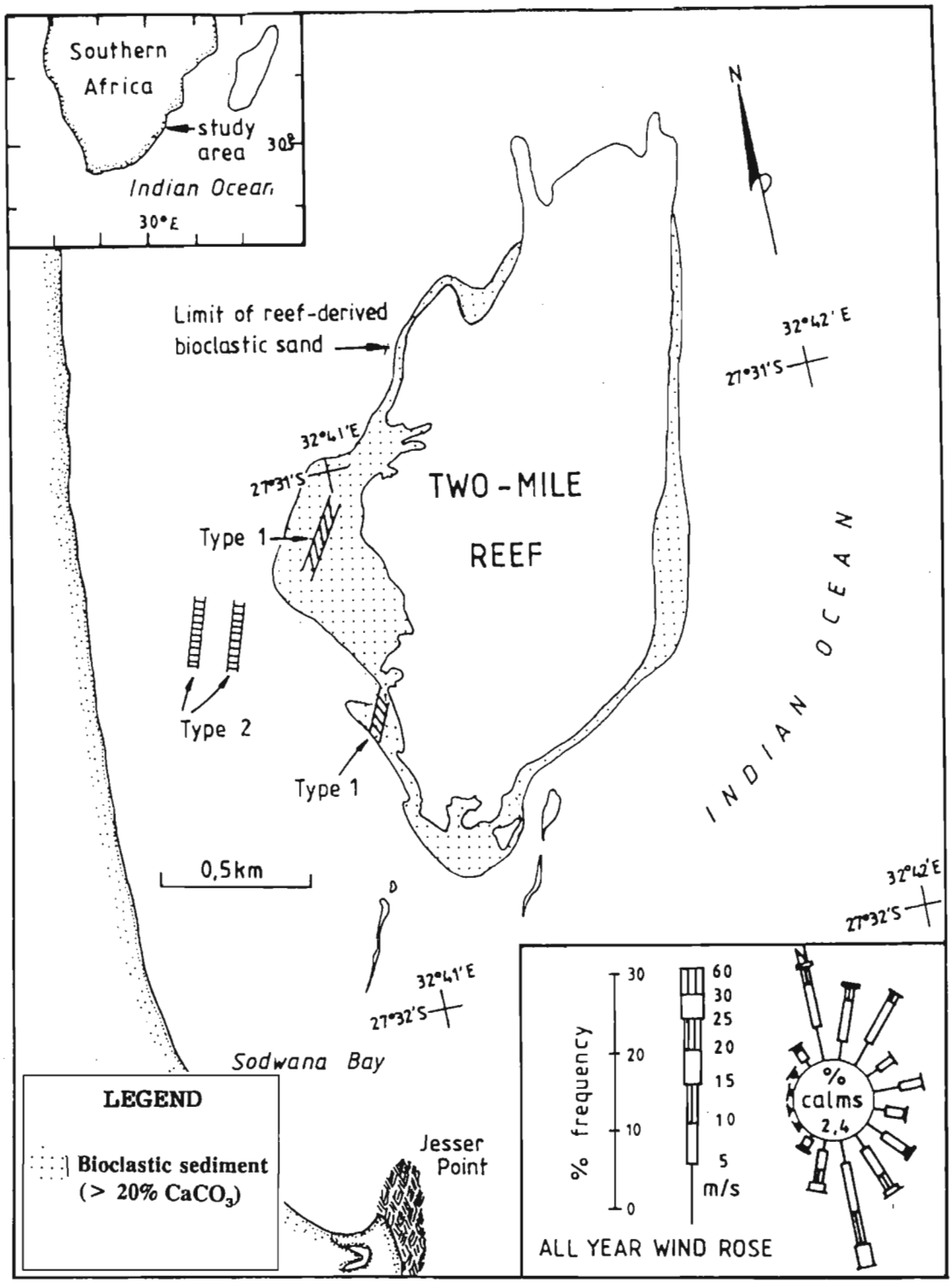

Figure 5.36. Locality map showing the geological setting of ladderback ripples. The reef-derived bioclastic carbonate fringe is illustrated, a wind rose is included, and orientation of Type 1 and 2 subtidal ladderback ripples at Sodwana Bay. Ripple size not to scale.

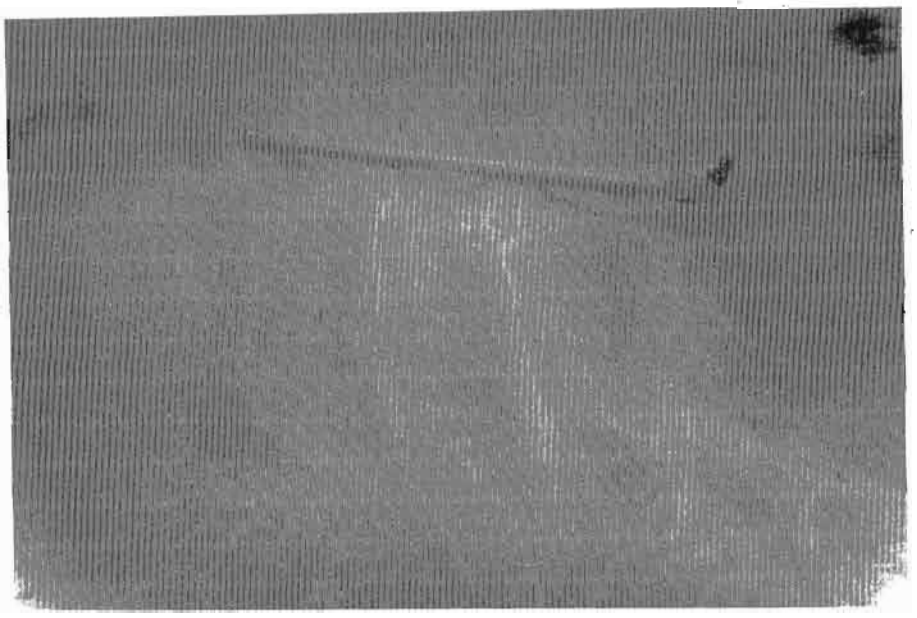

Figure 5.37. Type 1 ladderback ripples at a depth of 10 m in fine-grained quartzose shelf sand with fine bioclastic sediment along the ripple crests. In this instance the ladderback ripple set continues across the main ripple crests. This situation is, however, unusual in the author's experience of subtidal ladderback ripples. Scale in this underwater photograph is 1.5 m long.

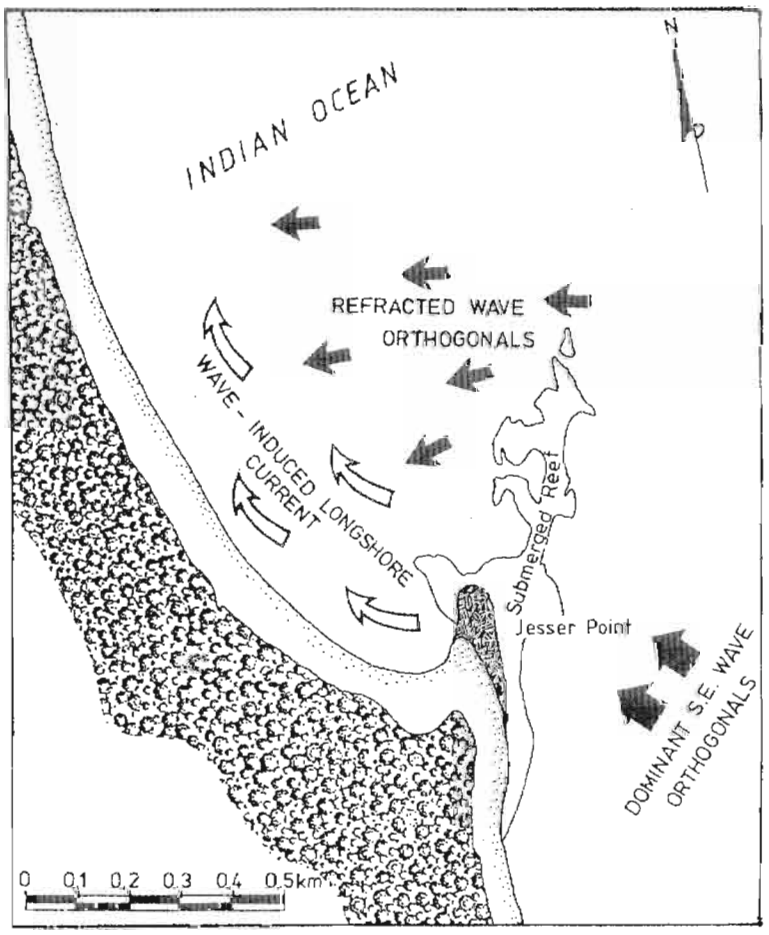

Figure 5.38. Sodwana Bay represents a typical Zululand embayment with dominant southeasterly wave orthogonals. Note how wave orthogonals are refracted around the rocky point and submerged reef. A wave-induced longshore current is produced by waves breaking over the shallow, submerged point.

and Murray, 1980). The critical velocity for bioclastic sediment movement is probably slightly lower than 0.34m/sec owing to the platy nature of the carbonate grains, although platy grains may lie lower in the current due a jamming effect with other grains. The observed variation in angles between the superimposed and the main ripple set (20-90°) may be explained by slight variations in the direction of the swell from the northeast. These ripples therefore form by a similar mechanism to the superimposed ripples described by Flemming (1979), the main difference being that for the ripples described in Zululand, the superimposed set is produced by waves of marked difference in amplitude and period, thus producing a distinctive ladderback pattern. It has been the author's experience that Type 1 ladderback ripples form after a strong northeasterly wind (generating northeasterly swells) of approximately 20 knots.

Type 2 ladderback ripples form in shallower water (-4m to -14 m) in coastal embayments with the current-derived superimposed ripple set being generated by a south-to-north longshore current. The northerly flowing longshore current is formed by waves from the southeast breaking over and refracting around the rocky points and submerged reefs of the coastal embayments (Fig. 5.38). The longshore current forms a superimposed ladderback ripple set without destroying the primary ripple orientation. A minimum bottom current velocity of 0.27m/sec is necessary to cause movement of terrigenous sediment with a mean grainsize of 0.153mm (Blatt, Middleton and Murray, 1980). The orientation of the superimposed set at 90° to the main set indicates that the presence of the main set affects the longshore current by channelling it into the ripple troughs. No variation from about 90° was noted. Type 2 ladderback ripples were observed less commonly than Type 1, and may be rare compared to the latter.

Following a strong 20 knot northeasterly wind that blew for 2 to 3 days, the main ripple set in quartzose sand at a depth of -5m to -8m changed orientation from a southeasterly swell-driven ripple set to a northeasterly wind-driven swell ripple set. At the same time the superimposed ladderback

ripple set changed orientation to that of a ripple set derived from a southeasterly swell. Thus an overall shift in ripple orientation of 90° occurred. This indicates that although the northeasterly swell became dominant, a minor component of the southeasterly swell was still present.

5.4 DISCUSSION

The Agulhas Current provides the geostrophic flow which controls the sedimentary processes on this extremely narrow shelf, producing a unique assemblage of interesting physical, sedimentological and biological phenomena. The narrow shelf is dominated by coral reefs which have colonised regressive aeolianite and beachrock outcrops. These outcrops define the positions of palaeocoastlines of the late Pleistocene. The shelf break has a steep gradient (up to 8°) and in places is dissected by submarine canyons. Sedimentary structures in unconsolidated shelf sediment include very large subaqueous dunes with superimposed smaller bedforms and the occurrence of subtidal ladderback ripples.

The consolidated lithologies on the shelf are late Pleistocene beachrock and aeolianite outcrops with or without an Indo-Pacific coral reef veneer. The outcrop area on the shelf of these lithologies amounts to 20% (11.7km^2) of the total shelf in the study area. This means that during the late Pleistocene regressions the formation of these lithologies generated a considerable sediment sink in the nearshore zone. This must have had a considerable effect on the coastline morphology and processes during the Holocene (Flandrian) transgression. Cooper (1991) noted that the formation of beachrock during stillstands or minor regressions in subtropical areas prevents grain transport in the littoral zone during later transgressions and regressions. In the short term, reduction of sediment supply through beachrock formation during a transgression would enhance the landward movement of the shoreline, but conversely the beachrock will afford better protection from erosion than loose sand (Cooper, 1991).

The dominant primary sedimentary structures found on the carbonate-cemented sandstone outcrops include high-angle planar cross-bedding and depositional dip bedding. The palaeocurrent directions suggest a combination of longitudinal and transverse dunes with generally coast-parallel wind directions, similar to those observed forming the modern dune systems. As a general rule the reef-crests of the reefs are aeolianites and the fore-reef environments are beachrock or intertidal facies. Erosional features evident on the submerged beachrocks and aeolianites include gullies trending in two dominant directions and sea-level planation surfaces with or without the presence of potholes.

The coral reef veneers capping the late Pleistocene beachrocks and aeolianites can be classified as patch reefs. The reef fauna is dominated by alcyonarian (soft) corals with scleractinian (hard) corals being common. The reefs can be divided into four morphological environments based on topography, depth, and geographical position: namely the back-reef, reef-crest, fore-reef, and deep reef-front environments (Ramsay, 1988; Ramsay, 1990a; Ramsay & Mason, 1990a&b). This morphological zonation is controlled by the underlying geology of beachrocks and aeolianites.

The unconsolidated sediment on the shelf is from two distinct sources: the shelf sand is composed mainly of terrigenous quartz grains; the bioclastic sediment is partially derived from biogenic sources. Wave-reworking of the quartzose shelf sand in shallower water results in greater sediment maturity than is noted in the geostrophic current-controlled sediment from deeper water. The quartzose shelf sand is derived by reworking of aeolian and beach sediments, deposited on the shelf during the period leading up to the Last Glacial Maximum (15 000 - 18 000 B.P.) when sea-level was -130m, during the Holocene (Flandrian) transgression.

The distribution of bioclastic sediment in the study area is widespread, with reef-derived and outer-shelf-derived populations being evident. The reef-derived bioclastic population is confined to depths less than -40m in close proximity to reef areas, whereas the shelf-derived bioclastic population occurs

at depths greater than -40m and is derived from carbonate-producing organisms from deep water reef and soft-substrate environments on the shelf. Higher carbonate contents, coarser grainsize and poorer sorting are evident in the reef-derived sediment due to the close proximity to the source. The only significant difference in bioclastic component distributions of the two biogenic populations is the increase in abundance of hexactinellid sponge spicule fragments on the outer-shelf compared to the mid- and inner-shelf environments.

Oscillation ripples are the most common sedimentary structure on the shelf in both bioclastic and quartzose sand. The formation these of ripples may be explained in terms of grain-size and bottom hydraulic conditions. The well-sorted, fine-grained quartzose sand is less mobile than the poorly sorted bioclastic sand. The mobility of the bioclastic sand results in more rapid hydraulic reworking of the sediment which forms larger oscillation ripple amplitudes and wavelengths in the bioclastic sand compared to the quartzose sand. The occurrences of ladderback ripples on the Sodwana Bay shelf at depths of -4m to -17m, supports Reddering's (1987a) observations and suggests that subtidal ladderback ripples may be more common than previously thought. The mode of formation is different from the classic late-stage emergent run-off model of intertidal occurrences (Klein, 1977). Ladderback ripples have a low preservation potential, and are difficult to recognise in the rock record. The author's observations indicate that they are not environment-specific.

Many reports of ladderback ripples in intertidal environments indicate that the main ripple set is often flat-topped (McKee, 1957 ; Allen, 1959 ; Evans, 1965 ; Wunderlich, 1972 ; Cooper, 1988); however non-truncated ladderback ripples have also been recorded (Davies et al., 1972 ; Reineck and Singh, 1973 ; Allen, 1984). Additional evidence of emergence is therefore necessary to support an intertidal setting: ladderback ripples alone are insufficient to prove an intertidal environment. Both the occurrences documented here and those reported by Reddering (1987a) are in microtidal settings. It remains to be seen if ladderback ripples occur subtidally in meso- or macrotidal areas.

Subaqueous dunes are a common feature on the Sodwana Bay shelf occurring as two distinct fields at depths -35m to -70m, the major sediment transport direction being towards the south. The larger, outer dune field appears to have originated as a system of climbing bedforms with three generations of bedforms being superimposed to form a giant bedform, while the inner dune field has a less complex construction. Flemming (1988) defined an equation relating the height and spacing of flow transverse subaqueous bedforms based on 1491 observations: $H = 0.0677\ L^{0.8098}$, where H is bedform height and L is spacing. The Sodwana Bay subaqueous dune statistics were plotted on Flemming's (1988) log-log plot of height versus spacing (Fig. 5.39). Based on this plot and Flemming's (1988) equation it can be seen that the height of large- and very large 2-D subaqueous from Sodwana Bay is less than predicted by the equation. The height to spacing ratio of medium 2-D dunes plot on the theoretical line defined by the equation. The non-compliance of the larger bedforms to the equation theory could be a result of the short-comings of the equation or insufficient height and spacing data from the Sodwana Bay shelf. Further research is required in this field.

Three bedload parting zones occur in the study area at depths of -45m, -47m and -60m; two in the inner dune field and one in the outer dune field. These are the result of two localised reversals in Agulhas Current, one offshore of Two-Mile Reef influences the outer and southern inner subaqueous dune fields, and the other offshore of Gobey's Point reverses the sediment transport direction in the northern part of the inner subaqueous dune field (Fig. 5.24). In these zones the dominant southerly sediment transport direction is reversed to become northerly. Bedload parting zones exist were the bedform migration direction changes from south to north. These zones are invariably located at the southern limits of large clockwise eddy systems (Flemming & Hay, 1988; Figs. 5.40 & 5.41). Such eddies appear to be the result of topographically induced vorticity changes in the geostrophic flow (Gill & Schumann, 1979) and/or the response to atmospheric forcing caused by coastal low-pressure system moving up the coastline (Bang & Pierce, 1978 ; Schumann, 1988).

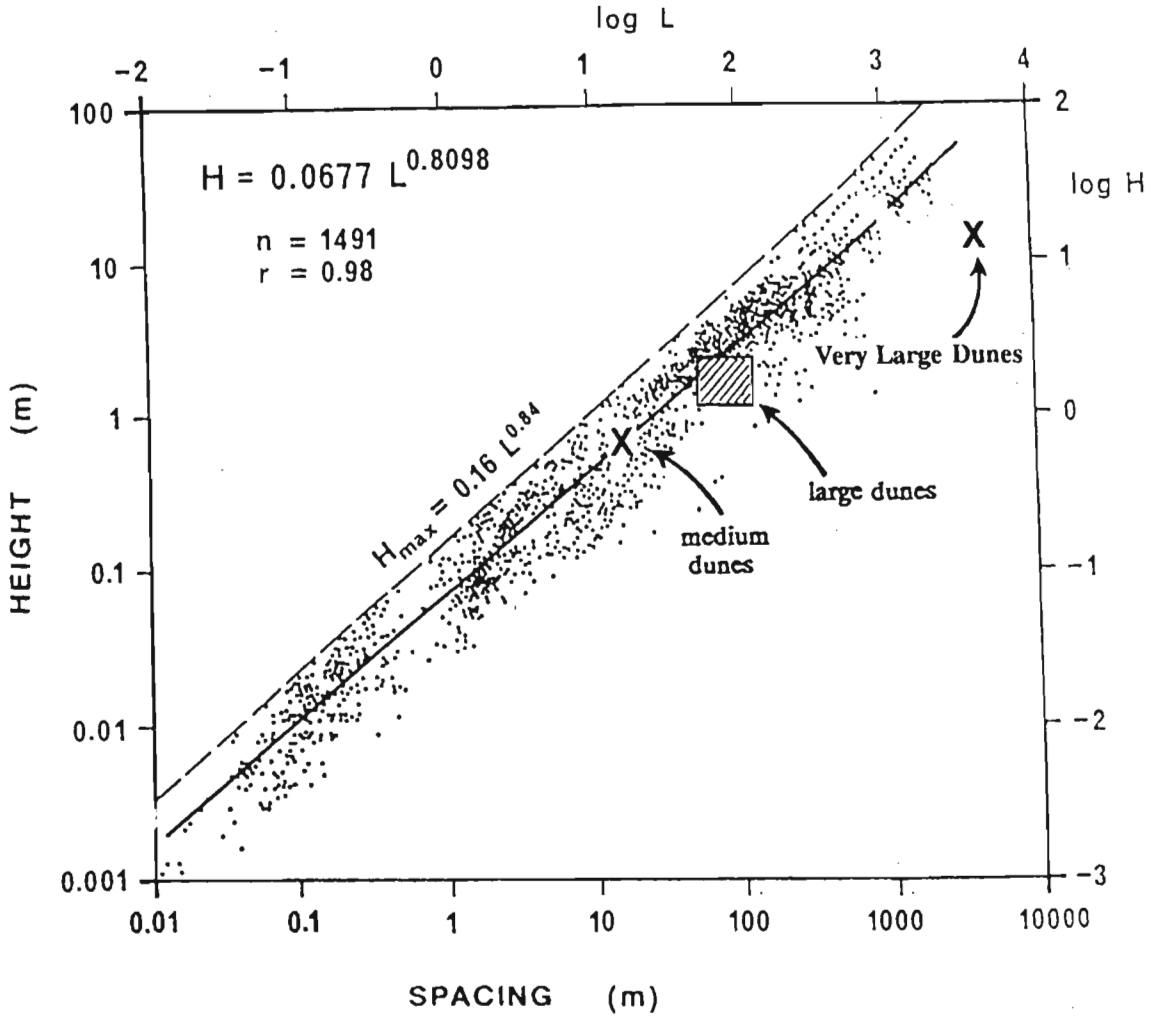

Figure 5.39. A log-log plot of height (H) versus spacing (L) of 1491 flow transverse subaqueous bedforms. The data appear to cluster into 2 populations separated by a paucity of forms at approximately 0.5m to 1.0m spacing. The smaller forms are ripples; the larger forms are dunes. The dimensions of the Sodwana Bay medium-, large-, and very large subaqueous dunes have been included as a comparison. (After Flemming, 1988).

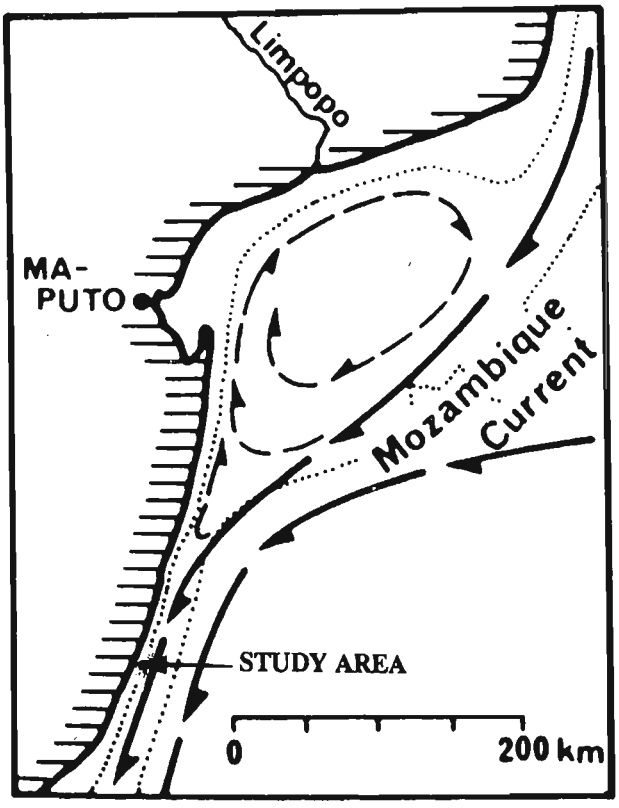

Figure 5.40. The Maputo eddy system formed in the lee of a structural offset in the Mozambican continental margin. Bedload parting zones are invariably located at the southern limits of these large clockwise eddy systems. (From Flemming, 1981).

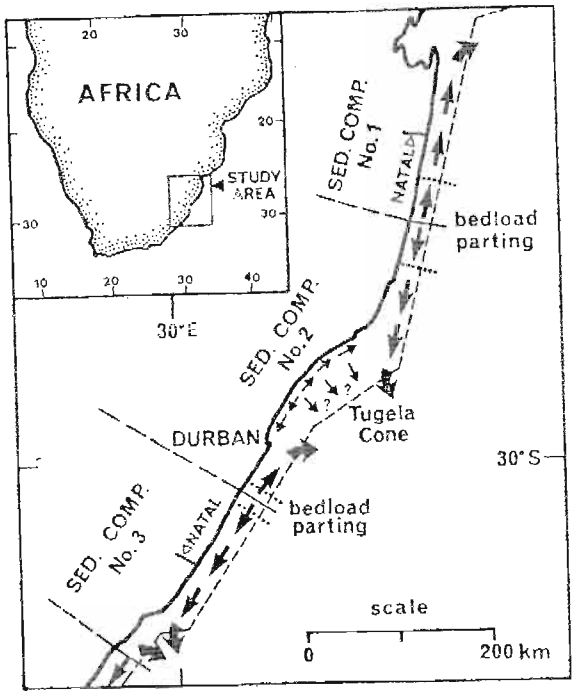

Figure 5.41. A schematic bedload dispersal model for the Natal continental shelf. (From Flemming & Hay, 1988).

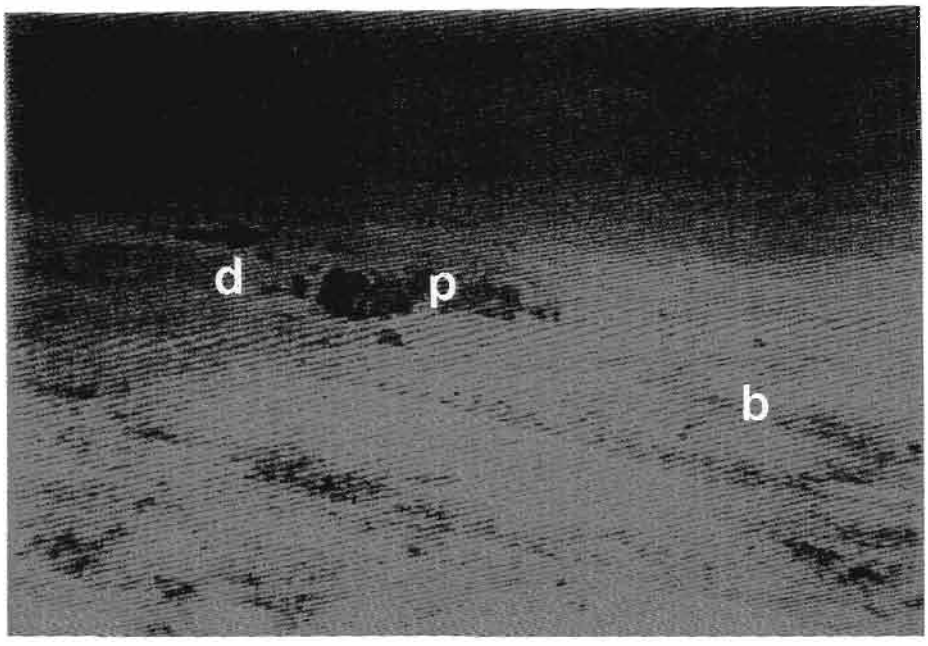

Figure 5.42. Pinna bivalves (p) in a dune trough have been partially buried by the northward advance (bedload parting zone) of the lee slope of a subaqueous dune (d) over a bioclastic-filled dune trough (b). The lee slope of this dune is bioturbated, indicating that it has not been active for a short period of time. The field of view is ± 3m. (X+3044179;Y+29339).

Observations taken on a SCUBA dive on one of these bedload parting zones indicated that the large 2-D dunes had been active fairly recently (a few months ago). Pinna bivalves in a dune trough had been partially buried by the northward advance of the lee slope of the dune over the bioclastic-filled dune trough (Fig. 5.42). The lee slope of this dune was now bioturbated, indicating that it was no longer active.

SCUBA diving observations on the inner subaqueous dune field have demonstrated that the large 2-D dunes were active in November 1990. On subsequent dives in February 1991 the lee slopes of these dunes were intensely bioturbated indicating the dunes had been inactive for a least 1-2 months. This demonstrates that the inner subaqueous dune sediment conveyor is not active all the time but only during periods of increased current strength when the Agulhas Current meanders inshore. No SCUBA diving observations have been made on the outer subaqueous dune field, but a remote video survey undertaken at night on the field showed that small-scale bedforms superimposed on the large 2-D dunes were migrating south. It is assumed that the large 2-D dunes were also migrating at that period and continue to do so at present: the current velocity on the shelf edge outer dune field is estimated to be higher than the velocity experienced on to the inner dune field. The very large 2-D dune which forms the outer dune field is probably not active at present: this is inferred due to the shallow angle of the mega-crest lee slope (8°).

The origin of bioclastic sediment in the troughs of subaqueous dunes is interesting in that the distribution has varied sources. The bioclastic sediment in the large 2-D dune troughs in the outer subaqueous dune field appears to be derived from a bioclastic pool source between Wright Canyon and the dune field itself. This bioclastic sediment originated from autochthonous shelf- and reef-derived sources. A similar origin of bioclastic trough sediment in the inner subaqueous dune field is envisaged: reef-derived bioclastic originating from the coral reefs and the shelf-derived bioclastic sediment from areas such as the Pinna muricata field.

The bioclastic sediment on the stoss dune slopes is very mobile and is easily transported by the current owing to the platy nature of the carbonate grains. These grains eventually avalanche down the dune lee slopes and accumulate in the dune troughs. The abundance of platy bioclastic sediment in the troughs causes a jamming effect between the constituent grains and reduces the mobility of the bioclastic trough sediment. As the lee slope of the dune migrates forward it buries the less-mobile trough bioclastic sediment and this forms a major bounding surface in the large 2-D dunes.

Positive-relief hummocks and negative-relief swale structures have been observed on two dives on the inner subaqueous dune field offshore of Two-Mile Reef. These appear to be transitional bedforms related to the reworking of medium 2-D subaqueous dunes. It is not certain if these hummocky structures are the modern equivalent of hummocky cross-stratification noted in the geological record. This will require further research in the form of regular SCUBA diving observations after storms to assess any wave-reworking of the smaller-scale bedforms on the inner subaqueous dune field. If these bedforms do represent the modern equivalent of HCS, then they are probably the first to have ever been observed underwater.

CHAPTER 6: PHYSIOGRAPHIC AND BIOLOGICAL ZONING OF CORAL REEFS

The Zululand coral reefs, on the southwestern margin of the vast Indo-Pacific faunal province, extend northwards from Leadsman Shoal (Leven Point) towards the South African/Mozambican border, a distance of 121km. The reefs consist of thin veneers of Indo-Pacific type corals which have colonised submerged, late Pleistocene dune and beach sequences (= reef-base), and may be classified as patch reefs (Ramsay, 1988; Ramsay & Mason, 1990b). The Zululand coral reefs generally occur 1km offshore, and extend parallel to the coastline.

Two-Mile Reef was chosen as the type physiographic and biological zoning model for Zululand coral reefs because of its large size, varied reef fauna and topography, and accessible geographical location. Two-Mile Reef lies in -9m to -35m of water, 1.3km north-northeast of Jesser Point at Sodwana Bay. Crossland's (1948) intertidal study of Natal corals, noted that the fauna was typical of a marginal belt and was characterised by the almost complete absence of the great reef-builder Acropora. Boshoff (1958) stated that the southernmost coral reefs in the southwestern Indian Ocean occur at Inhaca Island (26°10' S ; 32°58' E) off Mozambique and an annotated checklist of Scleractinia is available for the area (Boshoff, 1981).

A fossil coral fragment (Favia sp.), found in an intertidal beachrock sequence 35km north of Sodwana Bay, has been dated. It is envisaged that the fragment probably washed ashore during a storm and was included into a beachrock outcrop during the latter part of the Holocene. The modern northern Zululand beaches are often strewn with coral rubble after storm events (Fig. 6.1). A ^{14}C-age of 3780 ± 60 B.P. (laboratory analysis no. Pta-5052) was obtained from the coral fragment, and it is assumed that this date represents a minimum age for the Zululand patch reef assemblages.

Figure 6.1. Coral rubble washed ashore during a storm and deposited on the beach at the high-tide mark. Locality: 6km north of Jesser Point.

6.1 METHODS

Two-Mile Reef was initially mapped using panchromatic aerial photographs and echo-sounding profiles; followed by detailed mapping using side-scan sonar (see Chapters 3 & 5). Selected west-east underwater traverses were undertaken on Two-Mile Reef using SCUBA to collect physiographic and biological zoning data. Similar traverses undertaken on the other reefs were used to test the zones obtained from the Two-Mile Reef study. Underwater traverse lines were accurately coordinated using sextant bearings and position fixes using a GPS system. On each traverse the divers: (1) photographed and identified corals; (2) noted and measured coral cover/density and topographic features; (4) recorded depth measurements; (5) sampled the reef-base to determine the sedimentary facies (see Chapter 7). These data were supplemented by extensive snorkel-diving observations and sampling (to depths of -25m) along the entire reef system. Sediment grain size statistics were computed using a settling tube (see Chapter 3). A three-dimensional model of Two-Mile Reef was made to help visualise the morphology and zoning relationships of the reef (Ramsay, 1990b; see Chapter 4).

6.2 REEF SETTING

The Agulhas Current has provided the necessary biotic and abiotic factors which have allowed the Zululand coral reefs to thrive over the last few thousand years. Two-Mile Reef is a patch reef (Guilcher, pers. comm. 1988) which is always submerged. The reef lies 1km offshore and parallels the coastline for 2.1km; its maximum width is 0.9km. Water depths vary from -9m over the shallow central axis of the reef to -35m along the deep reef-front environment. The euphotic zone, below which little or no photosynthesis occurs, occurs at a depth of -30m along this section of coastline. Similar light intensity/depth coral growth criteria in other coral reef regions in the world have been observed by Agassiz (1898), Yonge (1940), Jaubert & Vasseur (1974), Mergner & Scheer (1974), Montaggioni

(1974), Reiss & Hottinger (1984), Jaap (1984), Tomascik & Sander (1985), and Chalker et al. (1986).

Hubbard & Pocock (1972) demonstrated the ability of isolated corals to survive under considerable sediment cover. Verwey (1931) stated that the physical effect of suspended sediment smothering corals and preventing growth is overrated; suspended sediment basically restricts light penetration. Since decrease in light is a major cause of the decline in coral growth rates with depth (Huston, 1985), reduced water transparency reduces carbonate productivity by corals. Kanwisher & Wainwright (1967) note that very little coral growth occurs when surface light levels fall to about 4%, but other workers (Chalker et al., 1986) state that corals are common down to about the 1% light level. This information can be used to predict how coral zonation will change if water transparency changes.

6.4 REEF ZONING

Earlier investigations on coral reefs viewed reef dynamics in terms of geomorphology (Barnes et al., 1971; Guilcher, 1971; Stoddart, 1969) or the biology of the reef system (Rosen, 1971; Scheer, 1971; Taylor, 1971). Regional variation and structural zonation of each reef are primarily caused by its geological history and its position in the open sea (Mergner & Scheer, 1974). Coral species distribution is influenced more by light exposure and light intensity than by other abiotic factors (Mergner & Scheer, 1974). Corals are the dominant animals on flourishing coral reefs and these determine the character of the physiographic zones within the reef by their horizontal or vertical sequence which results from the influence of changing ablotic factors (Mergner, 1971).

The physiographic and biological investigations of Two-Mile, Four-Mile, and Seven-Mile Reefs were made using coral sociological methods similar to those described by Mergner & Scheer (1974). The "zurich-montpellier" phytosociological method of coral abundance and sociability (surface coverage) described by Vasseur (1974) is too complex for large reef tract investigations. The extreme difficulty

of applying current coral classification meant that the reef corals were only identified to generic level. Underwater observations of the coral genera abundance/cover were either: (a) **r** = rare, very few specimens in the study area; the value of dominance or cover is insignificant; (b) **p** = present, coverage is poor; (c) **c** = common, a large number of specimens significantly contributes to reef cover; (d) **a** = abundant, many specimens and the value of dominance or cover is very significant.

In the absence of quantitative data, reefs are best compared using descriptive schemes based on physiographic and biological distribution patterns. The method is best suited to reefs showing pronounced zonation parallel to the reef edge, i.e. windward reefs (Stoddart, 1973). The Sodwana Bay reefs are windward reefs, and the criteria mentioned above were adopted to define eight distinct zones on the type area, Two-Mile Reef (Figs 6.2, 6.3, & 6.4).

Corals belong to the Phylum Cnidaria (Clarkson, 1979) and Zululand reefs host members of the two main orders: Scleractinia (hard corals) and Alcyonacea (soft corals). The other two subordinate anthozoan orders present are Gorgonacea (sea fans) and Antipatharia (black corals). The dominant alcyonarian corals comprise 60-70% of the total reef coral fauna and include the genera Lobophytum, Sinularia, Sarcophyton, and Dendronephthya. Faure (1974) noted a similar abundance of alcyonarians in the "Passe" Grand Bassin on Rodriguez Island and Fairbridge (1950a) quotes that patch and platform reefs in the outer parts of the Buccaneer Archipelago are dominated by bryozoans and alcyonarians. Williams (1989a&b) states that the alcyonarian contribution on Zululand reefs is typical of Indo-Pacific coral reef assemblages, and is dominated by the three genera Sinularia, Sarcophyton, and Lobophytum, with a relatively minor contribution being made by genera such as Dendronephthya, Nephthea, Alcyonium, Clavularia, Cladiella, Anthelia, Rumphella, Menella and Leptogorgia. Williams (1989a) also noted that the Zululand coral reef fauna is scanty compared to other Indo-Pacific areas such as the Red Sea. The most important Zululand scleractinian genera, in descending order of abundance, are Favia, Favites, Montipora, Acropora, Leptoria, Echinopora, Turbinaria, Pocillopora,

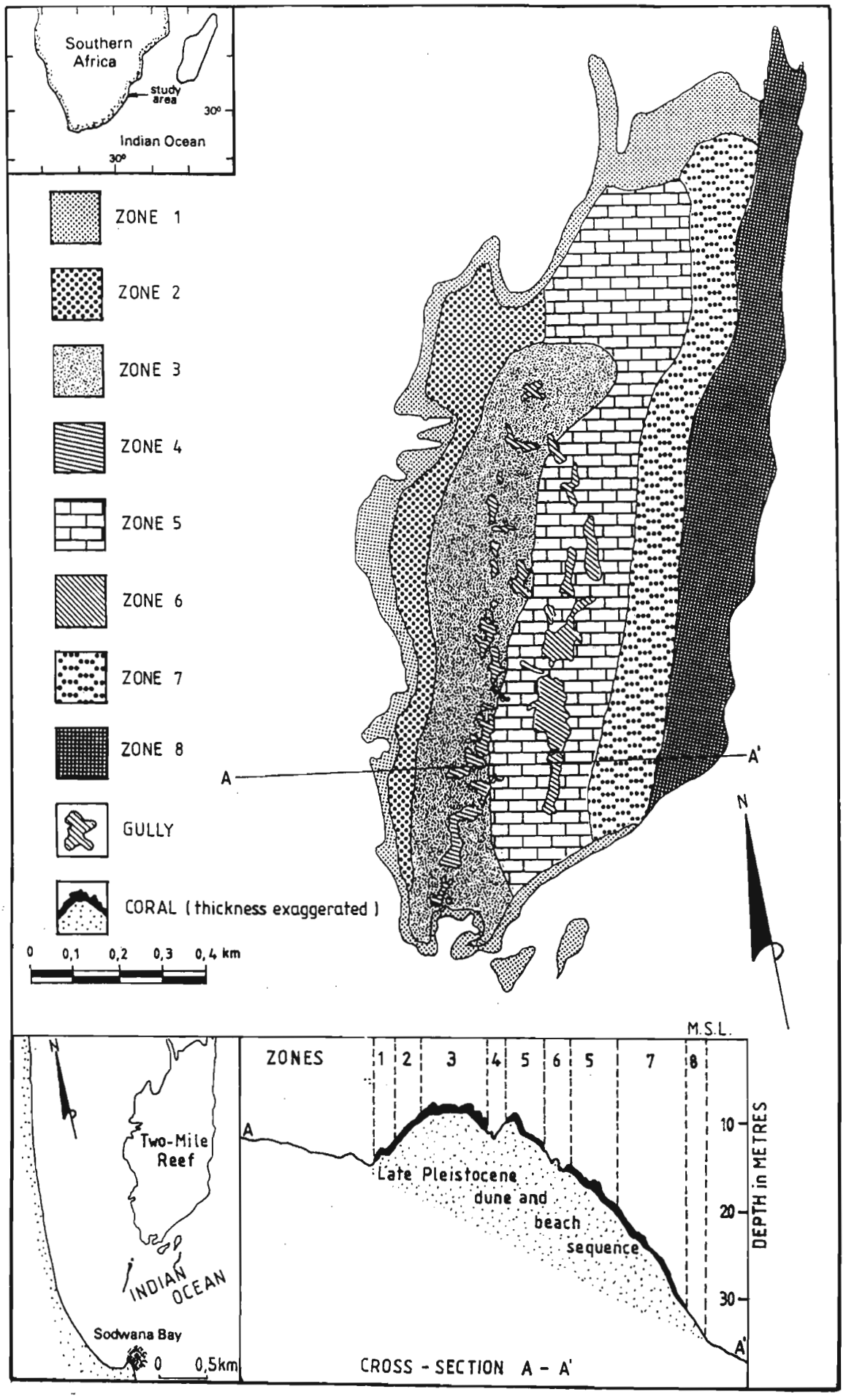

Figure 6.2. Location map of the study area showing the position of Two-Mile Reef and the "type" zonation scheme for Two-Mile Reef.

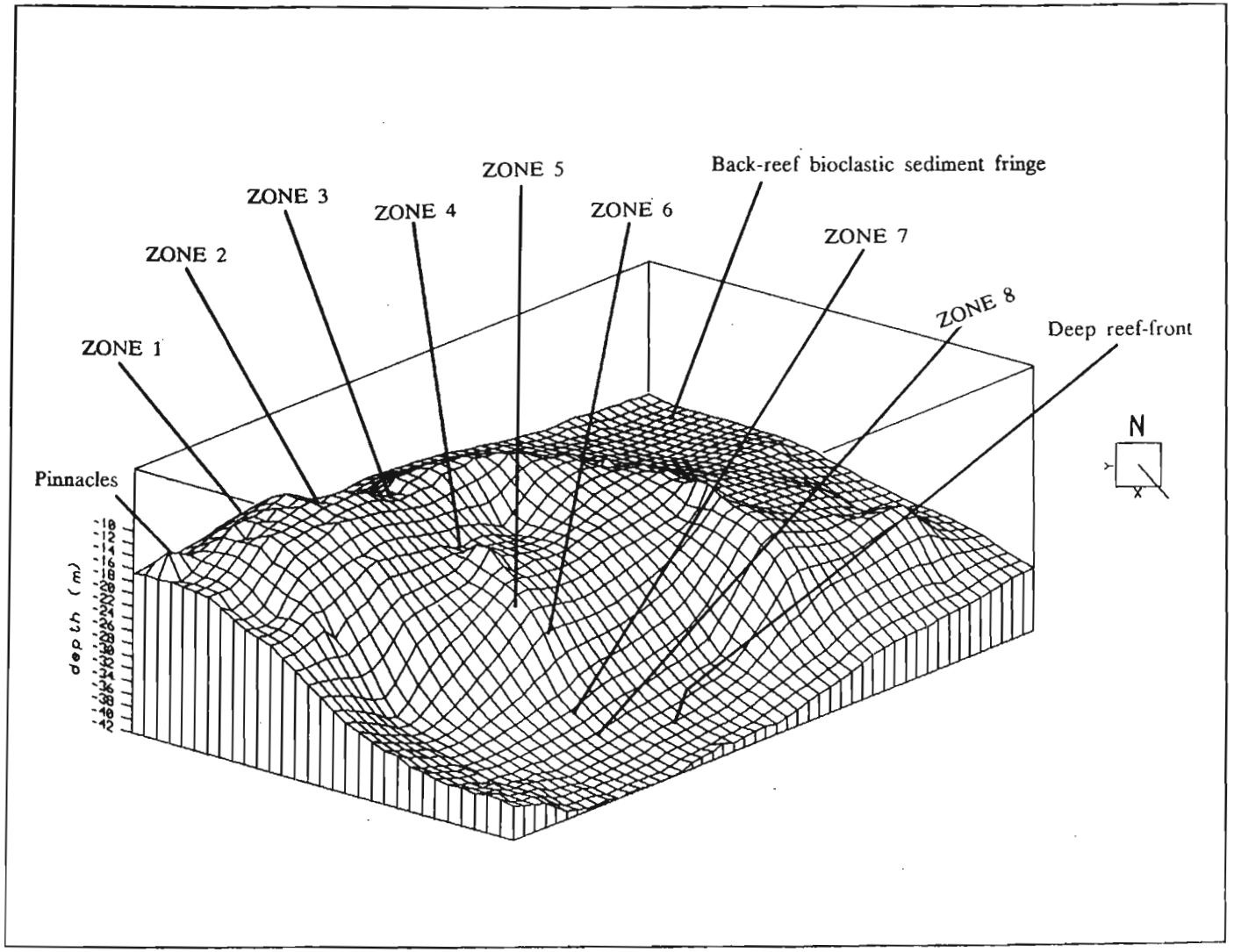

Figure 6.3. Computer-generated, three-dimensional surface model of Two-Mile Reef viewed from the southeast at a tilt angle of 20° above horizontal with the zonation scheme superimposed. The small legend next to the plot indicates the direction of view.

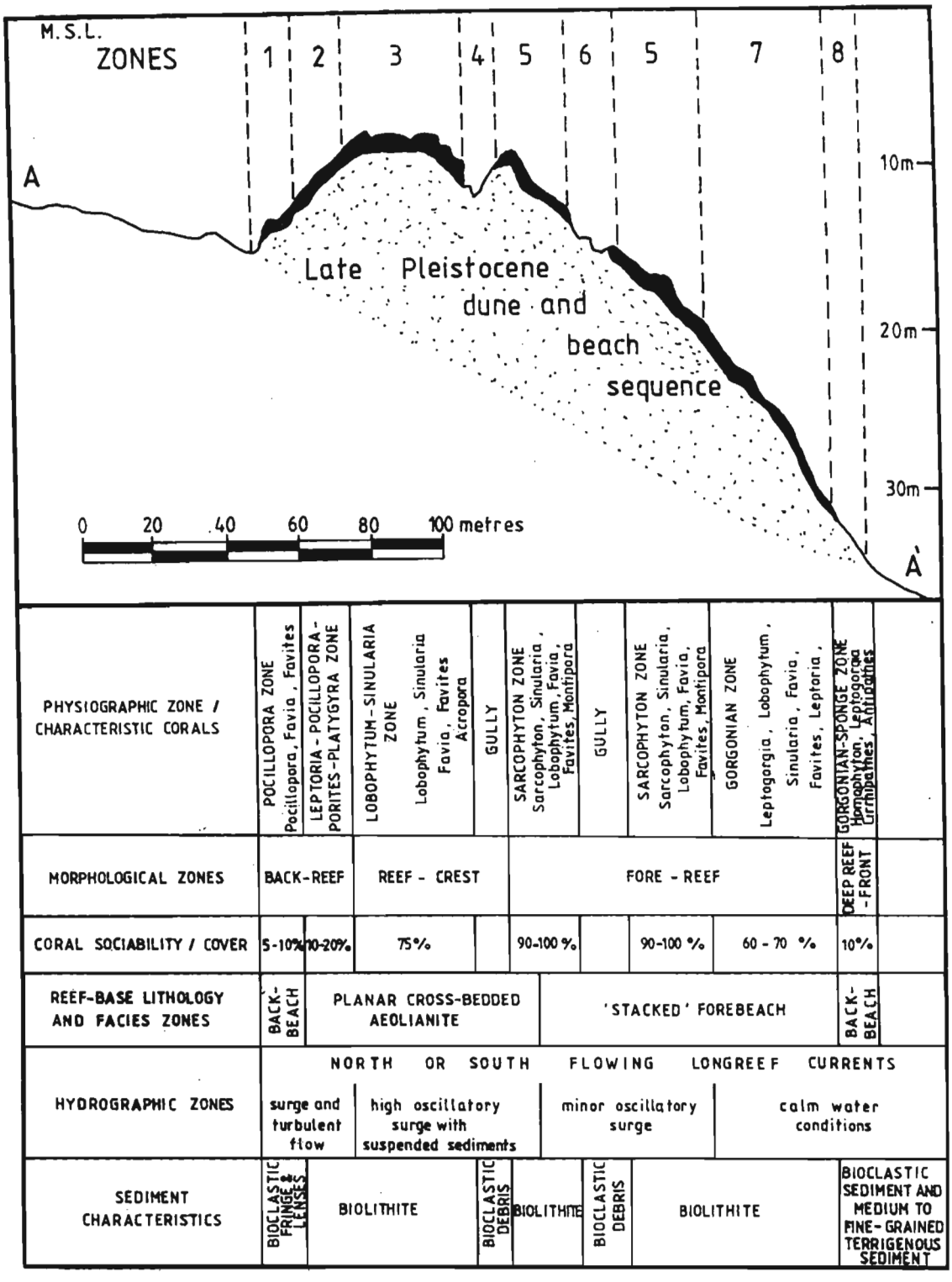

Figure 6.4. Reef cross-section A-A' on Two-Mile Reef indicating relationships of the physiographic, morphological, sociability, reef-base facies, hydrographic and sediment zones.

Porites, Platygyra, Astreopora, Symphyllia, Goniapora, Galaxea, Lobophyllia, Stylophora, Fungia, Anomastrea, Oxypora, Pavona, Pachyseris, Dendrophyllia, Coeloria, Hydnophora, Goniastrea, Oxyphyllia, and Oulophyllia (Fig. 6.5).

The eight defined physiographic and biological zones on Two-Mile Reef occur from the landward margin of Two-Mile Reef to the deep reef front zone (Figs. 6.2, 6.3, & 6.4).

Zone 1

Zone 1 is the landward margin of the reef and occasional "spur and groove" topography is developed. These ridges strike perpendicular to the shore and have a maximum height of 40cm. Within 20m of the reef margin they disappear under the fringe of bioclastic sediment which surrounds the reef (Fig. 6.6). Water depth varies from -15m to -21m and coral growth is sparse (approximately 5% coral cover or sociability), due to dynamic sediment movement on the reef fringe.

Soft alcyonarian corals are not as common in this zone as on other areas of the reef. The only abundant scleractinian genus is Pocillopora; Favia and Favites are however common. Pocillopora is the commonest genus in this zone, which is defined as the "Pocillopora Zone". The reef is fringed by skeletal biogenic carbonate sediment, mainly of molluscan origin, derived from the reef environment (Ramsay, 1988; Ramsay & Mason, 1990b). Subtidal ladderback ripples often form in this sediment after a strong northeasterly wind (Ramsay et al., 1989; see 5.3.3.2).

Zone 2

Zone 2 is a flat, subdued-relief zone with scattered coral colonies covering 10% of the area, though in some places the coral cover is much greater (Figure 6.6). Depths vary from -12m to -14m and less coral debris occurs here compared to Zone 1. Alcyonarian corals are less common in Zones 1 and 2 than on the rest of the reef. The most abundant corals are the scleractinian genera Leptoria,

TWO-MILE REEF

	ZONE 1	ZONE 2	ZONE 3	ZONE 5	ZONE 7	ZONE 8
ALCYONARIANS						
Lobophytum sp.	c/p	p	a	a/c	a	p
Sinularia sp.	c/p	p	a	a	a	
Sarcophyton sp.	p/r	p	c	a	c	p
Dendronephthya sp.	r	r	p	p	p	
SCLERACTINIANS						
Favia sp.	c	p	c	c	c	p
Favites sp.	c	p	c	c	c	
Montipora sp.			p	c	p	
Leptoria sp.	p	a	c	c	c	r
Acropora (plate)	r	p	c	c	c/p	p
Acropora sp.	p	p	c	c/p	p	
Echinopora sp.		p	c	c	c/p	r
Turbinaria sp.	p	p	p	p	p	
Pocillopora sp.	a/c	a	p	p	r	
Porites sp.	p	a	p	p		
Platygyra sp.	p	a	p/c	p		
Astreopora sp.		p	p	p		
Symphyllia sp.		p				
Goniapora sp.			p	r	r	r
Galaxea sp.			r	p/r		
Lobophyllia sp.			r	p/r	p	
Stylophora sp.			p	p/r		
Fungia sp.			p	p		
Anomastrea sp.	p		p/r			
Oxypora sp.			r			
Pavona sp.			r	r		
Pachyseris sp.						
Dendrophyllia sp.						
Coeloria sp.			p/r	r		r
Hydnophora sp.						
Goniastrea sp.						
Oxyphyllia sp.						
Oulophyllia sp.			r	r	r	
ANTIPATHARIANS						
Antipathes sp.			p/c	p	r	p
Cirrhipathes sp.					r	c/p
GORGONIANS						
Leptogorgia sp.			p	p	c/p	a
Homophyton sp.			p	p		a

Figure 6.5. Distribution of coral genera in the eight "type" zones of Two-Mile Reef. Underwater observations of the coral genera abundance/cover were either: (a) r = rare, very few specimens in the study area; the value of dominance or cover is insignificant; (b) p = present, coverage is poor; (c) c = common, a large number of specimens significantly contributes to reef cover; (d) a = abundant, many specimens and the value of dominance or cover is very significant.

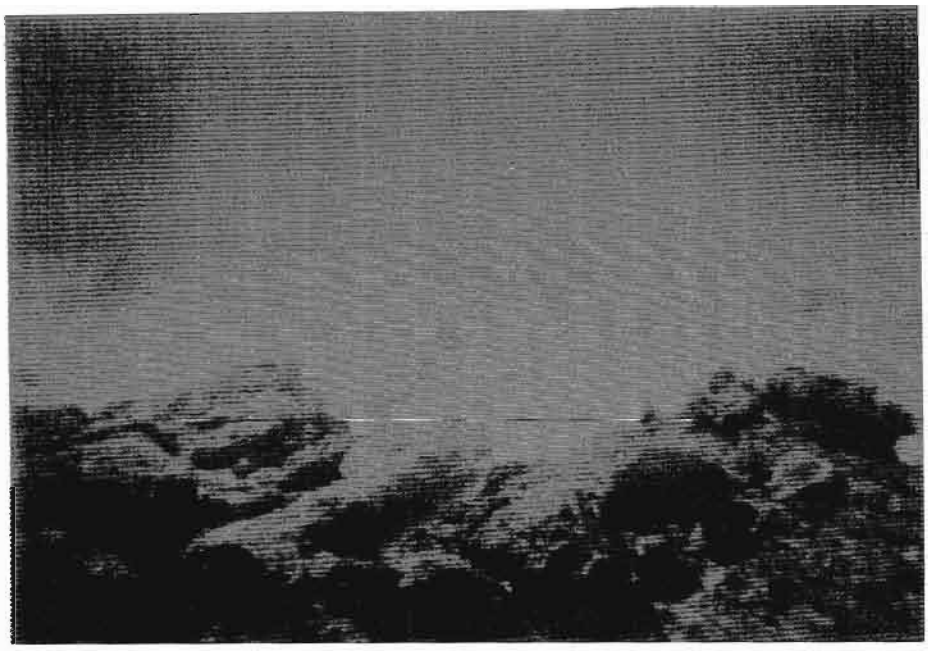

Figure 6.6. Underwater photograph of Zone 1 - Zone 2 (foreground) interface at -17m. This illustrates the carbonate sediment fringe on the landward margin of Two-Mile Reef. The foreground field of view is approximately four metres.

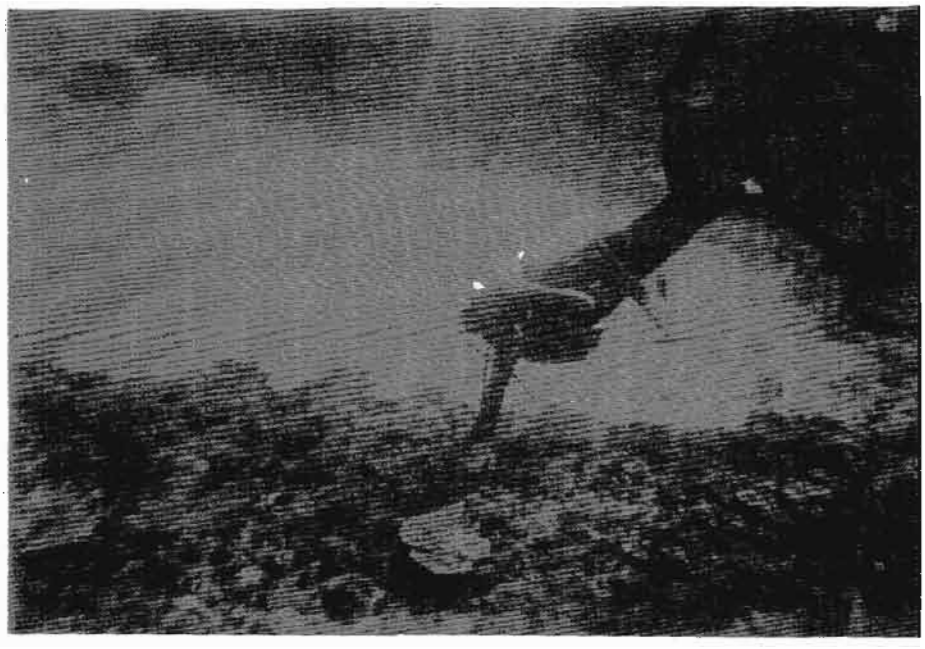

Figure 6.7. Underwater photograph of an inter-reef gully on the reef-crest (Zone 3) striking at 120°. Note the presence of rippled bioclastic debris in the gully. The depth is -13m.

Pocillopora, Porites, and Platygyra; a suitable name for the zone is the "Leptoria - Pocillopora - Porites - Platygyra Zone". Rocky outcrops in this zone tend to be covered by brown algae. Zones 1 and 2 form the back-reef environment which dips at 3° to the west.

Zone 3

Zone 3 is a shallow, high-energy, and rugged-relief central region of the reef which is parallel to the shore. This is the reef-crest zone, closest to the ocean surface, with numerous deep gullies, overhangs, and pinnacles, and depths varying from -9m to -13m (Figs. 6.7 & 6.8). The zone resembles the "spur and groove zone" described by Pichon (1974) on the fringing reefs of southwest Madagascar.

Corals are abundant in this zone with a total coral cover of about 75%. It is a stressful environment with a relatively high sediment load, and where the erosive effects of wave, surge, and tidal action are concentrated. Individual alcyonarian coral colonies tend to be larger, and species diversity is lower than in the deeper, seaward zones. According to Williams (1989a), these corals produce great quantities of mucus as an adaptation against the abrasive action of the high suspended sediment load in the water, and the mucus is an important nutrient source in coral reef food webs (Means & Sigleo, 1986). Other workers (Davies, 1984; Mitchell & Chet, 1975) have related excess mucus production to an excess of available nutrients within the surface waters. The reason for excess production of mucus by Zululand corals still needs to be investigated. The stressful conditions on the reef-crest result in alcyonarian colonies displaying a low relief with short and compact lobes on the upper surface as opposed to having elongate digitate processes (Williams, 1989a).

The most common coral genera include the dominant alcyonarians Lobophytum, Sinularia, Sarcophyton, and Dendronephthya whilst the most common scleractinians are Favia, Favites, Acropora, Leptoria, Echinopora, and Montipora. Antipatharians are represented by Antipathes. This high energy reef-crest zone has been named the "Lobophytum - Sinularia Zone". The lower part of the spur or gully side-wall is usually devoid of coral growth owing to dynamic sediment scouring in this

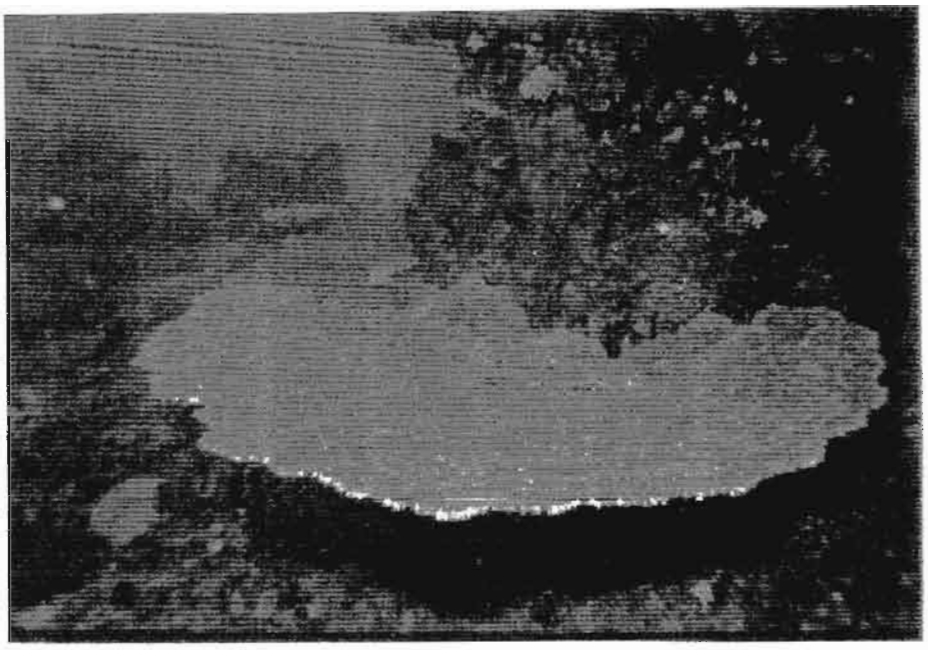

Figure 6.8. A large Acropora sp. plate coral (1 metre diameter) growing at the base of a pinnacle at a depth of 12 m on the reef-crest.

Figure 6.9. A narrow, 50 cm wide, sinuous inter-reef gully photographed in Zone 5 at a depth of -17m.

area. Antipatharians and gorgonians such as Rumphella tend to congregate on the spur side-walls (Williams, 1989a): corals are scarce. Pichon (1974) describes a lack of coral growth in similar areas of the reefs of southwestern Madagascar. Reef-derived debris, broken coral, and impact marks on soft and hard corals were observed here. These features were caused by a tropical cyclone which passed over the Zululand coast in January 1988, just before the initial zoning survey was carried out.

Zone 4

Zone 4 consists of 20-50m wide, north-south trending gullies which separate Zone 3 from Zone 5 (Map 2). Skeletal, reef-derived, bioclastic carbonate sediment occurs in the gullies and is underlain in places by medium- to fine-grained terrigenous quartz sand with a minor biogenic component. The bioclastic reef-derived sediment is moderately well-sorted, finely- to coarsely-skewed, and has a mean grain size of between 0.885-0.682mm. The origin of these gullies and those defining Zone 6 are discussed in 5.1.1.1.

Zone 5

Zone 5 is a flat, subdued-relief zone with a few pinnacles rising 2-3m above the average reef level. Depths are between -13m and -20m. The zone is dominated by regular, narrow, inter-reef gullies striking at approximately 120° (Fig. 6.9). The coral assemblage is diverse and soclability is 90-100%. The corals in this zone attain a maximum thickness of 20cm. This zone is named the "Sarcophyton Zone" as it is the dominant genus, often reaching 70cm in diameter (Fig. 6.10). Alcyonarian genera include Sarcophyton, Sinularia, and Lobophytum, whilst the common scleractinians are Favia, Favites, Montipora, Acropora, Leptoria, Echinopora, and Turbinaria. Reefal debris is less evident than in the other zones. This can be attributed to less tidal and wave action affecting the zone, thereby defining it as a lower energy regime.

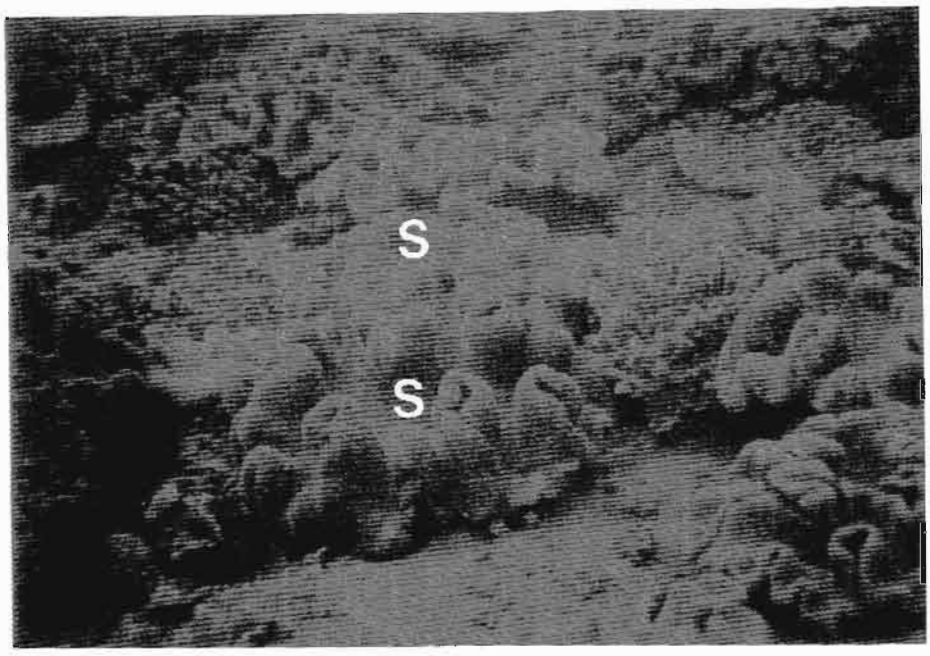

Figure 6.10. Numerous colonies of the characteristic Zone 5 soft coral Sarcophyton sp. (S); photographed at a depth of 18 m. Average colony diameter 30 cm.

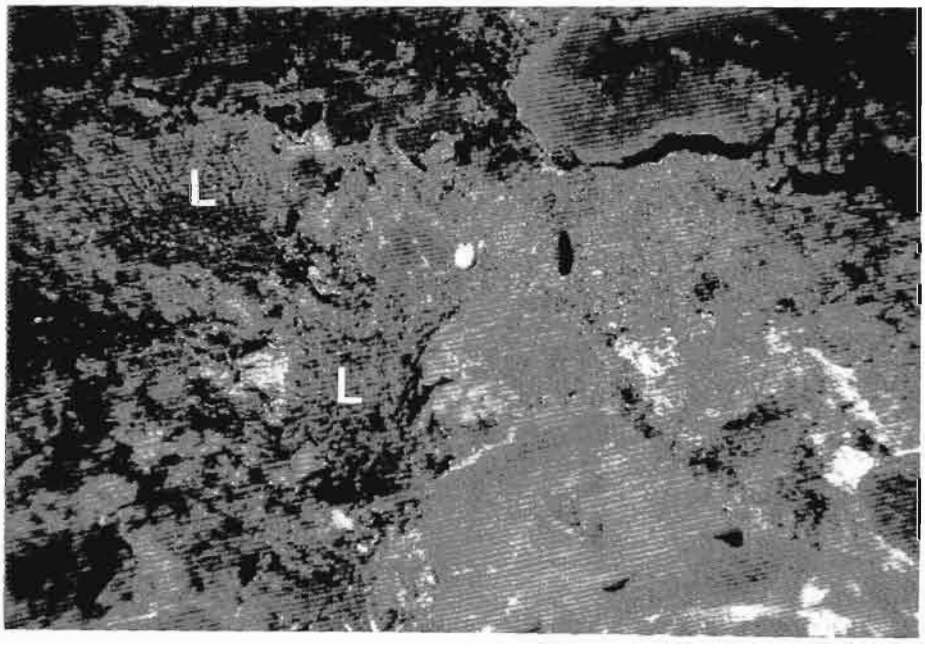

Figure 6.11. The appearance of numerous colonies of the red gorgonian Leptogorgia sp. (L) indicate the Zone 7 coral assemblage. Depth -21m.

Zone 6

An 80-100m wide set of north-south trending gullies occur at -17m within Zone 5 and this has been termed Zone 6 due to a change in physiography. The inter-reef gully sediment is typically reef-derived biogenic material with occasional mounds of dead coral rubble. The sediment is well- to moderately well-sorted and near-symmetrically skewed with a mean grain size between 0.803-0.578mm.

Zone 7

In Zone 7 there is a marked change in relief compared to Zone 5, with a range of 1.5m between gully bottom and reef level. Water depths vary from -21m to -28m in this zone and there are no true inter-gullies developed. Reef-base outcrops are seldom exposed beneath the extensive coral cover. Apart from the common hard and soft coral genera observed in the other zones, the hard coral Lobophyllia occurs along with colonies of red gorgonian sea fans (Leptogorgia sp.). This has given the zone its name: the "Gorgonian Zone" (Fig. 6.11). A reduction in abundance of Sarcophyton is also noted. Zones 5, 6 and 7 comprise the fore-reef environment which dips at an average of 3.5° seaward.

Zone 8

This -29m to -35m deep zone represents the deepest reef and reef-front environments of Two-Mile Reef. Potholes penetrate about 20% of the zone. Similar potholes, described by Coetzee (1975a), exist on the modern wave-cut platform and are formed by pebble grinding and diurnal carbonate solution and dissolution reactions (see 5.1.1.1). The relief is subdued and neither true inter-reef gullies nor "spur and groove" topography are well-developed. The reef front grades imperceptibly into terrigenous quartz sand, with a few biogenic grains: no topographic break is observed. Light penetration is poor at this depth, resulting in a low diversity coral assemblage. A sparse fauna of epifaunal algae, numerous sponges, gorgonians, black corals and occasional hard and soft coral varieties cap the underlying beachrock outcrop. Alcyonarians are usually Sarcophyton and Lobophytum colonies;

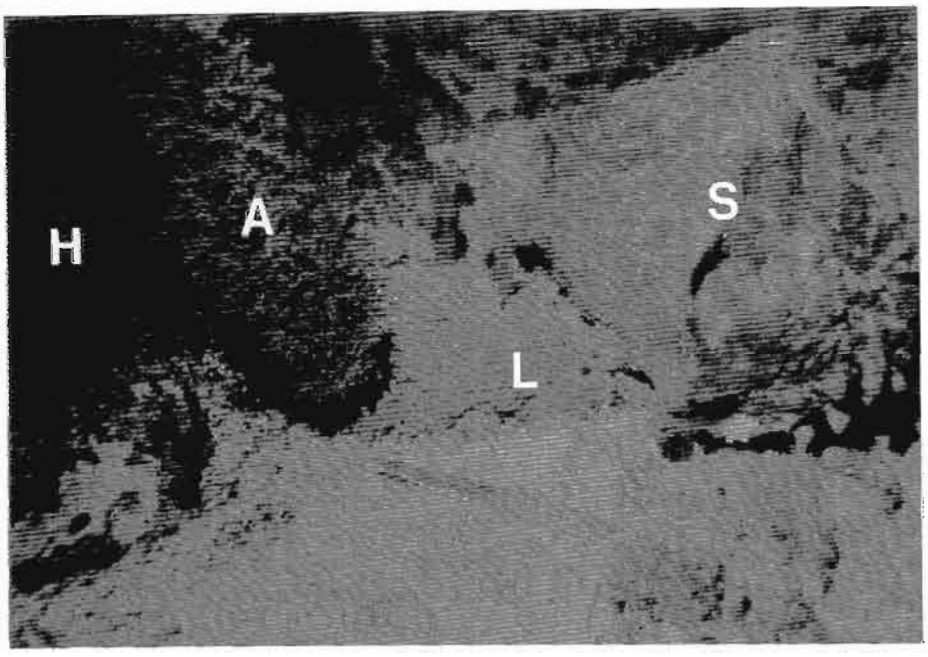

Figure 6.12. The deep reef-front zone (Zone 8) is characterised by the gorgonians Homophyton sp. (H) and Leptogorgia sp. (L) together with numerous large vase- and cup-shaped sponges (S) and Antipathes sp. black corals (A). Depth -32m.

scleractinians include Favia, Acropora, Leptoria, Coeloria, and Echinopora. Cup- and vase-shaped sponges are extremely common, as are gorgonians (Homophyton and Leptogorgia) and black corals (Antipathes and Cirrhipathes). A suitable name for this zone is the "Gorgonian-Sponge Zone" (Fig. 6.12).

6.5 APPLICATION OF THE TWO-MILE ZONING MODEL TO OTHER ZULULAND REEFS

6.5.1 Four-Mile Reef

Four-Mile Reef is a patch reef located 5.1km north-northeast of Jesser Point, Sodwana Bay, along the same strike as Two-Mile Reef (Fig. 6.13). The reef is 1.2km long and 1050m wide. Depths vary from -15m over the central reef axis to -35m on the deep reef-front zone (Fig. 6.14). The reef consists of flat ledges with few topographic high areas except on the reef-crest. The topographic highs are formed by resistant, planar cross-bedded aeolianite outcrops described in 5.1.1.1. The coral capping the homogeneous, ferruginous, calcareous aeolianite reef-base reaches a maximum thickness of 30-40cm with a sociability (surface cover) of 80-100%. A topographic break of 1.5m occurs between the fore-reef and the deep reef-front boulder tract. This boulder tract extends seaward for approximately 50m. Inter-reef gullies are not as well-developed as they are on Two-Mile Reef. This is probably due to lower hydraulic swell dynamics reducing the gully erosion rate acting on this subdued-relief reef structure.

Corals on the reef have a homogeneous distribution and are mostly scleractinian, comprising 60% of the coral reef fauna while alcyonarian corals make up the 40% balance (Fig. 6.15). The dominance of hard corals over soft corals shows that Four-Mile Reef is more like a true Indo-Pacific coral reef than the other Zululand coral reefs studied. The commonest scleractinians are Acropora (both branched and plate varieties) (Figs. 6.16 & 6.17), Favia, Favites, Montipora, and Echinopora. Sarcophyton

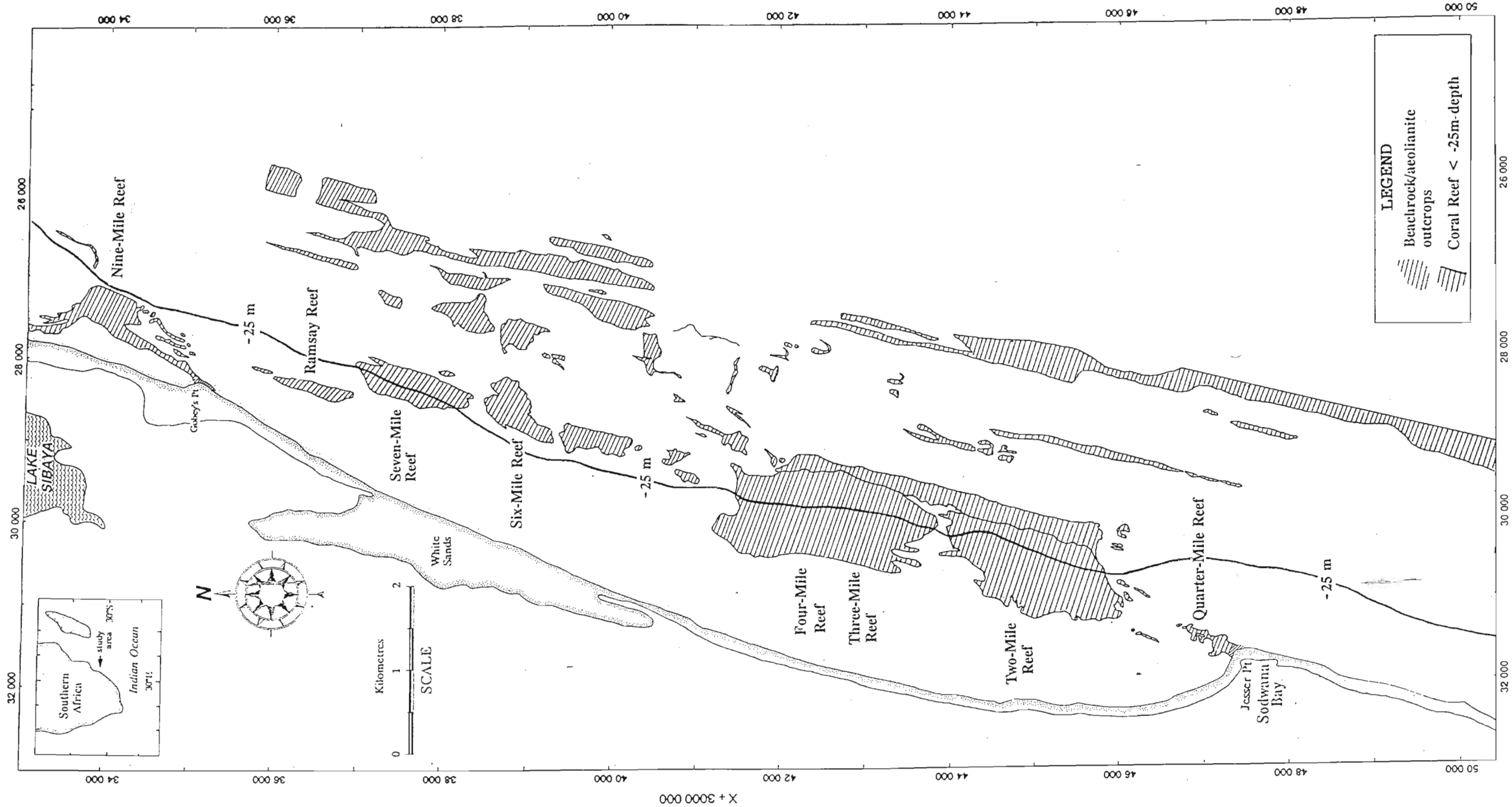

Figure 6.13. Location map of Two-Mile, Four-Mile, Seven-Mile, Ramsay, and Nine-Mile Reefs in relation to Sodwana Bay.

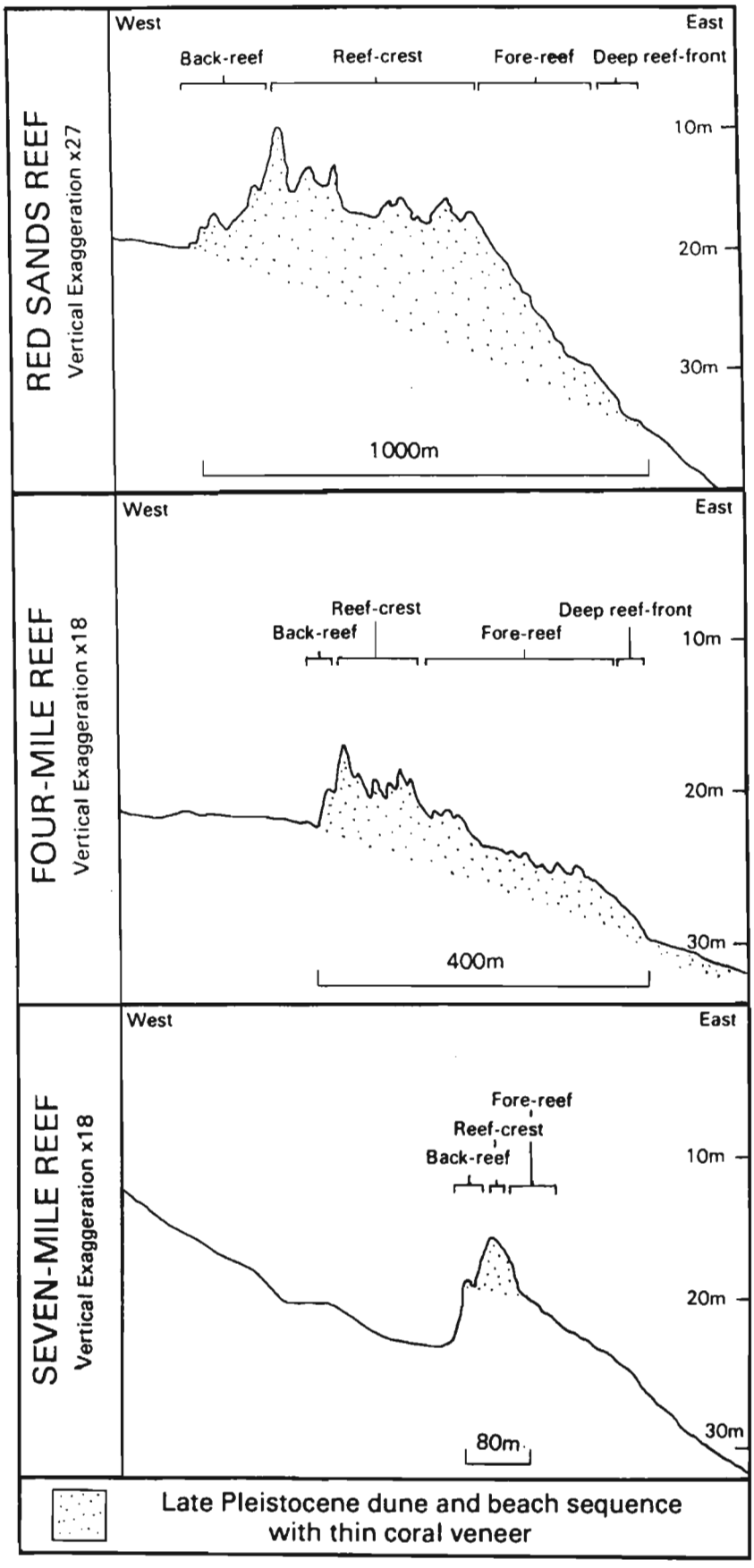

Figure 6.14. West-east cross-sectional profiles of Red Sands, Four-Mile, and Seven-Mile Reefs. The horizontal scales of the profiles differ.

	FOUR-MILE	SEVEN-MILE		
		Zone 1	Zone 2	Zone 3
ALCYONARIANS				
Lobophytum sp.	p	a/c	a/c	a/c
Sinularia sp.	c/p	a/c	a/c	a/c
Sarcophyton sp.	a	c/p	c/p	c/p
Dendronephthya sp.	r	p	p	p
SCLERACTINIANS				
Favia sp.	c	c	c	c
Favites sp.	c	c	c	c
Montipora sp.	c	c	c	c
Leptoria sp.	c/p	p	p	p
Acropora (plate)	a/c	c	c/p	c/p
Acropora sp.	a		c/p	p
Echinopora sp.	c	c/p	c/p	c/p
Turbinaria sp.	c/p	p	p	c/p
Pocillopora sp.				
Porites sp.	p	p	p	p
Platygyra sp.	c/p	p	p	
Astreopora sp.	p	p	p	p
Symphyllia sp.	p			
Goniapora sp.	p	p	p	p
Galaxea sp.	p	p	p	p
Lobophyllia sp.	r	p	p	p
Stylophora sp.				
Fungia sp.	c/p	p	p/r	p/r
Anomastrea sp.				
Oxypora sp.				
Pavona sp.	r			r
Pachyseris sp.				p
Dendrophyllia sp.	r			r
Coeloria sp.	p/r	p	p	p
Hydnophora sp.				
Goniastrea sp.			p	p
Oxyphyllia sp.	r			
Oulophyllia sp.	r			
ANTIPATHARIANS				
Antipathes sp.	p/r		p	p
Cirrhipathes sp.	r		p	p/r
GORGONIANS				
Leptogorgia sp.				p/r
Homophyton sp.				

Figure 6.15. Distribution of coral genera in the zones on Four-Mile and Seven-Mile Reefs.

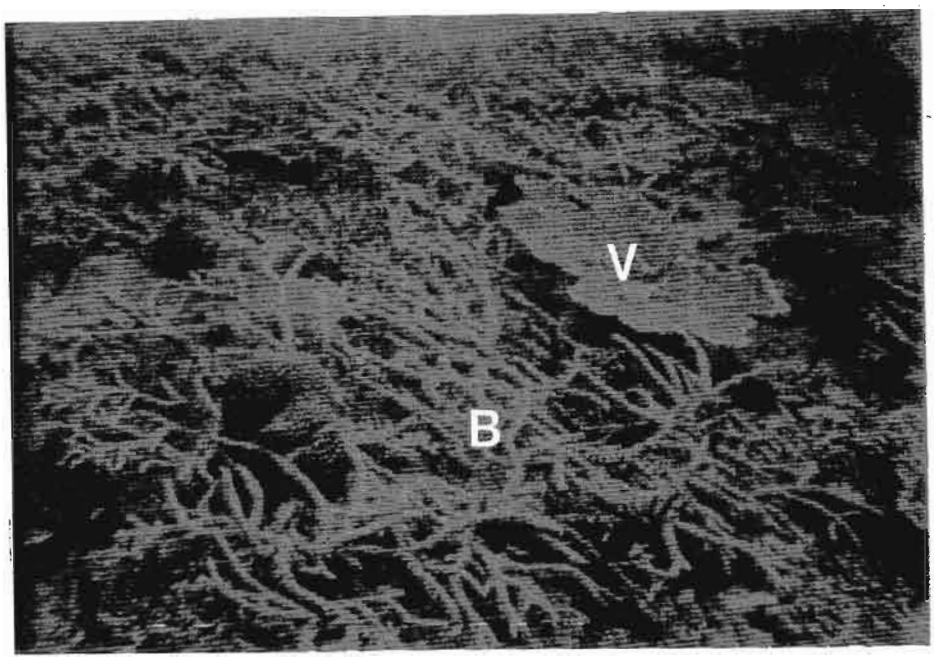

Figure 6.16. Acropora brueggemanni (Brook) and Acropora vasiformis (Brook) plate corals (B and V respectively) are abundant on Four-Mile Reef (-20m).

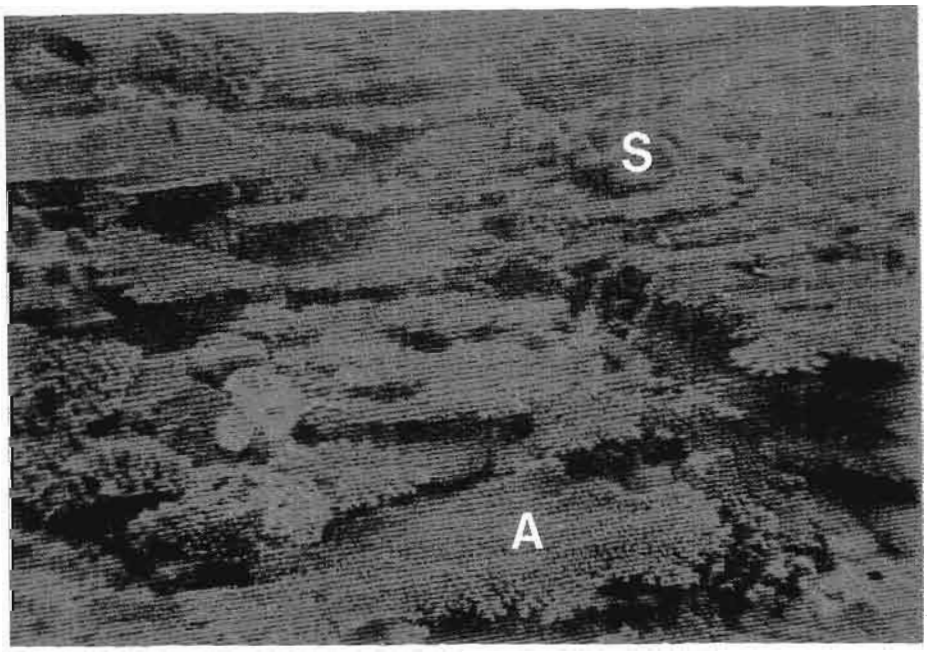

Figure 6.17. Extensive colonies of Acropora sp. (A) and the dominant soft coral, Sarcophyton sp. (S). Depth -21m.

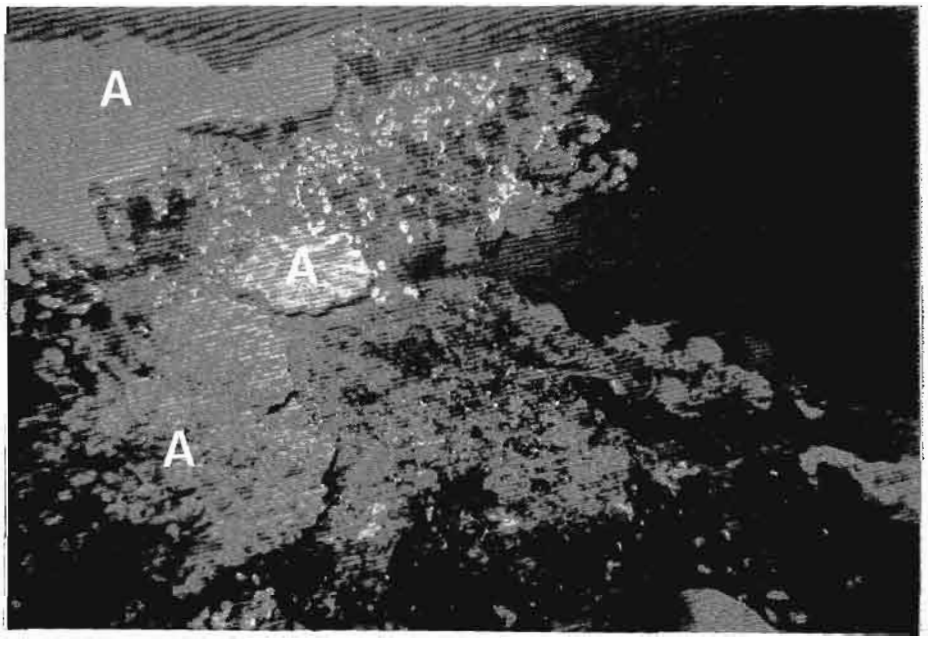

Figure 6.18. Underwater photograph of the reef-crest on Seven-Mile Reef (-15m) showing the dominance of alcyonarian corals (A).

dominates the soft coral component with Sinularia and Lobophytum being important. Sarcophyton is almost as abundant as Acropora; the name most applicable to the reef zone is "Acropora-Sarcophyton Zone". Four-Mile Reef is a mono-zone reef owing to the homogeneous distribution of the corals and the geomorphology of the reef.

If the zoning scheme of Two-Mile Reef is applied to Four-Mile Reef, Four-Mile Reef would fit into Zone 5 ("Sarcophyton Zone") of Two-Mile Reef. The major difference between them is the abundance of Acropora on Four-Mile Reef.

6.5.2 Seven-Mile Reef

Seven-Mile Reef is a small patch reef located 10.1km north-northeast of Jesser Point (Fig. 6.13). The reef is 1.4km long and 390m wide. Water depths vary from -15m on the reef-crest to -30m on the reef-front (Fig. 6.14). The reef coral veneer caps an aeolianite and beachrock ridge lying approximately 800-900m offshore. Reef coral thickness varies from 5-30cm. Alcyonarian and scleractinian abundance ratios are comparable to those on Two-Mile Reef and the coral sociability (surface cover) is approximately 70%. The reef comprises three geomorphological zones: back-reef, reef-crest, and fore-reef (Fig. 6.14). These define three physiographic and biological zones on Seven-Mile Reef. All three zones have similar abundances of the alcyonarian genera Lobophytum, Sinularia, Sarcophyton, and Dendronephthya (Fig. 6.15).

The **back-reef** environment (Zone 1) is characterised by a steep, shoreward-dipping slope. Depths in this zone vary from -22m on the reef margin/sandy sea-bed interface to -18m at the base of the reef-crest. The zone is distinguished by the lack of antipatharians and branched Acropora though Acropora plate varieties are common. Other common scleractinian corals include the ubiquitous Favia, Favites, Montipora, and Echinopora.

The reef-crest zone (Zone 2) has numerous deep gullies, overhangs, and pinnacles, and depths vary from -15m to -18m (Fig. 6.18). The relief from gully bottom to reef platform is as much as 5m. This zone is biologically characterised by the appearance of the antipatharians Cirrhipathes and Antipathes which are recorded as "present". On other Zululand reefs Cirrhipathes is much less abundant and is usually recorded as "rare" following the Mergner & Scheer's (1974) coral sociology scheme. A good correlation can be made between Zones 1 and 2 on Seven-Mile Reef and Zone 3 on Two-Mile Reef, on the basis of physiographic and biological criteria.

The -19m to -30m deep seaward margin of the reef is the fore-reef zone (Zone 3). The zone has a subdued relief with a few isolated pinnacles rising 1.5m above the reef level. Besides the common scleractinians that occur elsewhere on the reef, the rare genera Pavona, Pachyseris, and Dendrophyllia occur in small numbers in the fore-reef zone. The presence of the red gorgonian sea fan Leptogorgia is also characteristic of this zone. The geomorphology and coral fauna of the reef-front zone (Zone 3) correlates well with Zone 7 ("Gorgonian Zone") on Two-Mile Reef.

6.5.3 Other Sodwana Bay Reefs

Other coral reefs in the area include, from south to north, Six-Mile Reef, Ramsay Reef, and Nine-Mile Reef (Fig. 6.13). No detailed physiographic and biological zoning traverses have been undertaken on these reefs, although a general impression of the reef biota has been gained through numerous SCUBA dives on these reefs. Zones have been assigned to each of the reefs on a qualitative basis.

Six-Mile Reef is a medium- to small-sized patch reef 8.7km north of Jesser Point at depths of -25m to -40m. The topography is subdued with limited hard coral growth represented mainly by Acropora plates. The reef can be best categorised as a Zone 8-type or "Gorgonian-Sponge Zone" reef. Ramsay Reef is located 11.1km north of Jesser Point, in between Seven-Mile Reef and Nine-Mile Reef. The reef

axis is just under 1km in length with depths varying between -10m to -22m. The shallow, rugged, reef-crest passes seaward onto a subdued sea-level planation platform at -18m with well-developed potholes incised on it. The coral distribution on Ramsay Reef is similar to that found on the reef-crest of Two-Mile Reef and as such the reef can be classified as a Zone 3-type or "Lobophytum - Sinularia Zone" reef. Nine-Mile Reef, which lies 13.6km north of Jesser Point, can also be classified as a Zone 3-type or "Lobophytum - Sinularia Zone" reef. The depth of this very topographically rugged reef varies from -3m on the reef-crest to -22m on the deep reef-front zone.

6.5.4 Red Sands Reef

Although this reef is located outside the study area, it has been included as an analogue to Two-Mile Reef. Red Sands Reef is a patch reef lying 23km south of Jesser Point, Sodwana Bay (Fig. 6.19). The reef is larger than Two-Mile Reef, being approximately 5km long, 1km wide and 1km from the shore. The topography is very similar to that of Two-Mile Reef with depths varying from -9m on the reef-crest to -35m on the reef-front (Fig. 6.14). Inter-reef gullies are orientated in two directions; 000° and 124°. The physiographic and biological zoning of the reef resembles Two-Mile Reef. Zones 1 to 8 occur from the landward margin of the reef to the deep reef-front and are identical to those on Two-Mile Reef. Zone 1 is developed on the landward margin of the reef in water depths of -15m to -17m. Between -13m and -14m depth zone 2 is developed, with the reef-crest (zone 3) occurring at depths of -11m to -13m. Zone 3 has a more rugged and blocky relief than the corresponding zone on Two-Mile Reef. A set of north-south trending gullies at -13m depth, with an average width of 40m make up zone 4. The "Sarcophyton Zone" (zone 5) is well-developed at a depth of -14m to -19m and has the same characteristics as Zone 5 on Two-Mile Reef. Zone 6 (gully zone) was not observed on the reef traverse owing to the reconnaissance traverse being located in between two gullies. Zone 7 (-20m to -23m) is populated by the characteristic zone gorgonian, Leptogorgia, as on Two-Mile Reef. Minor gully structures are present in this zone and strike at an orientation of 124°. The interface between zone

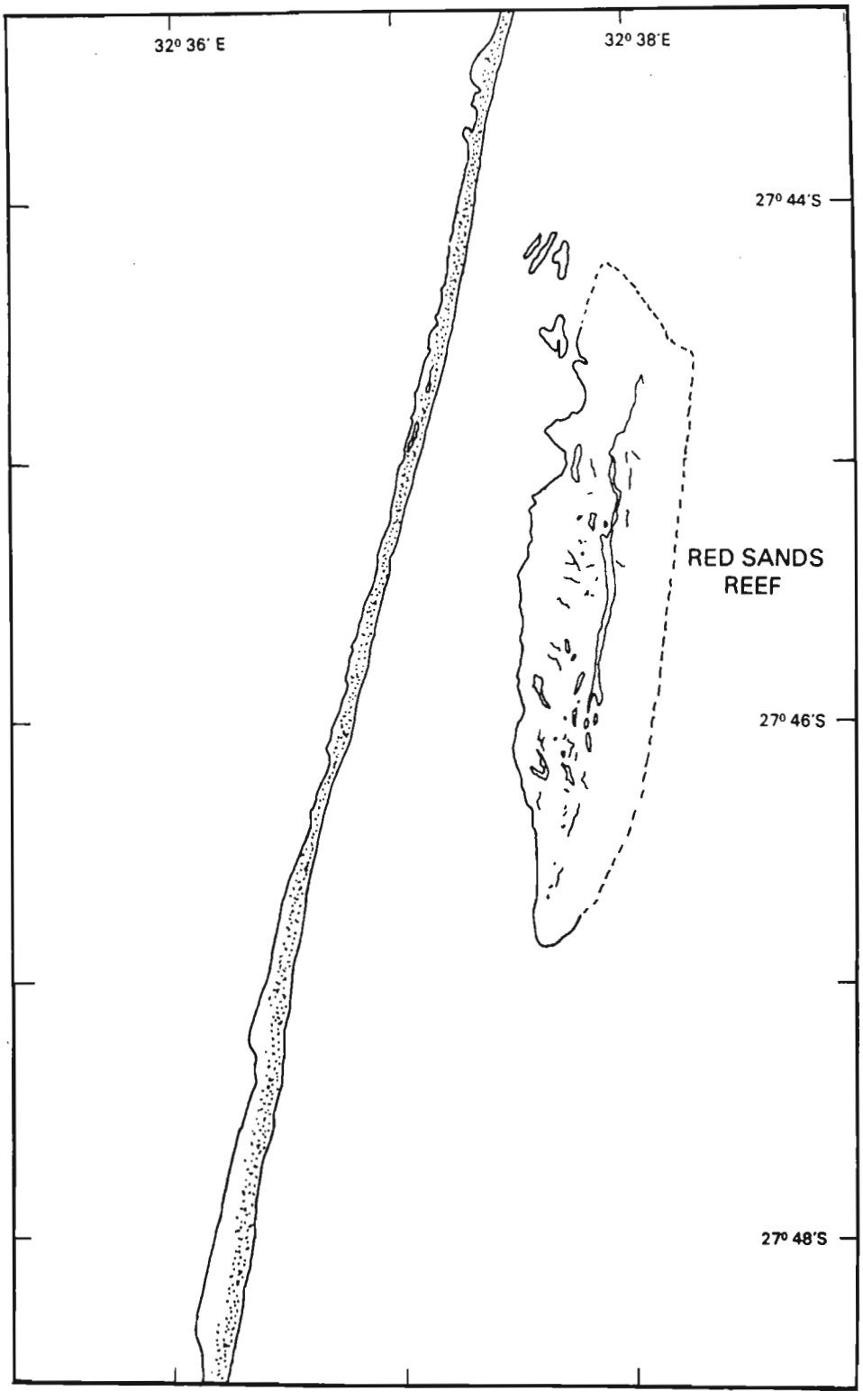

Figure 6.19. Location map of Red Sands Reef, 23 km south of Sodwana Bay.

7 and zone 8 occurs at a depth of -23m and is marked by the appearance of large vase- or cup-shaped sponges.

6.6 DISCUSSION

The "type" zoning scheme on Two-Mile Reef, Zones 1 to 8, is applicable on large Zululand coral reefs such as Red Sands Reef: controlling factors include similar depth controls and reef-base topography. Some of the Two-Mile Reef zones correlate well with zones on Four-Mile and Seven-Mile Reefs. Four-Mile Reef is a mono-zone reef with similar characteristics to Zone 5 ("Sarcophyton Zone") of Two-Mile Reef. A major difference between Two-Mile and Four-Mile Reefs is abundant Acropora on Four-Mile Reef. Acropora is more common on Four-Mile Reef due to quieter bottom conditions caused by the subdued topography of the reef. The back-reef (Zone 1) and reef-crest zones (Zone 2) on Seven-Mile Reef are very similar to Zone 3 on Two-Mile Reef with respect to physiographic and biological criteria. The reason why all the zones defined on Two-Mile Reef do not occur on all the reefs is that these other reefs have a compressed or restricted zonation because they are much smaller than the type area, Two-Mile Reef. Other large reefs on the Zululand coast, such as Leadsman Shoal (27°51.7' S ; 32°36.9' E), some 3.5km south of Red Sands Reef are predicted to have similar zoning characteristics to Two-Mile Reef because they will have similar abiotic factors such as light intensity and exposure, water exchange, and reef-base morphology. Leadsman Shoal is the largest and most southerly reef in the southwestern Indian Ocean; on the other side of the ocean, off southwestern Australia, reefs reach a higher latitude (29° S) (Guilcher, 1988) owing to the warm Leeuwin Current. Due to the location, a further detailed study of Leadsman Shoal would be worthwhile.

The maximum coral thickness found on the four reefs studied is only 30-40cm because:

(i) physico-chemical conditions for coral growth are not ideal in this marginal southwestern

fringe of the Indo-Pacific faunal province;

(ii) alcyonarians constitute 60-70% of the coral fauna on Two-Mile and Seven-Mile Reefs and as they are not reef builders this explains why the reef is merely a thin veneer;

(iii) the abundant soft corals, which are ahermatypic, compete for space on the reef with the hard coral varieties. Soft corals release terpenoid chemical compounds into the water which can cause local mortality, tissue necrosis (pathological death), and growth retardation in hard corals (Coll & Sammarco, 1986). The large numbers of soft corals, with their chemical defence mechanism, can retard the growth of hermatypic corals, thereby slowing down reef accretion.

CHAPTER 7: COMPUTER-AIDED REEF-BASE FACIES AND LITHOLOGICAL ANALYSIS

A new method of facies reconstruction has been devised to determine the late Pleistocene, carbonate-cemented, coastal sandstone environments (beachrocks and aeolianites) which formed the reef-base foundation of an offshore coral patch reef: Two-Mile Reef at Sodwana Bay. Ramsay (1990a) and Ramsay & Mason (1990a) devised the first successful method for defining detailed facies relationships of the regressive, aeollanites and beachrocks on the Sodwana Bay shelf.

7.1 METHODS

The facies analysis comprised:

(a) underwater observations of the reef-base sedimentary structures and general reef morphology (detailed in 5.1.1.1);

(b) a petrographic study of reef-base thin sections;

(c) a comparison of graphic settling statistics of acid-leached reef-base samples with modern unconsolidated dune/beach samples using cluster and discriminant analysis techniques.

A subsample of each reef-base sample was acid-leached with 36% hydrochloric acid to remove the carbonate cement. The residue was then rinsed to remove the HCl and oven-dried at 70°C. This fraction was split to the 1-2 g necessary for settling-tube analysis. The loss of carbonate skeletal grains (less than 5% of the total sample) due to acid-digestion is not considered important in the analysis. Cooper & Flores (1991), studied late Pleistocene coastal facies near Durban (South Africa) and noted that the loss of calcareous grains did not markedly alter the grain distributions of the original sediment. The graphic settling statistics of median (Φ), sorting (Φ), and skewness determined from the settling-tube analysis were compared to graphic statistics of modern unconsolidated coastal facies using cluster and discriminant analyses.

7.2 PETROGRAPHIC ANALYSIS OF AEOLIANITE/BEACHROCK

All of the samples described in this section were collected from submerged outcrops and petrographic descriptions are related to the morphological zones on the reef (Fig. 7.1). The sedimentary lithofacies of Two-Mile Reef, on which the modern corals are growing, comprises a carbonate-cemented, coastal sandstone: this is a beachrock/aeolianite sequence.

The rock fabric shows grains floating in a carbonate cement with occasional point-contacts: it has a high primary porosity. The average carbonate content of the reef-base is 32% with a range of 45-17%. The grains are mostly quartz (80-90%), with minor K-feldspar and plagioclase (5-10%). The lithic fragments comprise: (1) quartzite; (2) reworked beachrock/aeolianite; and (3) reworked Cretaceous composite grains. Occasional lithic fragments composed of lutecite, a length-slow variety of chalcedonic quartz, were noted in the samples; these indicate the former presence of evaporites (Folk & Pittman, 1973) which may have been derived from the Mozambique coastline. The rocks contain conspicuous organic grains including foraminifera, bivalve, echinoid, bryozoan, red algal, and occasional sponge spicule fragments; these commonly display replacement fabrics or iron-stained rims. The biogenic assemblage is similar to that noted by Siesser (1970) in the South African coastal limestones (beachrocks and aeolianites) between Saldanha Bay and Mossel Bay.

Thin section examination of the submerged coastal sandstones allowed them to be assigned to specific environments. The author recognises six sedimentary environments on the basis of petrography: this interpretation is supported by a statistical analysis and by underwater observations of sedimentary structures and reef morphology reported elsewhere (Ramsay, 1990a, Ramsay & Mason, 1990a&b).

Seaward margin of the reef-crest environment (-10m)

The rock is moderately well-sorted (0.58Φ), and very coarsely-skewed (-0.39) with a mean grainsize of

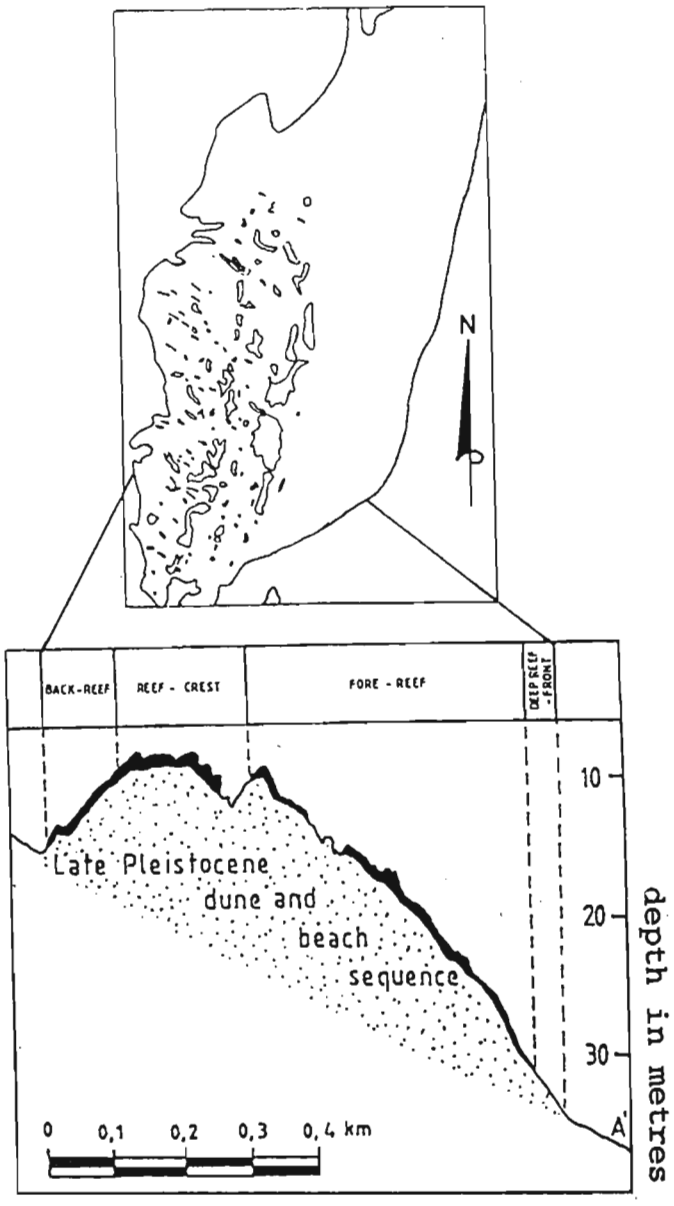

Figure 7.1. Map and cross-section of Two-Mile Reef showing depths and distribution of the reef's morphological environments.

0.283mm. The grains exhibit a rounded to sub-rounded character in all size classes. There are fewer lithic fragments than in other areas of the reef-base. The cementation history appears to have begun with the growth of an isopachous, equant rim cement around the grains, lithic fragments, and skeletal fragments. This was followed by cavity-filling equant sparite. Replacement fabrics include calcitisation and iron-staining of organic fragments and occasional replacement of quartz by calcite. The thin-section facies interpretation indicates a shallow, coastal marine environment probably at the dune/beach interface, based on biogenic components such as red algal fragments which are seen in the modern beach environment.

Back-reef and reef-crest gully-base environment (-11m)

The sediment is moderately sorted (0.73Φ), finely-skewed (0.20), with a mean grain size of 0.592mm, and the grains exhibit a sub-rounded to sub-angular character with the largest grains being rounded. In thin-section the grainsize population appears bimodal, but settling tube distribution statistics indicate a unimodal population. Lithic fragments appear to be derived from Cretaceous and ?Tertiary/Pleistocene lithologies. Bivalve fragments and other organic components, including sponge spicules, are common in this rock (Fig. 7.2). Cements include an initial isopachous rim cement and cavity-filling equant sparite cement: partial or complete replacement of organic fragments by micrite and sparry calcite are common (Fig. 7.3). The facies interpretation indicates formation in a shallow coastal or coastal fringe environment.

Upper to mid fore-reef environment (-12m to -16m)

The sediment is moderately sorted (0.82Φ), coarsely-skewed (-0.24), with a mean grainsize of 0.369mm. The grainsize population distribution in thin section appears bimodal with grains being sub-rounded to sub-angular or angular with the largest grains being sub-rounded; the settling tube grainsize distribution pattern indicates a unimodal population. The cementation history is the same as that found in the substrate of the back-reef environment. The facies interpretation indicates formation in

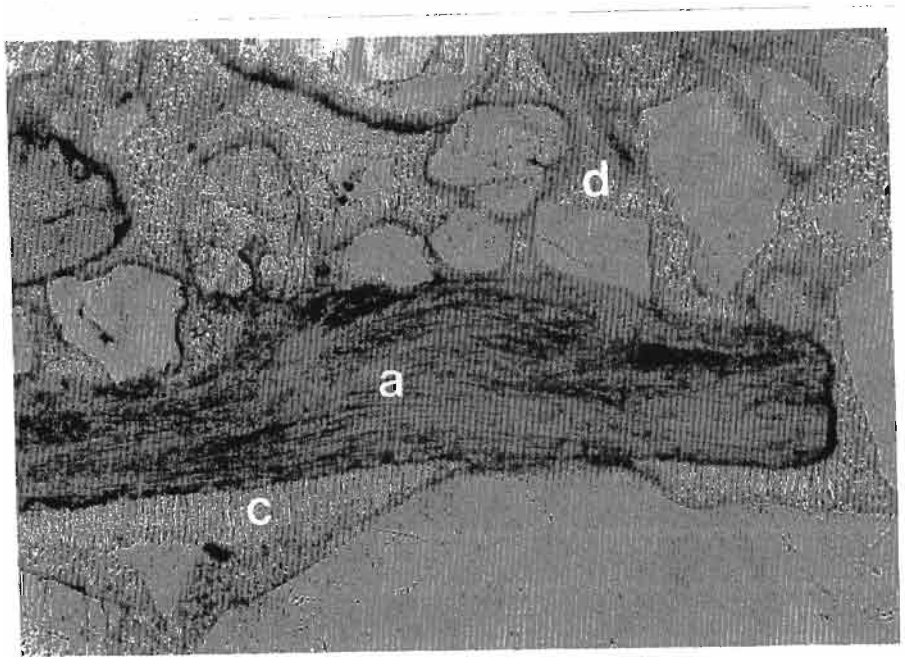

Figure 7.2. Thin section from the back-reef environment showing a bivalve fragment (a) with isopachous rim cement (c), angular quartz grains, and cavity-filling equant spar cement (d).

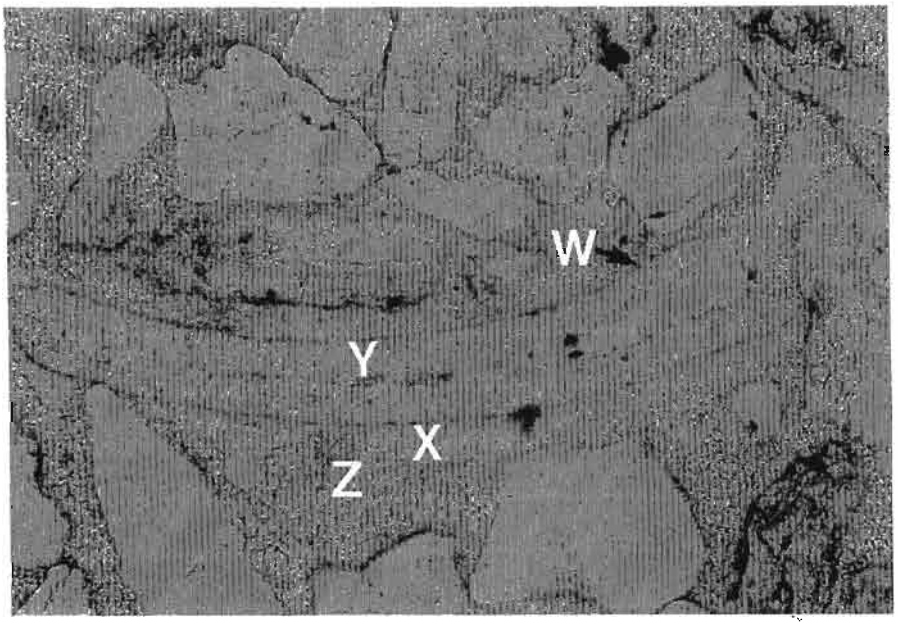

Figure 7.3. Thin section from the back-reef environment showing replacement of a bivalve fragment. The cementing episodes are:

(a) deposition of the bivalve fragment; (b) growth of a micrite grain coat on the biogenic fragment (W); (c) development of an isopachous rim cement on the grains (X); (d) dissolution of the bivalve fragment; (e) growth of internal replacement cement (Y); (f) growth of cavity-filling spar partly replacing cement (c) (Z).

a shallow coastal/coastal fringe environment.

Mid fore-reef environment (-18m)

The sediment is moderately well-sorted (0.64Φ), near-symmetrically skewed (-0.02), with a mean grainsize of 0.542mm. The grains are rounded and sub-rounded to angular as in samples 3,4, & 5 with a unimodal population distribution. The cementing episodes are different from the other samples examined. Sedimentary grains are partially or completely coated by primary micrite and grain throats are choked with opaque, non-pelleted micrite (Fig. 7.4). This was followed by an isopachous rim cement, which may have been aragonite, but has now inverted to sparry calcite. Finally, occasional voids were filled by clusters of micrite peloids of biogenic origin and subsequent cavity-filling equant sparite (Fig. 7.5). This indicates three generations of cement in the lithification process. The cementation process appears to have taken place in an intertidal environment.

Lower fore-reef environment (-23m)

The sediment is moderately well-sorted (0.51Φ), coarsely-skewed (-0.14), with a mean grainsize of 0.350mm, and the grains are rounded to sub-angular. Fewer marine organic fragments occur in this sample compared to the mid fore-reef environment. Cementation history began with micrite grain coats followed by partial cavity-filling sparite. A later event caused cavity-filling by micrite which in places is pelleted (Fig. 7.6). Micritisation of organic fragments followed and this explains why there are fewer organic fragments in this sample. The micrite which has replaced the organic fragments is lighter in colour than the micrite cavity-filling carbonate cement. An intertidal environment seems likely.

Deep reef-front environment (-34m)

The sediment is moderately well-sorted (0.59Φ), near-symmetrically skewed (-0.02), with a mean grainsize of 0.616mm. The grains are well-rounded to angular and are texturally more mature than

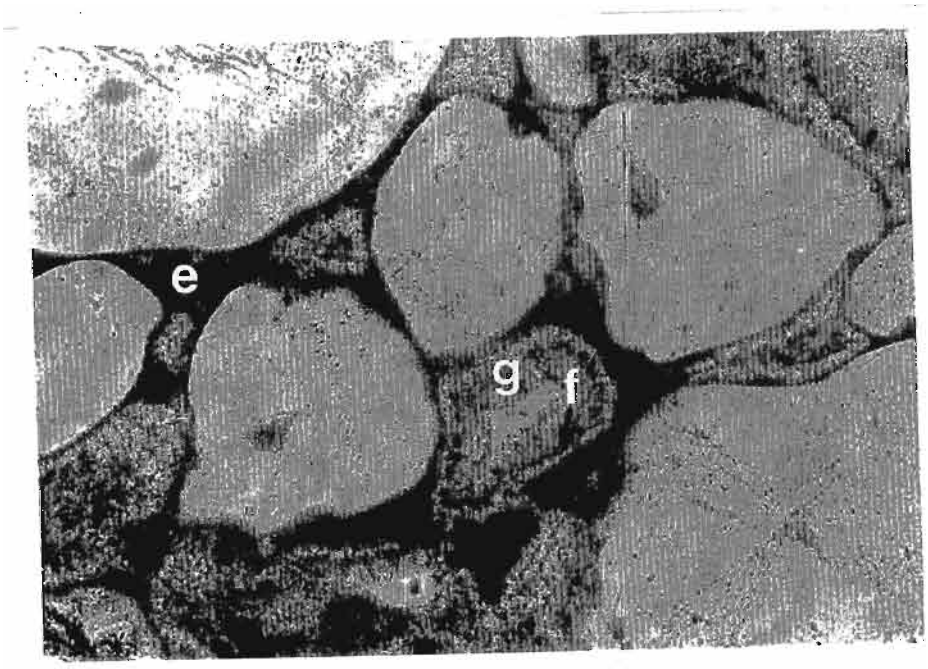

Figure 7.4. Thin section from the mid fore-reef environment showing grain throats choked with micrite (e) and later development of a sparry isopachous rim cement (f) and cavity-filling equant sparite (g).

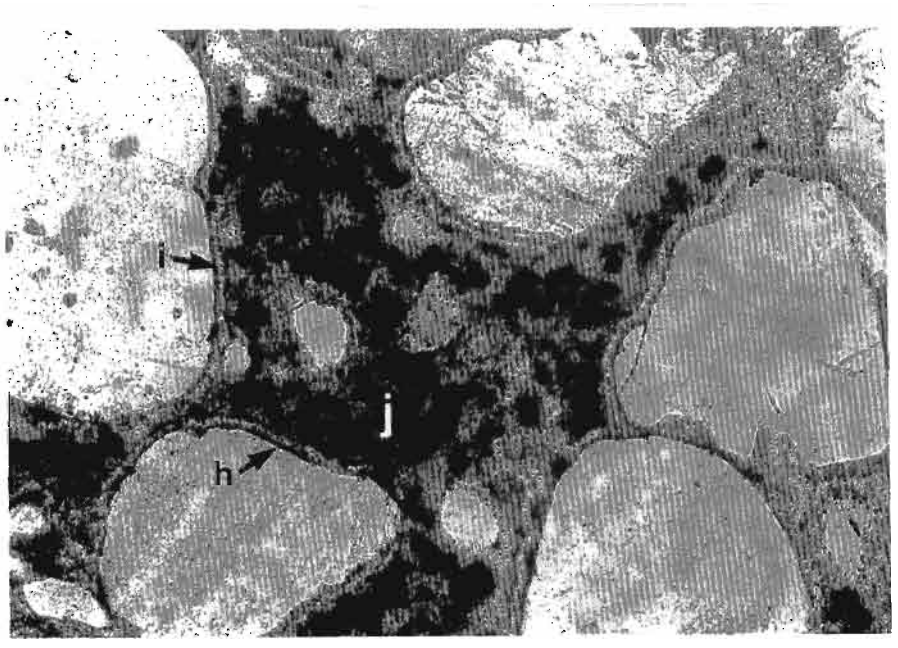

Figure 7.5. Same thin section as in Figure 7.3 showing three cementing episodes commencing with a micrite grain coat (h), later isopachous rim cement (i), and cavity-filling sparite. The micrite pelloids (j) filled the void during the pre-cavity-filling cementing episode.

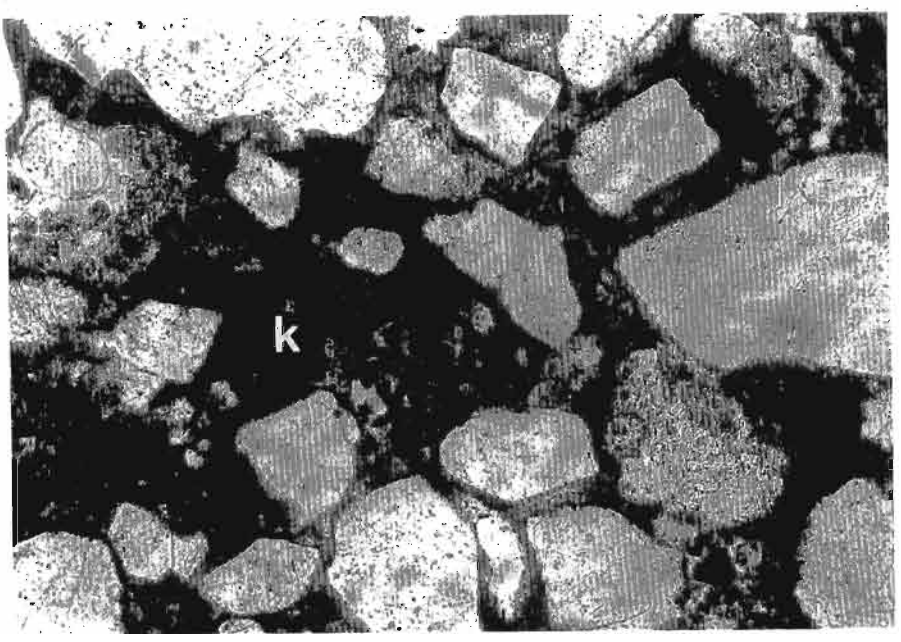

Figure 7.6. Thin section from the lower fore-reef environment showing a later cementing event of cavity-filling micrite (k) which in places is pelleted.

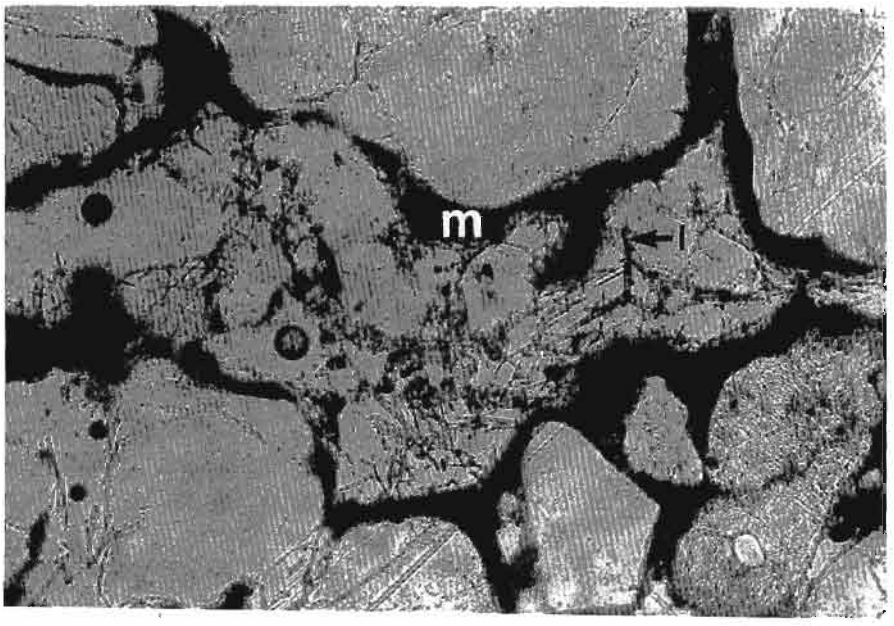

Figure 7.7. Thin section from the deep reef-front environment showing siliceous hexactinellid sponge spicules (l) in a void rimmed by micrite (m).

samples from the other areas of the reef. Siliceous hexactinellid sponge spicules are common and occasional remnants of sponge fragments can be seen in the voids (Fig. 7.7). Cementation began with a micrite grain coating, followed by an isopachous rim cement. A void-filling episode followed in which micrite, micrite pelloids, and equant sparite were introduced into the voids. A period of partial cement dissolution increased the rock's porosity considerably; this probably took place in the phreatic zone (Fig. 7.8). Decementation has been attributed to water table shifts (Blatt et al., 1980) associated with a subsequent transgression (Cooper & Flores, 1991). A backbeach palaeoenvironment seems reasonable, due to the mature nature and grainsize of the sediment together with the presence of large sponge fragments which are typical of modern backbeach environments of the northern Zululand coastline.

7.2.1 Review of carbonate cementation and beachrock/aeolianite formation

The origin of beachrock is controversial (Guilcher, 1988). Two favoured hypotheses are that cementation occurred by: (a) the action of fresh groundwater; (b) precipitation from seawater, as a result of evaporation (Komar, 1976). Field (1919) and Russell (1962) favour the former whilst Dana (1851), Daly (1924), Kuenen (1950), and Ginsburg (1953) favour the latter. Fairbridge (1950b) relates the formation of beachrock to percolation of carbonate-rich solutions carried down through the porous upper beach by rainwater and reprecipitation in the intertidal zone where the acid rainwater becomes neutralised by alkaline seawater and to carbonate oversaturation through solar heating at low-tides. Other workers favour this mode of formation (Coetzee, 1975b ; Guilcher, 1988). Although the action of groundwater has been invoked, beachrock occurs where there is no groundwater table (Guilcher, 1988). Beachrock cementation takes place under a 10-30cm cover of unconsolidated sediment; this subsurface cementation has been examined by Taylor & Illing (1969), Schmalz (1971), Davies & Kinsey (1973) and Leeder (1982). Fairbridge (1950b) predicted a theoretical maximum thickness for beachrock of 1.5m, although thicknesses of up to 5m have been recorded at Peron Point, Australia;

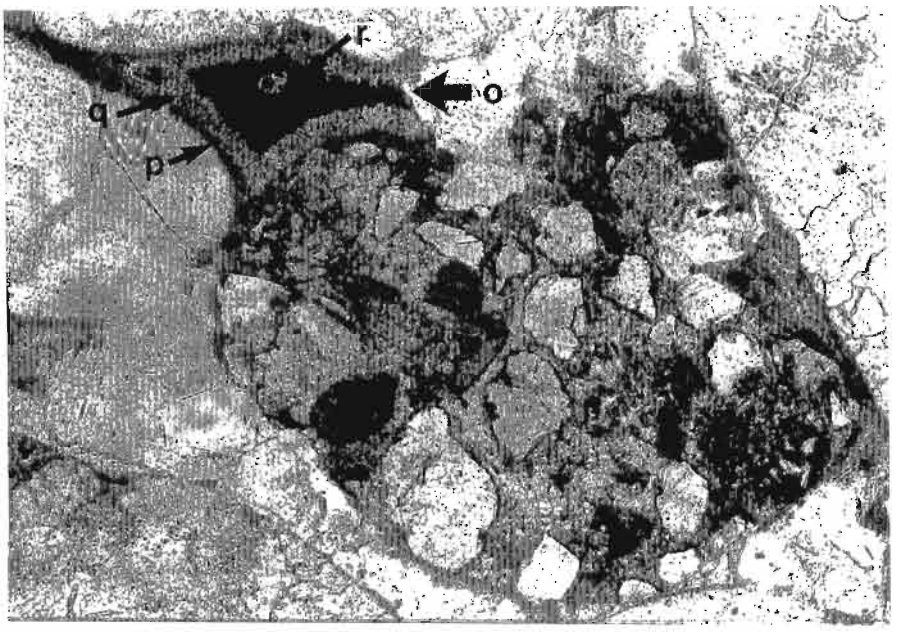

Figure 7.8. Thin section from the deep reef-front environment showing a lithic fragment of probable Cretaceous origin (n), three generations of cement, and phase of dissolution (o) which probably occurred in the phreatic zone. The three generations of cement include a micrite grain coat (p) succeeded by an isopachous rim cement (q). The final cementing episode introduced void-filling micrite (r) and equant sparite.

this was interpreted as beach formations formed through a period of changing sea-levels. It is not known how much cementation is phreatic marine, phreatic freshwater or vadose (Bathurst, 1974). Vadose cement in recent beachrocks is characterised by a stalactitic distribution, with thick fringes underneath the grains (Taylor & Illing, 1969). Not all solid pore-filling is cement; Taylor & Illing (1969) and Davies & Kinsey (1973) noted that carbonate mud adheres to the pore wails, trapped originally by organic films probably of algal origin. Schmalz (1971) and Davies & Kinsey (1973) indicate that precipitation of beachrock cement may be a nocturnal process, unrelated to the temperature or photosynthetic cycles, but showing a distinct relation between the mixing of meteoric with seawater and the precipitation of cement. Aragonite and high-magnesium calcite cement precipitation is a normal subtidal process in which no water mixing takes place (Bathurst, 1974). He goes on to say that intertidal mixing processes may well be responsible for the extremely rapid rate of beachrock cementation compared to that in its slower subtidal equivalent. Stoddart & Cann (1965) conclude that beachrock may form in more ways than one.

Rapid cementation was probably favoured at the vadose/phreatic interface. There, carbonate precipitation may be stimulated by evaporation of interstitial water (Taylor and Illing, 1969) and /or CO_2 degassing (Hanor, 1978); this can be enhanced by tidal pumping (Strasser et al., 1989). Mixing of marine and fresh water at the water table may also lead to cementation (Schmalz, 1971). Aragonite or calcite can be selectively precipitated by the influence that bacteria, fungi and algae in the sediment have on the pH and Eh conditions (Kitano and Hood, 1965; Mitterer and Cunningham, 1985). Strasser et al. (1989) state that superposition of different cements indicates changing parameters through time and space. Multiple cements in beachrock is well-documented by Stoddart and Cann (1965), Taylor and Illing (1969), Montaggioni and Pirazzoli (1984), Beier (1985), and Strasser and Davaud (1986). Strasser et al. (1989) also note that early consolidation is dominated by marine (phreatic to vadose) cements precipitating at, or close to, the water table. Beachrock situated above the water table undergoes freshwater diagenesis. Percolating rainwater locally dissolves unstable

aragonite and high-Mg calcite and precipitates low-Mg calcite. Freshwater cementation seals primary porosity and hardens the beachrock significantly (Strasser et al., 1989). Once exposed by erosion, beachrock may superficially be further cemented by freshwater diagenesis, or by carbonate precipitation from marine spray waters (Scoffin and McLean, 1978).

7.2.2 Cementing history of the Sodwana Bay beachrock/aeolianite

The cementation history of the submerged, carbonate-cemented, coastal sandstones from northern Zululand is very similar to the Holocene beachrock cementation described by Strasser et al. (1989) along the coast of southeastern Tunisia. Aragonite crystals commonly form isopachous rims around the grains, implying cementation in water-filled pores of a marine-phreatic diagenetic environment (Bathurst, 1975 ; Longman, 1980 ; Hird & Tucker, 1988). The isopachous rims are originally aragonite which inverts to calcite within a few hundred to thousands of years (Greensmith, 1979). Lowering of the water table during a regression causes the remaining pore space to be filled with equant sparite; this cement is normally associated with meteoric, vadose environments (Bathurst, 1975 ; Tucker, 1981 ; Weiss & Wilkinson, 1988). In the substrate of the mid fore-reef to deep reef-front environments (-18m to -35m) a micrite grain coat occurs around the grains and forms the base of the isopachous aragonite cement. This has been described in other parts of the world by Siesser (1970), Davies and Kinsey (1973), Pierson and Shinn (1985), Strasser and Davaud (1986), and Strasser et al. (1989). Micrite envelopes are usually attributed to the boring of skeletal fragments by algae or other organisms (Bathurst, 1966 ; Tucker, 1981). The minute algal-bored tubes within a grain's outermost surface are then presumably filled with micrite (Bathurst, 1966 ; Friedman, 1964). Siesser (1970), in his study of South African coastal limestones (beachrocks and aeolianites), noted the occurrence of micrite envelopes coating terrigenous grains. He concluded that algal boring was not the sole mechanism responsible for the formation of micrite envelopes but suggested that organisms may form micrite envelopes as a by-product of their own biological processes. Davies and Kinsey (1973)

suggested that the micrite coats originated from an organic mucus in which micritic carbonate was precipitated and trapped, and then served as nucleation site for the aragonite crystals. Beachrock from the mid fore-reef environment displays grain throats choked by micrite cement; this could represent meniscus cement linking the particles together, as described by Strasser et al. (1989). If this is the case, the meniscus cement would indicate cementation in the vadose zone (Longman, 1980). Strasser et al. (1989) also describes pores being completely filled by micrite cements (aragonite and/or high-Mg calcite) as is seen in the beachrock from the lower fore-reef and deep reef-front environments.

The cementation history of the late Pleistocene reef-base of Two-Mile Reef indicates lithification during a marine regression with beachrock and aeolianite forming on the present shelf close to the groundwater table. The result is a now submerged, stacked sequence of coastal aeolianites and beachrocks relating to various sea-levels during the regression.

7.3 PALAEOENVIRONMENTAL RECONSTRUCTION

Hutton's doctrine of uniformitarianism, "the present is the key to the past", is particularly relevant to the study of depositional processes and relict shorelines (Hails, 1983). In most cases coastal processes and weather patterns during the late Pleistocene were similar to modern conditions enabling direct comparisons to be made (Clifton et al., 1971 ; Dupré, 1984).

Textural and compositional features of individual sediment samples have long been used in an attempt to distinguish different environments of deposition (Siesser, 1972b). Known environments are sampled and the differences (if any) between them are recorded; these differences are then used to interpret ancient environments. Opinion is divided on the usefulness of this technique as some investigators have found significant differences while others did not (Siesser, 1972b).

Pettijohn et al. (1973) describe a refined method of sediment grain-size analysis obtained with a linear discriminant function. The discriminant function is a multivariate classifying function that assigns an unknown sample specified by several variables e.g. median (x_1), sorting (x_2), and skewness (x_3) to one or more populations of various environments (beach, dune, etc). For the three variables the discriminant has the form

$$D_3 = a_1x_1 + a_2x_2 + a_3x_3$$

where the a's are estimated from the data and D_3 is the discriminatory index. By determining x_1, x_2, and x_3 for unknown samples, they can be assigned to one of the parent populations.

Depositional environment fingerprinting assumes that the sediment has been winnowed by modern environmental processes to such a degree that the effects of inheritance are eliminated (Pettijohn et al., 1973). The orientation of the modern Zululand coastline has changed little since the Tertiary (Maud, 1968); this is demonstrated by analysis of the orientation of offshore coral reefs (Ramsay, 1988) and remnant, submerged dune cordons (Martin & Flemming, 1986). The modern northern Zululand coastline from Leven Point to Kosi Bay also has no rivers and this lack of fluvial contamination makes it ideal for comparative characterisation of the juxtaposed modern and ancient dune and beach environments.

7.3.1 Comparative reef-base settling analysis

This analysis set out to compare modern dune and beach environments along the northern Zululand coast with submerged ancient coastlines. The reef-base sediment is a carbonate-cemented sandstone and the analysis was carried out using a computer-based statistics programme called Statgraphics 4.0. The best way to compare such environments is to determine how the unknown facies relate to the known modern facies. This can be achieved by determining the graphic settling statistics of median (Φ), sorting, and skewness of the modern dune/beach facies and the reef-base facies and observing how

the known and unknown facies cluster together with respect to the graphic statistics. The type of clustering technique used is a seeded cluster analysis technique which relies on previously defined modern facies.

The cluster analysis procedure allows observations to be grouped from a multivariate data set into clusters of "similar" points. The seeded cluster method uses a "start-up" set of data points which the user specifies and these are used to initiate the clusters (Milligan, 1980 ; Statgraphics, 1989). Each additional case is then matched to the nearest seed point. Milligan (1980) recorded excellent cluster structure where starting seeds were obtained from valid a priori information (such as the defined modern coastal facies in northern Zululand). The cluster numbers corresponding to each observation can be saved for use in discriminate analysis for classifying observations (Statgraphics 4.0 manual, 1989). The discriminant analysis determines the linear combination of variables which produces the maximum difference between previously defined groups (Davis, 1973), and defines one or more functions of qualitative measurements to help discriminate among the groups. The author used the seeded cluster values as the classification factor and the median, sorting, and skewness values as the data vectors for the discriminant analysis.

The modern northern Zululand dune and beach environment was extensively sampled and divided into five facies, namely: aeolian, backbeach, forebeach, swash, and welded bar. These facies were differentiated on the basis of changes in beach profile and grainsize, the relationships of these facies can be seen in Figure 7.9. A representative sample of each of the five facies, based on the centroid of the median-sorting-skewness cluster, was chosen as the seed around which the unknown facies would cluster (Fig. 7.10). By using a seeded cluster analysis technique the unknown facies can be assigned to one of the modern coastal facies environments of the northern Zululand coastline.

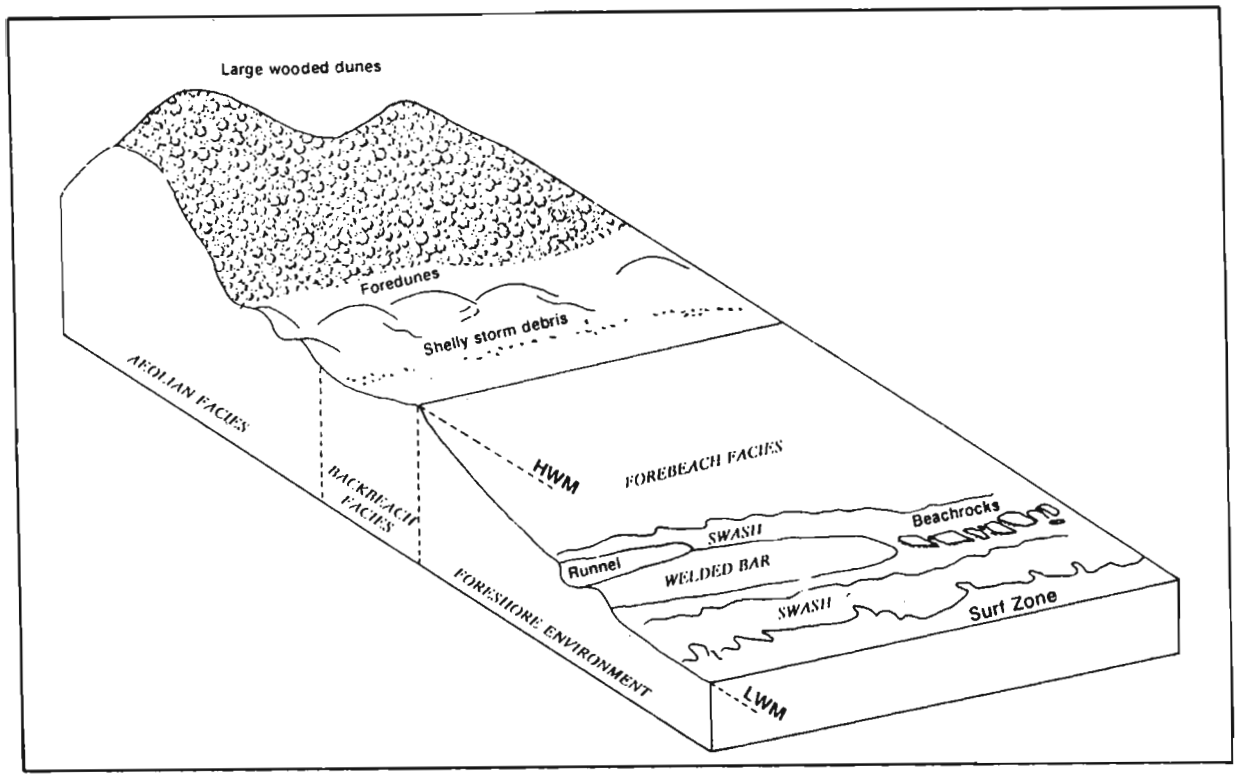

Figure 7.9. Idealised three-dimensional block diagram of modern coastal facies and facies relationships along the northern Zululand coastline.

FACIES CENTROIDS	MEDIAN (Φ)	SORTING (Φ)	SKEWNESS
Aeolian	1.56	0.31	-0.01
Backbeach	0.87	0.80	-0.22
Forebeach	1.66	0.29	-0.14
Swash	0.35	0.33	0.00
Welded bar	1.38	0.49	0.01

Figure 7.10. Graphic settling statistics of the five modern beach and dune facies along the northern Zululand coastline.

7.3.2 Cluster and discriminant results

The seeded cluster analysis separated the unknown reef-base facies into five clusters (Fig. 7.11) with the forebeach and welded bar facies being the most conspicuous facies, 31.58% respectively (Fig. 7.12). Most beachrocks form in the intertidal environment therefore this dominance of intertidal facies is to be expected. The backbeach is the next most dominant facies with aeolian and swash facies being the least common. If these facies are related to the morphological zones on the reef (Fig. 7.13), the substrate of the back-reef facies (at -13m to -17m depth) of Two-Mile Reef formed in a backbeach environment, whereas the substrate of the reef-crest (-9m to -13m) is an aeolian facies. A minor swash environment is developed on what is now the reef-crest/fore-reef interface. The substrate of the fore-reef facies may be ascribed to deposition in a forebeach/welded bar environment. The mid fore-reef (-18m) and the deep reef-front zone (> -30m) represents other backbeach facies.

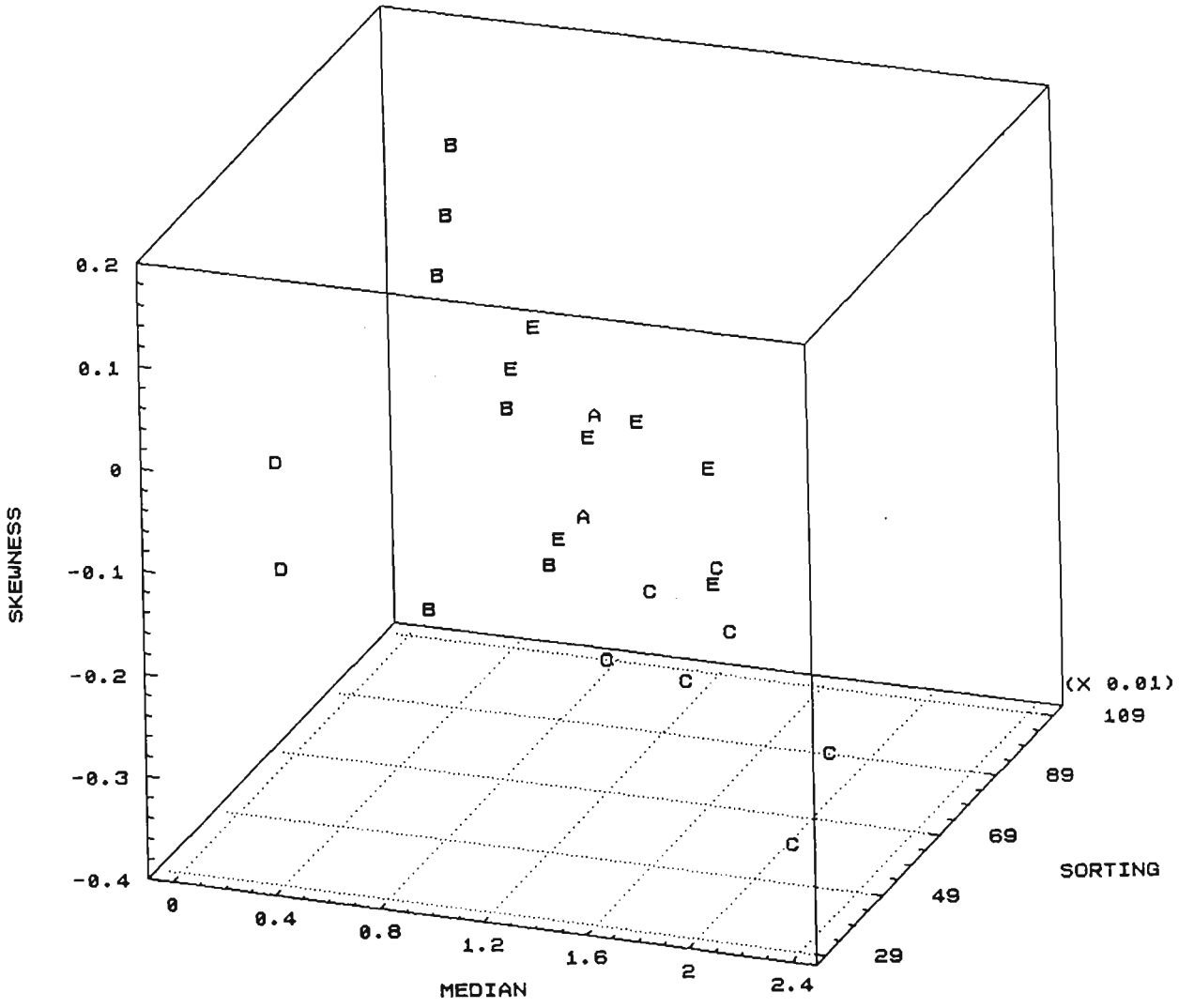

Figure 7.11. Seeded cluster analysis plot which separates the reef-base facies into the five defined modern coastal facies: (A) aeolian; (B) backbeach; (C) forebeach; (D) swash; (E) welded bar facies.

SEEDED CLUSTER	FREQUENCY	PERCENTAGE
Aeolian	1	5.26
Backbeach	5	26.32
Forebeach	6	31.58
Swash	1	5.26
Welded bar	6	31.58

Fig. 7.12. Frequency and percentages of five seeded cluster facies.

REEF-BASE SAMPLE	MEDIAN (Φ)	SORTING (Φ)	SKEWNESS	FACIES CLUSTER
1	2.05	0.58	-0.39	Forebeach
2	0.61	0.73	0.20	Backbeach
3	1.84	0.90	-0.40	Forebeach
4	1.58	0.74	-0.20	Welded Bar
5	1.49	0.81	-0.11	Welded Bar
6	0.90	0.64	-0.02	Backbeach
7	1.59	0.51	-0.14	Forebeach
8	0.65	0.67	0.15	Backbeach
9	0.74	0.50	-0.18	Backbeach
10	1.29	0.74	-0.05	Welded Bar
11	1.20	0.54	-0.11	Welded Bar
12	1.17	0.42	0.09	Welded Bar
13	0.68	0.61	0.11	Backbeach
414	1.94	0.32	-0.16	Forebeach
15	1.18	0.49	0.11	Welded Bar
16	2.00	0.42	-0.14	Forebeach
17	0.34	0.35	-0.11	Swash
18	1.61	0.31	0.09	Aeolian
19	1.92	0.45	-0.09	Forebeach

Fig. 7.13. Graphic settling statistics of reef-base samples and cluster facies correlation.

REEF-BASE FACIES	MEAN (mm)	MEDIAN (Φ)	SORTING (Φ)	SKEWNESS
Aeolian	0.320	1.61	0.31	0.09
Backbeach	0.592	0.72	0.63	0.05
Forebeach	0.299	1.89	0.53	-0.22
Swash	0.812	0.34	0.35	-0.11
Welded Bar	0.413	1.32	0.62	-0.05

Fig. 7.14. Mean values of the graphic settling statistics of reef-base samples correlated in their respective facies units.

The discriminant analysis (discriminant function 1 plotted against discriminant function 2) was used as a test to see if the clusters derived from the seeded cluster analysis were 'true' clusters or whether some overlap existed between the cluster groups (Fig. 7.15). Four of the five facies clusters separated out within the groups predicted in the discriminant analysis giving a correlation of 100%: there is no overlap between these facies groups (Fig. 7.16). The forebeach facies overlapped slightly into the aeolian facies group by 29%, therefore the difference between aeolian and forebeach facies must be confirmed by sedimentary structures (aeolian cross-stratification).

	Predicted Group					
Actual Group	1	2	3	4	5	TOTAL
1 (Aeolian)	100%	0	0	0	0	100%
2 (Backbeach)	0	100 %	0	0	0	100%
3 (Forebeach)	29%	0	71%	0	0	100%
4 (Swash)	0	0	0	100 %	0	100%
5 (Welded bar)	0	0	0	0	100 %	100%

Fig. 7.16. Classification of cluster facies based on discriminate analysis of seeded clusters.

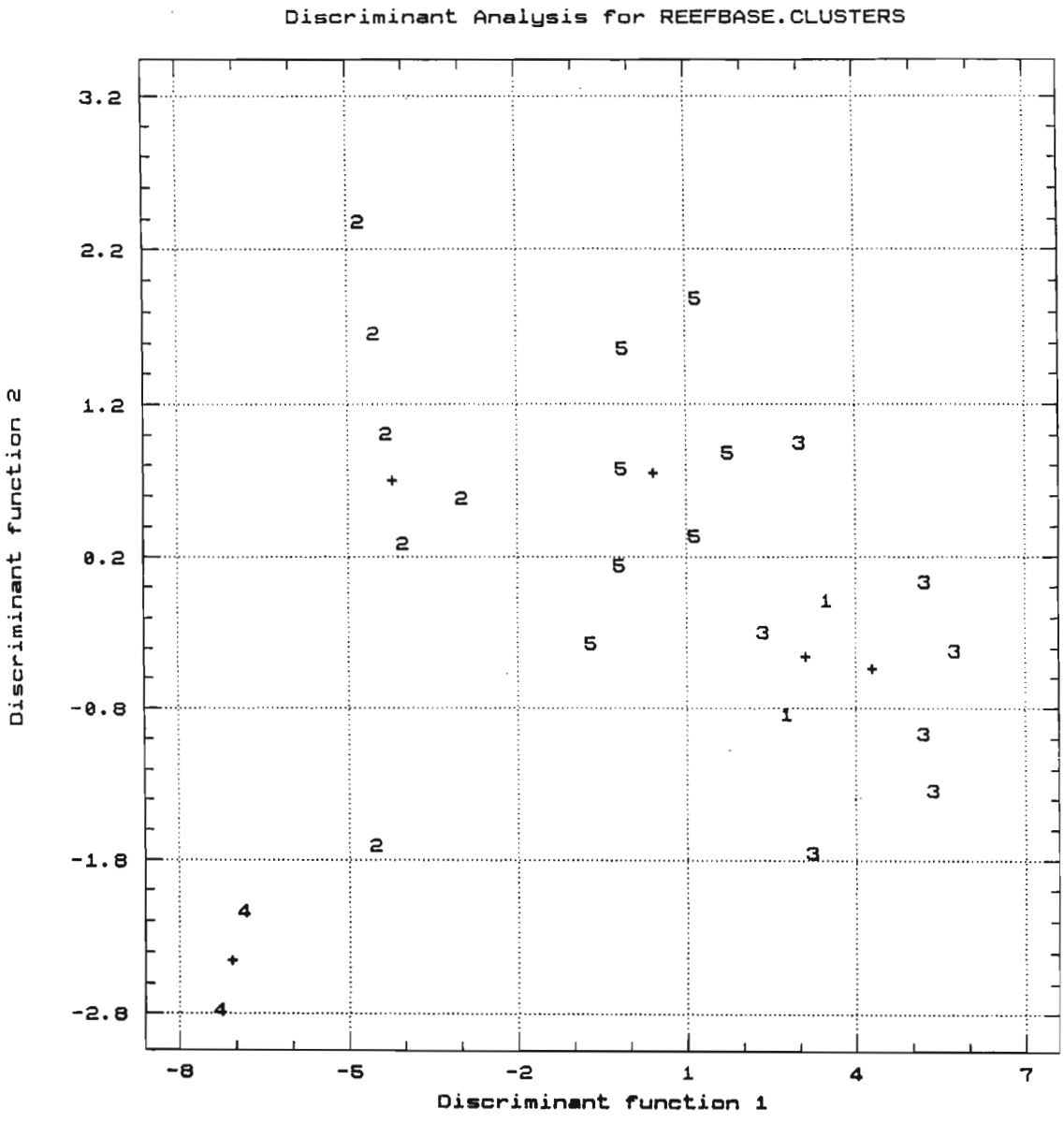

Figure 7.15. Discriminant analysis plot used to test cluster separation: (1) aeolian; (2) backbeach; (3) forebeach; (4) swash; (5) welded bar facies. Note the overlap (close proximity) between the aeolian facies cluster (1) and the forebeach facies cluster (3).

7.4 DISCUSSION

The cluster and discriminant analyses of the graphic settling statistics (median, sorting, and skewness) of modern dune and beach data compare very well with the acid-leached reef-base sedimentary environments and differentiated the reef-base into five facies: aeolianite, backbeach, forebeach, swash, and welded bar (Figs. 7.17 & 7.18). These can be related to the geomorphological zones on Two-Mile Reef.

SAMPLE	CLUSTER*	SED.STR	PETROLOGY	REEF MORPHOLOGY	FACIES
1	FB		Dune/beach	Reef-crest/fore-reef	Forebeach
2	BB		Beach	Back-reef	Backbeach
3	FB		Beach	Upper fore-reef	Forebeach
4	WB		Beach	Upper to mid fore-reef	Welded Bar
5	WB		Beach	Upper to mid fore-reef	Welded Bar
6	BB		Intertidal	Mid fore-reef	Backbeach
7	FB		Intertidal	Lower fore-reef	Forebeach
8	BB		Backbeach	Deep reef-front	Backbeach
9	BB		Backbeach	Deep reef-front	Backbeach
10	WB			Back-reef	Welded Bar
11	WB			Mid fore-reef	Welded Bar
12	WB			Seaward reef-crest margin	Welded Bar
13	BB			Deep reef-front	Backbeach
14	FB			Seaward reef-crest margin	Forebeach
15	WB			Reef-crest/fore-reef	Welded Bar
16	FB	Aeol X beds		Reef-crest	Aeolian
17	SW			Reef-crest/fore-reef	Swash
18	A	Aeol X beds		Landward reef-crest margin	Aeolian
19	FB			Upper fore-reef	Forebeach

* Where A is aeolian, BB is backbeach, FB is forebeach, SW is swash, and WB is welded bar facies.

Fig. 7.18. Cluster analysis results, reef-base sedimentary structures, facies petrology, sample position on the reef and derived facies environment based on the previously defined parameters.

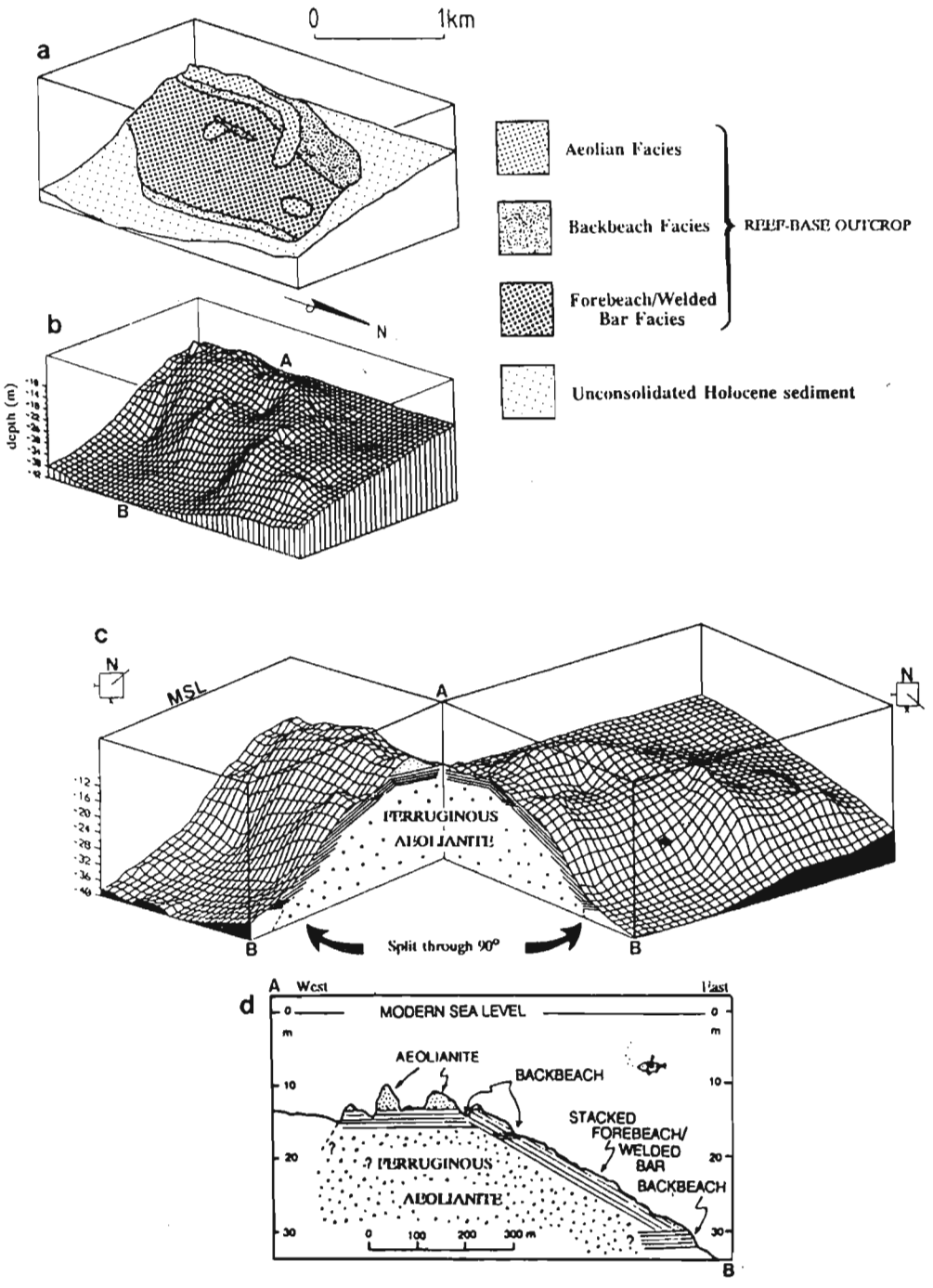

Figure 7.17. (a) and (b) show the three-dimensional reef-base facies distribution related to reef topography on Two-Mile Reef. (c) Three-dimensional reef topography plot split to show the underlying reef-base facies relationships. (d) detailed annotated cross-section A-B from diagram (c).

The back-reef-base facies of Two-Mile Reef formed in a backbeach environment, whereas the reef-crest is an aeolianite. Erosion of the aeolianite facies on the reef-crest reveals that it is underlain by backbeach facies, thereby defining the sequence as regressive. The backbeach facies implies a sea-level stillstand at approximately -13m. This correlates well with the sea-level stillstand at -11m described by Maud (1968). A minor swash environment is developed at the reef-crest/fore-reef area of Two-Mile Reef. The fore-reef-base may be ascribed to deposition in a forebeach/welded bar environment. The author envisages that multiple stacking of the forebeach/welded bar facies took place to explain a foreshore sequence with a vertical height of 17m. This implies a constant sea-level regression rate during the deposition of the forebeach facies. The stacked forebeach/welded bar sequence of the fore-reef environment was deposited under moderately regressive (progradational) conditions where the clastic depositional conditions resembled the modern, high-energy, wave-dominated, microtidal coastline. This facies is similar in most respects to what Short (1984) termed "ridge and runnel or low-tide terrace" beach state. The Holocene beachrock at present sea-level (^{14}C-age of 3780 ± 60 B.P.; laboratory analysis no. Pta-5052) displays evidence of "ridge and runnel structures" in the form of trough cross-bedding indicating northerly flowing palaeocurrents trending coast parallel with occasional 180° current reversals. At -18m there is a facies change on the mid fore-reef which represents an isolated outcrop of backbeach facies. The deep reef-front zone (> -30m) represents another backbeach facies formed by a lower (-30m to -35m) regressive sea-level stillstand. Maud (1968) describes stillstands at -18m and -36m along the Zululand coastline which correlate well with the mid fore-reef backbeach facies and the deep backbeach facies. Overlying the forebeach facies are isolated rocky pinnacles, which are regressive aeolianite outcrops. Two such pinnacles are found on the southern and northern margins of the reef at -18m and -22m respectively.

Inferred vertical thicknesses for each of the facies are:

Backbeach facies (1)	2.6 m
Aeolianite facies	3.8 m
Swash facies	0.5 m
Backbeach facies (2)	0.8 m
Forebeach/welded bar facies	3.0 m
Backbeach facies (3)	2.3 m

This regressive dune and beach sequence is underlain by a Pleistocene subreef-base lithofacies which is likely to be a red aeolianite, deduced from the local on- and offshore geology. Offshore evidence of this is seen in the reef-base of Four-Mile Reef, a reef 2km north of Two-Mile Reef. This is composed of a ferruginous aeolianite with northerly-dipping foresets and probably represents the northern extension of the Pleistocene subreef-base lithofacies of Two-Mile Reef.

The combined use of reef-base outcrop morphology, cluster and discriminant analyses of the graphic settling statistics of modern and reef-base facies, together with petrology, provides a good model for palaeocoastline reconstructions. This is especially useful for carbonate-cemented aeolianite and beachrock facies analysis where sedimentary structures are obscured or absent. This technique may be applicable to other carbonate-cemented sandstone successions where the inherited sedimentary grain characteristics have been modified by the environment in which the sediment was sampled. This would require a modern and ancient coastal environment relatively free of fluvial sediment contamination such as the northern Zululand coastline between Leven Point and Kosi Bay.

CHAPTER 8: SEA-LEVEL CHANGES, AEOLIANITE/BEACHROCK FORMATION, AND PALAEOCOASTLINE HISTORY

8.1 LATE PLEISTOCENE SEA-LEVEL CONTROVERSY

Anyone studying late Pleistocene sea-level curves will soon become aware of the controversy surrounding a high interstadial sea-level prior to the Last Glacial Maximum. Late Pleistocene sea-level histories described by Shepard (1963), Curray (1965), Milliman & Emery (1968), Maud (1968), and Thom (1973) indicate that there was a high interstadial near modern sea-level (approx. -10m) between 25 000 - 30 000 years B.P. Alternatively, Mörner (1971), Bloom et al. (1974), Chappell (1974), Tankard (1976), Williams et al. (1981), and Hails (1983) indicate that this interstadial was neither climatically nor glaciologically warm enough to create an ocean level at or about the present one. From glacio-climatic data Mörner (1971) expected a sea-level of -40m to -50m at about 30 000 years B.P. and Tankard (1976) suggests that a maximum sea-level of -20m occurred along the South African coastline. Mörner (1976) states that the high interstadial at about 30 000 years B.P., if not erroneous, could relate to the effect of geoid changes. The two schools of thought therefore are the "Emery camp" supporting a high interstadial at about 30 000 years B.P. and the "Mörner camp" who consider that sea-level was much lower during this time. The author does not favour a high interstadial at about 30 000 years B.P., thus siding with the "Mörner camp".

The eustatic late Pleistocene sea-level curve of Williams et al. (1981) has been used as a theoretical chronological control for the formation of aeolianite/beachrock sequences which define the late Pleistocene strandlines on the shelf (Fig 8.1). This sea-level curve was chosen as it has been previously used on this coastline by Martin & Flemming (1988) and closely resembles Barwis & Tankard's (1983) Quaternary sea-level for Southern Africa.

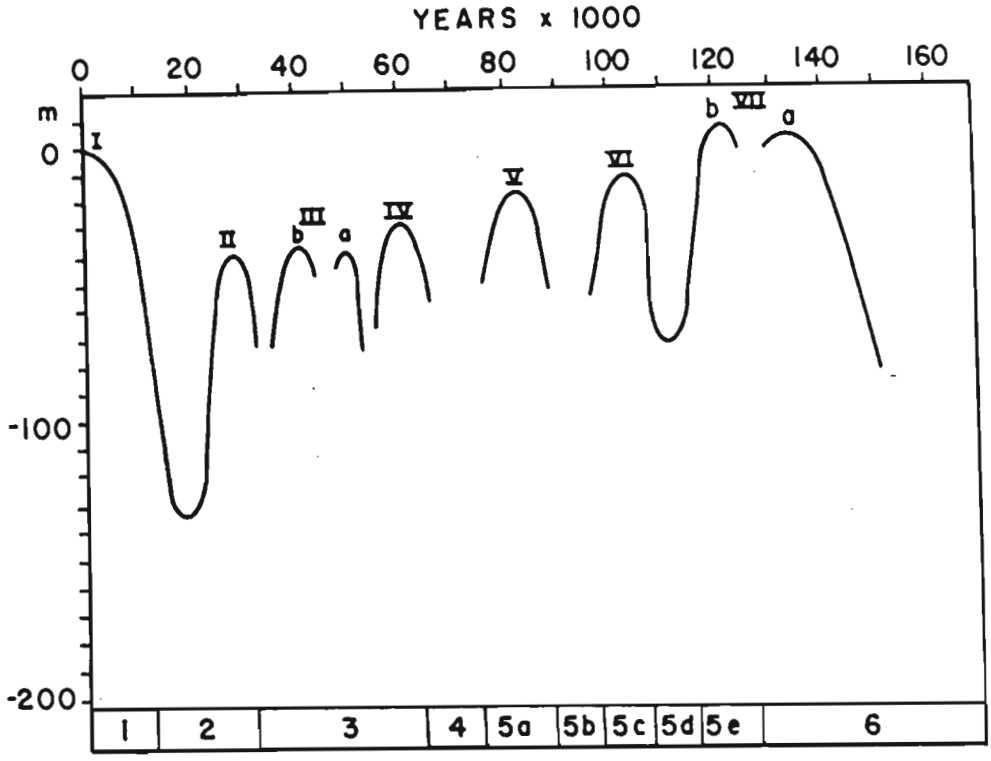

Figure 8.1. Sea-level curve for the last 150 000 years relative to present sea-level. Note high sea-levels I to VIIa and oxygen isotope stages 1-6. (After Williams et al., 1981).

8.2 AEOLIANITE/BEACHROCK PALAEOCOASTLINE EPISODES

The beachrocks and aeolianites outcropping on the shelf at Sodwana Bay are late Pleistocene in age, forming during the last interglacial between 120 000 and 30 000 years B.P. (Martin & Flemming, 1988; Ramsay, 1990a&b; Ramsay & Mason, 1990a&b). Based on global eustatic sea-level histories proposed by various authors, the author's current working hypothesis is that there are at least four possible periods in late Pleistocene times when these palaeocoastline sequences could have formed on the shelf. The major depth zones relating to the four palaeocoastline development episodes are (Fig. 8.2):

#1 -15m to -25m on the mid-shelf

#2 -13m to -45m on the mid-shelf

#3 -50m to -60m on the outer-shelf

#4 -70m to -95m on the outer-shelf

These palaeocoastlines episodes have been plotted onto the Williams et al. (1981) sea-level curve with age relationships derived from underwater facies evidence and depth relationships (Fig. 8.3). Sea-level stages and oxygen isotope stages are taken from Williams et al. (1981). The palaeocoastline episodes have been sub-divided based on side-scan sonar interpretations and underwater observations on the coast-parallel outcrops.

Chronologically, the oldest beachrock/aeolianite outcrop noted on the shelf is ferruginous aeolianite which forms the substrate of the reef-crest of Four-Mile Reef; this defines palaeocoastline episode #1 (Fig. 8.2), relating to a sea-level of approximately -27m. The degree of reddening has been used as a measure of age. This facies occurs as a transverse dune sequence formed by a dominant southerly wind (see 5.1.1.1). This sequence was deposited and cemented during an early post or pre-Eemian II high interstadial. Using Williams et al. (1981) eustatic sea-level curve, the earliest possible date for

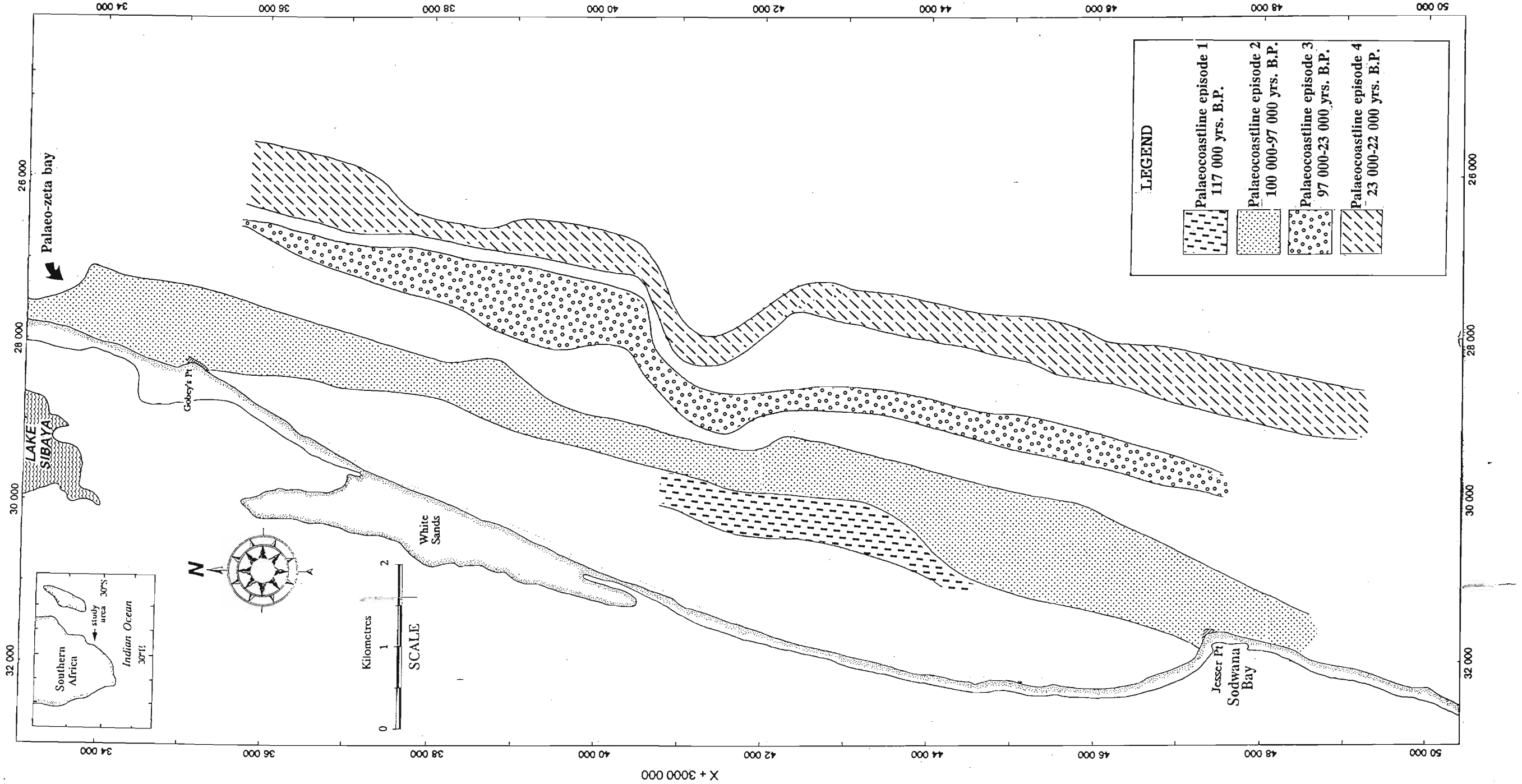

Figure 8.2. Late Pleistocene palaeocoastline episodes based on the occurrence and depth relationships of beachrock/aeolianite outcrops on the Sodwana Bay shelf. These coastal-facies outcrops were deposited and cemented between 117 000 and 22 000 years B.P. Note the presence of a palaeo-zeta bay in the north of the study area.

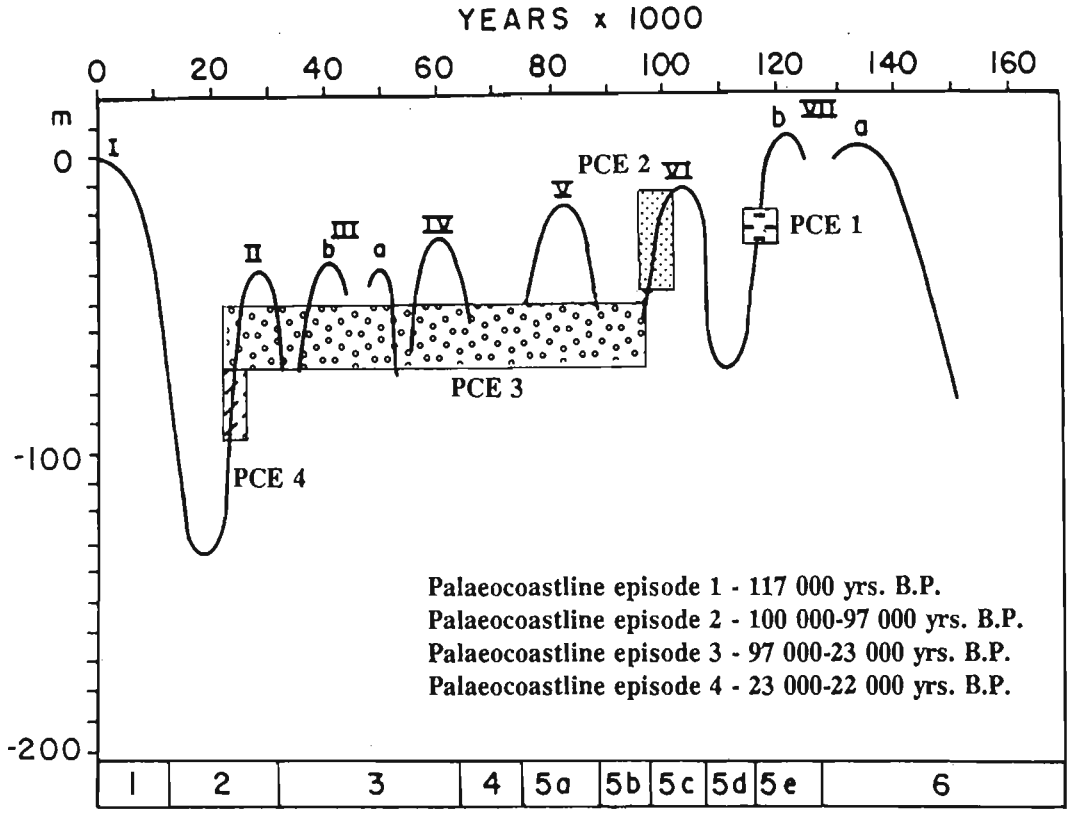

Figure 8.3. A plot of the major depth zones and stratigraphic (time) relationships of four palaeocoastline episodes evident on the Sodwana Bay shelf related to Williams et al. (1981) sea-level curve. This infers possible ages for each palaeocoastline episode.

the formation of the ferruginous aeolianite is ± 117 000 years B.P., this equates to just post sea-level stage VII and oxygen isotope stage 5e (Fig. 8.3). This ferruginous aeolianite may be synchronous with the milder period noted in the Cape coastal areas (after 90 000 years B.P.), associated with pedogenesis and ferruginous duricrust formation (Deacon, 1983).

Palaeocoastline #2 is a wide expanse of beachrock/aeolianite (up to 1.5km wide) which forms the substrate of the coral reefs on the mid-shelf (Fig. 8.2). Aeolianite palaeocurrent directions indicate an offshore wind regime with a minor onshore component (see 5.1.1.1). The beachrock sequences of this palaeocoastline episode dip seaward, and occasionally landward, at low angles of up to 5° (see 5.1.1.1). The deposition and cementation of the upper part of this sequence would have taken place when sea-level was approximately -13m below present sea-level, based on the aeolianite/beachrock relationship. A slow regression deposited the remaining reef-base down to -45m below present sea-level. Cementation developed post the earliest Wisconsin high interstadial just after sea-level stage VI, oxygen isotope stage 5c. This equates to the formation of the palaeocoastline episode starting at ± 100 000 years B.P. and continuing to ± 97 000 years B.P. (Fig. 8.3).

Beachrock/aeolianite outcrops on the outer-shelf between -50m and -60m define palaeocoastline episode #3 (Fig. 8.2). These outcrops were probably deposited and cemented during a regressive phase at any point between sea-level stage VI and II, corresponding to oxygen isotope stages 5b-2. These stages give a palaeocoastline episode age between 97 000 and 23 000 years B.P. (Fig. 8.3).

The final late Pleistocene palaeocoastline episode outcrops at -70m to -95m on the outer-shelf (Fig. 8.2). The beachrock/aeolianite outcrops associated with episode #4 formed post sea-level stage II (oxygen isotope stage 2) during the last phase of the regression leading to the Last Glacial Maximum. An age estimate for the formation of this palaeocoastline episode is 23 000-22 000 years B.P. (Fig. 8.3).

8.3 LATE PLEISTOCENE AND HOLOCENE HISTORY OF THE SHELF

Early- and mid Pleistocene outcrops which would have formed on the shelf during the numerous regressions have probably been eroded by the Pleistocene regression-transgression cycles.

The post-Eemian regressions during the late Pleistocene left a series of coast-parallel sand deposits covering 20% (11.7km^2) of the shelf in the study area. The lithification of these coastal sands was contemporaneous with their deposition; the carbonate cementing process responsible for the lithification of the sands was triggered by the action of groundwater super-saturated with $CaCO_3$ mixing with seawater and/or precipitation through solar heating at low-tides (see 7.2.1). The unconsolidated areas between the rocky outcrops indicate periods of little- or no carbonate cementation of the coastal sands. This probably represent an episode of accelerated sea-level regression or a minor transgressive phase which would hinder deposition and cementation. The development of beachrocks and aeolianites on the shelf during late Pleistocene regressions left a series of four distinct palaeocoastline episodes with possible ages between 117 000 and 22 000 years B.P. Glacial changes in sea surface temperatures were about 5°C lower than those in interglacial periods (Prell & Huston, 1979), therefore maximum sea temperature in this area was approximately 20°C. During periods of cooling the Agulhas Current was weaker and shallower (Prell et al., 1980). Figure 8.4 shows a smoothed version of oxygen isotope chronologies of the benthic foraminiferal record for core MD73-025 situated south of Madagascar at about 44°S, 51°E (Tyson, 1986).

During the regressive phase just prior to the Last Glacial Maximum the beachrock/aeolianite sedimentary sequence would have been exposed and was blanketed by shifting aeolian sands. The river that flowed into Lake Sibaya (Pongola River) entrenched itself into the unconsolidated sediments on the shelf, exploiting the route of least resistance: along the axes of White Sands and Wright Canyons (Fig. 8.5). Fluvial sediments carried by the Pongola River would have bypassed the shelf via Wright-

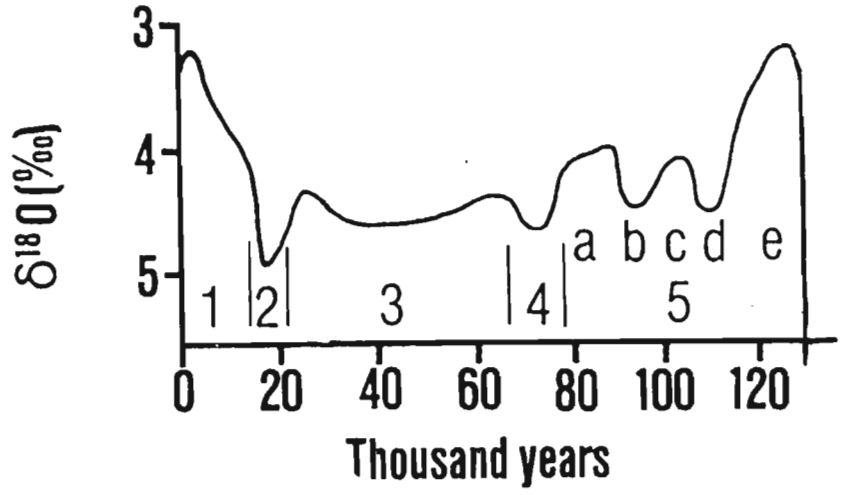

Figure 8.4. A smoothed oxygen isotope curve of the benthic record for core MD73-025 situated south of Madagascar. This indicates the extent to which climate fluctuated during the late Pleistocene, with alternating glacial and interglacial conditions. (From Tyson, 1986).

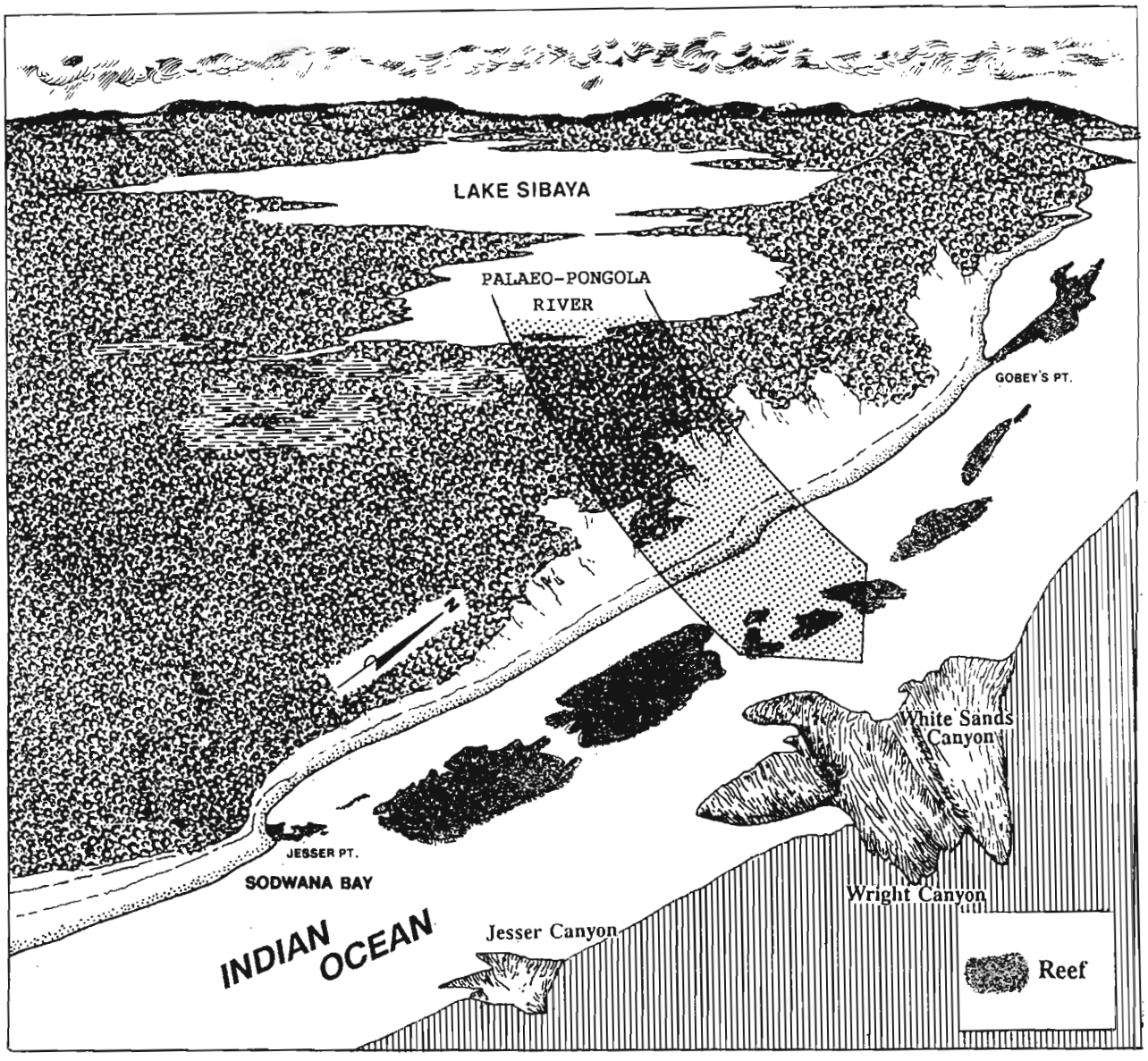

Figure 8.5. A three-dimensional sketch showing the palaeo-Pongola River channel which formed between Lake Sibaya and Wright Canyon during the period 15 000-18 000 years B.P.

and White Sands Canyons, and would have been deposited directly onto the continental slope. The erosion resulting from fluvial denudation in Wright Canyon caused this canyon to entrench to a deeper level and extensively breach the shelf to a distance of 2km offshore. Meyer & Kruger (1988) noted a deep palaeo-valley underlying Lake Sibaya to a depth of -140m below mean sea-level. This represents the deepest fluvial incision episode which occurred during the Last Glacial Maximum (15 000-18 000 years B.P.).

After the eustatic low at 15 000-18 000 years B.P., sea-level rose very rapidly with deglaciation (167cm/100 years; Tankard, 1976); this is referred to as the Flandrian transgression (Mörner, 1971). During the Flandrian transgression the unconsolidated sediment cover was eroded, exposing and submerging the beachrock/aeolianite sequence. As a result of sand movement along the coast, and in an onshore direction, sand bars developed across the outlet of Lake Sibaya's estuary. Insufficient fluvial flow allowed the extension of the coastal dune sands over these sand bars which finally sealed Lake Sibaya off from the sea, causing the river to become dammed behind the dune barrier. The barrier dune cordon developed on a pre-existing, remnant Pleistocene dune stub (McCarthy, 1967; Maud, 1968; Orme, 1973). Sediment sources for the development of the 130+m high dune barrier in the study area were:

1) reworking of the sediment prism on the shelf in an onshore direction; and

2) sediment derived from deltas and unconsolidated dune deposits further south along the shelf and transported north by southerly winds.

The formation of beachrock and aeolianite caused a nearshore reduction in sediment supply during the Flandrian transgression; this would tend to produce higher rates of erosion. Cooper (1991) states that the Holocene probably had the greatest erosion rate. Supporting evidence includes the location of Holocene shorelines some distance landward of the Last Interglacial (Eemian) shoreline, despite

the Holocene sea-level being lower by some 4-6m than the Last Interglacial sea-level (Cooper, 1991). The early formation of beachrock appears to favour overstepping during transgressions, or stranding during a regression (Cooper, 1991).

Post Glacial Maximum stillstands during the Flandrian transgression caused erosional features such as wave-planed terraces, potholes, and gullies to be incised into beachrock and aeolianite outcrops (see 5.1.1.1). Evidence of these stillstands have been observed on SCUBA dives at depths of -47m, -32m, -26m, -22m, -17m to -18m, and -12m.

Sea-level stabilised at its present level 7 000-6 000 years B.P. (Milliman & Emery, 1968; Mörner, 1971; Bloom et al., 1974; Tankard, 1976) and coral reef growth on the beachrock/aeolianite outcrops probably started at 5 000 years B.P. and has continued to proliferate ever since. Stoddart (1973) states that modern coral reef growth, related to present sea-level, began about 5 000 years B.P. Based on a ^{14}C-age of a fossil coral fragment (Favia sp.) found in an intertidal beachrock sequence 35km north of Sodwana Bay, the growth of coral patch reefs along this coastline began at least 3780 ± 60 years B.P. (laboratory analysis no. Pta-5052).

A +2m raised beachrock sequence occurs sporadically along the northern Zululand coastline, being best developed at the barrier dune/beach interface. This represents evidence of a mid Holocene transgression relating to the Climatic Optimum discussed by Tyson (1986). Reddering (1987b) found a +1.5m raised coastal terrace on the Cape south coast which formed around 5 180 years B.P. and also noted estuarine deposits which accumulated at present sea-level giving an age of 3 880 years B.P. A minor regression is envisaged, just before 3 880 years B.P. which caused sea-level to stabilise to its present level. A Holocene oxygen isotope temperature curve for the southern Cape (Tyson, 1986; Fig. 8.6) illustrates three Holocene temperature highs at 5 000, 3 500, & 1 000 years B.P.. The Sodwana Bay raised beach probably relates to the 5 000 year B.P. temperature high based on similar

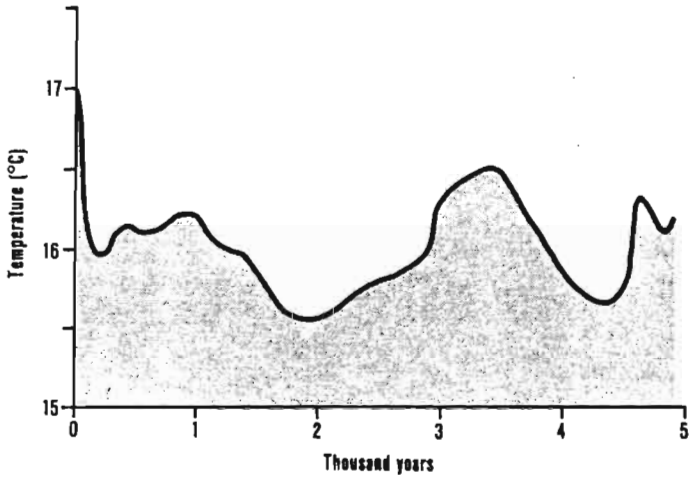

Figure 8.6. Holocene oxygen isotope curve for the southern Cape from Cango Cave. (From Tyson, 1986).

observations made by Reddering (1987b). The mid Holocene transgression had a profound effect on the coastline configuration of northern Zululand, causing the barrier dune system to be eroded and shifting the shoreline approximately 40m landward.

The Holocene sea-level rise, and its effect on the coastline configuration, can be used as a model for coastal erosion which will result from the predicted rise in sea-level over the next century. The International Panel for Climatic Change states that it is certain that human-induced increases in greenhouse gases will lead to a warming of the earth's surface by 1.8°C above pre-industrial levels by the year 2020 and 3.5°C by 2070 (IPCC, 1990). This temperature rise will induce a rise in sea-level and may alter the atmosphere and oceanic circulations causing further changes in local climate and sea-levels. The best estimate for the South African coastline indicate a 20 cm rise in sea-level within the next 35 years (IPCC, 1990; Thomas, 1987; Hughes & Brundrit, 1991), followed by a 1.5 m rise by the end of the next century (Thomas, 1987; Hughes & Brundrit, 1991). It was earlier demonstrated that a 2m rise in sea-level caused a landward shoreline translation of 40m, therefore a 1.5m rise in relative sea-level could result in the loss of 30m of coastline or a total South African land area loss of $\pm 90km^2$.

The impacts of sea-level rise on the coastal environment can be categorised into the areas of increased coastal erosion, increased salt water intrusion and raised groundwater tables, and increased vulnerability to extreme storm events (Hughes & Brundrit, 1991). These impacts must be viewed from both an economic and environmental standpoint. The economic standpoint considers the natural loss of development, infrastructure, and agriculture with rising sea-levels. The environmental standpoint considers the potential loss of biological diversity and resources that may occur as a result of poor planning procedures (Hughes & Brundrit, 1991).

This chapter on late Pleistocene and Holocene coastal evolution of the Sodwana Bay shelf represents

the author's current working hypothesis. This hypothesis will be tested and fine-tuned by an extensive U/Th-dating programme (in early 1992) which will provide the base data for a late Pleistocene eustatic sea-level curve.

REFERENCES

Agassiz, A. (1898). A visit to the Great Barrier Reef of Australia in the steamer "Croyden" during April and May, 1896. Harvard Mus. Comp. Zoology Bull., 28, 93-148.

Allanson, (Ed.) (1979). Lake Sibaya. Monographiae Biologicae, 36, W. Junk, The Hague, 364 pp.

Allen, J.R.L. (1984). Sedimentary Structures: Their Character and Physical Basis. Developments in Sedimentology, 30. Elsevier, 1256 pp.

Allen, P. (1959). The wealden environment, Anglo-Paris Basin. Phil. Trans. Roy. Soc. (London), Ser. B 242, 283-346.

Allen, P.A. (1985). Hummocky cross-stratification is not produced purely under progressive gravity waves. Nature, 313, 562-564.

Alexander, H. (1932). Pothole erosion. J. Geol., 40, 305-307.

Ashley, G.M. (1990). Classification of large-scale subaqueous bedforms: a new look at an old problem. J. Sediment. Petrol., 60, 160-172.

Ball, M.M. (1967). Carbonate sand bodies of Florida and the Bahamas. J. Sediment. Petrol., 37, 556-591.

Bang, N.D. (1968). Submarine canyons off the Natal coast. S. Afr. geogr. J., 50, 45-54.

Bang, N.D. & Pearce, A.F. (1978). Physical oceanography. In: A.E.F. Heydorn (Ed.), Ecology of the Agulhas Current Region. Trans. R. Soc. S. Afr., 43, 156-162.

Barnes, J., Bellamy, D.J., Jones, D.J., Whitten, B.A., Drew, E.A., Kenyon, L., Lythgoe, J.N. and Rosen, B.R. (1971). Morphology and ecology of the reef front of Aldabra. Symp. Zool. Soc. London, 28, 87-114.

Barwis, E.J. & Tankard, A.J. (1983). Pleistocene shoreline deposition and sea-level history at Swartklip, South Africa. J. Sediment. Petrol., 53, 1281-1294.

Bathurst, R.G.C. (1966). Boring algae, micrite envelopes and lithification of molluscan biosparites. Geol. J., 5, 15-32.

Bathurst, R.G.C. (1974). Marine diagenesis of shallow water calcium carbonate sediments. Annual Review of Earth and Planetary Sciences, 2, 257-273.

Bathurst, R.G.C. (1975). Carbonate Sediments and their Diagenesis. Elsevier, Amsterdam, 658 pp.

Begg, G.W. (1978). The Estuaries of Natal. Natal Town and Regional Planning Report, 41, 657 pp.

Beier, J.A. (1985). Diagenesis of Quaternary Bahamian beachrock, petrographic and isotopic evidence. J. Sediment. Petrol., 55, 755-761.

Birch, G.F. (1981). The bathymetry and geomorphology of the continental shelf and upper slope between Durban and Port St Johns. Annals of the Geological Survey of South Africa, 15/1, 55-62.

Blatt, H., Middleton, G. & Murray, R. (1980). Origin of Sedimentary Rocks, 2nd edition. Prentice-Hall, New Jersey, 141 pp.

Bloom, A.L. (1974). Geomorphology of reef complexes. SEPM Spec. Publ., 18, 1-8.

Bloom, A.L., Broecker, W.S., Chappell, J.M.A., Matthews, R.K. & Mesolella, K.J. (1974). Quaternary sea level fluctuations on a tectonic coast, new $^{230}Th/^{234}U$ dates from Huon Peninsula, New Guinea. Quaternary Research, 4, 185-205.

Boshoff, P.H. (1958). Development and constitution of the coral reefs. In: Macnae, W. & Kalk, M. (Eds.), A Natural History of Inhaca Island, Mozambique. Witwatersrand University Press, Johannesburg, 49-56.

Boshoff, P.H. (1981). An annotated checklist of southern African Scleractinia. Oceanographic Research Institute, Investigational Report, 49. South African Association for Marine Biological Research, Durban, 45 pp.

Boucher, K. (1975). Global Climate. The English Universities Press Ltd., London, 323 pp.

Bouma, A.H. & Rappeport, M.L. (1984). Verification of side-scan sonar acoustic imagery by underwater photography. In: Smith, P.L. (Ed.). Underwater Photography - Scientific and Industrial Applications. Van Nostrand Reinhold, New York, 279-294.

Chalker, B.E., Dunlap, W.C. and Jokiel, P.L. (1986). Light and corals. Oceanus, 29(2), 22-23.

Chappell, J. (1974). Geology of coral terraces, Huon Peninsula, New Guinea, a study of Quaternary tectonic movements and sea-level changes. Geol. Soc. America Bull., 5, 553-570.

Chappell, J. (1983). Evidence for smoothly falling sea-level relative to North Queensland, Australia, during the past 6 000 years. Nature, 302, 406-408.

Clarkson, E.N.K. (1979). Invertebrate Palaeontology and Evolution. Allen and Unwin, London, 323 pp.

Clifton, H.E., Hunter, R.E., & Phillips, R.L. (1971). Depositional structures and processes in the non-barred, high-energy nearshore. J. Sediment. Petrol., 41, 651-670.

Coetzee, F. (1975a). Solution pipes in coastal aeolianites of Zululand and Mozambique. Trans. Geol. Soc. S. Afr., 78, 323-333.

Coetzee, F. (1975b). Coastal aeolianites at Black Rock, northern Zululand. Trans. Geol. Soc. S. Afr., 78, 313-322.

Coll, J.C. and Sammarco, P.W. (1986). Soft corals: Chemistry and ecology. Oceanus, 29(2), 33-37.

Cooper, J.A.G. (1988). Sedimentary environments and facies of the subtropical Mgeni Estuary, southeast Africa. Geological Journal, 23, 59-73.

Cooper, J.A.G. (1991). Beachrock formation in low latitudes: implications for coastal evolutionary models. Marine Geology, 98, 145-154.

Cooper, J.A.G. & Flores, R.M. (1991). Shoreline deposits and diagenesis resulting from two late Pleistocene highstands near +5 and +6 metres, Durban, South Africa. Marine Geology, 97, 325-343.

Cooper, J.A.G. & Mason, T.R. (1987). Sedimentation in the Mgeni Estuary. S.E.A.L. Report, 2. Dept. of Geology & Applied Geology, University of Natal, Durban, 97 pp.

Crossland, C. (1948). Reef corals of the South African coast. Annals of the Natal Museum, 11(2), 169-205.

Curray, J.R. (1965). Late Quaternary history, continental shelves of the United States. In: H.E. Wright & D.G. Frey (Eds.), The Quaternary of the United States (INQUA volume). Princeton University Press, Princeton, New Jersey, 723-735.

Daly, R.A. (1924). The geology of American Samoa. Washington Carnegie Inst. Pub. no. 340, 93-143.

Dana, J.D. (1851). On coral reefs and islands. Am. J. Sci., series 2, 11, 357-372, 12, 25-51, 165-186, 329-338.

Davies, J.L. (1964). A morphogenic approach to world shorelines. Zeitschr. fur Geomorphol., 8, 27-42.

Davies, O. (1976). The older coastal dunes in Natal and Zululand and their relation to former shorelines. Annals of the South African Museum, 71, 19-32.

Davies, P.J. & Kinsey, D.W. (1973). Organic and inorganic factors in Recent beachrock formation, Heron Island, Great Barrier Reef. J. Sediment. Petrol., 43, 59-81.

Davies, P.S. (1984). The role of zooxanthellae in the nutritional energy requirements of Pocillopora eydouxi. Coral Reefs, 2, 27-35.

Davies, R.A., Jr., Fox, W.T., Hayes, M.O., Boothroyd, J.C. (1972). Comparison of ridge-and-runnel systems in tidal and non-tidal environments. J. Sediment. Petrol., 32, 413-421.

Davis, J.C. (1973). Statistics and Data Analysis in Geology. John Wiley & Sons, New York, 442-473.

Deacon, H.J. (1966). The dating of the Nahoon footprints. S.A. J. Sci., 62, 111-113.

Deacon, H.J. (1983). Another look at the Pleistocene climates of South Africa. S.A. J. Sci., 79, 325-328.

De Decker, R.H. (1987). The geological setting of diamondiferous deposits on the inner-shelf between the Orange River and Wreck Point, Namaqualand. Bulletin of the Geological Survey of South Africa, 86, 99 pp.

Dott, R.H. & Bourgeois, J. (1982). Hummocky cross-stratification: significance of its variable bedding sequence. Geol. Soc. Am. Bull., 93, 663-690.

Duck, R.W. & McManus, J. (1985). A side-scan sonar survey of a previously drawn-down reservoir: A control experiment. Int. J. Remote Sens., 6(5), 601-609.

Duke, W.L. (1985). Hummocky cross-stratification, tropical hurricanes and intense winter storms. Sedimentology, 32, 167-194.

Dupré, W.R. (1984). Reconstruction of palaeo-wave conditions during the late Pleistocene from marine terrace deposits, Monterey Bay, California. Marine Geology, 60, 435-454.

EG & G Instruction Manual (1984). Model 272-T Saf-T-Link tow fish with TVG. EG & G Environmental Equipment, Massachusetts.

EG & G Instruction Manual (1986). Model 260 image correcting side-scan sonar. EG & G Environmental Equipment, Massachusetts.

Emery, K.O. (1946). Marine solution basins. J. Geol., 54, 209-228.

Esterhuysen, K. & Reddering, J.S.V. (1985). Sedimentation in the Nahoon Estuary. R.O.S.I.E Report, 10. Dept. of Geology, University of Port Elizabeth, 98 pp.

Evans, G. (1965). Intertidal flat sediments and their environments of deposition in the Wash. Quart. Jour. Geol. Soc. London, 121, 209-245.

Fairbridge, R.W. (1950a). Recent and Pleistocene coral reefs of Australia. Jour. Geol., 58(4), 330-401.

Fairbridge, R.W. (1950b). The geology and geomorphology of Point Peron, Western Australia. J. R. Soc. Western Australia, 34, 35-72.

Fairbridge, R.W. (1961). Eustatic changes in sea-level. In: L.H. Ahrens et al. (Eds.), Physics and Chemistry of the Earth, IV. Pergamon Press, London, 99-185.

Fairbridge, R.W. & Teichert, C. (1953). Soil horizons and marine bands in the coastal limestones of Western Australia, between Cape Naturaliste and Cape Leeuwin. J. Proc. R. Soc. NSW, 86, 68-87.

Farre, J.A., McGregor, B.A., Ryan, B.F. & Robb, J.M. (1983). Breaching the shelfbreak: passage from youthful- to mature-phase in submarine canyon evolution. In: Stanley, D.J & Moore, G.T. (Eds.), The Shelfbreak: Critical Interface on Continental Margins. SEPM Special Publication, 33, 25-39.

Faure, G. (1974). Morphology and bionomy of the coral reef discontinuities in Rodriguez Island (Mascarene Archipelago, Indian Ocean). Proc. 2nd Internat. Symp. Corals and Coral Reefs 1973, 2, 161-172.

Field, R.M. (1919). Remarks on beachrocks in Dry Tortugas. Carnegie Inst. Yearbook, 18, 198 pp.

Flemming, B.W. (1978). Underwater sand dunes along the southeast African continental margin - observations and implications. Marine Geology, 26, 177-198.

Flemming, B.W. (1979). Underwater observations along a high-energy, cliffed coastline (Tsitsikama). Joint Geological Survey/University of Cape Town Marine Geoscience Unit, Technical Report 11, 57-61.

Flemming, B.W. (1980). Sand transport and bedform patterns on the continental shelf between Durban and Port Elizabeth (south-east African continental margin). Sedimentary Geology, 26, 179-205.

Flemming, B.W. (1981). Factors controlling shelf sediment dispersal along the southeast African continental margin. Marine Geology, 42, 259-277.

Flemming, B.W. (1988). Zur Klassifikation subaquatischer, stromungstransversaler Transportkorper. Boch. geol. u. geotechn. Arb., 29, 44-47.

Flemming, B.W. & Hay, E.R. (1988). Sediment distribution and dynamics on the Natal continental shelf. In: E.H Schumann, (Ed.), Coastal Ocean Studies off Natal, South Africa. Lecture Notes on Coastal and Estuarine Studies, 26, 47-80.

Flexor, J.M. & Martin, L. (1979). Sur l'utilisation des grès coquilliers de la région de Salvador (Brésil) dans la reconstruction des lignes de rivage holocènes. Proc. 1978 Internat. Symp. Coastal Evol. Quaternary, Sao Paulo, 343-355.

Folk, R.L. & Pittman, J.S. (1973). Length-slow chalcedony, a new test for vanished evaporites. J. Sediment. Petrol., 41, 1045-1058.

Friedman, G.M. (1964). Early diagenesis and lithification in carbonate sediments. J. Sediment. Petrol., 34(4), 777-813.

Gill, A.E.A. & Schumann, E.H. (1979). Topographically induced changes in the structure of an inertial coastal jet: application to the Agulhas Current. Journal of Physical Oceanography, 9, 975-991.

Ginsburg, R.N. (1953). Beachrock in south Florida. J. Sediment. Petrol., 23, 85-92.

Grapher Version 1.79 (1988). Golden Software Inc., Colorado.

Greensmith, J.T. (1979). Petrology of the Sedimentary Rocks. George Allen & Unwin, London, 241 pp.

Gründlingh, M.L. & Pearce, A.F. (1984). Large vortices in the northern Agulhas Current. Deep Sea Research, 31, 1149-1156.

Guilcher, A. (1971). Mayotte barrier reef and lagoon, Comoro Islands, as compared with other barrier reefs, atolls and lagoons in the world. Symp. Zool. Soc. London, 28, 65-86.

Guilcher, A. (1988). Coral Reef Geomorphology. Wiley, New York, 228 pp.

Hails, J.R. (1983). Shoreline development on mid- and low-latitude coasts. In: D.E. Smith & A.G. Dawson (Eds.), Shorelines and Isostasy, Inst. British Geographers Special Publ., 16, Academic Press, p.30.

Hanor, J.S. (1978). Precipitation of beachrock cements, mixing of marine and meteoric waters vs. CO_2-degassing. J. Sediment. Petrol., 48, 489-501.

Harris, T.F.W. (1978). Review of coastal currents in Southern African waters. South African National Scientific Programmes Report No. 30, CSIR, 103 pp.

Hayes, M.O. (1964). Lognormal distribution of inner continental shelf widths and slopes . Deep Sea Research, 11, 53-78.

Hayes, M.O. (1979). Barrier island morphology as a function of tidal and wave regime. In: S.P. Leatherman (Ed.), Barrier Islands from the Gulf of Mexico. Academic Press, New York, 3-22.

Hill, B.J. (1975). The origin of southern African coastal lakes. Trans. R. Soc. S. Afr., 41(3), 225-240.

Hird, K. & Tucker, M.E. (1988). Contrasting diagenesis of two Carboniferous oolites from South Wales, a tale of climatic influence. Sedimentology, 35, 587-602.

Hobday, D.K. (1973). Middle Ecca deltaic deposits in the Muden-Tugela Ferry area of Natal. Trans. Geol. Soc. S. Afr., 76, 309-318.

Hobday, D.K. (1976). Origin and development of the lagoonal complex, Lake St Lucia, Zululand. Annals of the South African Museum, 71, 93-113.

Hobday, D.K. (1979). Geological evolution and geomorphology of the Zululand coastal plain. In: Allanson (Ed.), Lake Sibaya. Monographiae Biologicae, 36, W. Junk, The Hague, 1-19.

Hubbard, J.A.E.B. and Pocock, Y.P. (1972). Sediment rejection by recent scleractinian corals: a key to palaeoenvironmental reconstruction. Geol. Rundschau., 61(2), 598-626.

Hughes, P. & Brundrit, G.B. (1991). Planning for our mistakes:- How to cope with rising sea-levels. Town & Regional Planning Report, 30, 10-13.

Hunter, I.T. (1988). Climate and weather off Natal. In: E.H Schumann, (Ed.), Coastal Ocean Studies off Natal, South Africa. Lecture Notes on Coastal and Estuarine Studies, 26, 81-100.

Huston, M. (1985). Variation in coral growth rates with depth at Discovery Bay, Jamaica. Coral Reefs, 4, 19-25.

IPCC Inter-governmental Panel for Climatic Change. IPCC Working Group 1. (1990).

Jaap, W.C. (1984). The ecology of the south Florida coral reefs: A community profile. U. S. Fish and Wildlife Service, FWS/OBS-82-08, 138 pp.

Jaubert, J.M. and Vasseur, P. (1974). Light measurements: duration aspect and the distribution of benthic organisms in an Indian Ocean coral reef (Tulear, Madagascar). Proc. 2nd Internat. Symp. Corals and Coral Reefs 1973, 2, 127-142.

Kanwisher, J.W. and Wainwright, S.A. (1967). Oxygen balance in some reef corals. Biological Bulletin, 133, 378-390.

Kuenen, Ph.H. (1950). Marine Geology. Wiley, New York, 568 pp.

Kitano, Y. & Hood, D.W. (1965). The influence of organic material on the polymorphic crystallisation of calcium carbonate. Geochim. Cosmochim. Acta, 29, 29-41.

Klein, G. de V. (1970). Depositional and dispersal dynamics of intertidal sand bars. J. Sediment. Petrol., 40, 1095-1127.

Klein, G. de V. (1977). Clastic Tidal Facies. CEPCO, Illinois, 31-39.

Knebel, H.J, Needell, S.W., & O'Hara, C.J. (1982). Modern sedimentary environments on the Rhode Island inner-shelf, off the Eastern United States. Marine Geology, 49, 241-256.

Komar, P.D. (1976). Beach Processes and Sedimentation. Prentice-Hall, New Jersey, 389-391.

Leeder, M.R. (1982). Sedimentology, Process and Product. George Allen & Unwin, London, 344 pp.

Longman, M.W. (1980). Carbonate diagenetic textures from nearsurface diagenetic environments. Bull. Am. Assoc. Pet. Geol., 64, 461-487.

Lutjeharms, J.R.E., Bang, N.D. & Duncan, C.P. (1981). Characteristics of the currents east and south of Madagascar. Deep Sea Research, 28, 879-899.

Martin, A.K. (1984). Plate tectonic status and sedimentary basin infill of the Natal Valley (SW Indian Ocean). Bulletin Joint Geological Survey/University of Cape Town Marine Geoscience Unit, 14, 208 pp.

Martin, A.K. & Flemming, B.W. (1986). The Holocene shelf sediment wedge off the south and east coast of South Africa. In: R.J. Knight & J.R. McLean (Eds.), Shelf Sands and Sandstones. Canadian Soc. Petrol. Geol., Memoir II, 27-44.

Martin, A.K. & Flemming, B.W. (1988). Physiography, structure, and geological evolution of the Natal continental shelf. In: E.H Schumann, (Ed.), Coastal Ocean Studies off Natal, South Africa. Lecture Notes on Coastal and Estuarine Studies, 26, 11-46.

Maud, R.R. (1968). Quaternary geomorphology and soil formation in coastal Natal. Zeitschr. fur Geomorphol., 7, 155-199.

Maud, R.R. (1980). The climate and geology of Maputaland. In: M.N. Bruton & K.H. Cooper (Eds.), Studies on the Ecology of Maputaland. Wildlife Society of South Africa, Durban, 1-7.

Maxwell, W.G.H. (1968). Atlas of the Great Barrier Reef. Elsevier, Amsterdam, 258 pp.

McCarthy, M.J. (1967). Stratigraphic and sedimentological evidence from the Durban region of major sea-level movements since the late Tertiary. Trans. Geol. Soc. s. Afr., 70, 135-165.

McKee, E.D. (1957). Primary structures in some recent sediments. Bull. Am. Assoc. Petrol. Geol., 41, 1704-1747.

McLachlan, I.R. & McMillan, I.K. (1979). Microfaunal biostratigraphy, chronostratigraphy, and history of Mesozoic and Cenozoic deposits of the coastal margin of South Africa. Geological Society of South Africa Special Publication, 6, 161-181.

Means, J.C. and Sigleo, A.C. (1986). Contributions of coral reef mucus to the colloidal organic pool in the vicinity of Discovery Bay, Jamaica, W.I. Bull. mar. Sci., 39(1), 110-118.

Mergner, H. (1971). Structure, ecology and zonation of Red Sea reefs (in comparison with south Indian and Jamaican reefs). Symp. Zool. Soc. London, 28, 141-161.

Mergner, H. and Scheer, G. (1974). The physiographic zonation and the ecological conditions of some south Indian and Ceylon coral reefs. Proc. 2nd Internat. Symp. Corals and Coral Reefs 1973, 2, 3-30.

Meyer, R. & Kruger, G.P. (1988). A sedimentological model for the northern Zululand coastal plain. Extended Abstract, 22nd Earth Science Congress of the Geological Society of South Africa, University of Natal, Durban, 423-425.

Mitchell, R. and Chet, I. (1975). Bacterial attack of corals in polluted seawater. Microbial Ecology, 2, 227-233.

Milligan, G.W. (1980). An examination of the effect of six types of error perturbation on fifteen clustering algorithms. Psychometrika, 45(3), 325-342.

Milliman, J.D. & Emery, K.O. (1968). Sea levels during the past 35 000 years. Science, 162, 1121-1123.

Mitterer, R.M. & Cunningham, R. Jr. (1985). The interaction of natural organic matter with grain surfaces, implications for calcium carbonate precipitation. In: N. Schneidermann & P.M. Harris (Eds.), Carbonate Cements. Soc. Econ. Palaeontol. Mineral., Spec Publ., 36, 17-31.

Moir, G.J. (1975). Preliminary textural and compositional analyses of surficial sediments from the upper continental margin between Cape Recife (34°S) and Ponta do Ouro (27°S), South Africa. Technical Report, Joint GSO/UCT Marine Geoscience Unit, 8, 68-75.

Montaggioni, L. (1974). Coral reefs and Quaternary shorelines in the Mascarene Archipelago (Indian Ocean). Proc. 2nd Internat. Symp. Corals and Coral Reefs 1973, 2, 579-593.

Montaggioni, L.F. & Pirazzoli, P.A. (1984). The significance of exposed coral conglomerates from French Polynesia (Pacific Ocean) as indicators of Recent relative sea-level changes. Coral Reefs, 3, 29-42.

Mörner, N.-A. (1971). The position of the ocean level during the interstadial at about 30 000 years B.P. - a discussion from a climatic-glaciologic point of view. Canadian Journal of Earth Sciences, 8, 132-143.

Mörner, N.-A. (1976). Eustasy and geoid changes. J. Geol., 84(2), 123-151.

Orme, A.R. (1973). Barrier and lagoon systems along the Zululand coast, South Africa. Office of Naval Research Technical Report 1, 181-217.

Pearce, A.F. (1978). Seasonal variations of temperature and salinity on the northern Natal continental shelf. South African Geographical Journal, 60, 135-143.

Pettijohn, F.J., Potter, P.E. & Siever, R. (1973). Sand and Sandstone. Springer-Verlag, New York, 86-88.

Pichon, M. (1974). Dynamics of benthic communities in the coral reefs of Tulear (Madagascar), succession and transformation of the biotypes through reef tract evolution. Proc. 2nd Internat. Symp. Corals and Coral Reefs 1973, 2, 55-68.

Pierson, B.J. & Shinn, E.A. (1985). Cement distribution and carbonate mineral stabilisation in Pleistocene limestones of Hogsty Reef, Bahamas. In: N. Schneidermann & P.M. Harris (Eds.), Carbonate Cements. Soc. Econ. Palaeontol. Mineral., Spec Publ., 36, 153-168.

Prell, W.L. & Huston, W.H. (1979). Zonal temperature anomaly maps of the Indian Ocean surface water: modern and ice-age patterns. Science, 206, 454-456.

Prell, W.L., Huston, W.H. & Williams, D.F. (1980). The Subtropical Convergence and late Quaternary circulation in the Southern Indian Ocean. Marine Micropalaeontology, 4, 225-234.

Ramsay, P.J. (1987). The Sedimentation, Distribution and Zonation of Two-Mile Reef, Sodwana Bay. (unpubl.) Bsc (Hons) thesis, 63 pp.

Ramsay, P.J. (1988). Physiographic and biological zoning of Two-Mile Reef, Sodwana Bay. Extended Abstract, 22nd Earth Science Congress of the Geological Society of South Africa, University of Natal, Durban, 483-486.

Ramsay P.J. (1990a). A new method for reconstructing late Pleistocene coastal environments, Sodwana Bay, Zululand. SA Geological Survey Report, 1990-0227, 44 pp.

Ramsay, P.J. (1990b). The use of computer graphics software to produce a three-dimensional morphological and bathymetric model of a Zululand coral reef. S.A. J. Sci., 86(3), 130-131.

Ramsay, P.J., Cooper, J.A.G., Wright, C.I. & Mason, T.R. (1989). The occurrence and formation of ladderback ripples in subtidal, shallow marine sands, Zululand, South Africa. Marine Geology, 86(2/3), 229-235.

Ramsay, P.J. & Mason, T.R. (1990a). Zululand coral reefs as palaeocoastline indicators. Abstract: Oceans '90, 7th National Oceanographic Conference, San Lameer, South Africa.

Ramsay, P.J. & Mason, T.R. (1990b). Development of a type zoning model for Zululand coral reefs, Sodwana Bay, South Africa. J. Coastal Research, 6(4), 829-852.

Reddering, J.S.V. (1987a). Subtidal occurrences of ladderback ripples: their significance in palaeo-environmental reconstruction. Sedimentology, 34, 253-257.

Reddering, J.S.V. (1987b). Evidence for a middle Holocene transgression, Keurbooms estuary, South Africa. Palaeoecology of Africa, 19, 79-86.

Reineck, H.E. & Singh, I.B. (1973). Depositional Sedimentary Environments. Springer-Verlag, Berlin, 439 pp.

Reiss, Z. and Hottinger, L. (1984). The Gulf of Aqaba, Ecological Micropalaeontology. Ecological Studies No. 50. Springer-Verlag, New York, 354 pp.

Rosen, B.R. (1971). The distribution of coral reef genera in the Indian Ocean. Symp. Zool. Soc. London, 28, 263-299.

Rossouw, J. (1984). Review of existing wave data, wave climate and design waves for South African and South West African (Namibian) coastal waters. CSIR Report T/SEA 8401, Stellenbosch, 66 pp.

Russell, R.J. (1962). Origin of beach rock. Zeitschr. fur Geomorphol., 6, 1-16.

Saetre, R. & Da Silva, A.J. (1984). The circulation of the Mozambique Channel. Deep Sea Research, 31, 485-508.

Scheer, G. (1971). Coral reefs and coral genera in the Red Sea and Indian Ocean. Symp. Zool. Soc. London, 28, 329-367.

Schmalz, R.F. (1971). Formation of beachrock at Eniwetok Atoll. In: O.P. Bricker (Ed.), Carbonate Cements. Johns Hopkins, Baltimore, Md., 17-24.

Schink, J.C, Stockwell, J.H. & Ellis, R.A. (1978). An improved device for gasometric determination of carbonate in sediment. J. Sediment. Petrol., 48, 651-653.

Schumann, E.H. (1988). Physical Oceanography off Natal. In: E.H Schumann, (Ed.), Coastal Ocean Studies off Natal, South Africa. Lecture Notes on Coastal and Estuarine Studies, 26, 101-130.

Schumann, E.H. & Orren, M.J. (1980). The physico-chemical characteristics of the south-west Indian ocean in relation to Maputaland. In: M.N. Bruton & K.H. Cooper (Editors), Studies on the Ecology of Maputaland. Wildlife Society of South Africa, Durban, 8-11.

Scoffin, T.P. (1987). An Introduction to Carbonate Sediments and Rocks, Blackie, London, 273 pp.

Scoffin, T.P. & McLean, R.F. (1978). Exposed limestones of the Northern Province of the Great Barrier Reef. Philos. Trans. R. Soc. London, 291, 119-138.

Shackleton, N.J & Opdyke, N.D. (1973). Oxygen isotope and palaeomagnetic stratigraphy of equatorial Pacific core V28-238: Oxygen isotope temperatures and ice volumes on a 10^5 and 10^6 year scale. Quaternary Research, 3, 39-55.

Shepard, F.P. (1963). Thirty-five thousand years of sea level. In: T. Clements (Ed.), Essays in marine geology in honour of K.O. Emery. Univ. S. Calif. Press, Los Angeles, California, 1-10.

Short, A.D. (1984). Beach and nearshore facies, southeast Australia. Marine Geology, 60, 261-282.

Sidekick Version 1.56A (1985). Borland, Inc.

Siesser, W.G. (1970). Carbonate components and mineralogy of the South African coastal limestones of the Agulhas Bank. Trans. Geol. Soc. s. Afr., 73, 49-63.

Siesser, W.G. (1972a). Relict algal nodules (rhodolites) from the South African continental shelf. J. Geol., 80, 611-616.

Siesser, W.G. (1972b). Environmental discrimination of coastal limestones by conventional and electron microscopic methods. Trans. Geol. Soc. s. Afr., 75(3), 295-298.

Siesser, W.G. (1974). Relict and recent beachrock from southern Africa. Geol. Soc. Am. Bull., 85, 1849-1854.

Smith, A.M. (1989). A lower Permian sandwave-containing shelf sequence exposed at Zungwini Mountain, Republic of South Africa. Sedimentary Geology, 64, 127-142.

Smith, A.M. (1990). Gradation from shelf to terrestrial deposition in the lower Permian Ecca Group near Vryheid, northern Natal, Republic of South Africa. 13th International Sedimentological Congress (Abstracts), Nottingham, England, 507-509.

Smith, A.M. & Tavener-Smith, R. (1988). Early Permian giant crossbeds near Nqutu, South Africa, interpreted as part of a shoreface ridge. Sedimentary Geology, 57, 41-58.

Statgraphics 4.0 (1989). Statistical Graphics Corp., USA.

Stoddart, D.R. (1969). Ecology and morphology of recent coral reefs. Biol. Rev., 44, 433-498.

Stoddart, D.R. (1973). Coral reefs of the Indian Ocean. In: O.A. Jones & R. Endean (Eds.), Biology and Geology of Coral Reefs. Academic Press, New York, 51 - 92.

Stoddart, D.R. & Cann, J.R. (1965). Nature and origin of beach rock. J. Sediment. Petrol., 35, 243-247.

Strasser A. & Davaud, E. (1986). Formation of Holocene limestone sequences by progradation, cementation, and erosion, two examples from the Bahamas. J. Sediment. Petrol., 56, 422-428.

Strasser, A., Davaud, E., & Jedoui, Y. (1989). Carbonate cements in Holocene beachrock, example from Bahiret el Biban, southeastern Tunisia. Sedimentary Geology, 62, 89-100.

Supercalc Version 5.00A (1989). Computer Associates International, Inc.

Surfer Version 3.00 (1987). Reference Manual. Golden Software Inc., Colorado, USA.

Swart, D.H. and Serdyn, J.de V. (1981). Statistical Analysis of Visually Observed Wave data from Voluntary Observing Ships for South African East Coast. Volume 9. Unpublished CSIR Report, 141 pp.

Swift, D.J.P., Alberto, G.F., Jr., Freeland, G.L. & Oertel, E.F. (1983). Hummocky cross-stratification and megaripples: a geological double standard. J. Sediment. Petrol., 53, 1295-1318.

Swift, D.J.P. & Nummedal, M.F. (1987). Discussion: hummocky cross-stratification, tropical hurricanes and intense winter storms. Sedimentology, 34, 338-344.

Swinchatt, J.P. (1965). Significance of constituent composition, texture, and skeletal breakdown in some recent carbonate sediments. J. Sediment. Petrol., 35, 71-90.

Sydow, C.J. (1988). Stratigraphic control of slumping and canyon development on the Zululand continental margin, east coast, South Africa. (unpubl.) BSc (Hons) thesis, University of Cape Town, 58 pp.

Tankard, A.J. (1976). Cenozoic sea-level changes, a discussion. Ann. S. Afr. Mus., 71, 1-17.

Taylor, J.C.M. & Illing, L.V. (1969). Holocene intertidal calcium carbonate cementation, Qatar, Persian Gulf. Sedimentology, 12, 69-107.

Taylor, J.D. (1971). Reef associated molluscan assemblages in the western Indian Ocean. Symp. Zool. Soc. London, 28, 501-534.

Thom, B.G.C. (1973). The dilemma of high interstadial sea levels during the last glaciation. Progr. in Geogr., 5, 170-246.

Thomas, R.H. (1987). Future sea-level rise and its early detection by satellite remote sensing. Prog. Oceanog., 18, 23-40.

Tomascik, T. and Sander, F. (1985). Effects of eutrophication on reef-building corals: I. Growth rate of the reef-building coral Montastrea annularis. Marine Biology, 87, 143-155.

Tucker, M.E. (1981). Sedimentary Petrology, An Introduction. Blackwell, London, 252 pp.

Tyson, P.D. (1986). Climatic Change and Variability in Southern Africa, Oxford University Press, Cape Town, 219pp.

Van Bruggen, A.C. & Appleton, C.C. (1977). Studies on the ecology and systematics of the terrestrial molluscs of the Lake Sibaya area of Zululand, South Africa. Zool. Verh., Leiden, 154, 1-44.

Van Heerden, I.L. & Swart, D.H. (1986). An assessment of past and present geomorphological and sedimentary processes operative in the St. Lucia Estuary and environs. CSIR Research Report, 569, 1-60.

Vasseur, P. (1974). The overhangs, tunnels and dark reef galleries of Tulear (Madagascar) and their sessile invertebrate communities. Proc. 2nd Internat. Symp. Corals and Coral Reefs 1973, 2, 143-159.

Verwey, J. (1931). The depth of coral reefs in relation to their oxygen consumption and the penetration of light in the water: Treubia (Buitenzorg). Coral Reef Studies, 13, 169-198.

Weiss, C.P. & Wilkinson, B.H. (1988). Holocene cementation along the central Texas coast. Jour. Sediment. Petrol., 58, 468-478.

Williams, G.C. (1989a). A review of recent research on the sublittoral coral reefs of northern Natal with a provisional assessment of findings regarding the distribution of octocorals on Two-Mile Reef, Sodwana Bay. S.A. J. Sci., 85(3), 140-141.

Williams, G.C. (1989b). A provisional annotated list of octocorallian coelenterates occurring on the sublittoral coral reefs at Sodwana Bay and Kosi Bay, northern Natal, with a key to the genera. S.A. J. Sci, 85(3), 141-144.

Williams, S.J. (1982). Use of high resolution seismic reflection and side-scan sonar equipment for offshore surveys. U.S. Army, Corps of Engineers, Coastal Engineering Tech. Aid, Report No. 82-5.

Williams, D.F., Moore, W.S., & Fillon, R.S. (1981). Role of glacial Arctic Ocean ice sheets in Pleistocene oxygen isotope and sea-level records. Earth and Planetary Science Letters, 56, 157-166.

Wright, C.I. (1990). The sedimentation of Lake Sibaya, north Kwa-Zulu. S. A. Geological Survey Report, 1990-0147, 25 pp.

Wunderlich, F. (1970). Genesis and environment of the 'Nellenkopfchenschichten' (lower Emsian, Rheinian Devon) at the locus typicus in comparison with modern coastal environment of the German Bay. J. Sediment. Petrol., 40, 102-130.

Wunderlich, F. (1972). Georgia Coastal region, Sapelo Island, U.S.A. Sedimentology and biology, III. Beach dynamics and beach development. Senckenbergiana Marit., 4, 47-79.

Yonge, C.M. (1940). The biology of reef-building corals: Great Barrier Reef Expedition 1928-1929. British Mus. Nat. History Sci. Repts., 1(13), 353-391.

Zeuner, F.E. (1959). The Pleistocene Period, 2nd Edition. Hutchinson, London.

APPENDIX

The following data are available on disk in the following formats:

Shelf bathymetric data - Surfer data file

Unconsolidated sediment grain statistics and distributions - Word Perfect 5.1 & Supercalc 5

Consolidated sediment grain statistics and distributions - Word Perfect 5.1 & Supercalc 5

Bioclastic component distributions - Supercalc 5

Cluster and discriminate analysis data - Statgraphics 4.0

Reef coordinates - Word Perfect 5.1